

This item was submitted to Loughborough's Institutional Repository (<https://dspace.lboro.ac.uk/>) by the author and is made available under the following Creative Commons Licence conditions.



CC creative commons
COMMONS DEED

Attribution-NonCommercial-NoDerivs 2.5

You are free:

- to copy, distribute, display, and perform the work

Under the following conditions:

BY: **Attribution.** You must attribute the work in the manner specified by the author or licensor.

Noncommercial. You may not use this work for commercial purposes.

No Derivative Works. You may not alter, transform, or build upon this work.

- For any reuse or distribution, you must make clear to others the license terms of this work.
- Any of these conditions can be waived if you get permission from the copyright holder.

Your fair use and other rights are in no way affected by the above.

This is a human-readable summary of the [Legal Code \(the full license\)](#).

[Disclaimer](#) 

For the full text of this licence, please go to:
<http://creativecommons.org/licenses/by-nc-nd/2.5/>

Interactions Between Charge Conditioning,
Knock and Spark-Ignition Engine Architecture

James William Griffith Turner

M.Eng.

A Doctoral Thesis submitted in partial fulfilment of the requirements for the award
of Doctor of Philosophy of Loughborough University

April 2011

© 2011 J.W.G. Turner

CERTIFICATE OF ORIGINALITY

This is to certify that I am responsible for the work submitted in this thesis, that the original work is my own except as specified in acknowledgments or in footnotes, and that neither the thesis nor the original work contained therein has been submitted to this or any other institution for a degree.

..... (Signed)

..... (Date)

Abstract

There are currently many factors motivating car manufacturers to reduce the tailpipe CO₂ emissions from their products. One of the major routes to achieving reduced CO₂ emissions in spark-ignition 4-stroke engines is to 'downsize' the swept volume which, among other advantages, reduces the proportion of fuel energy expended on pumping losses. The full-load performance deficit caused by reducing the swept volume of the engine is normally recovered by pressure charging.

One of the limits to pressure charging is combustion knock, which is the unintended autoignition of the last portion of gas to burn in the combustion chamber after combustion has been initiated. This thesis presents results from investigations into a number of methods for suppressing knock, including (1) tests where the density of the intake air is closely controlled and the effect of charge air temperature is isolated, (2) where the latent heat of vaporization of a fuel is used to reduce the outlet temperature of a supercharger, and (3) where the engine architecture is configured to minimize exhaust gas residual carryover to the benefit of stronger knock resistance. Extensive comparison of this resulting engine architecture is made with published data on other strategies to reduce the effect of the knock limit on engine performance and efficiency. Several such strategies, including cooled EGR, were then investigated to see how much further engine efficiency (in terms of brake specific fuel consumption) could be improved if they are adopted on an engine architecture which has already been configured with best knock limit performance in mind.

Within the limits tested, it was found that if the charge air density is fixed then the relationship between knock-limited spark advance and air temperature is linear. This methodology has not been found in the literature and is believed to be unique, with important ramifications for the design of future spark-ignition engine charging systems.

It was also found that through a combination of an optimized direct-injection combustion system, an exhaust manifold integrated into the cylinder head, and a 3-cylinder configuration, an engine with extremely high full-load thermal efficiency can be created. This is because these characteristics are all synergistic. Against the baseline of such an engine, other technologies such as excess air operation and the use of cooled EGR are shown to offer little improvement.

When operating a pressure-charged engine on alcohol fuel, it was found that there exists a maximum proportion of fuel that can be introduced before the supercharger beyond which there is no benefit to charge temperature reduction by introducing more. Strategies for reducing the amount of time when such a system operates were developed in order to minimize difficulties in applying such a strategy to a practical road vehicle.

Finally, a new strategy for beneficially employing the latent heat of vaporization of the fuel in engines employing cooled EGR by injecting a proportion of the fuel charge directly into the EGR gas is proposed. This novel approach arose from the findings of the research into pre-supercharger fuel introduction and cooled EGR.

Acknowledgements

I am an unreconstructed internal combustion engine man, and this thesis is an embodiment of that fact. During my career and in the researching of this work it has been my privilege and pleasure to meet and interact with many like-minded individuals, without whom what little understanding of the subject I have would not have come about. I cannot possibly thank them all, but they have my profound gratitude. There are, however, some who must be singled out for my thanks.

Firstly I would like to thank my supervisor, Colin Garner, who has become a firm friend over the six years that this thesis has been in the making, and who has an intelligence and clarity of thought which have been very supportive during those dark days when the enormity of the task seemed about to overwhelm me. There is no way that I would have got to this point without his mentorship and I hope that the technical discussions we have had continue, without the background task of completing this research looming large over them.

I also wish to deeply thank Richard Pearson for his friendship and encouragement over the 13 years we have known each other – a better friend I could not hope to find. Not a day goes by when I do not find myself amazed by his intelligence, together with his accessibility and knack of explaining truly complex things in ways that I, at least, can understand. I cannot speak highly enough of his intellect. Also, if it had not been for him setting me on this path, I would not have started on this endeavour.

I must mention all of the very talented designers, engineers and technicians at Lotus Engineering who have been involved in the various engine projects that included the work I have done and reported here. Designing, developing and testing an engine is a major group effort and no single person can be fully responsible for all aspects of such an undertaking. However, I do claim that the major concepts reported here have been created by myself. Primarily these are

the control strategy for the pre-supercharger fuel injection system reported in Chapter 5 being based on alcohol content as well as load, the asymmetric close-spaced direct-injection combustion system of the HOTFIRE engine which was subsequently incorporated into the Sabre engine, and the general specification of that engine (including its combination of combustion system, 3-cylinder configuration, integrated exhaust manifold and the use of its switching tappets to promote increased tumble and swirl at part load while simultaneously dethrottling it) which has provided such excellent full-load fuel consumption. The specific tests reported utilizing increased turbine inlet temperature and cooled EGR were also formulated by myself and formed the basis of an ongoing research stream into downsized engine performance. It is with due deference to, and acknowledgement of, the very many talented people with whom I have worked on these projects that I write this thesis.

I also wish to thank the management of Lotus Engineering for permitting me to do this work and then allowing me to publish the results.

The research boys – or ‘Q Branch’ as I like to think of them – must also be mentioned, especially Dave Blundell, Graham Pitcher, Clive Card, James Young, Rish Patel and Dave Gedge. They have helped me to ‘keep it real’ in the nine years which I have spent doing what I consider to be the best job in the world, and have always been quick to offer a particular brand of humour when (or when not) required. I salute them all. What they really think of me is anyone’s guess.

Alan Nobbs deserves a special mention for many years ago taking an under-experienced but over-enthusiastic young engineer under his wing and showing him the glories of 4-stroke engine performance. His dry sense of humour was similarly formative. He may never know the profound influence he had on me.

I would like to mention a further debt of inspiration to the great aero engine engineers Sir Stanley Hooker and Major Frank Halford, both of whom had amazing careers spanning pressure-charged piston engines and then gas turbines. The conceptual similarity of modern downsized engines to the Rolls-

Royce Merlin in particular has always struck me. Perhaps one day the automotive industry will also dispense with the 'heavy and complicated bit' between the compressor and turbine and similarly replace it with a simpler combustion chamber as series hybridization takes hold, and so I like to think this thesis represents a possible embodiment of my old school motto, *Sapiens qui prospicit* – wise is the man who looks ahead. We'll see.

Above all others, I have been inspired by one engine since very early in my career – the Napier Nomad. Such dedication to efficiency and synergy between individual subsystems probably drove me to think habitually in these terms. My belief is that the CFR engine is the most important reciprocating engine ever built; however, in my opinion, the Napier Nomad is easily the greatest, despite being over 60 years old.

I must profoundly thank my parents (and grandparents) for providing the best upbringing and education possible and for encouraging my curiosity in whatever topic took my interest. While it's strange to reflect that as a result of this I might have become a palaeontologist, I hope that they know that I'm intensely glad I settled on engine engineering as a career path. While some people may see the internal combustion engine as a dinosaur, as a result of whatever skills I may have acquired I will do my utmost to ensure that it doesn't become extinct any time soon.

Lastly, and definitely most importantly, I wish to thank my wife Rachael and my daughter Imogen. While they probably don't see much beauty in the process of hydrocarbon combustion, they know that I do, and they were generously prepared to allow me the time – effectively *their* time – to do this research. They also encouraged me when I needed it most. This is truly love beyond the call of duty and, in turn, I love them deeply for it. And I promise that they can have full access to our kitchen in the evenings from now on.

Contents

Certificate of Originality	2
Abstract.....	3
Acknowledgements	5
Contents	8
Co-Authorship Statement.....	14
Notation and Abbreviations	15
Chapter 1: Introduction	19
1.1 Historical perspective	20
1.2 The CO ₂ challenge	20
1.3 Gasoline as a fuel for internal combustion engines	26
1.4 The Otto cycle	29
1.4.1 Induction.....	31
1.4.2 Compression	32
1.4.3 Combustion	33
1.4.4 Expansion.....	34
1.4.5 Exhaust	35
1.4.6 Otto cycle mean effective pressures and air standard cycle efficiency.....	36
1.5 Objective of this research	39
1.6 Thesis overview.....	40
1.7 Contributions to the body of knowledge from the work presented in this thesis.....	42
1.8 Literature arising from work undertaken for this thesis	44
1.8.1 Book chapter written as lead author	44
1.8.2 Conference papers written as lead author.....	44
1.8.3 Conference papers written as co-author.....	46
1.8.4 Journal papers written as co-author	47
1.9 Summary and concluding remarks	47

Chapter 2: Pressure Charging and Engine Downsizing to improve Vehicle Fuel Consumption	49
2.1 Supercharging	50
2.1.1 Roots superchargers	54
2.1.2 Lysholm twin-screw superchargers	56
2.1.3 Centrifugal compressors.....	59
2.1.4 Axial-flow superchargers	62
2.2 Turbocharging	64
2.3 Compound charging	69
2.4 Turbocompounding	70
2.5 The use of pressure charging to reduce road vehicle fuel consumption...	72
2.6 The use of cooled EGR, excess air and turboexpansion to extend the knock limit of pressure-charged engines	78
2.7 Summary and concluding remarks	82
 Chapter 3: Literature Review of Spark-Ignition Combustion Knock and Means of Counteracting It.....	85
3.1 The spark-ignition engine combustion process	86
3.2 General discussion of spark-ignition engine knock.....	89
3.3 The knock rating of fuels	95
3.4 Approaches to extend the relevance of RON and MON ratings	108
3.5 Other factors influencing the occurrence of knock.....	111
3.6 Knock suppression by charge dilution	117
3.7 Employing the latent heat of vaporization of a fuel to increase the knock limit.....	120
3.8 Other means of suppressing knock	123
3.9 Summary and concluding remarks	132
 Chapter 4: Previous Work.....	136
4.1 Pressure-charged engine work utilizing the benefits of the latent heat of spark-ignition engine fuels.....	136
4.2 Development of the turboexpansion concept as a fuel economy technology	139

4.3	Design of the ‘Nomad’ research engine and initial turboexpansion system dynamometer testing	143
4.4	Summary and concluding remarks	150
Chapter 5: Supercharged Engine Tests with Alcohol-Based Fuel		152
5.1	Alcohols as alternative fuels for spark-ignition engines	153
5.2	Base supercharged test engine	158
5.3	Fuelling philosophy adopted: the use of pre-supercharger injection to maximize the benefit of alcohol fuel	161
5.4	Dynamometer testing and results	164
5.4.1	Fuelling tests to investigate the effect of pre-supercharger injection of alcohol-based fuel	166
5.4.2	Engine performance on E85 and comparison with 95 RON gasoline.....	173
5.5	Discussion of test results	180
5.5.1	Practical considerations in applying a pre-supercharger injection operating strategy with E85.....	184
5.6	Concepts to improve the efficiency of flex-fuel engines.....	188
5.7	Summary and concluding remarks	191
Chapter 6: Single-Cylinder Engine Tests at Constant Charge Air Density		194
6.1	Single-cylinder test engine	194
6.2	Charge air conditioning rig.....	198
6.3	Test cell equipment	201
6.3.1	General measuring equipment	201
6.3.2	Intake and exhaust systems	202
6.4	Test results.....	207
6.4.1	Test conducted to determine relative air-fuel ratio for the test programme	207
6.4.2	Tests conducted to determine the valve timing for the fixed-air-density tests.....	210
6.4.3	Testing at constant charge air density while varying charge inlet temperature	215
6.5	Summary and concluding remarks	219

Chapter 7: The Sabre 3-Cylinder Downsized Demonstrator Engine Concept...	221
7.1 The Sabre engine project	221
7.2 Sabre engine design	222
7.3 The concept of swirl-enhanced combustion and a brief overview of part-load results	232
7.4 Initial full-load test results	234
7.5 Scavenging advantages of 3-cylinder groups in turbocharged spark-ignition engines	237
7.6 Sabre engine results in comparison to competing technologies.....	240
7.6.1 Comparison of Sabre with compound charging systems.....	240
7.6.2 Comparison of Sabre with 4-cylinder engines employing 180° CA exhaust cam period to eliminate pulse interaction	241
7.6.3 Comparison of Sabre with an external water-cooled exhaust manifold ..	243
7.6.4 Comparison of Sabre with excess air combustion strategies	246
7.6.5 Comparison of Sabre with cooled EGR.....	247
7.6.6 Comparison of Sabre with higher turbine inlet temperatures.....	249
7.6.7 Comparison of Sabre with some combinations of other technologies	251
7.7 Summary and concluding remarks	253
 Chapter 8: Experiments with Concepts to Further Improve the Full-Load Fuel Consumption of the Sabre Downsized Demonstrator Engine.....	 256
8.1 Experiments on the effect of turbocharger matching	256
8.2 Experiments on the effect of increasing turbine inlet temperature.....	259
8.3 Experiments with cooled EGR.....	269
8.3.1 Modifications to the Sabre engine for cooled EGR testing	269
8.3.2 Effect of cooled EGR system dead volume	270
8.3.3 Configuration of cooled EGR system tested.....	272
8.3.4 Means of introduction of cooled EGR into the intake air flow	273
8.3.5 Effect of cooled EGR on SI engine combustion systems	275
8.3.6 Cooled EGR test results	277
8.4 Comparison of results for increased turbine inlet temperature and cooled EGR	286

8.5	A new concept to reduce the complexity of cooled EGR systems.....	293
8.6	Summary and concluding remarks	298
Chapter 9: Conclusions and Further Work.....		300
9.1	Summary of the thesis.....	300
9.2	Major conclusions.....	303
9.3	Recommendations for further work	305
References.....		307
Appendix I: Original Spreadsheet for Turboexpansion Concept		342
Appendix II: Notes on Accuracy of Results		343
Appendix III: Further Details of the CFR Fuels Testing Engine.....		345
Appendix IV: Notes on the Performance of the Charge Air Conditioning Rig....		351
Appendix V: Comparison of the Effects of Different EGR Routes on the Sabre Downsized Demonstrator Engine		352
A5.1	Effect of EGR route on the performance of the charging system of the Sabre engine	354
A5.2	Effect of EGR route on combustion in the Sabre engine	367
A5.3	Summary and concluding remarks	371
Appendix VI: Listing of Input Variables for Modelling of the Single-Cylinder Engine in Chapter 6.....		373
Appendix VII: Reproductions of Various Websites Given as References		375
A7.1	EC (2010).....	376
A7.2	SMMT (2011)	377
A7.3	MCE-5 (2010).....	378
A7.4	Website (2011a).....	380
A7.5	Website (2011b).....	381

For Rachael and Imogen

Thank you.

Co-Authorship Statement

The work presented in this thesis was conceived, conducted and disseminated by the doctoral candidate. The co-authors of the manuscripts that comprise part of this thesis made contributions only as is commensurate with a thesis committee or as experts in a specific area as it pertains to the work. The co-authors provided direction and support. The co-authors reviewed each manuscript prior to submission for publication and offered critical evaluations; however, the candidate was responsible for the writing and final content of these manuscripts.

Notation and Abbreviations

4vpc	Four-valves-per-cylinder
ACEA	European Automobile Manufacturers' Association
AFR	Air-fuel ratio
AN	Army-Navy (performance number)
ASME	American Society of Mechanical Engineers
ATDC	After top dead centre
BDC	Bottom dead centre
BMEP	Brake mean effective pressure
BOM	Bill-of-material
BSAC	Brake specific air consumption
BSFC	Brake specific fuel consumption
BTDC	Before top dead centre
BTE	Brake thermal efficiency
c_p	Specific heat capacity at constant pressure
CA	Crank angle
CA50	Position of 50% mass fraction burned
CAC	Charge air conditioning
CARB	California Air Resources Board
CCR	Critical compression ratio
CFR	Cooperative Fuels Research
CO	Carbon monoxide
CO ₂	Carbon dioxide
COV	Coefficient of variation
CPS	Cam profile switching
CR	Compression ratio
CSTR	Continuously-stirred tank reactor
CVCP	Continuously-variable camshaft phasing
DCVCP	Dual continuously-variable camshaft phasing
DEP	Divided exhaust period
DI	Direct injection

DISI	Direct-injection spark-ignition
EBP	Exhaust back pressure
EC	European Commission
EGR	Exhaust gas recirculation
EIVC	Early intake valve closing
EMS	Engine management system
EOCT	End-of-compression temperature
EPSRC	Engineering and Physical Sciences Research Council
ETC	Exothermic centre
EU	European Union
EVO	Exhaust valve opening
FMEP	Friction mean effective pressure
GDI	Gasoline direct injection
h	Specific enthalpy
HC	Hydrocarbons
HCCI	Homogeneous charge compression ignition
HMN	Heptamethyl nonane
HSDI	High-speed direct-injection
HUCR	Highest usable compression ratio
IEM	Integrated exhaust manifold
IMEP	Indicated mean effective pressure
IQT	Ignition Quality Tester
IVC	Inlet valve closing
KLSA	Knock-limited spark advance
LBDI	Lean Boost Direct Injection
LBT	Leanest fuelling for best torque
LES	Lotus Engine Simulation
LHV	Lower heating value
LIVC	Late intake valve closing
\dot{m}	Mass flow rate
MBT	Minimum ignition advance for best torque
MFB	Mass fraction burned

MOP	Maximum opening point
MON	Motor octane number
MTBE	Methyl <i>tert</i> -butyl ether
NA	Naturally-aspirated
NEDC	New European Drive Cycle
NMEP	Net mean effective pressure
NO	Nitric oxide
NO ₂	Nitrogen dioxide
NO _x	Oxides of nitrogen
NTC	Negative temperature coefficient
OEM	Original equipment manufacturer
OI	Octane index
ON	Octane number
p	Pressure
PCI	Pre-compressor (fuel) injection
PFI	Port fuel injection
PMEP	Pumping mean effective pressure
ppm	Parts per million
PRF	Primary reference fuel
\dot{Q}	Heat flow rate
r	Compression ratio
R_{Th}	Thermal ratio
RAT	Radial aperture tube
RCM	Rapid compression machine
RON	Research octane number
rpm	Revolutions per minute
s	Specific entropy
S	Octane sensitivity
SAE	Society of Automotive Engineers
SI	Spark-ignition
SMMT	Society of Motor Manufacturers and Traders
SOCT	Start-of-compression temperature

SVC	Saab Variable Compression
t	Time
T	Temperature
TDC	Top dead centre
TEL	Tetraethyl lead
TIT	Turbine inlet temperature
TML	Tetramethyl lead
TWC	Three-way catalyst
V	Volume
VCR	Variable compression ratio
VGT	Variable-geometry turbine
\dot{W}	Power
WOT	Wide-open throttle

Greek letters

γ	Ratio of specific heats
ϕ	Equivalence ratio
λ	Relative air-fuel ratio
η	Efficiency
τ	Autoignition delay time

Subscripts

C	Clearance
LHV	Lower heating value
S	Swept
TEL	Tetraethyl lead

Chapter 1: Introduction

This thesis presents research into spark-ignition (SI) engine downsizing for improving fuel economy in road vehicles. It shows how the control of gasoline engine knock is crucial to being able to reduce the swept volume of an engine to improve fuel economy. The latter is because such engine downsizing reduces the effect of the throttling losses inherent in the 4-stroke cycle at road loads.

The effects of fuel properties, and how they may beneficially be used to increase downsizing, were investigated in a supercharged engine. The effects of charge air temperature and pressure were aspects investigated in a test programme using a single-cylinder engine supplied with air by an independently-driven rig. The architecture of this single-cylinder engine was carried over to a 3-cylinder research engine which showed that a synergistic approach to engine configuration can produce results at least equal to the best which can be achieved with supplementary technologies at engine loads equivalent to current downsized vehicle engines. Finally, some tests were conducted applying some of these 'add-on' technologies to the 3-cylinder engine, which showed that only minimal improvements could be made with these approaches, thus showing that the baseline was genuinely a near-optimum configuration.

This first chapter reviews the historical reasons for mankind's mobility and the rise of the 4-stroke Otto cycle engine in supplying that mobility. The fossil fuel such engines use and the importance of reducing fuel consumption as a means of controlling the accumulation of CO₂ in the atmosphere are discussed. The Otto cycle is described so that a framework is provided for the discussion of pressure charging and knock in the following two chapters. Finally, the structure of the thesis is described together with the contributions to the body of knowledge that it makes.

1.1 HISTORICAL PERSPECTIVE

The desire for mobility is one of the defining characteristics of mankind. Man has always sought to move throughout the world he inhabits in order to colonize new land and to ensure survival of his species. Gradually the importance of this turned to the ability to move goods and soldiers in order to drive economic and political growth. This in turn gave rise to the development of an infrastructure of roads and bridges by past civilisations. As a by-product of the creation of these communication networks, citizens could also use them to move relatively easily from place to place, at different rates depending upon the form of transport to which they had access.

Consequently, personal freedom of movement has developed into what is often perceived as a basic human right. This is not something which is going to be given up lightly by any population, regardless of socio-political factors, market forces or climatic concerns.

Following Karl Benz's creation of the first workable automobile in the 1885 (employing a spark-ignition version of the 4-stroke cycle attributed to Nikolaus Otto in 1876) the growth of personal transport due to the automobile has been remarkable. The end result of this social and engineering development is that mankind places a significant reliance on the hydrocarbon fuels that fuel the automobile. Modern economic and availability pressures demand that attempts be made to improve engine fuel economy.

1.2 THE CO₂ CHALLENGE

The need to reduce the amount of fossil fuel that mankind consumes is driven by several economic and geopolitical factors. This need is also linked to a growing concern that mankind's accelerating usage of fossil carbon-based fuels is beginning to affect the climate of the Earth through the release of carbon dioxide (CO₂), a so-called 'greenhouse gas'. The economic factors are straightforward in that the balance of trade of nations is affected by the amount and value of the

fuels that they import or export. The geopolitical factors are governed primarily by the desire of several Western nations not to be dependent upon crude oil from the Middle East, which is seen as a geopolitically unstable region. In the past it was precisely these factors that led to military intervention in these areas to ensure energy supply, with over-reliance by the West on these areas for fuel increasing the concern that those nations with the capability to meet the demand for oil can exert undue influence over the 'developed' world.

The need to reduce the amount of greenhouse gases (such as CO₂) released into the atmosphere is driven by recent evidence that their accumulation in the atmosphere is causing its temperature to increase. Estimates have been made that 400 billion tonnes of CO₂ have already been released into the atmosphere by mankind by burning fossil fuels, and that if man were to burn all of the fossil fuels available to him, the atmospheric temperature would increase by 13°C by 2100 (Pearce, 2006a). Even before all of this CO₂ is released, if the atmospheric temperature is allowed to reach a high enough value, climatic change could ensue as a result of the polar ice caps melting. For northern Europe there is the added concern that as salinity levels in the North Atlantic reduce, there is the danger that the North Atlantic Conveyor (i.e. the 'Gulf Stream') will move south, and a generally colder climate will result. Such an event has been predicted to result in an average temperature reduction of 5-10°C (Website, 2006a).

Therefore, there is now a great amount of political pressure put upon society in general, and the vehicle original equipment manufacturers (OEMs) in the automobile industry in particular, to reduce the rate at which CO₂ is emitted from motor vehicles. This pressure was enacted chiefly by the Kyoto Protocol to the United Nations Framework Convention on Climate Change of December 1998 (Website, 2006b). Since the Kyoto Protocol was ratified, there has been significant further legislation passed in the form of the California State Government's Assembly Bill 1493, lobbied for by the Californian Air Resources Board (CARB) (Website, 2002). In this bill, CARB sought to make legal requirements on the OEMs to reduce the amount of CO₂ that their products

release. This is *de facto* a route to reduced fuel consumption since CO₂ production is directly linked to hydrocarbon fuel consumption, but it can also be argued to be a legislatable exhaust tailpipe gas, which is all CARB is currently empowered to legislate upon. While CO₂ limits are enacted by the bill, at the same time, vehicles must continue to comply with limits on the three existing mandated primary pollutants of hydrocarbons (HC), carbon monoxide (CO) and oxides of nitrogen (NO_x).

Simultaneously in Europe, the European Automobile Manufacturers Association, ACEA, came under pressure from the European Union (EU) as a result of the Kyoto Protocol. The result was a voluntary undertaking by ACEA to reduce the average passenger vehicle tailpipe CO₂ output of its entire fleet to 140g of CO₂ per kilometre (gCO₂/km) by 2008, as measured on the New European Drive Cycle (NEDC). After some promising initial results (ACEA, 2005), caused primarily by a market shift away from gasoline towards diesel engines (and itself driven by CO₂-based taxation policies within some member states of the EU), the target was missed. This is illustrated by Figure 1.1, which is data released by the European Commission (EC) and the Society of Motor Manufacturers and Traders (SMMT) for vehicles sold in the EU and UK after 1997 on a year-by-year basis, respectively (EC, 2010 and SMMT, 2011). Note that the European average is lower because of the historical preference for diesel-engined vehicles in Europe versus the UK. A proportion of the improvement is due to a rising share of diesel engines. Also note that the two sets of data are converging because of the increasing popularity of diesels in the UK as a result of government incentives through the company car tax system.

The result of this failure by ACEA to meet the voluntary agreement was that the EU decided to mandate fines for failure to achieve fleet-averaged fuel economy targets. While the targets are based upon vehicle mass, the net effect is that in 2012 exceeding the target will result in a fine of €35 for each gram of CO₂ per kilometre over the target, rising to €95 in 2015. The target is set to achieve an average tailpipe CO₂ emission of 130 gCO₂/km across the vehicle fleet, of which a further 10 gCO₂/km will be removed by fuel-related measures, i.e. increasing

the renewable energy component in the fuels supplied. Figure 1.1 shows that the rate of improvement between 2007 and 2009 must be maintained if the EU target of 130 gCO₂/km is to be met.

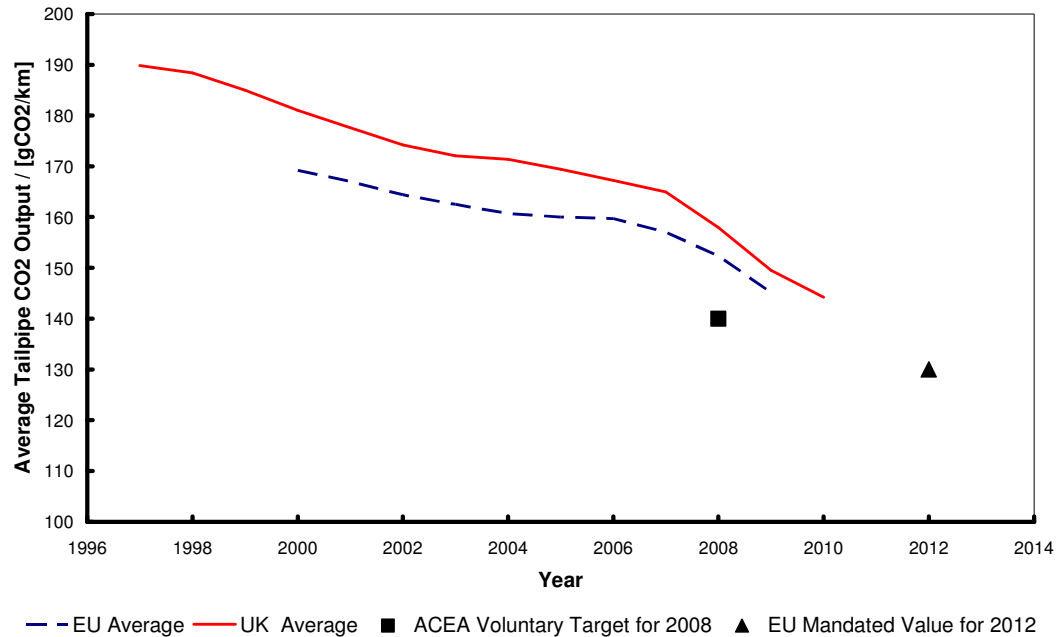


Fig. 1.1: Average tailpipe CO₂ emitted by passenger vehicles sold per year in the European Union and the UK, as measured on the NEDC. Also shown is the voluntary ACEA target for 2008 (140 gCO₂/km) and EU mandated figure for 2012 (130 gCO₂/km). Data taken from EC (2010) and SMMT (2011)

Since the Kyoto Protocol was enacted, various new technologies have been and are being developed by OEMs in order to meet its challenge (Turner *et al.*, 2005b). As has been stated previously, an increase in the market share of light-duty diesel engines across Europe has allowed a general reduction in CO₂ output. However, since CO₂ output is dependent upon mass of carbon burnt and *not* on the volume of fuel, there is a reduced benefit in favour of the diesel engine compared to its gasoline counterpart. This is because diesel contains less energy per unit CO₂ released than gasoline (Coe, 2005). The diesel engine also faces significant challenges in the form of its exhaust emissions, whereas SI

engine exhaust emissions can be dealt with relatively simply and robustly by a three-way catalyst. As a result, much effort is being spent in the area of SI engine technology. Furthermore, after years of continual development, the modern light duty diesel is arguably well defined in its general specification of common-rail fuel injection equipment, turbocharger and chargecooler with cooled EGR being used to reduce NO_x emissions. Conversely gasoline engines show, at present, a much greater variation in their specification, with natural aspiration, turbocharging and/or supercharging with chargecooling, direct fuel injection and variable valve trains of varying levels of sophistication all being employed, together with increasing use of cylinder deactivation (Turner *et al.*, 2005b). There is also a general shift towards increasing electrification of the vehicle, with series hybridization also being best served by gasoline engines (Bassett *et al.*, 2010 and Turner *et al.*, 2010b). The use of these technologies on SI engines and how they can be used to improve fuel consumption in vehicles with mechanical transmissions will be returned to in Chapter 2.

At the same time, so-called 'alternative' fuels such as natural gas, propane, ethanol and hydrogen are being adopted for SI engines, although gasoline still dominates the market. These alternative fuels have the potential to reduce CO₂ production in road vehicles, particularly those which can be obtained from biomass, since for such fuels a significant proportion of the CO₂ that is emitted in their combustion has already been removed from the atmosphere by the plants which are used in their manufacture. This fact is driving a move to bioethanol and also the consideration of a methanol-based energy economy, which can help to create a 'closed CO₂ cycle', as is shown in Figure 1.2 (Olah *et al.*, 2006 and Pearson *et al.*, 2009b).

A fuel with a fully-closed CO₂ cycle can be created if CO₂ scrubbed from the atmosphere is used as a feed stock to chemically liquefy hydrogen (Olah *et al.*, 2006, Lackner, 2008 and Pearson *et al.*, 2009b). Providing all of the energy used in the process of creating and distributing the fuel is carbon-free, its subsequent combustion yields no net accumulation of CO₂ in the atmosphere. This process allows the ready implementation of a practical fossil-carbon free fuel without the

significant challenges and costs associated with implementing the 'hydrogen economy' or the full electrification of the automobile (Olah *et al.*, 2006 and Pearson *et al.*, 2009b).

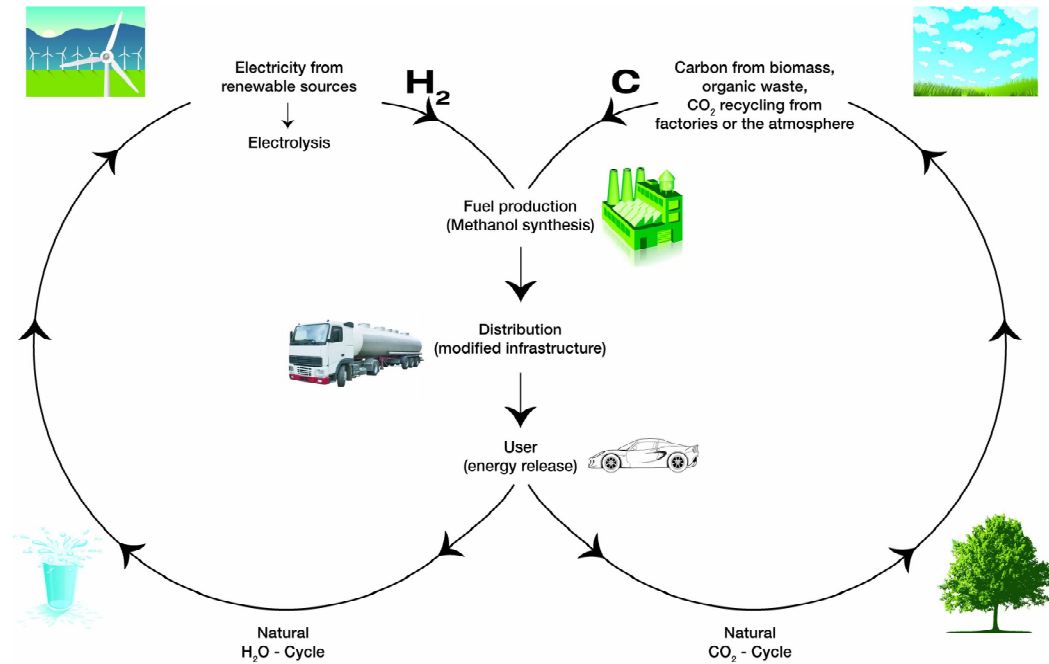


Fig. 1.2: Illustration of fully-closed fuel cycle utilizing CO₂ and hydrogen to provide methanol for use as a transportation fuel. (Illustration courtesy Lotus Engineering)

Importantly, the two low-carbon-number alcohol fuels are also arguably better fuels for internal combustion engines than gasoline, since they possess higher octane ratings than common gasoline formulations used for road transport, together with a higher latent heat of vaporization (Germane, 1985 and Owen and Coley, 1995). These characteristics permit higher engine thermal efficiency than is possible with gasoline, with thermal efficiency defined as

$$\eta_{th} = \frac{\dot{W}}{\dot{Q}_{LHV}}$$

Eqn 1.1

where η_{th} is the thermal efficiency of the engine, \dot{W} is the usable shaft power out and \dot{Q}_{LHV} is the total chemical energy per unit time carried by the fuel being supplied to the engine. Thermal efficiency is usually expressed as a brake value measured on a dynamometer, but is occasionally expressed in indicated terms, where the work of the cycle is calculated as the power liberated by combustion.

The prime reason why alcohol fuels can allow an SI engine to operate at higher thermal efficiency is because the knock limit of the engine is extended by the use of the higher octane fuel. The flame speed is also higher, which leads to faster and hence more optimally-timed combustion (Institution of Automobile Engineers, 1924 and Turner *et al.*, 2007a). Despite performance and efficiency being of great importance in aircraft, they have not been rigorously investigated there because of their low volumetric energy content. Nonetheless, they have been used as octane-enhancing blending agents for many years together with other oxygenated compounds such as ethers (Drell and Branstetter, 1950). They have also been used as a separate agent injected into the entry to a supercharger to help increase power (Gunston, 1995).

Despite the obvious advantages of low-carbon-number alcohols in SI combustion systems, fossil-based gasoline has become the dominant fuel for Otto-cycle engines. The Otto cycle itself is discussed in greater detail in Section 1.4 of this chapter, and the subject of SI engine combustion and knock and how it relates to engine efficiency will be returned to in Chapter 3 of this thesis, but the next section briefly describes the reason for the dominance of gasoline as a light-duty vehicle fuel.

1.3 GASOLINE AS A FUEL FOR INTERNAL COMBUSTION ENGINES

For transportation purposes the predominant hydrocarbon fuels are gasoline and diesel. Of these, gasoline was the fuel chosen by Nikolaus Otto for his four-stroke engine in Germany in 1876 (Gibbs, 1993). Since Otto produced the first practical SI engine, he was, of course, at liberty to choose the fuel upon which it

operated. Consequently, because gasoline was the fuel originally specified by Otto, Benz's use of gasoline for the first production automobile was logical and understandable, and this choice has influenced road vehicles ever since.

At the time that Otto designed his first engine, gasoline was sold as a solvent from apothecaries and was therefore easy to obtain in small quantities. It was also cheap because it was merely a chemical which, in terms of the volume produced, was a rather troublesome by-product of the petrochemical industry of the time (Dickinson, 1929). It had not even been commercially developed until 1863, when it and kerosene began to be used as a raw material for lighting systems (Gibbs, 1993), gradually replacing whale oil. This followed the first commercial oil well being drilled in Titusville, Pennsylvania, in 1859 (Olah *et al.*, 2006). It was because of its volatility that gasoline was the fuel chosen by Otto, and with hindsight the near-simultaneous development of fuel and engine must be seen as fortuitous for the development of personal transport as we know it.

As a fuel for SI engines, gasoline has several advantages. In addition to its volatility, it is simple to store and transport, easy to ignite (although this characteristic must be treated with the necessary respect) and, with a lower heating value of about 43 MJ/kg (Bosch, 2000), its calorific content is higher than most other SI engine fuels such as liquid oxygenated hydrocarbons, e.g. the alcohols and ethers, allowing more energy to be stored in a given vehicle fuel tank volume (Germane, 1985).

Gasoline is now seen as an everyday product in the modern world and has enabled engine designers to develop engines without concern for variation in fuel quality. Dickinson (1929), however, states that until 1910 gasoline was merely an *ad hoc* term for all of the volatile material which was a by-product of kerosene refining. Indeed, despite increasing numbers of automobiles (and aircraft) no specification for gasoline existed until 1919 (Gibbs, 1996). Once the importance of a systematic approach to the development of the SI engine and its fuel was established, better properties for base gasoline stock have continually been sought. This systematic approach was primarily driven by the pioneering work of

the Cooperative Fuel Research (CFR) Committee in the USA (Dickinson, 1929 and Horning, 1931) and Ricardo in the UK (Institution of Automobile Engineers, 1924). At the same time, additives have been developed to improve knock resistance, combat combustion chamber deposits and carburettor icing, and improve other characteristics such as fuel injector cleaning (Dickinson, 1929, Boyd, 1950, Dorn and Mourao, 1984, Gibbs, 1990 and Kalghatgi, 1990). The subject of the work of the CFR Committee and other pioneers in the area of fuel research (such as the General Motors Research Laboratories and members of the Empire Motor Fuels Committee) will be returned to in Chapter 3.

Despite its advantages, gasoline does, however, have the disadvantage that relative to many other potential gaseous and liquid hydrocarbon fuels for SI engines, it is relatively prone to autoignition under certain conditions (Owen and Coley, 1995). Unfortunately, these conditions are frequently found in engines. Autoignition is that characteristic of a fuel to spontaneously ignite when its temperature and pressure are increased such that, subsequently, it combusts without external energy input (such as by an initiating spark or by a deflagrating flame front consuming it). This was a problem identified very early in the development of the SI engine (Campbell *et al.*, 1930 and Boyd, 1950) and is a subject which will be discussed in detail in Chapter 3 of this thesis, because it limits the efficiency which is attainable from such an engine.

Autoignition, in itself, is not necessarily damaging to an engine, but under certain conditions of local exothermicity, inhomogeneity and the desorption of reactive species from the combustion chamber wall, autoignition can lead to combustion knock, which can in turn, in very short periods, produce damage in an engine, the consequences of which can be catastrophic. This subject is discussed in great detail by Konig *et al.* (1990), Nates and Yates (1994) and Fitton and Yates (1996), and will be discussed in detail in Chapter 3, including the disadvantage of the long-chain structure of gasoline hydrocarbons. The size and structure of these hydrocarbon molecules is what makes them liquid, but they also make it extremely difficult to model and predict the combustion of gasoline when it is under the conditions prevalent in an SI engine.

Because of these disadvantages it could almost be considered unfortunate that Benz decided upon gasoline as the fuel for his Otto-cycle-engined vehicles, when compared to, say, a renewable alcohol such as ethanol. Nevertheless, the situation is that gasoline is one of the dominant types of fuel used by modern society for passenger vehicles, and with the imperative of reducing mankind's increasing CO₂ output, engineers must find ways of enabling Otto cycle engines to burn this fuel more efficiently, at least until fuels with superior characteristics and better potential for renewability, such as ethanol and methanol, become mainstream.

Finally, it should also be remembered that Otto's choice of gasoline has, in addition to the vehicle manufacturers, also had a significant effect on the petrochemical industry. Ever since the automobile became the largest consumer of gasoline in 1908, the petrochemical industry has had to develop ever more efficient means of increasing gasoline yield from each barrel of crude oil (Gibbs, 1993 and Schmidt and Forster, 1984). Historically, as the number of vehicles using gasoline has increased, the refining industry has always found ways of establishing an equilibrium such that the yield of gasoline and diesel from each barrel of crude oil is economical to obtain at the near-equal amount of each that is currently used (Louis, 2001). Significant developments with regard to increasing the yield of gasoline per barrel of crude oil include the introduction of thermal cracking at high pressure in 1913 and the catalytic cracking process in 1936 (Olah *et al.*, 2006). Keeping the ratio of the yield of gasoline to diesel from a barrel of crude oil in an optimum range in itself helps to keep the cost of the fuel low (before taxes are added).

1.4 THE OTTO CYCLE

Up to this point in 2011, all production automotive passenger car gasoline engines operate on a 4-stroke SI cycle, commonly referred to as the Otto cycle after the German inventor to whom it is attributed, Nikolaus Otto. In most engines the phases of the cycle correspond approximately to what are the

'strokes' of a Watt crank-rod-slider mechanism, which is used to perform the various functions of the cycle by motion of the crankshaft, connecting rod and piston. The cycle is termed a 4-stroke cycle since it takes four strokes, or movements of the piston from one end of the cylinder to the other, to complete itself.

The most common way of admitting fresh charge and expelling burnt gases from the combustion chamber of such 4-stroke reciprocating engines is by 'poppet' valves in the cylinder head, usually driven by an overhead camshaft mechanism. Some aircraft engines used sleeve valves for gas exchange, but for passenger cars, the only recent dissenter from the crank-rod-slider-and-poppet-valve configuration was the Wankel rotary piston engine recently manufactured by the Mazda Motor Corporation (Yamamoto, 1981 and Ohkubo *et al.*, 2004). Elsewhere, the poppet-valve reciprocating piston engine reigns supreme, and from henceforth it will be described here as the 4-stroke engine.

In a 4-stroke engine the maximum and minimum volume of the working chamber is defined to be at bottom dead centre (BDC) and top dead centre (TDC) respectively. These dead centres correspond to when the piston gudgeon pin, crankshaft big end and crankshaft main journals are all in line. Balancing of the forces arising from the acceleration and deceleration of the reciprocating masses in these engines gives rise to the common cylinder configurations which are often found. While the combustion loads within the cylinder do not affect the state of free-body vibration of the engine, they do have an affect on torsional vibration (Thomson, 1978).

In the Otto cycle there are five phases: induction, compression, combustion, expansion and exhaust. These are inter-linked to various degrees and will now be discussed with respect to the indicator diagram for the Otto 4-stroke cycle shown in Figure 1.3. Such an indicator diagram shows the log of the pressure in the cylinder versus the log of the cylinder volume during the cycle (Heywood, 1988). The example in Figure 1.3 is for an engine operating at part load, and shows the swept volume normalized between TDC and BDC and the different

phases of the cycle, together with arrows indicating the direction in which the cycle proceeds.

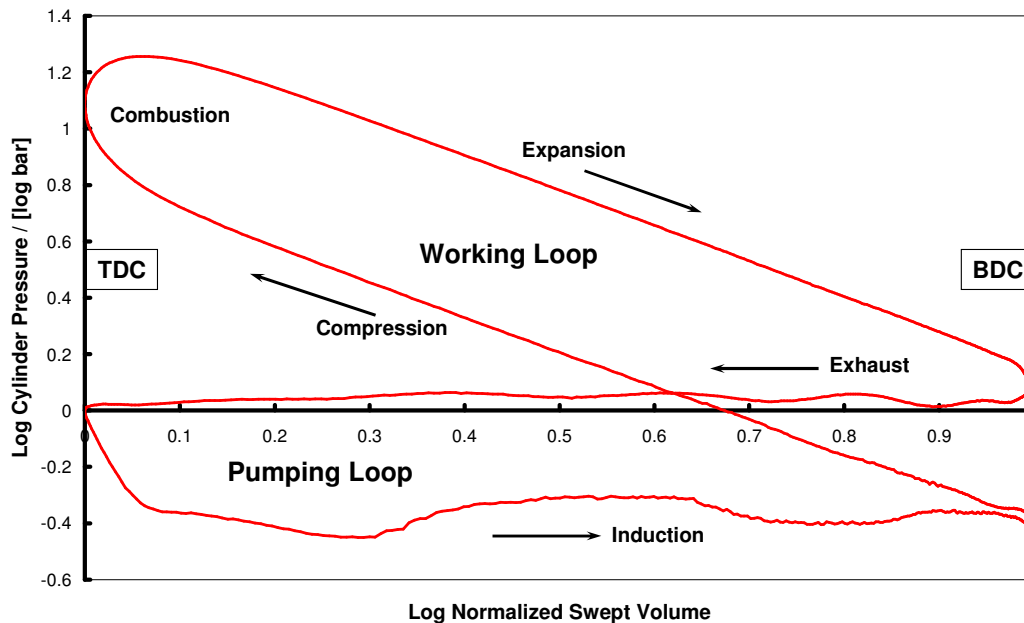


Fig. 1.3: Example of Otto cycle indicator diagram for an engine operating at part load

1.4.1 Induction

During the induction (or intake) stroke, air is drawn into the engine when the piston descends. If the engine utilizes a carburettor or port fuel injection (PFI) to prepare the mixture external to the cylinder, fuel is also inducted. This air and fuel mixture is termed the charge. The process begins when the intake valve opens, conventionally just before TDC. If the engine is aspirated 'naturally' and operating at below its full load producing capacity (i.e., operating at part load), this operation is normally performed against a partially-closed throttle plate. The throttle causes a reduction in the density of the intake charge. The mass of charge entering the engine, and thus the power it can produce, is therefore controlled by 'throttling'. The vacuum necessary to cause the expansion is

produced by the piston. Since it is descending, this is negative work and has an impact on fuel consumption which will be discussed in more detail later. In general, note that for any given crankshaft torque required, the larger the swept volume of the engine, the higher the parasitic losses due to throttling.

In a direct-injection engine, the fuel will be introduced into the cylinder via a nozzle positioned in the wall. A high-load operating condition will generally see the fuel being sprayed while the intake valves are open in order to maximize fuel-air mixing and provide as homogeneous a charge as possible, as would be provided by external fuel preparation such as PFI. Stratified operation is another possibility with direct injection, but if used, it is generally currently only adopted as a part-load operating condition.

The induction phase ends at intake valve closing (IVC). This point in the cycle does not have to coincide with the BDC of the piston at the end of the associated stroke, although it is usually somewhere near to it.

1.4.2 Compression

After the induction process is complete, the charge is compressed during the following upward stroke of the piston. This occurs in an approximately adiabatic manner across a compression ratio which is defined geometrically by reference to the piston dead centre positions as

$$r = \frac{V_s + V_c}{V_c} \quad \text{Eqn 1.2}$$

where r is the compression ratio of the engine, V_s is the swept volume of the engine cylinder and V_c is the clearance volume of the combustion chamber. It can readily be seen that while the geometric compression ratio is a simple measure of two simply-obtained volumes, the *effective* compression ratio of the engine is actually a function of IVC timing and the pressure in the chamber at that

point in the cycle. Furthermore, the pressure itself is in turn a function of the degree of throttling applied to the engine to reduce the load it produces. Thus at part-load conditions the engine operates at a low effective compression ratio, to the detriment of thermodynamic efficiency. This is returned to below. (Note that the expansion ratio of the engine is similarly affected by the exhaust valve timing after the combustion event. Exhaust valve timing is affected by the need to discharge sufficient mass from the cylinder under residual pressure before positive scavenging later in the cycle. This is described in Section 1.4.5.)

1.4.3 Combustion

At a pre-determined time in the cycle the compressed charge is ignited by a spark and proceeds to burn. Since the Otto cycle is referred to as a 'constant volume' combustion cycle, ideally (from an ideal thermodynamic point of view) this would occur instantaneously at TDC. However, since it takes a finite period of time for the combustion event to occur, combustion necessarily straddles TDC 'Firing' by being initiated during the end of piston stroke associated with compression and ending during the piston stroke likewise associated with expansion. This causes the event to appear to be curved on an indicator diagram, as shown in Figure 1.3.

Combustion itself is a complicated process during which what is ideally a deflagatory flame sweeps across the combustion chamber completely consuming the charge in the process. This combustion event releases the chemical energy of the charge which causes the gas temperature to rise, and hence in an enclosed volume the pressure to increase and the piston to be forced towards bottom dead centre, turning the crankshaft via the connecting rod and producing power. There is, however, great danger in that the process of combustion will not proceed in an ideal manner, and an uncontrolled autoignition event (e.g. knock) can occur instead. This can be damaging to both the engine's structure and its efficiency.

The earlier combustion is initiated the greater the pressure build up while the piston is still rising during the end of the compression stroke and hence the greater the amount of negative work done. Additionally, the pressure and hence temperature of the burning charge will build up faster with further advance, which heats the last portion of charge to burn in the cycle, and can cause it to autoignite. This last portion is known as the 'end gas'. An ideal fuel would, therefore, be one of high resistance to autoignition and with a fast flame speed, minimizing negative work and allowing greater freedom in setting optimum ignition timing to best phase the combustion event to obtain the best possible thermal efficiency. Note that in addition to having higher octane numbers than gasoline fuels, alcohols have a high adiabatic flame speed. This adds to the ability of alcohol fuels to realize higher thermal efficiency than gasoline blends.

The timing of spark initiation is one of the major factors in whether autoignition occurs or not, as well as having a significant effect on engine fuel energy conversion efficiency through its influence on the position of peak cylinder pressure during the cycle. These factors are inter-dependent, as will be discussed further in the literature review in Chapter 3.

1.4.4 Expansion

Practically, the expansion phase is the only part of the cycle that produces useful work. This is because positive work results only when the piston is descending with a positive pressure differential across it, or rising with a negative pressure differential. Negative work results when the opposite occurs. Thermal losses to the wall cause a reduction in efficiency during the expansion phase.

If the engine is at an idle condition, then the work released during the expansion stroke is balanced exactly by the parasitic losses of friction and pumping (including throttling losses). Expansion ends shortly after the exhaust valve opens near BDC and the gas pressure in the cylinder has fallen to that of the exhaust system back pressure. The period between exhaust valve opening (EVO) and the gas in the cylinder achieving this pressure is called 'blowdown'.

1.4.5 Exhaust

The burned gas is physically expelled during the exhaust phase. A proportion of the burned gas exits the cylinder during the 'blowdown' period, when the residual pressure of the expanded gases is used to force a proportion of it from the cylinder. This ensures that the pressure that the piston has to work against during the following upstroke is reduced to exhaust back pressure so that less pumping work has to be performed by the piston during the upwards exhaust stroke. If the exhaust ducts and system are too restrictive, the engine has to work against the restriction during the upward exhaust stroke, and this again results in increased negative work.

Despite what was stated in Section 1.4.4, note that a small amount of useful work can still be extracted from the gas during the blowdown phase even after the closed-valve expansion phase has ceased. This occurs only if the exhaust back pressure is higher than crankcase pressure, since this still results in a positive pressure on the piston while it is still moving downwards. In reality, the amount of work it is possible to obtain in this manner is extremely small in Otto cycle engines, since the pressure differential across the piston is low, although it can be significant in highly turbocharged diesel engines.

Following the exhaust phase the cycle begins again. A final point of importance is that, if not all of the burnt gas is scavenged from the cylinder, some residuals will be left to mix with the incoming fresh charge. While some of these may be radical species which are still chemically active, they also cause heat energy to be transferred to the fresh charge, and can form exothermic centres in their own right. The trapping of residuals has two effects: firstly the volumetric efficiency, defined here as

$$\eta_{\text{vol}} = \frac{m_{\text{trapped}}}{m_{\text{manifold}}} \qquad \text{Eqn 1.3}$$

where η_{vol} is the volumetric efficiency, m_{trapped} is the mass of charge trapped inside the cylinder and m_{manifold} is the mass of air equivalent to the swept volume of the cylinder at intake manifold conditions, reduces¹, and secondly the temperature of the charge during the cycle is higher. This latter effect has a significant bearing on knock, as will be discussed in Chapter 3.

1.4.6 Otto cycle mean effective pressures and air standard cycle efficiency

The Otto cycle comprises therefore two pressure-volume 'loops'. The first is the high-pressure loop associated with compression, combustion and expansion, and is also termed the working loop. The work of this loop is characterised by the indicated mean effective pressure (IMEP) which is defined as the equivalent pressure which, when acting on a single stroke of the piston, performs the same work as the working loop. The second loop is that associated with the gas exchange phases of exhaust and induction, and is termed the pumping loop. Similarly, it has a pumping mean effective pressure (PMEP) associated with it. The net work of the cycle is defined as the positive work minus the pumping work, such that when PMEP is subtracted from IMEP the net mean effective pressure (NMEP) is obtained. When friction, in the form of friction mean effective pressure (FMEP), is subtracted from this result one obtains the useful work at the crankshaft, as measured on the engine dynamometer or 'brake'. This is the brake mean effective pressure (BMEP). Therefore,

$$\text{BMEP} = \text{IMEP} - \text{PMEP} - \text{FMEP}. \quad \text{Eqn 1.4}$$

Pumping work itself comprises all of the work done by the engine overcoming gas friction during the charging and exhaust processes and also the work done during the throttling process.

The cycle shown in Figure 1.3 is at a part-load condition, with the areas of the working and pumping loops shown being nearly equal. This signifies that the

¹ Note that despite its name, volumetric efficiency is actually the ratio of masses.

engine will be producing little useful work, and nearly all of the work produced during the working loop is absorbed in pumping work. Conversely, at full load, the working loop is large and the pumping loop is small, which is because there is no throttling occurring (the engine is at the wide-open throttle, or WOT, condition). Hence the net work of the engine will be much higher, and there are minimal gas exchange losses at full load.

Therefore, throttling losses are very significant at part load (Ricardo and Hempson, 1968 and Heywood, 1988), and it can be said that this characteristic of the Otto cycle does not truly suit real world usage in a passenger vehicle. This is because as the load on the engine is reduced, its parasitic losses rise significantly. Note that this unfortunate characteristic of the Otto cycle is not shared by the 2-stroke cycle in which there are no distinct intake and exhaust strokes and therefore no throttling losses specifically associated with them. The work associated with the scavenging process in the 2-stroke engine instead manifests itself as frictional loss (Ricardo and Hempson, 1968 and Nahum *et al.*, 1994).

Much of the work currently being undertaken to improve the fuel consumption of Otto cycle 4-stroke-engine-equipped vehicles on drive cycles is focussed on reducing the impact of throttling losses at part load (Schausberger *et al.*, 2001, Kiefer *et al.*, 2004 and Turner *et al.*, 2005b). One means to achieve this is to reduce the swept volume of the engine in conjunction with pressure charging it to maintain installed engine power. This is commonly referred to as 'downsizing' and will be discussed in the following chapter. Since such engines will still be operated at part load conditions, downsizing still needs to be achieved while maintaining the highest possible compression ratio, since the ideal Otto Cycle Efficiency is related to compression ratio such that

$$\eta_{\text{ideal}} = 1 - \frac{1}{r^{\gamma-1}}$$

Eqn 1.5

where η_{ideal} is the ideal cycle efficiency, r is the geometric compression ratio and γ is the ratio of specific heats of the working fluid. This relationship is shown graphically in Figure 1.4.

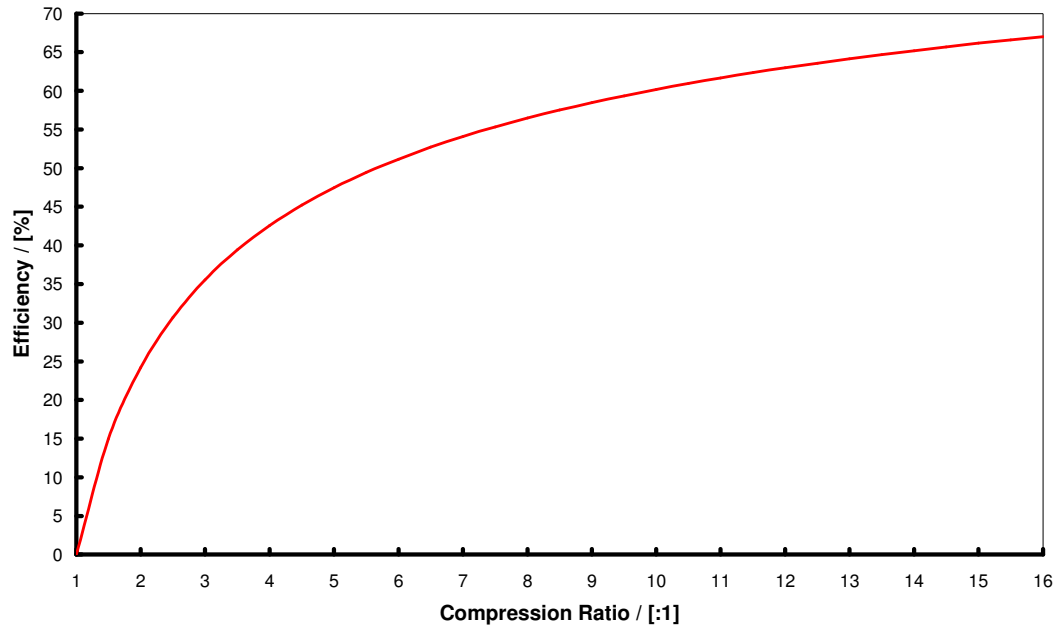


Fig. 1.4: Air standard cycle efficiency for Otto cycle versus compression ratio

As mentioned in Section 1.4.1, in conventional SI engines, throttling reduces the mass of charge that flows into the engine and is therefore used to control the load it produces. The load has to be controlled in this manner because, in a spark-ignition combustion system, a deflagrating flame is used to burn the mixture throughout the chamber, and such a flame can only be supported by a narrow range of air-fuel ratios near to the stoichiometric, or chemically-correct, value (Griffiths and Barnard, 1995, Heywood, 1988). Throttling also reduces the effective compression ratio that the engine operates at, since at lighter loads it takes further into the compression stroke to exceed atmospheric pressure, which can be taken as the point from which effective compression starts. Figure 1.4 shows that any reduction in the compression ratio of an engine causes an exponential decrease in the ideal cycle efficiency.

Two things become apparent as a result. Firstly, it is important to maintain as high a compression ratio as possible at full load in order to start from as high a value of efficiency as possible when the engine is throttled. Secondly, a variable compression ratio mechanism would yield significant benefits for Otto cycle engines. This has been shown to be the case in practice where the increase in geometric compression ratio at part load, coupled with the increased downsizing offered by the ability to reduce compression ratio under highly pressure-charged conditions, has improved drive cycle fuel economy by ~30% (Drangel and Bergsten, 2000, Schwaderlapp *et al.*, 2002 and Roberts, 2003). This subject will be returned to in Chapter 2.

Finally, it should be noted that only improvements to the engine operating map, and not vehicle mass reduction or aerodynamic improvements, give *pro-rata* benefits with regard to in-vehicle fuel consumption improvements (Wurms *et al.*, 2003). This is because the effect of vehicle mass on fuel economy manifests itself only under acceleration and similarly aerodynamic and rolling resistance effects assume greater importance only as vehicle speed is increased. For these reasons, engine researchers and developers continue to be primarily responsible for reductions in road vehicle fuel consumption and hence CO₂ emissions.

1.5 OBJECTIVE OF THIS RESEARCH

The objective of this research was to investigate the knock limit of gasoline engines and how this can be improved by using the characteristics of the fuel and the architecture of the engine. The 'knock limit' is that amount of ignition advance that the engine will tolerate beyond which unacceptable knocking combustion is generated. This can be affected by a variety of means, some of which are inherent in the architecture of an engine and some of which require modification of the charge itself, e.g. its temperature, an improvement in some characteristic of the fuel, or the use of a diluent to influence its temperature- and pressure-history in the period prior to combustion. In investigating these factors the research presented in this thesis will help to yield a fuller understanding of the

potential routes to optimization of pressure-charged spark-ignition engines. This in turn will enable a better understanding by engine designers and developers of the importance of, and merit in, pursuing more effective architectures and subsystems in such engines. The end result will enable the compression ratio of newly-designed pressure-charged SI engines to be increased, to the benefit of reduced fuel consumption and CO₂ output in passenger vehicles.

Specifically, the primary tasks were to establish the following:

1. The potential benefit of targeted use of the latent heat of a fuel in a pressure-charged engine through its introduction before the pressure-charging device.
2. The relationship between charge air temperature and knock, when the density of the charge air and the air-fuel ratio are held constant.
3. The benefit of employing a new engine architecture which separates the exhaust pulses in a turbocharged engine and which utilizes a cooled exhaust manifold, integrated into the cylinder head. This will ensure that the minimal amount of hot residual is trapped in the cylinder to cause a reduction in combustion efficiency and the need for component thermal-protection over-fuelling.
4. To gauge the benefit of the approach outlined in point 3 by operating the engine with competing fuel-consumption-improvement technologies and gauging their effect versus the baseline.

1.6 THESIS OVERVIEW

This first chapter has discussed the use and importance of gasoline as a fuel for passenger car transportation to society. The requirement to reduce the CO₂ emissions from such vehicles has also been reviewed, particularly with respect to the reported threat of climate change. The characteristics of gasoline and its

development alongside the engines it powers has also been mentioned. The important characteristics of the Otto cycle have been discussed and the effects on fuel economy of throttling a 4-stroke spark-ignition engine to bring about its operation at part load have been briefly described. The overall objective of the research has been stated and its importance to future CO₂ reduction explained.

Chapter 2 discusses in greater detail the pressure charging of gasoline engines, including methods for achieving this, and its importance with respect to improving the fuel economy of spark-ignition engines in the future. This approach is also discussed in the context of other competing fuel consumption reduction technologies for gasoline engines. The phenomenon of gasoline combustion knock is further discussed.

Chapter 3 reviews work on knocking combustion reported in the literature.

Chapter 4 describes work by the author in the area of knock limit extension of spark-ignition engines. This includes the development of a research programme to investigate 'turboexpansion', a charging system to over-cool charge air with respect to what can be achieved with a simple chargecooler system. The results from this work are reviewed and the requirements for the subsequent work put into context.

Chapter 5 describes an experimental investigation into the use of fuel properties to improve the efficiency of a pressure-charged engine, where the latent heat of vaporization of a high-blend alcohol-based fuel is used to cool the charge air before its induction into the charging system. The benefit of this is quantified through a systematic approach to varying the proportion of the total fuel mass introduced in this manner.

Chapter 6 describes the design of a new single-cylinder research engine and its use, together with a newly-specified charge air conditioning rig, to investigate the interaction between charge air temperature and the knock limit when using port

fuel injection. The use of modelling to assist in the specification of the intake and exhaust systems of this engine is also described.

Chapter 7 describes the design of a new direct-injection 3-cylinder downsized engine based on the cylinder geometry developed for the single-cylinder engine described in Chapter 6. The performance of this engine is compared in detail with competing approaches to increase the knock limit. It is shown that engine architecture itself can be used to improve high-load fuel economy to a level where these competing technologies are not required, for the same level of engine performance.

Chapter 8 presents results from operating the 3-cylinder engine described in Chapter 7 with some of the competing technologies, and it is shown that the magnitude of the improvement possible is significantly lower than that which they give on less-optimized engines. This reinforces the original benefit of a synergistic approach to engine configuration.

Chapter 9 presents conclusions from this work and details some potential areas for future research.

1.7 CONTRIBUTIONS TO THE BODY OF KNOWLEDGE FROM THE WORK PRESENTED IN THIS THESIS

The research work presented in this thesis has led to a greater understanding of the value of developing more effective architectures and subsystems for Otto cycle engines. Specifically the major findings are:

1. Within the limits tested here, at fixed charge air density the relationship between knock-limited spark advance and air temperature is linear. The approach of fixing density has not been seen anywhere else in the literature and is believed to be unique, with particularly important ramifications for the design of future charging systems.

2. Through a combination of an optimized direct-injection combustion system, an exhaust manifold integrated into the cylinder head and a 3-cylinder configuration, an engine with extremely high full-load thermal efficiency can be created. This is because these characteristics are all synergistic. The high-load efficiency of this configuration is such that its brake specific fuel consumption at maximum power is better than has been demonstrated in the literature for other practical, self-contained engines with efficiency-enhancing technologies.
3. When used on such an engine, competing technologies such as excess air operation and the use of cooled EGR offer little improvement. While in such an engine the use of cooled EGR *will* increase efficiency, it is at the cost of some significant extra practical complications. The benefit seen was far from the level reported by other researchers utilizing more compromised engine concepts for their research.
4. When operating a pressure-charged engine on alcohol fuels, the latent heat of vaporization can be utilized in reducing supercharger (or compressor) outlet temperatures through the use of pre-compressor fuel injection. There is a clearly-defined amount of fuel beyond which there is no benefit in introducing more fuel at the entry to the supercharger, at least in terms of charge temperature reduction. Control strategies to reduce the amount and occurrence of pre-compressor injection based on alcohol content and throttle position can readily be created with modern electronic engine management systems.
5. Alternatively the latent heat of the fuel can also be used beneficially in engines employing cooled EGR by injecting a proportion of the fuel charge directly into the EGR gas to evaporatively cool it. This helps to reduce the amount of physical cooling that has to be performed which reduces the extra thermal load which cooled EGR puts onto the vehicle cooling system.

1.8 LITERATURE ARISING FROM WORK UNDERTAKEN FOR THIS THESIS

One book chapter and several technical papers have been written as a result of work undertaken as part of this research. The more significant and peer-reviewed ones are listed below.

1.8.1 Book chapter written as lead author

1. Turner, J.W.G. and Pearson, R.J., "The turbocharged direct-injection spark-ignition engine", in Zhao. H. (ed.), Direct injection combustion engines for automotive applications: Science and technology. Part 1: Spark-ignition engines, Woodhead Publishing Limited, Cambridge CB21 6AH, UK, 2009, ISBN 1-84569-389-2.

1.8.2 Conference papers written as lead author

1. Turner, J.W.G., Pearson, R.J., Bassett, M.D. and Oscarsson, J., "Performance and Fuel Economy Enhancement of Pressure Charged SI Engines through Turboexpansion – An Initial Study", SAE paper number 2003-01-0401 and SAE 2003 Transactions, June 2004.
2. Turner, J.W.G., Pearson, R.J., Bassett, M.D., Blundell, D.W. and Taitt, D.W., "The Turboexpansion Concept - Initial Dynamometer Results", SAE paper number 2005-01-1853.
3. Turner, J.W.G., Pitcher, G., Burke, P., Garner, C.P., Wigley, G., Stansfield, P., Nuglisch, H., Ladommatos, N., Patel, R. and Williams, P., "The HOTFIRE Homogeneous GDI and Fully Variable Valve Train Project - An Initial Report", SAE paper number 2006-01-1260.
4. Turner, J.W.G., Kalafatis, A. and Atkins, C., "The Design of the NOMAD Advanced Concepts Research Engine", SAE paper number 2006-01-0193.

5. Turner, J.W.G., Pearson, R.J., Milovanovic, N. and Taitt, D., "Extending the knock limit of a turbocharged gasoline engine via turboexpansion", 8th I.Mech.E. Conference on Turbochargers and Turbocharging, London, May 2006.
6. Turner, J.W.G., Pearson, R.J. and Milovanovic, N., "Reducing the Octane Appetite of Pressure-Charged Gasoline Engines using Charge Air Conditioning Systems", JSAE paper number 20065414, Yokohama, Japan, May 2006 and JSAE Transactions No. 3-06, pp.11-16.
7. Turner, J.W.G., Pearson, R.J., Holland, B. and Peck, B., "Alcohol-Based Fuels in High Performance Engines", SAE paper number 2007-01-0056, SAE Fuels and Emissions Conference, Cape Town, South Africa, January 2007.
8. Turner, J.W.G., Peck, B. and Pearson, R.J., "Flex-Fuel Vehicle Development to Promote Synthetic Alcohols as the Basis of a Potential Negative-CO₂ Energy Economy", SAE paper number 2007-01-3618, 14th Asia-Pacific Automotive Engineering Conference, Los Angeles, California, USA, August 2007.
9. Turner, J.W.G., Coltman, D., Curtis, R., Blake, D., Holland, B., Pearson, R.J., Arden., A. and Nuglisch, H., "Sabre: A Direct Injection 3-Cylinder Engine with Close-Spaced Direct Injection, Swirl-Enhanced Combustion and Complementary Technologies", JSAE paper number 20085014 and JSAE 2008 Proceedings No. 79-08, pp.5-10, ISSN 0919-1364, JSAE 2008 Congress, Yokohama, Japan, 21st-23rd May 2008.
10. Turner, J.W.G., Pearson, R.J., Curtis, R. and Holland B., "Improving Fuel Economy in a Turbocharged DISI Engine Already Employing Integrated Exhaust Manifold Technology and Variable Valve Timing", SAE paper

number 2008-01-2449, SAE International Powertrain Fuels and Lubricants Meeting, Rosemont, Illinois, USA, October 2008.

11. Turner, J.W.G., Pearson, R.J., Curtis, R. and Holland B., "Effects of Cooled EGR Routing on a Second-Generation DISI Turbocharged Engine employing an Integrated Exhaust Manifold", SAE paper number 2009-01-1487, SAE 2009 World Congress, Detroit, Michigan, USA, April 2009.
12. Turner, J.W.G., Pearson, R.J., Purvis, R., Dekker, E., Johansson, K. and Bergström, K. ac, "GEM Ternary Blends: Removing the Biomass Limit by using Iso-Stoichiometric mixtures of Gasoline, Ethanol and Methanol", SAE paper number 2011-24-0113, The 10th International Conference on Engines and Vehicles, Capri, Naples, Italy, 11th-16th September, 2011.

1.8.3 Conference papers written as co-author

1. Stansfield, P.A., Wigley, G., Garner, C.P., Patel, R., Ladommatos, N., Pitcher, G., Turner, J.W.G., Nuglisch, H. and Helie, J., "Unthrottled Engine Operation using Variable Valve Actuation: The Impact on the Flow Field, Mixing and Combustion", SAE paper number 2007-01-1414, SAE 2007 World Congress, Detroit, Michigan, USA, April 2007.
2. Coltman, D., Turner, J.W.G., Curtis, R., Blake, D., Holland, B., Pearson, R.J., Arden., A. and Nuglisch, H., "Project Sabre: A Close-Spaced Direct Injection 3-Cylinder Engine with Synergistic Technologies to achieve Low CO₂ Output", SAE paper number 2008-01-0138, SAE 2008 World Congress, Detroit, Michigan, USA, April 2008.
3. Pearson, R.J., Turner, J.W.G. and Peck, A.J., " Gasoline-ethanol-methanol tri-fuel vehicle development and its role in expediting sustainable organic fuels for transport", 2009 I.Mech.E. Low Carbon Vehicles Conference, London, UK, 20th-21st May, 2009.

4. Pearson, R.J. Turner, J.W.G., Eisaman, M.D. and Littau, K.A., "Extending the Supply of Alcohol Fuels for Energy Security and Carbon Reduction", SAE paper number 2009-01-2764, SAE Powertrain, Fuels and Lubricants Meeting, San Antonio, Texas, USA, 2nd-4th November, 2009.

1.8.4 Journal papers written as co-author

1. Taitt, D.W., Garner, C.P., Swain, E., Pearson, R.J., Bassett, M.D., and Turner, J.W.G., "An Automotive Engine Charge-Air Intake Conditioner System: 1st Law Thermodynamic Analysis of Performance Characteristics", Proc. Instn Mech. Engrs Journal of Automotive Engineering, Vol. 219, Part D, no. 6, pp. 389-404, 2005.
2. Taitt, D.W., Garner, C.P., Swain, E., Blundell, D., Pearson, R.J. and Turner, J.W.G., "An Automotive Engine Charge-Air Intake Conditioner System: Analysis of Fuel Economy Benefits in a Gasoline Engine Application", Proc. Instn Mech. Engrs Journal of Automotive Engineering, Vol. 220, Part D, no. 9, pp. 1293-1307, 2006, ISSN: 0954-4070.

1.9 SUMMARY AND CONCLUDING REMARKS

This chapter has discussed the symbiotic reasons for the development of both gasoline fuel and spark-ignition internal combustion engines, and how both are the result of mankind's desire for mobility. The coincidence of the near-simultaneous creation of gasoline (as a by-product of kerosene refining) and the Otto cycle engine with which it would become synonymous has ultimately resulted in a well-developed system. The system must be further refined in the future in order to reduce the rate at which CO₂ is released into the atmosphere. This is to help avoid climate change on such a scale that catastrophic results might ensue for planet Earth's ecosystem.

The need to address the parasitic losses which increase CO₂ production in real-world engine operation leads to the desire to reduce throttling losses in 4-stroke

Otto cycle engines. In order to do this, various technologies have been proposed, with engine downsizing and pressure charging emerging as a near-term direction for the development of the Otto cycle engine.

The chapter has also described various contributions to knowledge gained as a result of undertaking this research, and listed some papers which have arisen as a result of it.

The next chapter will review downsizing technology in more detail and will also discuss how it relates to others being developed to reduce the fuel consumption and CO₂ output of spark-ignition-engined passenger vehicles.

Chapter 2: Pressure Charging and Engine Downsizing to improve Vehicle Fuel Consumption

This chapter will discuss engine downsizing and the various types of pressure charging device commonly used to achieve it. The advantages and disadvantages of these devices will be discussed and some of the means of combining them to the benefit of overall system efficiency described. The use of downsizing to improve vehicle fuel economy is then discussed together with some of the challenges which must be overcome in employing the technique. Finally some of the advanced means of improving the knock resistance of downsized engines are discussed before a description of one of the more likely future formats of such engines is made.

'Downsizing' is an attempt to shift the operating points of an Otto cycle engine, when following the road load of the vehicle, to a regime with greater thermal efficiency than is the case with conventional engine operation. This is because, as discussed in Chapter 1, normal part-load operation of a 4-stroke SI engine results in throttling losses which cause a significant part of the fuel consumption of a road vehicle under real-world conditions.

Downsizing can only be achieved to a small degree using conventional naturally-aspirated (NA) engine tuning techniques. It is more normal to use intake pressure charging techniques. The purpose of the pressure charging system is to increase air flow such that the installed power of the engine can be maintained despite the reduction in swept volume. Downsizing, therefore, results in an increase in engine specific power output. This is so that vehicle performance is not impaired through the reduction in engine swept volume. For any given road load, a downsized engine requires less throttling, and therefore its pumping losses are reduced as discussed in Chapter 1. Downsizing is only one of several potential techniques being developed for the near future (Walzer, 2001 and Turner *et al.*, 2005b), but is currently of great interest to the world's automotive manufacturers.

The intention of any form of pressure charging is to raise intake charge-air density above the prevailing atmospheric conditions so that more air mass is delivered to the cylinder, and hence more fuel can be injected and burnt by the engine (Kemble, 1921a, Hooker *et al.*, 1941, Ricardo and Hempson, 1968, Mezger, 1978, Watson and Janota, 1986 and Richter and Hemmerlein, 1990). This is done in a separate compression stage before the combustion engine. The engine is thus given a 'boost' by the charging system and this is the term given to the increase in pressure forced on the engine intake port by the charging system. Hence 'forced induction' is another phrase often used to denote the concept.

Compression of the charge air is normally performed either by a blower or compressor (known as a 'supercharger') that is either mechanically-driven by the crankshaft of the engine or driven by an exhaust gas turbine (in which case it is known as a 'turbosupercharger' or more commonly a 'turbocharger'). Other devices, such as the pressure-wave supercharger, also exist (Allard, 1982 and Guzzella *et al.*, 2000). Occasionally, a compound charging system employing more than one compressor is used with the intention to offset the disadvantages of one of the pressure-charging devices by building on the advantages of the other. For SI engines, this has been performed by a combination of a positive displacement supercharger and a turbocharger (Robson, 1986, Middendorf *et al.*, 2005 and Krebs *et al.* 2005a and 2005b), by an axial-flow aerodynamic compressor and a turbocharger (Doble, 1987) and also by a high-pressure and low-pressure turbocharger in series (Sauerstein *et al.*, 2010). All of these various pressure charging methods will be discussed in the following sub-sections.

2.1 SUPERCHARGING

Sir Dugald Clerk has been credited as being the first person to investigate the concept of supercharging a combustion engine when he applied pressurized air to an engine in 1901 (Allard, 1982). While some early racing cars employed supercharging, it was first widely used as a means of increasing power in aircraft

engines both for take-off and at higher altitudes (Kemble, 1921a, Hooker, 2002, Gunston, 1995 and Whitworth, 2000), although in tandem with this the development of the variable pitch propeller was necessary in order to allow that power to be used efficiently both at take-off and under cruise conditions (Kemble, 1921b).

In a supercharged engine, the engine drives an air pump (the supercharger) which forces charge air into the engine over and above what can be achieved with natural aspiration from the atmosphere. This allows more fuel to be injected and more charge to be burnt per unit time than is the case if the engine is naturally aspirated. The term 'supercharged' was therefore created. A schematic of a typical supercharged engine layout is shown in Figure 2.1.

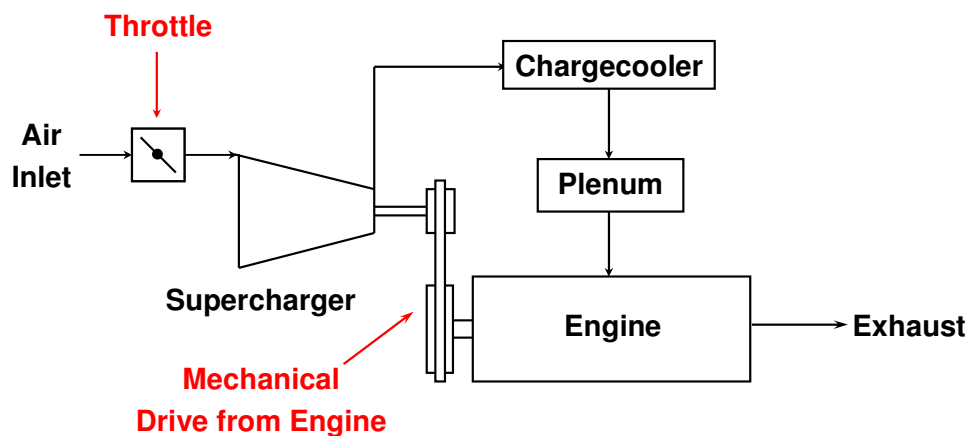


Fig. 2.1: Schematic of the layout of a supercharged engine. Arrows depict flow of charge through engine

In Figure 2.1 the drive system from the engine is shown schematically as a belt drive (as is normally the case with automotive engines), although in aero and racing engines the drive is conventionally by gears and/or shafts to improve reliability. Unsurprisingly, the racing world was very quick to see the potential in supercharging technology and between the First and Second World Wars many supercharged racing engines were built (Ludvigsen, 2001).

In Figure 2.1 a 'chargecooler' is also shown between the supercharger and engine. This reduces the charge air temperature, thus simultaneously increasing power through a combination of both the increased charge air density (thus increasing the mass air flow through the engine) and the increased knock resistance during combustion afforded by the lower charge temperature. This subject will be returned to later in Chapter 3. Chargecoolers are also variously termed 'intercoolers' or 'aftercoolers'.

Superchargers function as compressors to pressurize the charge air. Unless the compression is isothermal the compression process usually leads to an increase in the charge air temperature. The required power input is defined by

$$\dot{W}_c = \dot{m}(h_2 - h_1) = \dot{m}c_p(T_2 - T_1) \quad \text{Eqn 2.1}$$

where \dot{W}_c is the power consumption of the compressor, \dot{m} is the mass flow through it, c_p is the specific heat capacity at constant pressure of the working fluid, h denotes specific enthalpy, T denotes temperature, and the subscripts 1 and 2 are the inlet and outlet conditions, respectively. The adiabatic outlet temperature of the compressor is a function of the pressure ratio that it is working across, such that

$$T_2' = T_1 \left(\frac{p_2}{p_1} \right)^{\left(\frac{\gamma-1}{\gamma} \right)} \quad \text{Eqn 2.2}$$

where T_2' is the adiabatic outlet temperature, p_1 and p_2 are the inlet and outlet pressures, respectively, and γ is the ratio of specific heat capacities of the working fluid. The actual outlet temperature T_2 is related to the adiabatic outlet temperature T_2' by

$$\eta_{\text{adiabatic}} = \frac{T_2' - T_1}{T_2 - T_1} \quad \text{Eqn 2.3}$$

where $\eta_{\text{adiabatic}}$ is the adiabatic efficiency of the compressor, as measured on a test stand and including bearing friction.

For all practical applications, the major factor affecting the temperature increase due to compression is the pressure ratio that the compressor is working across. Its adiabatic efficiency, while very significant, is generally of lesser importance. Therefore, minimizing the amount of boost pressure necessary to reach the performance desired in a supercharged engine is one of the most important factors in reducing supercharger power consumption. This, in turn, is important because this power has to be wholly supplied by the engine crankshaft. A chargecooler contributes to minimizing supercharger power consumption because (at conditions of equal supercharger mass airflow) it contributes to the increase in charge density at the engine by rejecting heat at constant pressure and therefore reducing the amount of boost pressure required. (This, of course, neglects skin friction in the chargecooler and hence any pressure drop across it.) The subject of the effectiveness of chargecoolers will be returned to later.

It should be noted that some of the work done on the charge air is recovered directly by the engine in pneumatic form during the intake stroke. In Section 1.4, the Otto Cycle was described and it was stated that positive work results if there is a positive pressure differential across the piston from the working volume to its underside and the piston itself is moving downwards. This is exactly the case in any pressure-charged engine working with a charge air pressure greater than that in the crankcase. Hence some pneumatic power is recovered, affected also by the charge air temperature (since mass flow and pressure both affect power). Indeed, Ricardo and Hempson (1968) state that, in highly boosted piston aero engines, this pneumatic work can approach 50% of the work performed on the charge air by the supercharger.

Superchargers themselves broadly fall into two types: 'positive displacement' and 'aerodynamic'. The two most common types of positive displacement supercharger are Roots blowers and screw compressors, while the aerodynamic types divide primarily into centrifugal- and axial-flow types. These will be discussed in the following sections.

2.1.1 Roots superchargers

This type of supercharger was originally patented in 1860 by Philander and Francis Roots as a machine to ventilate mine shafts (Turner and Pearson, 2009). In a Roots-type supercharger two rotors, typically with the same number of lobes, inter-mesh and draw air in on the suction side, trapping it in two volumes on the outside of the machine before transporting it around to the discharge side. The discharge is isolated from the intake by the rotors themselves. A partly-disassembled Roots supercharger is shown in Figure 2.2. It should be noted that compression of the air does not occur until the outlet port opens and the air is pushed by the rotors against the restriction caused by the engine itself. Thus a Roots supercharger does not perform any compression internally and as a consequence its adiabatic efficiency is lower than the types of supercharger that do, being typically 50-60% (Turner *et al.*, 2004c and Bonello *et al.*, 2005). This lack of any internal compression leads to the term 'blower' frequently being applied to this device, rather than 'compressor'.

A typical automotive Roots supercharger installation is represented by the General Motors 2.0 litre supercharged engine in Figure 2.3. The supercharger was manufactured by the Eaton Corporation. Here the drive to the device is by poly-Vee belt and incorporated into the front end accessory drive, with the supercharger drive pulley positioned in the belt run between the air conditioning compressor and the alternator. This application has a water-cooled chargecooler incorporated into the engine plenum chamber downstream of the supercharger itself, and so can be considered to be typical of the system shown schematically in Figure 2.1.

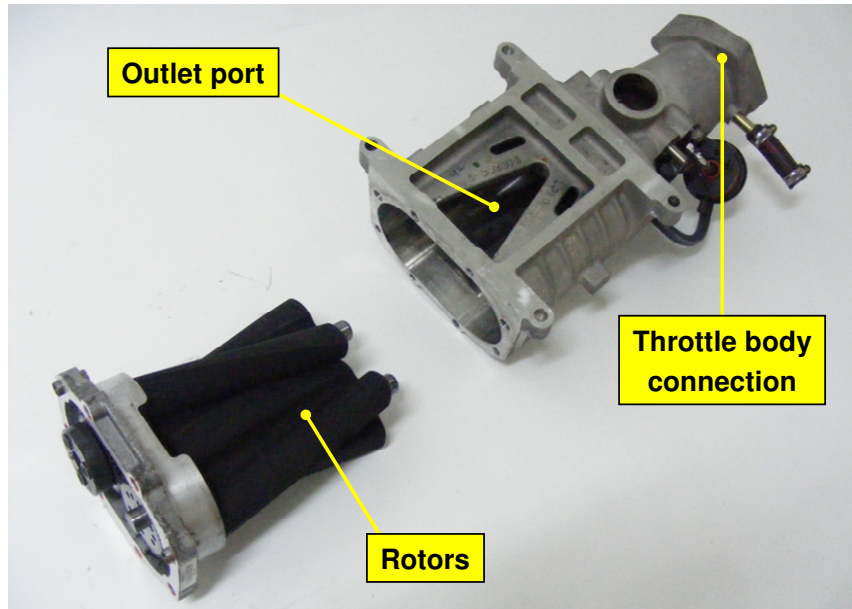


Fig. 2.2: Disassembled Roots supercharger manufactured by Eaton Corporation. Air flows in via the throttle body connection at top right and out from the rotors via the triangular discharge port. (Photograph courtesy Lotus Engineering)

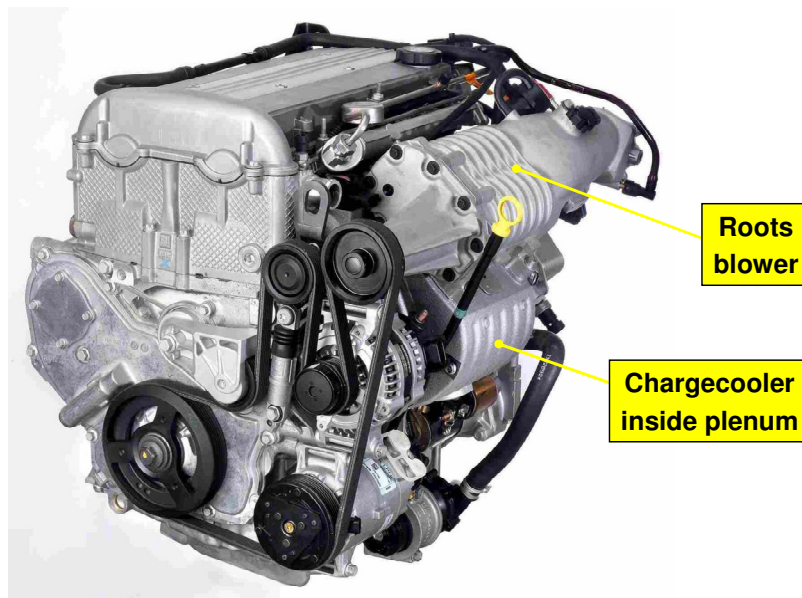


Fig. 2.3: General Motors 2.0 litre supercharged 4-cylinder engine using Roots blower manufactured by Eaton Corporation. This engine uses the supercharger shown in Fig. 2.2. (Photograph courtesy Lotus Engineering)

The Roots supercharger has for many years been applied to gasoline engines in both experimental and production forms (Kociba and Parr, 1991, Uthoff and Yakimow, 1987, Richter and Hemmerlein, 1990, Joyce, 1994, Joos *et al.*, 2000, Kato *et al.*, 1986, Overington and de Boer, 1984, Turner *et al.*, 2004c, Bonello *et al.*, 2005, Fitzen *et al.*, 2008 and Sandford *et al.*, 2009). It can therefore be considered both robust and commonplace.

2.1.2 Lysholm twin-screw superchargers

The other type of positive displacement supercharger commonly used in automotive engines is the Lysholm twin-screw type. This type of air compressor was first proposed and developed in the 1940s (Lysholm, 1942) and has been developed for both supercharger applications and for large scale compressor plant for air conditioning purposes (Carre, 1987 and Stosic *et al.*, 2003). It has some similarity to the Roots blower in that it employs two intermeshing rotors. Conventionally, these do not have the same number of lobes and are termed male and female rotors. Figure 2.4 shows the manner in which the two rotors mesh.

A Lysholm twin-screw compressor has broadly the same configuration and types of components as a Roots blower, although the principle of operation is quite different. As discussed above, in a Roots blower, air travels around the outside of the rotors, trapped by the rotor housing and both end plates. In a twin-screw compressor there are a male and a female rotor which, because they do not normally have the same number of lobes, do not rotate at the same speed. These draw air in axially and mesh together forming an air seal between them to provide part of the surface constraining the air. The rest of the surface is formed by the housing and one of the end plates. The air is thus trapped in what would appear to be a 'V'-shaped volume, if this volume was unwrapped from the rotors. This V-shaped volume reduces in size as the rotors rotate and the air is thus compressed internally against the end plate until the outlet port opens. From this point further compression can be carried out against a back pressure (i.e. the engine intake system in automotive applications). Importantly, since a proportion

of the compression is done internally, these devices have significantly higher adiabatic efficiency and hence also consume less power. This is because the amount of charge-air heating they perform is less, and thus, from Equation 2.1, for equivalent mass flow the power consumption reduces proportionately.

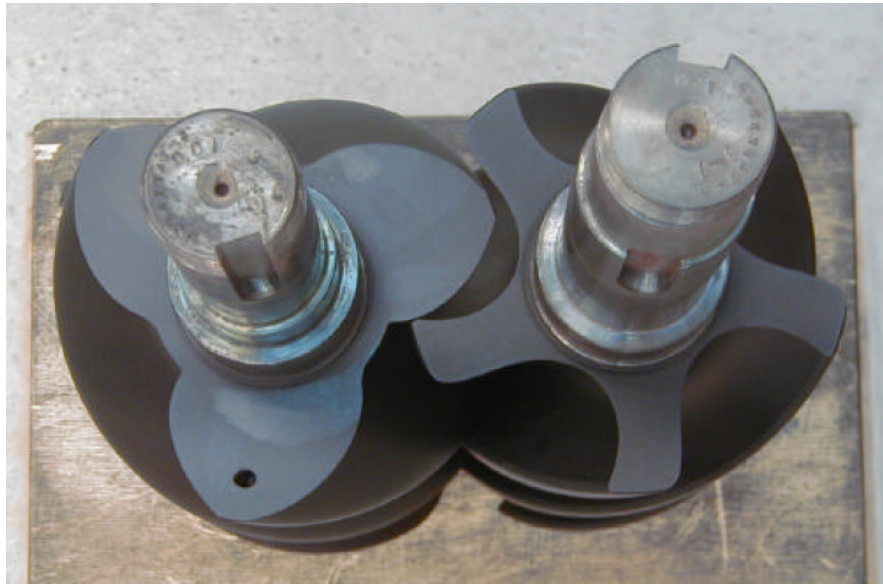


Fig. 2.4: Lysholm twin-screw compressor rotors, showing different mesh arrangement to a Roots blower. Three-lobe male rotor is to left, five-lobe female rotor to right. (Photograph courtesy of City University Centre for Positive Displacement Compressor Technology)

An example of a development engine fitted with a twin-screw compressor manufactured by Opcon AB is shown in Figure 2.5. This engine, reported by Turner and Pearson (2001), employed pre-compressor injection of part of the fuel mass in a 'wet compressor' application, to reduce charge-air heating without recourse to a chargecooler by exploiting the latent heat of vaporization of the fuel as beneficially as possible. This not only resulted in a lowering of charge air temperature and an increase in mass air flow rate, it also reduced the power necessary to drive the compressor. Such a technique has also been reported by Rosenkranz *et al.* (1986) in a turbocharged engine, and has been commonly used in aero engine and racing applications (Hooker *et al.*, 1941, Gunston, 1995,

Whitworth, 2000 and Ludvigsen, 2001). It is particularly beneficial with alcohol fuels, and the results of an investigation using such an approach are discussed later in Chapter 5. Water and methanol has also been introduced into the air stream in this manner to permit higher boost at aircraft take-off through extension of the knock limit (Hooker *et al.*, 1941 and Vandeman and Heinecke, 1945). As a blending agent (in an emulsion), Owen and Coley (1995) reported that water can increase the research octane number (RON) of gasoline by nearly 9 octane numbers, and they also state that separate injection of water into the charge air can have a significant effect in reducing the propensity of the charge to knock. They also discuss the attractiveness of methanol as a blending agent in gasoline in high performance applications. The importance of octane numbers with regard to combustion knock will be returned to in Chapter 3.



*Fig. 2.5: Development engine application of Opcon AB twin-screw compressor on Rover K-Series engine, employing pre-compressor injection in place of charge air cooling and described by Turner and Pearson (2001). The pre-compressor injectors are visible and positioned at the entry to the supercharger rotors.
(Photograph courtesy Lotus Engineering)*

Single-stage twin-screw compressors can have internal pressure ratios of up to 8:1 when oil-flooded operation is used, as is possible in air conditioning plant (Stosic *et al.*, 2003). However, flooding the compressor with oil to cool the device is not practical for automotive applications. The metallurgical limit of the rotors and housings restricts the internal pressure ratio to a maximum of ~2:1, because of the temperature rise of the air due to internal compression. This was the amount of internal compression used in the Lysholm twin-screw compressor employed by Saab in their variable compression 'SVC' engine, in which the outlet air temperature was limited to 185°C (Drangel and Bergsten, 2000).

Other advantages of screw compressors over Roots blowers include smaller size and lower mass for a given mass air flow capacity. These are both due to their higher operating speed, although a corollary of this is greater amounts of noise from the gears used to phase the rotors. Perhaps their biggest disadvantage is that during part load operation, because they possess internal compression, they always perform work on whatever air is passing through them, and therefore they consume power at part load. This in turn means that either a clutch and bypass or a decompression device is desirable, with the associated control challenge (Drangel and Bergsten, 2000). This operational disadvantage is not shared by the Roots blower, which, having no internal compression, does no work on the air passing through it and is thus arguably better suited to part-load operation in typical automotive applications.

2.1.3 Centrifugal compressors

The centrifugal compressor is a type of aerodynamic compressor. It typically operates at much higher speeds than positive-displacement types (Allard, 1982). Its best adiabatic efficiency can exceed 75%. In such a supercharger, air is compressed by centrifugal action in an impeller before being decelerated in a diffuser, which further increases its pressure. Approximately half of the compression work is done in each (Watson and Janota, 1986). However, due to the characteristic of increasing pressure ratio with increasing mass flow,

centrifugal superchargers with fixed-ratio drives from the engine crankshaft are more suited to aircraft use than automotive engines. This is because the delivery characteristics of such compressors closely match a propeller load line (Kemble, 1921a and 1921b, Whitford, 2000 and Hooker *et al.*, 1941). An example of this type of mechanically-driven compressor is shown fitted to the rear of a Rolls-Royce Merlin engine in the drawing in Figure 2.6. This particular type of engine had a two-stage supercharger and a water-cooled chargecooler. The two stages were on the same shaft and so can be considered to comprise a single unit.

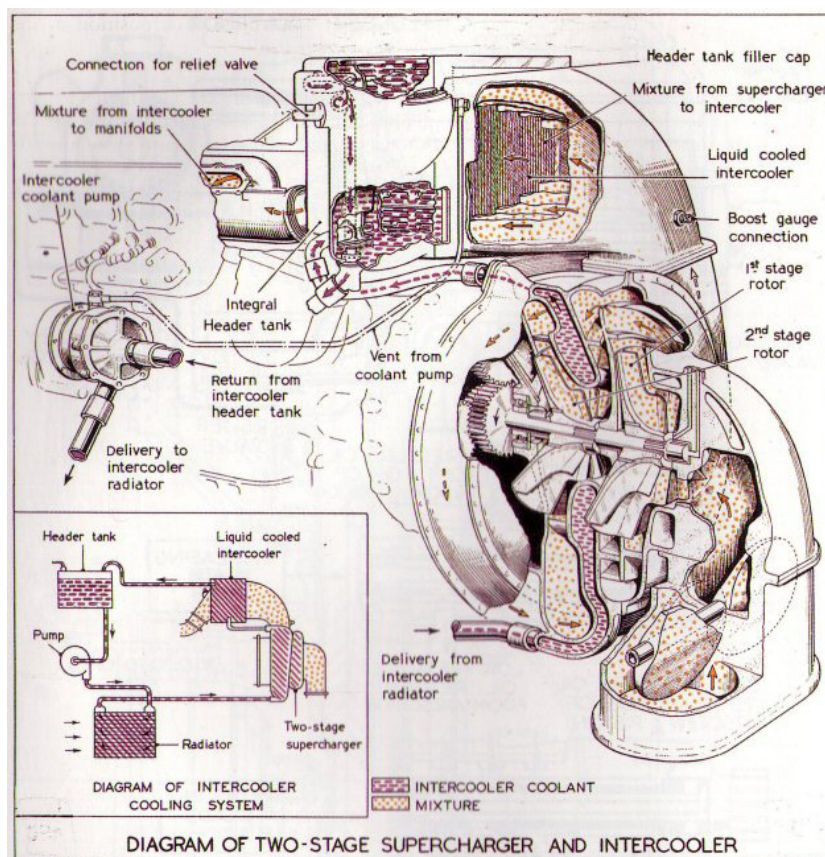


Fig. 2.6: Two-stage centrifugal supercharger as fitted to Rolls-Royce 60-series Merlin engines. Also note the use of a water-cooled chargecooler and throttle positioned before the supercharger entry. (Taken from Rubbra (1990), courtesy Rolls-Royce Heritage Trust)

In a conventional mechanically-driven centrifugal supercharger application the throttle is fitted before the compressor, as is visible in Figure 2.6. This is to avoid surge at part load. Because centrifugal compressors operate at high wheel tip speeds, in addition to having higher adiabatic efficiency than positive-displacement types, they can also be more compact. However, providing the necessary high drive ratio to the crankshaft is in itself a challenge and any gearing mechanism used to achieve this is often compounded, adding to mass and cost. In aero engines the supercharger is conventionally mounted to the rear end of the engine for aircraft aerodynamic reasons (a notable exception being the Daimler-Benz DB601 series, where it was mounted on the side (Gunston, 1995)), and could be large in diameter as a result, affording a simpler gearing arrangement. Greater air flow can also be achieved by using a double-sided impeller, and this system was used on some aero engine applications (Sheffield, 1944) where it also has the benefit of balancing axial thrust on the impeller wheel bearings. However, this is unlikely to be a practicable solution for automotive use because of the cost implications of a more complex impeller arrangement.

It is difficult to match the air flow characteristics of a centrifugal compressor operating at a fixed speed ratio to the crankshaft to the requirements of an automotive engine, although this has been achieved with some success in racing engines (Pomeroy, unknown date). Thus, the general delivery characteristics of centrifugal superchargers suggest that a variable-ratio drive, controllable dependent on engine load, would be desirable, particularly considering that all of the compression is performed internally within these devices. This promotes the same observation on drive cycle fuel economy as in the previous section on Lysholm twin-screw compressors. While the Daimler-Benz DB601 did employ a variable-speed drive mechanism (by slipping clutches (Gunston, 1995)), two-speed gearboxes have also been used (Sheffield, 1944 and Harvey-Bailey and Piggott, 1993) and electrical drive systems for such superchargers have also been developed (Pallotti *et al.*, 2003). However, the subject of the most common type of variable speed drive for aerodynamic compressors – the exhaust-gas-driven turbine – will be returned to in Section 2.2.

2.1.4 Axial-flow superchargers

The axial-flow compressor is commonplace in gas turbine engines, but, while its adiabatic efficiency can be higher than centrifugal types, its pressure ratio versus mass flow characteristic is generally even less well matched to the positive displacement swallowing requirements of the internal combustion engine. For this reason they have not found favour on automotive engines, although they have been developed and used both separately and in compound charging systems (Unknown Author, 1958 and Doble, 1987). They have been successfully applied to the Napier Nomad 2-stroke aircraft diesel engine, for which Sammons and Chatterton (1955) reported that a variable-ratio drive system was also used. A similar system was also specified on the Napier Deltic high-speed diesel engine for marine and rail traction (Chatterton, 1956). These last two engines will be briefly returned to under the subject of turbocompounding, below.

One type of spark-ignition engine application of an axial-flow supercharger is shown in Figure 2.7, the L9 research engine built by Lotus Engineering for the contemporary Formula 1 regulations in the mid-1980s. Doble (1987) described it as a compound-charged engine, with two different types of compressor in series. The axial compressor was the first stage of the charging system and is visible in Figure 2.7 on top of the engine with anti-surge throttles fitted in front of it. It was driven by a gear and shaft system at an input speed 4.685 times that of the crankshaft and discharged into two turbochargers in parallel (one for each bank of this V6 engine). The engine also used direct injection (DI). A schematic of the charging system layout used is shown in Figure 2.8.

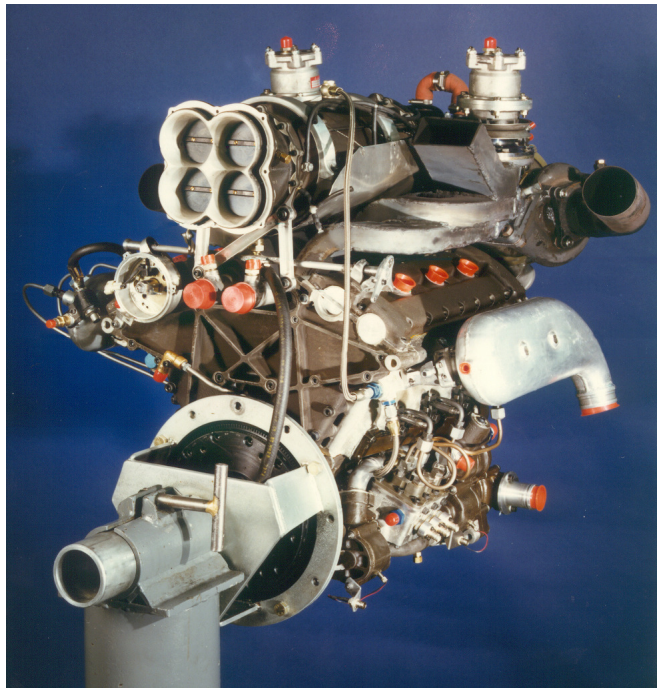


Fig. 2.7: L9 research Formula 1 racing engine built by Lotus Engineering, with axial-flow supercharger fitted to top of engine, described by Doble (1987).
(Photograph courtesy Lotus Engineering)

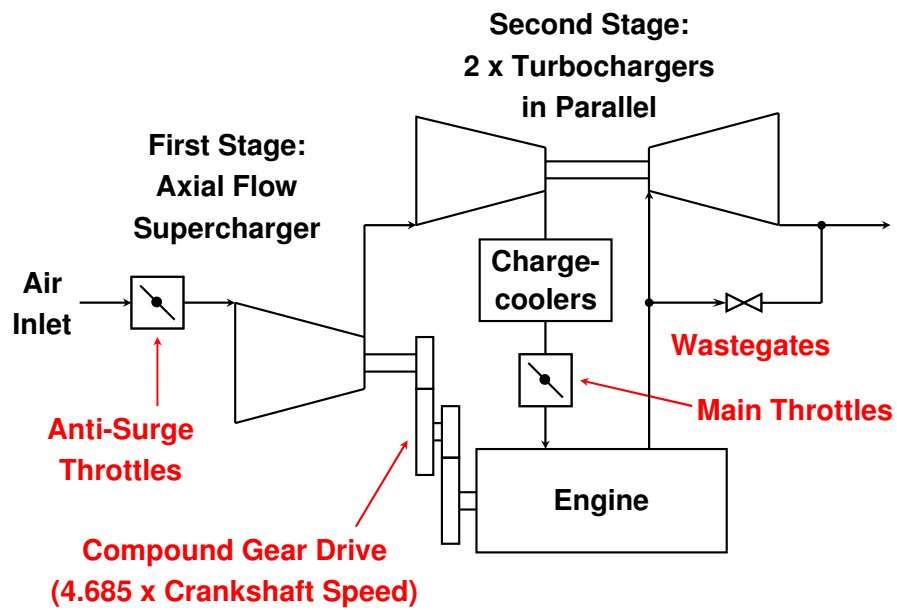


Fig. 2.8: L9 research Formula 1 racing engine charging system concept

The subject of compound charging will be returned to in Section 2.3, but in the specific case of axial-flow superchargers for automotive engines, their cost and highly specialized nature has meant that they have not found widespread popularity. The cost of the device is clear from the description of Doble (1987), who described the L9 supercharger itself as having six separate stages grouped onto two separate shafts, with inlet guide vanes in addition to the anti-surge throttles (main load control was performed by port throttles close to the intake valves). These two shafts operated at different speeds, the front at 90% of the rear, facilitated by cycloidal gearing provided between the shafts. In this case the fact that this compressor had a best adiabatic efficiency of 83% was seen as worthwhile versus the 75% a (much simpler) centrifugal compressor could achieve, but only because of the less severe cost constraints of Formula 1 racing.

2.2 TURBOCHARGING

Turbocharging – the use of a turbine in the exhaust gas stream to drive the supercharging compressor – was first patented by the Swiss engineer Alfred Büchi in 1905 (Patent, 1905). Unlike in an engine supercharged by a mechanically-driven device, where all of the power to compress the charge air is taken from the crankshaft, in a turbocharged engine the power for the compressor comes from expansion of the exhaust gas in the turbine stage. Hence the device was originally termed a ‘turbosupercharger’, although this word is now generally contracted to ‘turbocharger’. Figure 2.9 is a photograph of a Lotus Type 918 V8 engine, in which the turbocharger on the right-hand cylinder bank is visible, each bank having its own device fitted.

In a manner similar to that of the power consumed by a compressor, the power produced by the turbine is

$$\dot{W}_t = \dot{m}(h_3 - h_4) = \dot{m}c_p(T_3 - T_4) \quad \text{Eqn 2.4}$$

where \dot{W}_t is the power produced by the turbine, \dot{m} is the mass flow through it, c_p is the specific heat capacity at constant pressure of the working fluid (in this case, exhaust gas), h denotes specific enthalpy, T denotes temperature and the subscripts 3 and 4 are the inlet and outlet conditions of the turbine, respectively.



*Fig. 2.9: Photograph of a Lotus Type 918 V8 engine. The turbocharger for the right-hand cylinder bank is visible beneath the right-hand cylinder head.
(Photograph courtesy Lotus Engineering)*

The use of an exhaust gas turbine to drive the compressor makes use of some of the waste heat from the engine, although the back pressure on the engine necessarily increases, increasing both negative work during the exhaust stroke (see Chapter 1) and the density of the residuals trapped inside the combustion chamber at the exhaust valve closing point. This is to the detriment of the engine knock limit, a subject that will be returned to later in Chapter 3. A schematic of a simple turbocharged engine is shown in Figure 2.10.

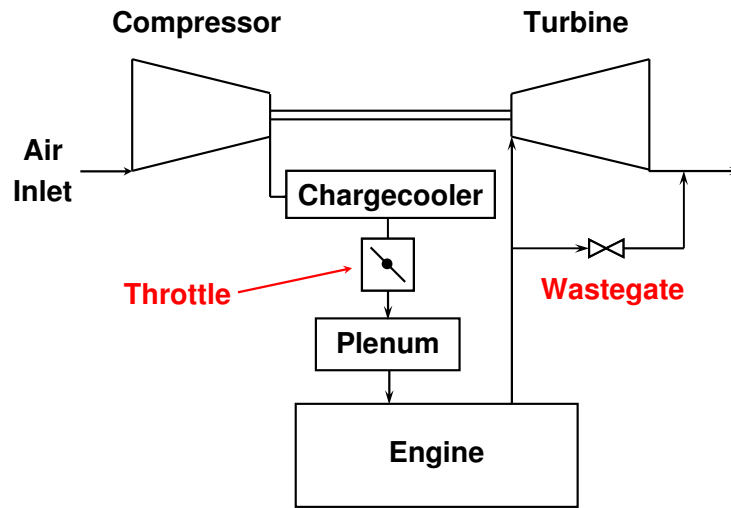


Fig. 2.10: Schematic of a turbocharged engine

The first turbocharged automotive engine, built by the aero engine designer Major Frank Halford for his 'Halford Special' racing car in 1923 (Taylor, 1999), used a turbocharger of his own design. This engine is shown in Figure 2.11, which also shows the use of a chargecooler and pre-compressor introduction of fuel, the advantage of which will be discussed later. With its double overhead camshafts and twin ignition system, this engine is of remarkably modern configuration, despite being nearly 90 years old.

Halford's turbocharger was of simple design, being matched such that the turbine stage exactly balanced the power consumed by the compressor. Such a device is termed a 'free-floating' turbocharger. This approach is acceptable on large stationary engines where maximum fuel economy is the aim, but leads to driveability problems in automotive use since it takes a long period of time for the turbine to supply sufficient power to the compressor to allow it to react to any load change on the engine. In automotive applications, at low mass air flow conditions there is thus a desire to have the capability to drive the compressor harder than a turbine matched solely to the maximum air flow requirements of the engine can achieve. Consequently the convention is to use a turbine capable of producing excess power at full load, and to bypass part of the flow when the desired charge

pressure is achieved. Thus the schematic of Figure 2.10 shows, in addition to a chargecooler, such a bypass valve, which is normally termed a wastegate.

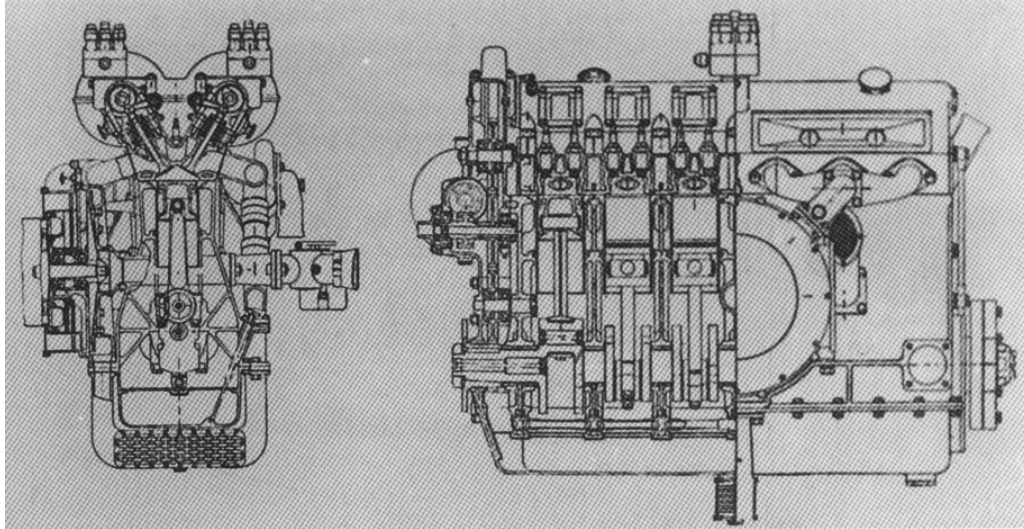


Fig. 2.11: Sections of the first turbocharged car engine, developed by the aero engine designer Major Frank Halford in 1923. The use of an chargecooler is shown, as is the pre-compressor introduction of fuel. (Taken from Taylor (1999), courtesy Rolls-Royce Heritage Trust)

The use of a wastegated turbine capable of providing excess power is advantageous in road vehicles both to overcome the time it takes to produce steady-state boost pressure at low engine speed (then being limited by the surge line of the compressor) and the effect of lag resulting from the turbocharger system as a whole (because of the dynamics of the turbocharger and the filling time associated with the induction system). However, using such a turbine would exponentially increase the power it produces, and so the purpose of the wastegate is to reduce the mass flow through the turbine, limiting the power it produces according to Equation 2.4, and hence control the boost pressure delivered to the engine. This is the common means of matching a turbocharger to a gasoline engine, primarily because the wastegate is a simple and robust device and SI engines produce very high exhaust gas temperatures at high power outputs (typically 950-1050°C).

Adopting such a wastegating strategy increases the back pressure on the engine above that which a 'free-floating' turbocharger provides. Since the pre-turbine pressure is a function of both expansion ratio and the exhaust system back pressure downstream of the turbine, the disadvantages of this approach are compounded in a road vehicle with its catalyst and silencing system versus a racing or aero engine (where silencing requirements are minimal). This in turn means that for a larger area of their operating map such racing and aero engines have a mean inlet pressure higher than the mean pre-turbine pressure (the point at which this reverses often being termed 'boost cross-over'). Thus with no silencing, turbocharged racing and aero engines scavenge better than NA engines and they are not affected by trapped exhaust residuals to the same degree. These are particularly important factors in why such turbocharged racing engines can give better fuel consumption than NA ones (Mezger, 1978).

As a means of circumventing the fixed expansion ratio of a wastegated turbocharger, so-called variable-geometry turbines (VGTs) have been developed and become commonplace on diesel engines. This is possible because diesel engines typically have $\sim 200^{\circ}\text{C}$ cooler exhaust gas temperatures (Heywood, 1988). Instead of altering the mass flow through the turbine as a wastegate does, a VGT adjusts the expansion ratio directly and hence extracts some work from all of the exhaust gas mass flow, which facilitates a lower expansion ratio at full load. Recently, they have been developed by Porsche for high performance gasoline engine use, which has required development of significantly higher-specification materials (Kerkau *et al.*, 2006). Better load-change response coupled to lower back pressure on the combustion chamber is the chief benefit of this technology. The lower pre-turbine pressure of such devices results in reduced residual rate in the cylinder. They have also been shown to have significant benefits in engines with separated exhaust gas pulses to the turbine (Sauerstein *et al.*, 2009).

Note that the throttle in a turbocharged engine can be positioned anywhere in the air path. This is unlike in an engine mechanically supercharged by an

aerodynamic device, and is because in a turbocharger the compressor shaft speed is not a fixed multiple of the crankshaft speed, instead being free to float with air flow rate. It is normal, however, to position the throttle downstream of the compressor, obviating the need for the compressor to be fitted with oil seals to prevent carryover of oil into the charge air. This is the configuration shown in the schematic of Figure 2.10.

2.3 COMPOUND CHARGING

As mentioned above, compound charging is the use of two different pressure-charging devices on an engine, the aim of which is to offset the disadvantages of one of the devices with the advantages of another. In Otto cycle engines, systems employing a Roots blower and turbocharger in series have mostly been used (Robson, 1986, Middendorf *et al.*, 2005a and Krebs *et al.* 2005a and 2005b). One such system is illustrated schematically in Figure 2.12, being a representation of the 1.4 litre Volkswagen TSI 'Twincharger' production engine described by Krebs *et al.* (2005a and 2005b). The charging system of this engine comprised a Roots blower and wastegated turbocharger in series. Note that to control the air charge into this engine, four devices were required: the throttle, wastegate, supercharger bypass and clutch actuator, and thus the system made significant demands on the engine management system employed.

Systems with an axial-flow compressor and turbocharger in series have also been built (Doble, 1987) and also some with two turbochargers in parallel, switched sequentially as necessary (Tashima *et al.*, 1994). Light-duty diesel engines are starting to employ series turbocharged systems with bypasses controlling switchover between the devices (Sweetland and Grissom, 2003 and Steinparzer *et al.*, 2004), and there is also an expectation that these systems will eventually appear on series production SI engines (Kleeberg *et al.*, 2006 and Bandel *et al.*, 2006). The increase in flow range and engine performance possible with such regulated two-stage turbocharging systems when applied to SI engines is discussed by Sauerstein *et al.* (2010), who state that specific power outputs of 120 kW/l (161 bhp/l) are possible while still producing BMEPs of 24 bar

at 1500 rpm. As a consequence of this, higher levels of downsizing will be achieved with compound-charged engines.

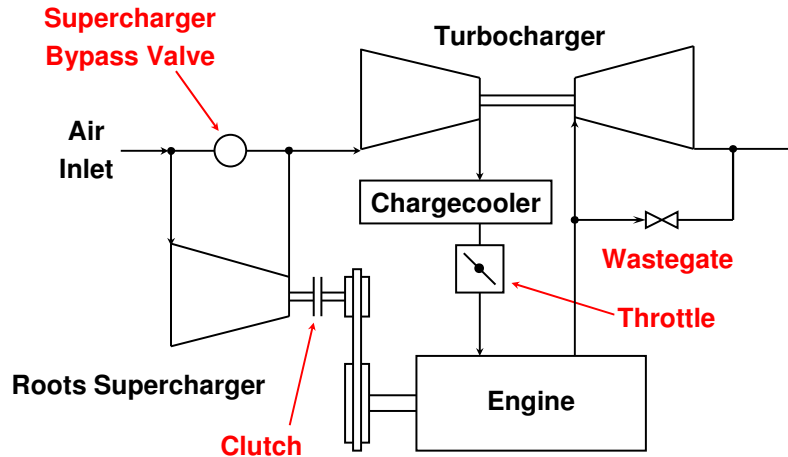


Fig. 2.12: Schematic representation of the compound charging system of the Volkswagen TSI 1.4 litre 'Twincharger' engine

Compound-charged engines sometimes employ inter-stage chargecooling as well as the more normal post-compression chargecooler (Robson, 1986).

2.4 TURBOCOMPOUNDING

Turbocompounding is the use of a turbine stage to extract mechanical work from the exhaust gas. Historically this has chiefly been applied to diesel engines. Sammons and Chatterton (1955) describe the Napier Nomad 2-stroke aircraft engine with such a system, employing axial-flow compressor and turbine on the same shaft, compounded to the crankshaft via a variable speed 'Beier' drive. This compressor-turbine system was also specified for the Napier Deltic engine (Chatterton, 1956). Scania have also commercialized a turbocompound heavy duty diesel engine (Website, 2011a).

Since the act of obtaining extra work from the exhaust gas results in a higher expansion ratio across the turbine, the density of the residuals trapped inside the

cylinder increases. This is not an issue for diesel engine combustion, which does not suffer from combustion knock in the same manner as an SI engine (Heywood, 1988). In Otto cycle engines, however, combustion knock becomes a major limit on engine fuel efficiency. Nonetheless, there has been one productionized gasoline turbocompound engine, the Wright R-3350 Turbo Cyclone aero engine, which utilized three turbines (one for each group of six cylinders on this twin-row 18-cylinder radial engine) and hydraulic drive to return power to the crankshaft (Gunston, 1995). However, the same observation can be made for this technology as for racing applications of turbochargers: because the Turbo Cyclone was an aircraft engine, and hence there was no significant downstream exhaust back pressure, overall pressure on the combustion chamber was much reduced and the knock limit was still sufficiently far away for the technology to be of benefit. It could be, however, that with the advent of gasoline VGTs described in Section 2.2, this technology may once again become applicable to gasoline engines in the future, although the gearing would continue to be an issue for mechanical power recovery.

The subject of fuel characteristics, and their bearing on combustion knock, will be discussed in Chapter 3, but it should be pointed out that the symbiotic development of gasoline with the SI engine it is associated with has led to fuels with very advantageous properties compared to the fluid used by Benz to power his first automobile. The types of combustion system common to the pressure-charged engines described above place ever greater demands on the fuel they operate on, and such fuels have an important part to play in the ability of current and future engines to deliver better fuel consumption. One means by which this may be done, pre-compressor injection (as used by Halford in his engine, and by many aero engines such as the Rolls-Royce Merlin) will be discussed in Chapter 5.

2.5 THE USE OF PRESSURE CHARGING TO REDUCE ROAD VEHICLE FUEL CONSUMPTION

In Chapter 1 the Otto cycle was explained in detail, and it was stated that one of its main disadvantages is the presence of pumping losses attributable to throttling the engine. Throttling is the normal mechanism applied to 4-stroke SI engines to control load, since the charge will only burn within a tightly-defined air-fuel ratio (AFR) band near to the stoichiometric value. This means that the amount of air entering the engine has to be restricted as well as the fuel.

The AFR that the engine is operating at is usually termed λ , where

$$\lambda = \frac{\text{AFR}_{\text{actual}}}{\text{AFR}_{\text{stoichiometric}}} \quad \text{Eqn 2.5}$$

where $\text{AFR}_{\text{actual}}$ is the AFR that the engine is operating at and $\text{AFR}_{\text{stoichiometric}}$ is the chemically-correct AFR. Operation at stoichiometric conditions is usually termed $\lambda = 1$, and operation at fuel rich conditions (where there is insufficient oxygen for complete combustion) is indicated by $\lambda < 1$, and fuel-lean conditions $\lambda > 1$ (i.e. there is an excess of oxygen for complete combustion). At $\lambda = 1$ the gaseous exhaust emissions of an SI engine can be simply controlled by a three-way catalyst (TWC). In engines where operation at $\lambda = 1$ is the strategy for exhaust emissions control, and where consequently the amount of air entering the engine has to be heavily restricted, throttling losses can be minimized by adopting different approaches. These include the use of valve trains which limit the opening period of the intake valves to enable the gas exchange to be conducted at higher manifold pressures (Tuttle, 1980 and 1982, Turner *et al.*, 2004b and 2005b), the use of cylinder deactivation at part load (Turner *et al.*, 2005b) or downsizing the swept volume and recovering the lost power output by some form of pressure charging. With downsizing, as well as a reduction in throttling losses, there are also supplementary benefits in the form of reduced

friction (for engines where the number of cylinders is reduced) and reduced thermal losses at part load.

To illustrate the benefit of the approach, Schwaderlapp *et al.* (2002) predicted an 18% reduction in fuel consumption when pressure charging was used in a downsized engine fitted with conventional port-fuel injection (PFI) and single-stage turbocharging with chargecooling versus a baseline NA one. However, there are limits to the amount of downsizing that can be applied, in the form of abnormal combustion, and especially combustion knock.

The challenge of using pressure-charging devices on a spark-ignition engine is a severe one and has been studied and reported in detail ever since this method of increasing engine specific output was invented (Hooker *et al.*, 1941, Watson and Janota, 1986, Esch and Zickwolf, 1986 and Bruestle and Hemmerlein, 1994). This is because in increasing the pressure of the charge air by compressing it non-isothermally (e.g. approximately adiabatically), a simultaneous increase in its temperature occurs. With this increase in charge air temperature the propensity of an SI engine to knock increases.

Knock occurs within the combustion chamber when some proportion of the end gas (the portion of the charge to be consumed last by the advancing flame front) autoignites and the charge combusts extremely rapidly. The autoignition is a result of the temperature and pressure history the charge has been subjected to during the cycle. Because the near-stoichiometric mixture contains a large amount of energy, autoignition of the end gas results in extremely high pressures being reached. Furthermore, high-pressure waves traverse the combustion chamber which can cause catastrophic to damage the engine. This subject will be returned to in Chapter 3.

As described in Chapter 1, since the maximum thermodynamic efficiency an SI engine can achieve is a function of the effective in-cylinder compression ratio (CR) it is operating at, it is of utmost importance that the CR be as high as possible for minimum fuel consumption in a vehicle. In a pressure-charged

engine, after external compression in the charging system, the further compression inside the engine heats the charge further. Clearly the start-of-compression temperature (SOCT) of the charge delivered to the engine by the charging system has a major bearing on the end-of-compression temperature (EOCT) reached, as this is the temperature from which the charge is adiabatically compressed inside the cylinder according to the relationship defined in Equation 2.2.

There are thus two conflicting requirements when using pressure charging to increase the 'downsizing factor' of an engine when improved vehicle fuel consumption is the aim: there is the need to increase charge air density to increase specific output and retain installed power, but there is also the requirement to reduce the compression ratio as the charge air temperature is increased to mitigate the likelihood of knock occurring in the engine at full load. This is the reason for the development of variable compression ratio (VCR) mechanisms, and why they are particularly pertinent to pressure-charged SI engines. Schwaderlapp *et al.* (2002) predicted a further 9% improvement by employing a VCR mechanism over their results for a conventionally-downsized engine, and Drangel and Bergsten (2000) reported up to a 30% improvement in drive cycle fuel economy over a basic turbocharged type of engine for their supercharged VCR engine.

In spark-ignition engines improved charge air cooling systems can bring improvements in engine performance (Wood and Bloomfield, 1990). However, since chargecooler effectiveness is analogous to the thermal ratio of the heat exchanger under the operating conditions it is being used at, this being defined as

$$R_{Th} = \frac{T_{in} - T_{out}}{T_{in} - T_{ambient}} \quad Eqn 2.6$$

where R_{Th} is the thermal ratio, T_{in} and T_{out} are the entry and exit temperature of the air flowing through the chargecooler and $T_{ambient}$ is the atmospheric or 'sink' temperature, there is a limit on how much heat energy can be removed from the charge air. This is because, since it cannot be of infinite size, no chargecooler can be 100% effective, and even if this were possible the minimum charge air temperature that can be achieved is the prevailing atmospheric temperature. The above holds whether the cooling medium is air or water (Bromnick *et al.*, 1998).

It should be mentioned that intake valve closing (IVC) variation can also be used to reduce the EOCT since it influences the effective CR. Extreme versions of this approach are commonly referred to as operating on the Miller cycle, and are also sometimes incorrectly termed 'operating the engine as an Atkinson cycle engine'. (The Atkinson cycle engine requires a very specific crank train arrangement, much more complicated than the traditional Watt crank-rod-slider mechanism, allowing as it does the entire 4-stroke cycle to be completed in one revolution of the engine output shaft.) A great deal of work has been done in this area since the throttling losses of the engine are also reduced. Furthermore, since the intention of raising the compression ratio of an engine is actually to increase the effective expansion ratio (and thus to increase the work ratio of the high pressure to low pressure loops of the Otto cycle) there are important secondary benefits at the same time.

The effect of differential expansion can be achieved by either late or early intake valve closing (LIVC or EIVC) (Tuttle, 1980 and 1982). However, fully realizing the benefit in an NA engine without sacrificing an unacceptable amount of engine power at full load requires employing a variable valve train (Schausberger *et al.*, 2001, Turner *et al.*, 2002b and Kiefer *et al.*, 2004). When used in conjunction with fixed valve timing, Miller-cycle operation is normally combined with pressure charging to offset the effect of the reduced effective swept volume that the valve timing realizes, and supercharged Miller cycle engines have been productionized that have shown benefits in fuel economy over equivalent capacity and power output NA engines (Goto *et al.*, 1994). Therefore, pressure charging the engine

is fundamental to maintaining vehicle performance, and this cannot really be termed a downsizing approach because the engine swept volume is typically not greatly reduced, if at all.

Employing a VCR mechanism to vary the compression ratio (CR) is a means to avoid combustion knock at high engine loads by reducing the temperatures the end gas is subjected to during compression and combustion. Additionally, the CR can be increased at part load up to and over what is conventionally used even in NA engines, which results in superior thermodynamic efficiency and especially reduced idle fuel consumption (Drangel and Bergsten, 2000). From these observations, VCR is of special benefit in pressure-charged engines which, as mentioned, normally have to be configured with a low, fixed, CR because of combustion knock. Furthermore, versus a LIVC or EIVC Miller-cycle approach, VCR engines provide the benefit of fixed effective swept volume since the compression ratio is not adjusted by advancing or retarding IVC.

Direct injection (DI) of SI engines is an important enabler for the current trend in downsizing since it shows clear synergies with pressure charging (Wirth *et al.*, 2005, Ranini and Monnier, 2001, Lake *et al.*, 2004, Krebs *et al.*, 2004, Wurms *et al.*, 2004, Lang *et al.*, 2005, Klütting *et al.*, 2005 and Meyer, 2005). The benefit of DI in pressure-charged SI engines is primarily a result of the latent heat of vaporization of the fuel being taken preferentially from the air and not the structure of the engine itself. This cools the charge by reducing SOCT to allow a simultaneous increase in volumetric efficiency and compression ratio since it reduces the propensity of the engine to knock. In all DISI engines, there is also a potential supplementary benefit if the fuel is introduced after intake valve closure, insofar as the volume of the fuel itself does not displace incoming air (Anderson *et al.*, 1996).

Lang *et al.* (2005), in a study of the relative benefits of charge air cooling and oxygen displacement have shown that, if the fuel is injected during the intake stroke, 8% more air mass can be inducted due to charge cooling, whereas if all the fuel is injected after IVC then 2% greater mass is inducted due to reduced air

displacement. As they point out, however, considering the finite time available for injection, the actual magnitude of the increase in volumetric efficiency available is between these theoretical maxima. This is echoed by Anderson *et al.* (1996), who also showed that retarding the injection event later into the compression phase of the cycle tends to benefit charge cooling with respect to knock suppression and advancing it favours volumetric efficiency improvement. This results in a fairly wide window for injection timing (with respect to full load BMEP) which can be used, for any given injector orientation within an engine architecture, to offset the danger of excessive fuel impingement on the cylinder bore walls or piston crown through the ability to inject at a more favourable point in the cycle.

In supercharged DISI engines, the full range of potential benefits is only partially available. The knock limit is extended to the benefit of thermal efficiency through both the latent heat of vaporization of the fuel and forced scavenging of the chamber by boost pressure (fuel being absent in the air passing through the engine), but the turbocharged DI engine enjoys further advantages over both supercharged DI and turbocharged PFI engines. This is primarily because at low speeds the engine can be extremely effectively scavenged by increasing the valve overlap through the use of a variable camshaft phasing system in the same manner as the supercharged engine, which in the turbocharged case also allows a shift in operating point of the compressor (Wirth *et al.*, 2000, Lang *et al.*, 2005 and Kleeberg *et al.*, 2006). Furthermore, this is coupled with beneficial harnessing of secondary oxidation of CO in the exhaust manifold to increase the enthalpy of the exhaust gases flowing into the turbine, and so to increase its available work at the low mass air flow typical of low engine speeds (Klütting *et al.*, 2005 and Schmid *et al.*, 2010).

In combination, these effects result in a widening of the maximum BMEP plateau of the turbocharged DI engine versus the PFI type (particularly in the low speed range) which is further augmented by the fact that this can be achieved at lower boost pressure because of the increase in volumetric efficiency provided by the DI system mentioned above. As a consequence, turbocharged DI engines have

reduced 'turbolag' than PFI ones and require less enrichment fuelling at full load to protect the turbine, as Krebs *et al.* (2004) have shown. This latter situation is aided by the fact that the exhaust manifold air-fuel ratio (AFR) is decoupled from the in-cylinder AFR such that, before the boost cross-over point, fresh air can be blown through the engine to reduce the turbine inlet temperature. This in turn means that the in-cylinder fuelling can be increased to the benefit of knock suppression and power output while still resulting in $\lambda = 1$ at the catalyst inlet. Furthermore, Krebs *et al.* (2004) show that variable valve timing, in conjunction with a split injection event, can be used at start-up to light the catalyst more quickly after a cold start.

In addition to VCR and DI, new combustion and charging systems are being proposed to allow an increase in either compression ratio or specific output through an extension of the knock limit. These include cooled EGR at full load, excess air at full load, and turboexpansion. These will be discussed further in the next section.

2.6 THE USE OF COOLED EGR, EXCESS AIR AND TURBOEXPANSION TO EXTEND THE KNOCK LIMIT OF PRESSURE-CHARGED ENGINES

As mentioned previously, there is a significant compromise to be accepted in increasing the specific output of pressure-charged engines if improved vehicle fuel consumption is the aim. This is the requirement to reduce the compression ratio for knock limit protection at full load versus the need for a high CR for good part-load vehicle fuel consumption. Traditionally, the approach has been to set the CR as high as feasible for full-load operation while using excess fuelling to absorb some of the heat released in combustion and thus to give a good clearance to the knock limit. This use of excess fuel is termed 'enrichment cooling'. Ignition retard is also used to control end gas temperature, but this has the effect of causing increased cylinder gas temperatures at EVO and a consequent increase in exhaust gas temperature. Further excess fuelling is often used to protect components in the combustion chamber and exhaust stream from thermal overload. As the degree of downsizing increases, the engine will operate

more frequently in the region of enrichment, because it will operate at high BMEP more often. This has clear implications for vehicle fuel consumption and CO₂ emissions.

In order to alleviate this problem, Stokes *et al.* (2000) proposed a combustion system in which excess air is supplied at full load instead of excess fuel. The intention here was to use the excess air – which dilutes the charge and is hence termed a ‘diluent’ – to slow down the heat release rate and hence limit the propensity of the combustion system to knock. However, in a similar study of the potential of excess air as a knock suppressant, Hiroshi *et al.* (2004) suggested that instead of suppressing knock to the extent imagined, the excess air actually reduces the knock limit, because the higher ratio of specific heats of air causes the end gas temperature to increase at a greater rate than is the case for other diluents. Others, notably Grandin *et al.* (1998 and 1999), Duchaussoy *et al.* (2003) and Cairns *et al.* (2006 and 2008) have proposed the use of cooled EGR as a diluent instead, showing that it offers similar benefits to using excess air with the significant added benefit of still being able to make use of simple three-way catalysis at full load. It is interesting to note that these combustion systems were all originally proposed and investigated by Ricardo (1919).

Work by Cairns *et al.* (2006) and Hattrell *et al.* (2006) has approached the issue of which of the three practical diluents for knock limit extension (fuel, air or cooled EGR) is the most pragmatic in an experimental study and a related theoretical one. They concluded quite firmly that cooled EGR is the most attractive solution if the intention is to avoid excessive fuel consumption at high load. However, they do concede, as with others studying the use of cooled exhaust gas as a diluent, that there is a significant challenge to supply sufficient cooled EGR to the engine at a low enough temperature so as not to impact the knock limit negatively. The mass flow rate of gas recirculated in this manner approaches 10% in their studies, and in their work this was supplied pre-compressor. As a consequence, compressor discharge temperatures exceeded 220°C in their tests. There was then a major requirement in terms of heat rejection placed on the chargecooler that the combined flow of charge air and EGR passed through.

Taylor *et al.* (2010) have repeated this work with an architectural modification to a DISI engine in the form of a water-cooled exhaust manifold, with the same conclusion as Cairns *et al.* (2006) and Hattrell *et al.* (2006).

Separately, Turner *et al.* (2002a, 2003, 2005a, 2006c and 2006d) and Whelan and Rogers (2005 and 2006) have proposed a 'turboexpansion' system to extend the knock limit of high compression ratio, high specific output engines. This is analogous to an air refrigeration cycle. Such systems have been proven in lean-burning natural gas engines before (Crooks, 1959 and Helmich, 1966) and have also been proposed for diesel engines (Meyer and Shahed, 1991). One possible configuration of such a system is shown in Figure 2.13. The temperature-entropy diagram for this system is shown in Figure 2.14.

In Figure 2.14 it is clear that the charge air is initially compressed from atmospheric conditions to an 'upper' system pressure represented by the line to point X, after which conventional charge air cooling is conducted from points X to Y. The charging system to this point in the air path might be considered a 'conventional' pressure-charged one, albeit at higher pressure, since it comprises similar hardware to that shown in Figure 2.9. There is, however, an extra stage in the form of an expansion through a cold air turbine back down to plenum pressure which, in addition to reducing the pressure of the charge air, further reduces its temperature in accordance with Equation 2.4 (this stage is represented by the line YZ in Figure 2.14).

There are three additional points of interest in this approach. Firstly, because of the necessarily higher pressure ratio of the compressor, the air temperature into the chargecooler is high and thus it has a larger temperature difference across it than in the 'conventional' systems. The chargecooler can thus reject a larger amount of heat energy for the same thermal ratio, according to Equation 2.5. Secondly, the expansion turbine produces power, and this must either be wasted or collected by some means for useful ends. Finally, since the final stage is one of adiabatic expansion, it is possible to achieve high pressure (and hence high

charge air density) in the plenum at a temperature lower than that which could be achieved by a simple single-stage pressure-charging-and-chargecooler system.

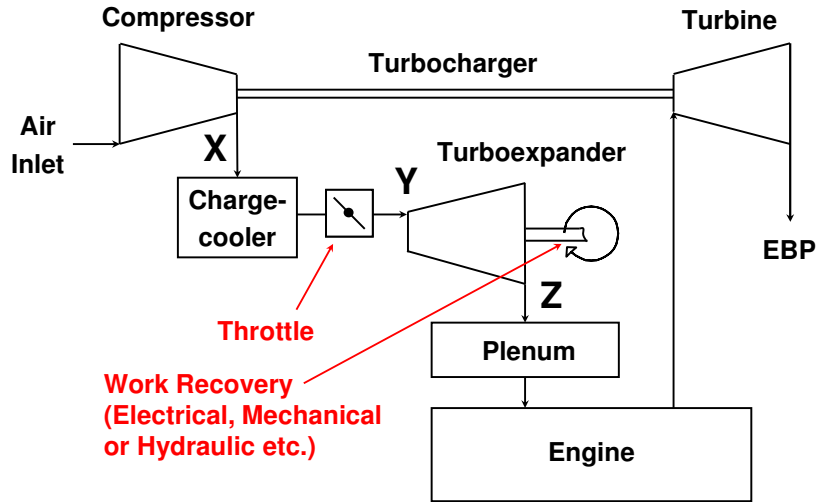


Fig. 2.13: Schematic of one possible turboexpansion system for a turbocharged engine. EBP = Exhaust Back Pressure. X, Y and Z refer to states in the temperature-entropy diagram shown in Fig. 2.14, below

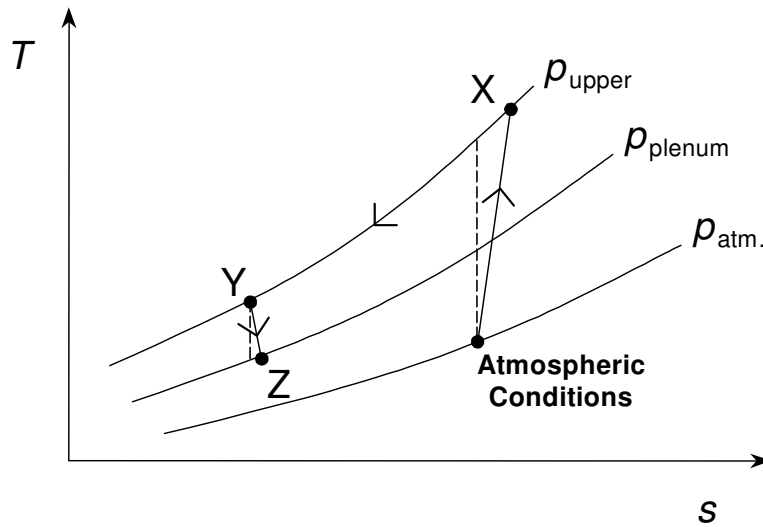


Fig. 2.14: Temperature-entropy diagram for the turboexpansion system shown schematically in Fig. 2.13

The subject of system coefficient of performance has been dealt with by Taitt *et al.* (2005 and 2006) in research related to this work. This and the detail of the system tested by the author will be returned to in Chapter 4.

Thus, if one of the means discussed in this section can afford an increase in the CR of a spark-ignition engine through delaying the onset of knock at high load, then the fuel consumption of a vehicle to which it is fitted can be expected to improve. This relates to the primary aims and objectives of the research here which are to investigate whether or not the knock limit of a downsized engine can be improved by adopting advanced charging techniques and new architectures, or by using an advanced combustion system such as cooled EGR. This will help to address the question of whether an increase in engine CR can be enabled through an extension of the knock limit in this manner.

2.7 SUMMARY AND CONCLUDING REMARKS

This chapter has discussed different configurations of engine pressure charging systems and their use to improve fuel economy of SI engines in downsizing strategies. As a consequence of the desire to reduce vehicle fuel consumption, in the design of such SI engines for higher fuel efficiency it is important to maintain as high a compression ratio as is possible. While modern gasoline fuels are suited to this approach (and alcohols even more so), if the formulation of gasoline fuel is not to change significantly, then mechanisms such as VCR and DI linked to turbocharging will become more attractive for the reasons discussed. Consequently much research work is ongoing in these areas. Both of these approaches are expensive and can also increase the bill-of-material and/or assembly costs. Nevertheless, the requirement to increase compression ratio while suppressing knock will be paramount.

As a result of this, a picture of one of the likely 'standard formats' for the spark-ignition engine of the future thus emerges:

1. It will very likely be downsized and have a reduced swept volume that will in turn reduce both throttling loss and friction (which can be decreased further through a reduction in the number of cylinders);
2. It will employ a pressure-charging system to provide the full-load power output necessary for vehicle performance to be kept equivalent to that provide by current, larger-displacement NA engines;
3. DI will become increasingly common, specifically to extend the knock limit and to improve driveability in turbocharged engines through compressor map shifting;
4. Variable camshaft phasing devices will be used to maximize the potential of the decoupled cylinder and exhaust manifold AFR and to increase air flow to increase compressor efficiency and turbocharger shaft speed.

Klüting *et al.* (2005), state that all of these improvements can be compounded further if a high degree of stratification can be supported at part load, although due to the excess oxygen in general operation, the after treatment of exhaust gases (especially oxides of nitrogen) then becomes more problematic and expensive. There is also a conflict in that as the degree of downsizing increases, the area of the operating map where it is possible beneficially to operate in a stratified manner reduces. Similar comments are made by Cairns *et al.* (2006) on the subject of the adoption of homogeneous charge compression ignition combustion systems in such engines. Hence, unless a very high power output is required (from a large swept volume), the downsized type of DISI engine is increasingly likely to remain a homogeneous charge type operating at or close to stoichiometric, since this permits simple exhaust gas after treatment by using three-way catalysts, although advanced start-up strategies such as split injection may be used to accelerate catalyst light-off.

VCR may be used widely at some future point as the degree of downsizing increases, particularly for its ability to optimize the operating point of the engine

while avoiding the likelihood of knock occurring at full load, thus allowing high part-load efficiency. However, new combustion systems, such as the use of cooled EGR at full load, or more advanced charging systems such as turboexpansion (if successfully developed) or compound charging, may make the complication of VCR less attractive.

Therefore, since downsizing is likely to be a major trend, combustion knock is a major constraint on future automotive engine design and development. The causes, effects and means of combating combustion knock will therefore be discussed in detail in Chapter 3.

Chapter 3: Literature Review of Spark-Ignition Combustion Knock and Means of Counteracting It

The purpose of this chapter is to survey the spark-ignition (SI) engine knock literature from fundamentals, and relate this to the needs of current downsized SI engines. This will culminate in a specific set of aims for the research.

The chapter will start with a general review of SI combustion and the phenomenon of knock before discussing, among other things, the apparatus used to quantify the knocking behaviour of fuels and improve their knocking behaviour through the blending of different components. Various means of suppressing knock via engine and charging system design will also be described, including the targeted use of the latent heat of vaporization of the fuel, cooled EGR, and some other more unusual methods which have recently been proposed.

As stated in Chapter 2, engine downsizing is one possible future technique to improve the fuel consumption of vehicles fitted with SI engines when operated at part load (Walzer, 2001, Turner *et al.*, 2005b, Fraidl *et al.*, 2005 and Bandel *et al.*, 2006). This is due to a shift in the road load locus in the operating map, reducing throttling losses and improving mechanical efficiency (Andriessse *et al.*, 2006). To enable a downsized SI engine to deliver equivalent absolute performance to a non-downsized naturally-aspirated (NA) one, the downsized engine is frequently pressure-charged to increase its full-load BMEP such that the power output is maintained (Emmenthal and Manz, 1982, Torella *et al.*, 2001, Pallotti *et al.*, 2003 and Petitjean *et al.*, 2004). Unfortunately, this can frequently lead to SI combustion knock, which is potentially extremely damaging to an engine and which leads to a reduction in power output, an increase in heat rejection and consequently a reduction in thermal efficiency (Heywood, 1988 and Lee and Schaefer, 1983).

A literature survey on the subject was carried out and additional information was gathered as a result of personal contacts at conferences and in other companies, etc. The literature survey also included a targeted patent search. Despite the prolific amount of literature on the subject, it is believed that the following represents a valuable survey of knocking combustion in SI engines, its importance, causes and effects, and various methods to suppress it in the interests of increasing SI engine thermal efficiency in the future.

3.1 THE SPARK-IGNITION ENGINE COMBUSTION PROCESS

In a typical Otto-cycle internal combustion engine the mixture is induced, compressed and then ignited by a spark from a spark plug at a predetermined point in the cycle. A flame kernel is formed between the spark plug electrodes which itself is affected by convective flow and turbulence in the combustion chamber and which can stretch it into a 'C' or horseshoe shape (Maly, 1994). This flame kernel is therefore subject to a great deal of variation, which in turn gives rise to much of the cyclic irregularity associated with SI combustion, since the flame must proceed from it (Griffiths and Barnard, 1995). Further irregularity occurs in the first few centimetres of flame travel (Curry, 1963). While the kernel itself only comprises 0-2% of the fuel mass (Maly, 1994), its irregularity dominates the first 10% of mass fraction burned (MFB), and this is the reason why other characteristics such as 10-90% MFB and the position of 50% MFB (or 'CA50') are predominantly used to define the performance of a spark-ignited combustion system.

After the flame kernel has formed and stabilized, a flame front starts to travel away from the ignition source and combustion continues in a deflagratory manner into the rest of the combustion chamber, consuming the mixture and releasing heat energy. This heat energy causes the burnt gas to expand and the pressure to rise so providing work to the piston. The difference between the pressure increment due to compression and that due to combustion is used to establish the MFB at any given crank angle (Rassweiler and Withrow, 1938).

Since it takes a finite time for the flame to sweep across the combustion space, all of the mixture is not consumed immediately. The last portion to be consumed, typically at the edge of the combustion space, is termed the 'end gas'. This is heated both by compression due to piston motion (before TDC) and by the expansion of the burnt gas, as well as by flame radiation. Some heat is lost by rejection to the combustion chamber walls. Conventional deflagratory combustion is essentially a chaotic process, which can be affected and accelerated by the level of turbulence, and CFD is sometimes used to investigate bulk trends in conjunction with optical techniques (Robinson *et al.*, 1991).

Turbulence is very important in ensuring that the combustion process proceeds in a rapid manner, and can increase the actual speed of the flame by a significant factor above the 'laminar flame speed', i.e. the speed of the flame in stagnant conditions (Hamori and Watson, 2006). The laminar flame speed is also affected by the temperature, pressure and equivalence ratio of the charge ϕ , defined as

$$\phi = \frac{\text{AFR}_{\text{stoichiometric}}}{\text{AFR}_{\text{actual}}} \quad \text{Eqn 3.1}$$

where $\text{AFR}_{\text{actual}}$ is the AFR that the engine is operating at, and $\text{AFR}_{\text{stoichiometric}}$ is the chemically-correct AFR. Note that ϕ is the inverse of λ (the relative AFR), and hence rich conditions are denoted by $\phi > 1$.

An increase in unburned charge temperature tends to increase the laminar flame speed and an increase in pressure will decrease it (Westbrook and Dryer, 1980). With pure hydrocarbon fuels and alcohols, laminar flame speed shows a maximum slightly on the rich side of stoichiometric at ϕ of about 1.1 to 1.2 (i.e. $\lambda = 0.91$ to 0.83) (Metgalchi and Keck, 1982, Westbrook and Dryer, 1980, Gülder, 1984 and Vancoillie *et al.*, 2011). The laminar flame speed is a characteristic of the type of fuel: for example, low-carbon-number alcohols tend to have a significantly higher laminar flame speed than the paraffins which typically constitute the majority of gasoline components (Metgalchi and Keck, 1982), and

can, even when blended in relatively low proportions, significantly increase the laminar flame speed of paraffins (Gülder, 1984).

It is interesting to note that since the gas near the spark plug burns first and is subsequently compressed as the pressure in the chamber increases due to combustion, the initially-burnt gas reaches the highest temperature in a conventional non-knocking cycle. Hence the spark plug is at the hottest part of the combustion chamber and cooling it is of utmost importance if it is not to become a hot-spot initiator for unintended combustion such as preignition. This observation is also true in the case of a knocking cycle, although the temperature is higher still due to the greater compression as a result of the knock event (Rassweiler and Withrow, 1935), and the heat transfer to the combustion chamber walls in such a knocking cycle is higher still because of the breakdown in the thermal boundary layer. It should also be noted that a similar degree of attention must be paid to cooling the fuel injector in 'close-spaced' direct-injection SI engines, a subject which will be returned to in Chapter 8.

As it is being heated by all of the events occurring in the chamber, the end gas, also being an ignitable mixture, will autoignite if and when the Livengood-Wu integral equation

$$\int \frac{1}{\tau} dt = 1 \quad \text{Eqn 3.2}$$

is satisfied (Livengood and Wu, 1955). The parameter τ in this case is the Livengood-Wu induction time representing the autoignition delay time for the mixture, and is defined by an Arrhenius rate equation of the form

$$\tau = Ap^{-n} \exp\left[\frac{B}{T}\right] \quad \text{Eqn 3.3}$$

where A , n and B are constants which vary for different fuels at different conditions in different engines, i.e. fuels with different 'octane indices'. The definition and determination of octane indices will be returned to later.

When autoignition occurs, if conditions are correct, a flame front can then traverse the remaining end gas at more than 10-20 times the normal flame speed, in turn causing molecular vibration and excitation of the engine structure (Curry, 1963 and Spicher *et al.*, 1991). This is transmitted to the outside of the engine and heard as a metallic ringing or knocking sound, from which the name 'knock' is taken.

From a historical perspective, it is interesting to note that the process has been understood in what might be considered a modern form since very early in the development of the internal combustion engine. In his text book, Lichty (1939) describes the process in fundamentally the same way as it is outlined above and attributes the formation of the theory of autoignition as being due to temperature increase in the end gas to Ricardo (1919).

3.2 GENERAL DISCUSSION OF SPARK-IGNITION ENGINE KNOCK

Knock is a result of the uncontrolled autoignition of the end gas giving rise to extremely high pressure oscillations in the combustion chamber. It should be noted that autoignition itself is not knock, even if it is a necessary precursor to knock occurring: autoignition can occur without knock but not *vice-versa* (Schreiber *et al.*, 1991). This non-knocking form of autoignition is the basis of homogeneous charge compression ignition (HCCI), a subject of a great deal of research in recent years, but which is not a form of SI combustion. HCCI is discussed in detail by Zhao (2007).

Very early in the history of the SI engine knock was understood to be damaging to the engine, and that steps would have to be taken to suppress it in the interests of both fuel efficiency and engine durability (Ricardo, 1919 and 1920,

Tizard and Pye, 1922, Clerk, 1926 and Maly *et al.*, 1990). This has guided spark-ignition engine designers ever since (Maly, 1994).

There are three main theories to explain the knocking phenomenon mentioned in the literature (Oppenheim, 1984, König and Sheppard, 1990, Puzinauskas, 1992 and Pan and Sheppard, 1994). These are:

1. **The autoignition theory** which postulates that if the end gas is subjected to certain conditions, autoignition will occur, which can lead to knock;
2. **The detonation theory** where sonic waves reflect from the walls of the combustion chamber and reinforce the normal deflagration wave until a supersonic speed is achieved and knock occurs;
3. **The rapid-entrainment theory** in which the normal deflagratory flame front is believed to accelerate to a high subsonic speed causing a rapid rate of pressure rise.

Pastell (1950) mentions an earlier explanation, the nuclear theory, in which detonation of the end gas was supposed to be initiated by nuclear particles of carbon. This has since fallen from favour and indeed of all the theories, the autoignition theory is now believed to be the only one which explains the physical and chemical events during the knock process. Pastell's work was fundamental in accepting this, since his motored engine method subjected a mixture to a varying temperature- and pressure-time history. This approach ensured that over a timescale representative of engine operation, various chemical processes could occur in the mixture in a similar manner to those occurring in the end gas of a firing engine. As a result, Pastell's motored engine approach has been adopted by later researchers.

In general, the chemistry of the process that leads to knock is now commonly divided into three regimes; low, intermediate and high temperature (Li *et al.*, 1994b). These are divided as follows:

1. Low temperature: < 650 K
2. Intermediate temperature: 650-1000 K
3. High temperature: > 1000 K.

Much effort has been expended in understanding the kinetic process by which autoignition occurs, with different types of apparatus being used for this purpose. For paraffins, low temperature chemistry is dominated by the process of abstraction of a hydrogen atom from a fuel molecule, subsequent addition of an oxygen molecule, internal isomerization of the resulting radical, then molecular breakdown processes, chain branching, further oxygen addition and termination processes (Li *et al.*, 1994a, Tanaka *et al.*, 2003, Kawahara, *et al.*, 2006, Curran *et al.*, 1998 and 2002, Sahatchian *et al.*, 1990 and 1991, Viljoen *et al.*, 2007). Some of these steps are reversible, depending on pressure, with different rates in the forward and reverse directions. This gives rise to a negative temperature coefficient (NTC) behaviour, where the reaction rate of the compound can slow down with increasing temperature. This phenomenon is especially found in paraffinic fuels. Often, it is preceded by 'cool flame' activity.

Cool flame chemistry has been the subject of much research, since it adds thermal energy to the autoignition process. Ball (1955) presented images of cool flame development in an engine and Pastell (1950) and Cornelius and Caplan (1952) related the appearance of cool flames to the increase in pressure due to precombustion reactions occurring in the combustion chamber. The relationship is shown in Figure 3.1, reproduced from Cornelius and Caplan (1952). Later, Leppard (1987) employed a variable compression ratio (VCR) 'cooperative fuels research' (CFR^{TM2}) engine to show that light emission varied with pressure in the combustion chamber during the cool flame period, as shown in Figure 3.2. The CFRTM engine itself is discussed in Section 3.3 and Appendix III.

² CFR is the registered trademark of Dresser, Inc., DresserWaukesha.

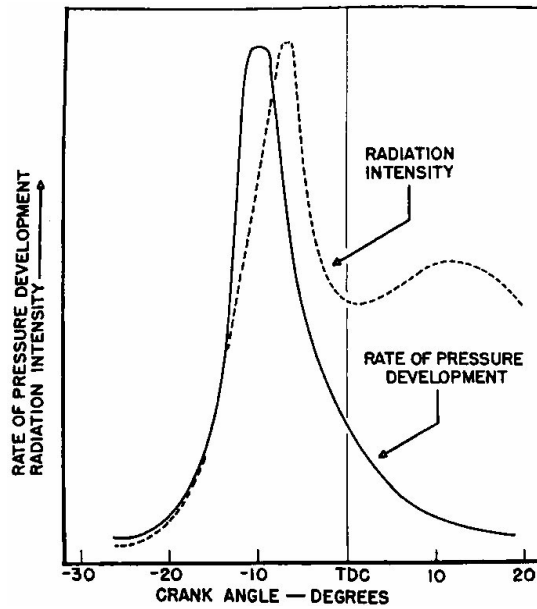


Fig. 3.1: Comparison of cool flame radiation intensity and rate of precombustion reaction pressure development for a 70 octane blend of isooctane and n-heptane. (Reproduced from Cornelius and Caplan (1952), reprinted with permission from SAE Transactions, Vol. 6, pp. 488-510, © 1952 SAE International)

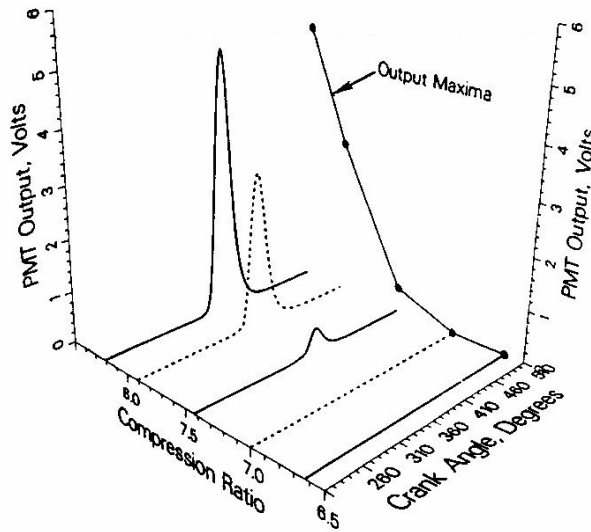


Fig. 3.2: Measured visible radiation as a function of crank angle and compression ratio. (Reproduced from Leppard (1987), reprinted with permission from SAE paper number 872150, © 1987 SAE International)

Levedahl (1955) compared results from a modified CFR engine (with a special cross-head piston arrangement to eliminate the danger of lubricating oil contaminating the charge) with those from a rapid compression machine (RCM) to assert that the main contribution of cool flame chemistry to the autoignition process is to provide a heat input to enable the later hot ignition process. By use of a sampling valve in the cylinder and analysis of cylinder pressure he showed that the low temperature chemistry phase preceding the appearance of cool flames, while not in itself exothermic, is a necessary precursor to cool flame activity. This was reiterated by Green *et al.* (1987). Ballinger and Ryason (1971) showed that at low pressure, a temperature rise of ~200°C can be associated with the appearance of cool flames. Lignola and Reverchon (1987) investigated cool flame behaviour extensively in a continuously-stirred tank reactor (CSTR), showing how it relates to the NTC behaviour of some hydrocarbons, which in turn plays a role in the oscillatory nature of cool flames.

In comparison to the low temperature chemistry, the high-temperature ignition process is much simpler and dominated by the build-up of HO₂ radicals created by straight hydrogen abstraction from the fuel molecule by an O₂ molecule. When a sufficient level of HO₂ radicals in the charge is reached, thermal runaway occurs. Maly (1994) discussed how anti-knock compounds either retard low-temperature oxidation and chain-branching reactions or inhibit the high-temperature HO₂ route. Richardson *et al.* (1961a, 1961b and 1963) describe how tetraethyl lead (TEL) and tetramethyl lead (TML) work to do this, and how 'lead extenders' can delay the point in the cycle at which TEL and TML work best to scavenge the radicals and extend the knock limit. They also state that the effect of TML is stronger with aromatic compounds than TEL.

The concept of a global low-temperature chemistry, with all of the end gas sharing the same temperature-time history, would give rise to the simultaneous autoignition of all of the unburned charge when it reached the conditions necessary for it to occur. In fact, global autoignition of the end gas is very rare, because of inhomogeneities either of temperature or gas composition, meaning discrete sub-volumes of the end gas reach an autoignitive state first. The subject

of inhomogeneity in the unburned charge and how it affects knock will be returned to later, but Pan and Sheppard (1994) have studied temperature gradients in the end gas and determined the sort of thermal event that can be expected as a result. These they describe as follows:

1. **Deflagration:** typical thermal gradient = 100 K/mm
2. **Developing detonation:** typical thermal gradient = 12.5 K/mm
3. **Thermal explosion:** typical thermal gradient = 1.25 K/mm.

The last two terms were originally defined by Zel'dovich *et al.* (1970). 'Deflagration' is a typical flame front-type event where the temperature difference across the flame front is very high, and Pan and Sheppard (1994) state that preconditioning of the end gases to this state could be beneficial in accelerating the later stages of combustion. A 'thermal explosion' is when all of the charge ignites effectively simultaneously: this is the state aimed for in HCCI, although when that combustion process is used with gasoline, significant amounts of EGR are used to slow the resulting combustion process down (Sheppard *et al.*, 2002). Neither of these two modes give a particularly damaging level of knock. However, Pan and Sheppard (1994) show that 'developing detonation' is the most destructive condition since it releases sufficient energy that the chemistry becomes coupled to the thermal event, producing extremely rapid flame speeds and, they assert, higher levels of pressure oscillations than can be measured with currently-available equipment. They also show how two exothermic centres, when sequentially ignited, can lead to highly damaging levels of knock, the first raising the temperature such that a developing detonation can start from the second.

As well as creating soot (König and Sheppard, 1990), the audible manifestation of knock is symptomatic of why it needs to be avoided. When it occurs, extremely high pressure waves move at supersonic speeds across the combustion chamber, in various modes of vibration (Draper, 1938 and Blunsdon

and Dent, 1994). These compression waves can often ignite unburnt charge in the top piston ring land, causing severe local overpressures and hence characteristic damage patterns (König *et al.*, 1990, Maly *et al.*, 1990, Klein *et al.*, 1994, Nates and Yates, 1994 and Fitton and Nates, 1996). Furthermore, the high bulk gas velocities induced by knock result in a reduction in engine power due to extremely high rates of heat transfer (Blunsdon and Dent, 1994). There is a corresponding reduction in exhaust temperature (Heywood, 1988). Catastrophic damage to the piston and cylinder head flame face from these pressure and heat transfer effects can occur if an engine is run in a knocking condition for long periods.

3.3 THE KNOCK RATING OF FUELS

A standardized rating for the knocking propensity of a fuel was sought very early in the development of the internal combustion engine. For such a rating system, lower and upper limit fuels are required. n-Heptane was chosen very early as the lower limit fuel, since it is easily made (Campbell *et al.*, 1930), but the upper limit fuel was the subject of some debate and research. Ricardo, Tizard and Pye described the mechanism of knock and proposed that a 'toluene number' be employed to rate different fuels (Clerk, 1926 and Nahum *et al.*, 1994). They chose the aromatic molecule toluene (C_7H_8 , or methyl benzene) because it was known to have a very high knock resistance. Campbell *et al.* (1930) investigated several different compounds, including toluene, with respect to their suitability as an upper-limit fuel for knock rating, and recommended the use of isooctane. This was because its response when blended in n-heptane was more linear than that for benzene, toluene or an alcohol over the range of knock resistance of the gasoline formulations then commonly available. This is illustrated in Figure 3.3, taken from their work, which also shows the use of a critical compression ratio (CCR) in defining the knock resistance of a fuel. This concept will be returned to later, but essentially the higher the CCR, the more knock-resistant the fuel. It was accepted by Campbell *et al.* (1930) that a wider rating range could be obtained by using an alcohol or aromatic fuel as the upper limit, but the chosen lower-limit hydrocarbon, n-heptane, is a straight-chain paraffin. The paraffins (or

alkanes) are very common in gasoline and have different physical properties to aromatics and alcohols. On this basis (as well as the linearity of the useful range) it was believed that a mixture of two paraffins would provide a better basis for any rating scale subsequently adopted.

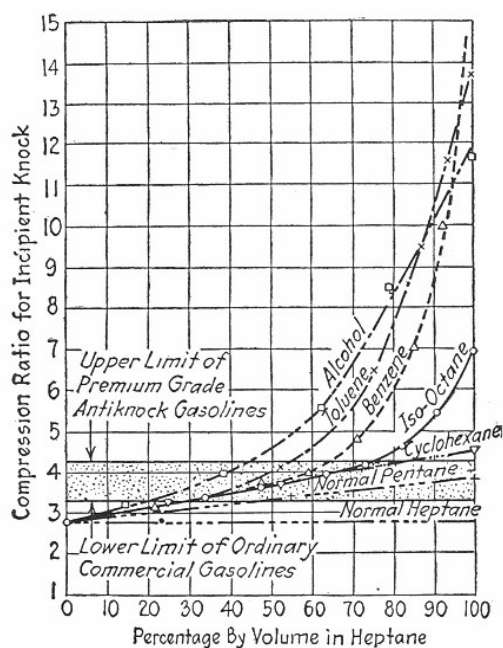


Fig. 3.3: Knocking characteristics of several fuels in admixture with n-heptane from 0 to 100% by volume. Shaded area represents range of gasolines commonly available in 1930. (Reproduced from Campbell et al. (1930), reprinted with permission from SAE Transactions, Vol. 25, pp. 126-131, © 1930 SAE International)

Isooctane (or 2,2,4-trimethyl pentane) is a highly-branched paraffin molecule with the highest practically-attainable knock resistance for a saturated hydrocarbon at the time that Campbell *et al.* (1930) conducted their tests. As mentioned, n-heptane was at that time an easily manufactured straight-chain paraffin with extremely low knock resistance. Edgar (1927) had been the first to suggest that these two chemicals could be used as rating fuels and describes a production method for isooctane together with a summary of the physical properties of both it and n-heptane, showing their similarities and hence suitability for blending

together. This is a result of the fact that, being paraffins, both are saturated hydrocarbons. As a consequence of this work, isooctane and n-heptane were adopted as the upper and lower rating fuels respectively, and were termed the primary reference fuels (PRFs).

At a similar time to Ricardo's work and with knowledge of Campbell *et al.*'s investigations, the Cooperative Fuels Research (CFR) Committee, together with the American Society of Mechanical Engineers (ASME), defined a series of test methods intended to establish what was to become known as the octane number (ON) of a fuel. This will be defined later. These test methods employ a variable compression ratio engine especially developed to become a standard test engine and hence to enable consistency of knock testing across the industry³. The engine created by the CFR committee is the Cooperative Fuels Research (CFR™) engine (Horning, 1931 and Baxter and Yeo, unknown date), which is still manufactured by the DresserWaukesha division of Dresser, Inc. A photograph of the current version of this engine is shown in Figure 3.4. Some further illustrations and more details of the engine are presented in Appendix III.

In these rating methods, a test fuel is tested at preset intake charge conditions and the equivalent mixture of isooctane and n-heptane (by volume) is then established by trial and error for the same level of knock. The percentage of isooctane in the mixture is then the octane number (ON) of the fuel under those rating conditions. These rating tests are discussed in the following paragraphs.

The two most commonly-used methods defined by the CFR committee for determining the octane rating of an automotive fuel are those establishing a 'Research Octane Number' (RON) and 'Motor Octane Number' (MON) for it (ASTM International 2007a and 2007b). The former is termed the 'F1' method

³ The CFR Committee was originally set up in the US to enable and promote closer cooperation between engine manufacturers and fuels suppliers and to work towards setting standards for fuels to the benefit of both. The Society of Automotive Engineers (SAE) was also heavily involved in its creation. Dickinson (1929) discusses some of its early results before the creation of the original version of the fuels rating engine it designed. It is now the Coordinating Research Council, Inc. (Heywood, 1988). Note that in Great Britain, the work of the Empire Motor Fuels Committee predated the creation of the CFR engine (Institution of Automobile Engineers, 1924).

and the latter the 'F2'. There is also equipment available to enable the CFR engine to be used for the 'F4' 'ASTM Supercharge' method, but (as with the 'F3' 'ASTM Aviation' method) this test is usually reserved for aircraft engine fuels and as such is not widely used now because of the decline in use of high-performance piston engines for aircraft use. The 'supercharged 17.6' test also exists but this is not performed using the CFR engine; a much larger single-cylinder engine with an air-cooled cylinder is used, based upon the Wright R-1820 radial engine (Drell and Branstetter, 1950). In contrast, the CFR engine is cooled by an evaporative liquid cooling system (Horning, 1931).⁴



Fig. 3.4: The CFR™ variable compression ratio test engine, adopted as the standard fuels rating engine across the automotive and petroleum industries.

(Photograph provided compliments of DresserWaukesha)

⁴ The CFR engine can also be fitted with 'F5' test equipment for determination of the cetane number of a fuel. A new piece of test equipment, the 'Ignition Quality Tester' (IQT) is also being introduced to perform the same function. This is a form of combustion bomb. Both the CFR F5 engine and the IQT, however, have a fairly small range of accuracy, which is an issue with synthetic diesel fuels which can be manufactured by methods such as the Fischer-Tropsch process (Yates *et al.*, 2007).

The operating conditions of the CFR engine for the widely-used Research and Motor methods are summarized in Table 3.1 (from Heywood, 1988 and ASTM International, 2007a and 2007b). The MON test is widely assumed to be the more severe of the two, since it encompasses higher intake temperature and 6-13° crank angle (CA) more ignition timing. Against this is set an engine speed ratio of 1.5 versus the RON test which will tend to increase the knock limit due to there being less time for autoignition of the end gas to occur. Both methods make use of the CFR engine's VCR system, which is configured so that the valve timing does not vary as the CR is changed.

Table 3.1: Operating conditions for CFR engine for RON and MON tests

Parameter	Research ('F1') method	Motor ('F2') method
ASTM number	D-2699	D-2700
Inlet temperature (°C (°F))	52 (125)	149 (300)
Inlet pressure	Atmospheric	Atmospheric
Engine speed (rpm)	600	900
Spark advance (° BTDC)	13 (fixed)	19-26 (varies with compression ratio)
Air/fuel ratio	Adjusted for maximum knock	
Humidity (kg / kg dry air)	0.0036-0.0072	
Coolant temperature (°C (°F))	100 (212)	

Operationally, the test methods are similar (ASTM International, 2007a and 2007b). The procedure is firstly to operate the engine on the test fuel and to find the maximum knock value (as determined by the standard ASTM knock meter equipment supplied with the CFR engine) at the conditions for the method being used. The CR is then adjusted to give a standard level of knock, presently required to be a value of 50 on the knock meter supplied with the equipment, but this value has been reduced from an original value of 55 (Swarts *et al.*, 2005). With the CR fixed at this value, different binary mixtures of the PRFs are tested until two PRF mixtures which bracket the test fuel in knock intensity are found. These must be to within two percent of the volume of isoctane in the PRF blend. To facilitate this process the CFR engine has a rapid switchover capability between three fuels, being the test fuel and two PRF blends. By interpolating the

percentage by volume of isooctane in the bracketing PRF blends between the meter readings for them and that of the test fuel, the octane rating of the fuel is obtained (Heywood, 1988).

Since the PRFs are the fuels used as the reference for both tests, they always have the same RON and MON values. This, therefore, applies to any binary mixture of the two. However, this does not follow for non-PRF fuels because clearly the octane number of a fuel is dependent on the test method being used. The difference between RON and MON for any fuel is termed the octane sensitivity of the fuel (S), and again, by definition PRFs and their mixtures have a sensitivity of zero. The subject of octane sensitivity will be returned to later.

When the rating methods were originally laid down, most commercial hydrocarbon fuels effectively had an octane rating of less than 100, with specialized fuels such as benzene and toluene and some of the alcohols being known to be more knock resistant (Campbell *et al.*, 1930). However, practical fuels have been developed in the intervening years with greater knock resistance than isooctane, necessitating that some means be found of extending the octane scale. This was done by taking 'clear' (i.e. pure) isooctane and adding TEL to it to increase its knock resistance, TEL having been developed to have strong antiknock capability since the original adoption of isooctane as the upper limit fuel (Heywood, 1988 and Boyd, 1950)⁵. For octane values above 100, the octane number is calculated from:

$$ON = 100 + \frac{28.28V_{TEL}}{1.0 + 0.736V_{TEL} + \sqrt{1.0 + 1.472V_{TEL} - 0.035216V_{TEL}^2}} \quad Eqn\ 3.4$$

where ON is the derived octane number, and V_{TEL} is the number of millilitres of TEL added per US gallon of isooctane (Heywood, 1988). Therefore, TEL could be considered to be a 'third' PRF, but this view is not found in the literature.

⁵ TEL has the chemical formula $(C_2H_5)_4Pb$ and contains 64.06% by weight lead. 1 ml of TEL contains 1.06 g of lead (Heywood, 1988).

The author has observed fuels testing in a CFR engine. There is no doubt that it is a relatively robust process. However, it is immediately apparent that the test conditions themselves are very different to those pertaining in modern engine designs, which is also true of the general architecture of the CFR engine itself. It could be argued that the CFR engine actually 'measures what the CFR engine measures', and that modifications to the results it gives are needed to give the results relevance to current engine designs. This subject is returned to in Section 3.4.

Swarts *et al.* (2005 and 2007) discuss some of potential shortcomings of the CFR equipment, not least the fact that the standard magnetostrictive knock meter pickup was painstakingly developed as an electrical analogue of the Midgley 'bouncing pin' apparatus. This effectively limits the range of frequency it can detect. Swarts (2006) contends that what the equipment actually defines as 'knock' is in reality an inflection in the cylinder pressure curve which occurs as a result of flame acceleration because of a preconditioning of the end gas. This is a form of cascading autoignition and appears to be a peculiarity of the CFR engine design itself. Therefore, the CFR equipment does not reveal knock as a high-frequency phenomenon, its detection instead coinciding with when the flame acceleration causes deflection of the cylinder diaphragm originally used in the Midgley bouncing pin equipment. In turn, this helps to explain why fuels of markedly different autoignition characteristics can share the same RON or MON ratings (Swarts, 2006).

Lovell (1948) showed how many paraffin and other hydrocarbon fuels relate to each other in terms of knock resistance, indicating that few easily-manufactured pure hydrocarbons have higher knock resistance than isooctane. One such is 'triptane' (2,2,3-trimethyl butane), an isomer of heptane. Triptane is difficult to manufacture in large quantities and so is more usually used as a blending agent in gasoline for very-high-performance piston aircraft engines. Its adoption as the upper rating fuel would have made for a 'wider' rating scale and the two components of the mixture would have been even more similar in terms of

density, heating value etc., than isooctane and n-heptane. This is because, while isomers of the same compound are known to share these characteristics, they can differ markedly in autoignition resistance as a result of increased branching in the molecule (Curran *et al.*, 1995)⁶. In Figure 3.5, Lovell (1948) shows the knock resistance of various paraffins in terms of CCR and how it relates to isomerization of the molecules, including the PRFs isooctane and n-heptane.

Note that triptane is the most knock-resistant paraffin shown in Figure 3.5 (disregarding methane). This illustration has also been used in discussion of knock resistance by other authors, notably Germane (1985). Heywood (1988) combines elements of other illustrations in Lovell's work to compare the performance of some paraffins, olefins and aromatics. In the same work Lovell (1948) discusses the effect of increased chain branching in a molecule and describes the way in which a molecule's knock resistance changes with isomerization. Figure 3.6 illustrates how knock resistance, defined in terms of CCR, changes for the different isomers of octane. Westbrook (2000) also discusses the effect of isomerization in pentane molecules, showing that although the three isomers n-pentane, neopentane (2,2-dimethyl propane) and isopentane (2-methyl butane) all ignite at the same temperature following compression in a rapid compression machine, the different induction times are attributable to the amount and rate of heat created during the first stage of the autoignition process. The order of ignition is the same as the increase in CCR as shown in Figure 3.5 (see the isomers shown for five-carbon-atom molecules on the x-axis).

⁶ At this point, there is an interesting comparison to the Primary Reference Fuels presently used for rating diesel fuels as defined by the ASTM D613 procedure used for that purpose. The two fuels currently in use for this rating scale are n-hexadecane (also known as n-cetane, from which the scale takes its name) and 2,2,4,4,6,8,8-heptamethyl nonane (also known as HMN), which is a highly-branched isomer of n-hexadecane. Thus these fuels share similar characteristics in density, lower heating value etc., but have markedly different autoignition characteristics which would have been advantageous in the Primary Reference Fuels used for octane testing. n-Hexadecane has a cetane value of 100.0, and HMN has a cetane value of 15.0. Yates *et al.* (2004) discuss some of the shortcomings of the present approach to cetane ratings and also apply their own autoignition ignition delay model to the autoignition of diesel fuels in later work (Yates *et al.*, 2007).

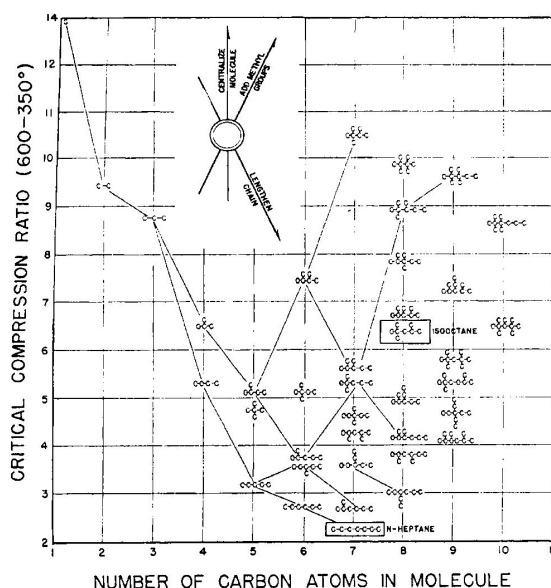


Fig. 3.5: Knock resistance of various straight-chain and branched paraffins expressed in terms of critical compression ratio, showing the primary reference fuels isooctane and n-heptane adopted for rating purposes. Triptane, a highly-branched isomer of heptane, has the highest knock resistance after methane on this figure, with a CCR of 10.5. The term '600-350°' on the y-axis relates to engine speed in rpm and intake air temperature in °F for the test engine used. (Reproduced from Lovell (1948), by permission of the American Chemical Society)

While for paraffins isooctane has the highest anti-knock capability that was practically available when the RON and MON procedures were being formulated (Edgar, 1927), as discussed earlier some newer compounds and fuels have greater anti-knock capabilities (Lovell, 1948), and the scale has had to be extended using TEL addition to clear isooctane (Heywood, 1988). This increase in octane value above 100 is required especially in the case of some partially-oxidized fuels such as the low-carbon-number alcohols methanol and ethanol (CH_3OH and $\text{C}_2\text{H}_5\text{OH}$, respectively) and some, but not all, of the ethers (Drell and Branstetter, 1950 and Leppard, 1991). An example of one of these high-octane ethers is methyl *tert*-butyl ether (MTBE), which has often used as a blending agent in gasoline (Fieweger *et al.*, 1997).

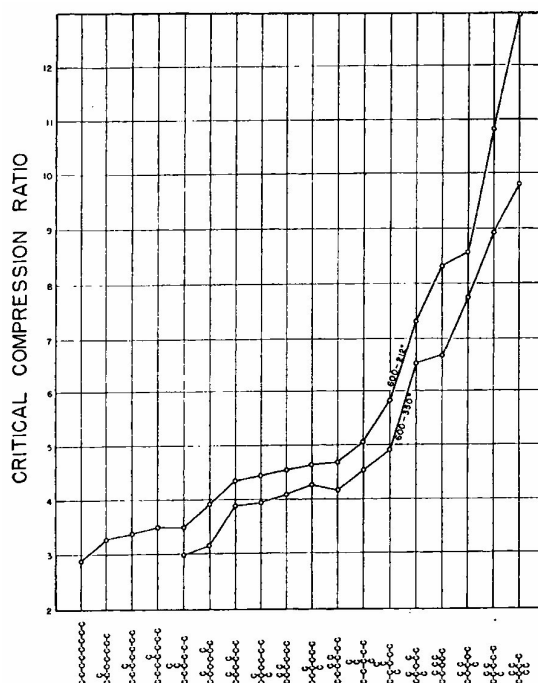


Fig. 3.6: Effect of isomerization on knock resistance in C_8H_{18} molecules (expressed in terms of critical compression ratio). The 'upper limit' primary reference fuel for knock testing, isooctane (or 2,2,4-trimethyl pentane), is fifth from the right of the 18 isomers of octane shown. (Reproduced from Lovell (1948), by permission of the American Chemical Society)

Although the RON and MON tests are precisely set down, both could be regarded as critical compression ratio (CCR) tests. Ricardo was a proponent of a pure CCR method, which he termed the 'highest usable compression ratio' (HUCR) of a fuel (Institution of Automobile Engineers, 1924). A test to determine the CCR (or HUCR) would commonly use a fixed ignition advance and intake conditions with the CR being increased until the knock limit was reached (Institution of Automobile Engineers, 1924). Much data exists comparing fuels in terms of CCR, albeit it at different values of engine intake conditions, spark advance etc., and most of Lovell's comparison work uses this as the rating scale, as shown in Figures 3.5 and 3.6 (Lovell, 1948). It could be argued that the extra step in the RON and MON tests of finding the mixture of PRFs to give an octane

rating to a fuel is perhaps a redundant one, since CCR is a direct step on the path to obtaining the octane rating. However, in order to do this, all of the test equipment around the world would have to be absolutely identical. Hence the extra step of finding the binary mixture of PRFs which yields the same knock value as the test fuel at a given CR removes most of the influence of the test equipment and makes the process robust.

Perhaps one operational change to further remove variability from the process would be to fix the AFR at which the knock test is conducted, instead of merely stating that it should be that for maximum knock (see Table 3.1). An ideal would perhaps be to specify stoichiometry. In recognition of the fact that non-specified λ introduces some uncertainty, there are guides issued with the RON and MON tests which show the relationship between ON as measured with the CFR engine and CR (Yates *et al.*, 2005). These relationships are shown in Figure 3.7. Clearly evident is the non-linear nature of ON with CR in this test, and the fact that the two tests yield curves with different shapes, a function of the different engine speeds, intake conditions and ignition advance used with each procedure.

Westbrook (2000) presented data taken by Leppard which showed a clear relationship between CCR and octane rating, gathered under motored conditions equating to the intake conditions for the RON test and at stoichiometric AFR. This was compared to calculated results and is reproduced in Figure 3.8, below. It clearly suggests that in fired tests, if the AFR were fixed, the extra step to find the octane index could be made redundant as discussed above. Westbrook also made the observation that in these motored test results, "*a rather smooth curve results ... indicating that octane rating is a rather nonlinear scale*". This reinforces the earlier data of Campbell *et al.* (1930) for mixtures of n-pentane and isooctane and presented in Figure 3.3 above. Note that the difference between the lowest CCRs shown in the Figures 3.3 and 3.8 is due to the motored nature of the results presented by Westbrook.

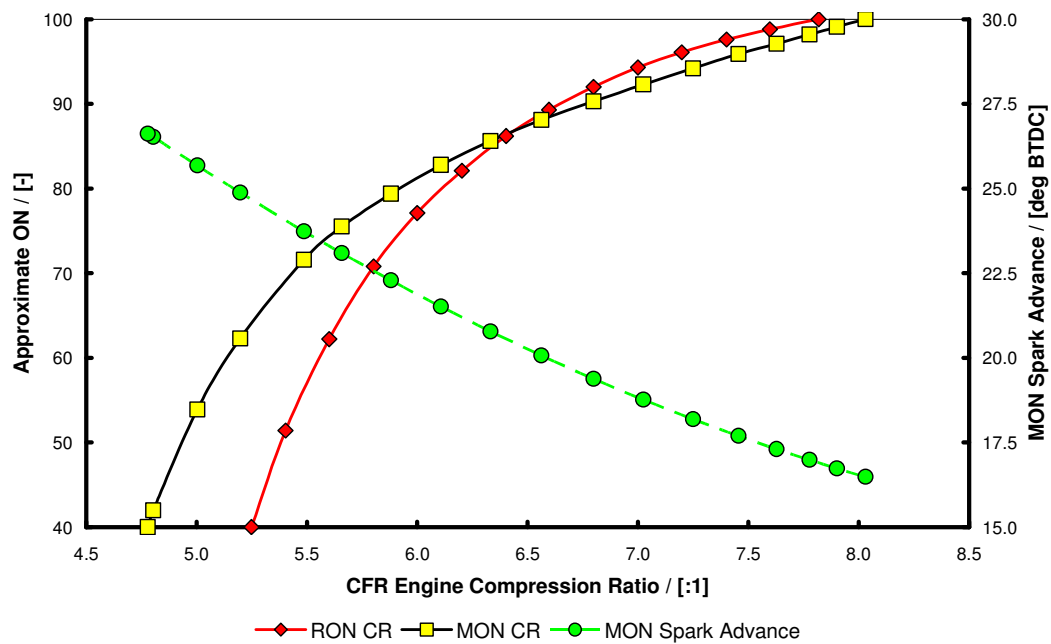


Fig. 3.7: Guide for the relationship between compression ratio and approximate ON for the CFR engine when conducting RON and MON tests. MON test spark advance as shown. For the RON test, the spark advance is fixed at 13° BTDC. (Data courtesy of Sasol Advanced Fuels Laboratory, University of Cape Town)

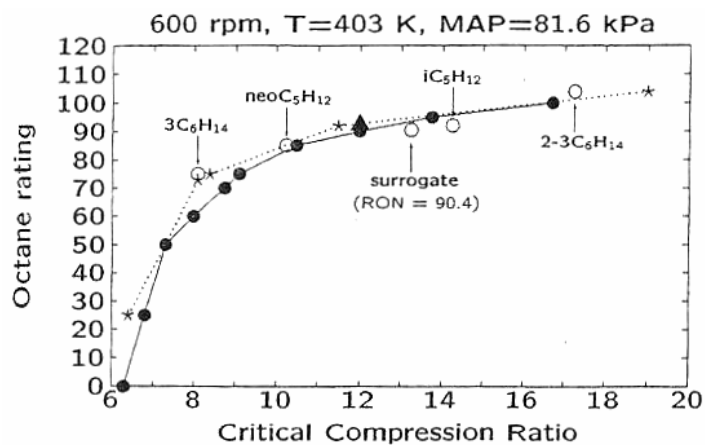


Fig. 3.8: Correlation of computed CCR with RON under motoring conditions. Solid circles are PRF mixtures, open circles are isomers of hexane and pentane and a gasoline surrogate, and stars are experimentally-measured values. (Reproduced from Westbrook (2000), by permission of Elsevier)

Another fuel rating procedure is the US Army-Navy Performance Number (or AN Performance Number). This has effectively been made obsolete by the demise of the piston engine as a powerplant for high-performance aircraft. Much literature employing this rating scale exists up to about 1960, and Mason and Hesselberg (1954) show a relationship between AN number and CCR in terms of the two PRFs. This is reproduced in Figure 3.9. Kerley and Thurston (1956) also relate AN Performance Number to RON and MON in a method using nomograms to establish the response of engines to changes in fuel property.

Finally, Lignola and Reverchon (1987) have investigated the use of a CSTR to determine MON directly, and show that the frequency of periodic cool flames in such apparatus correlates with the MON rating of fuels by conventional means.

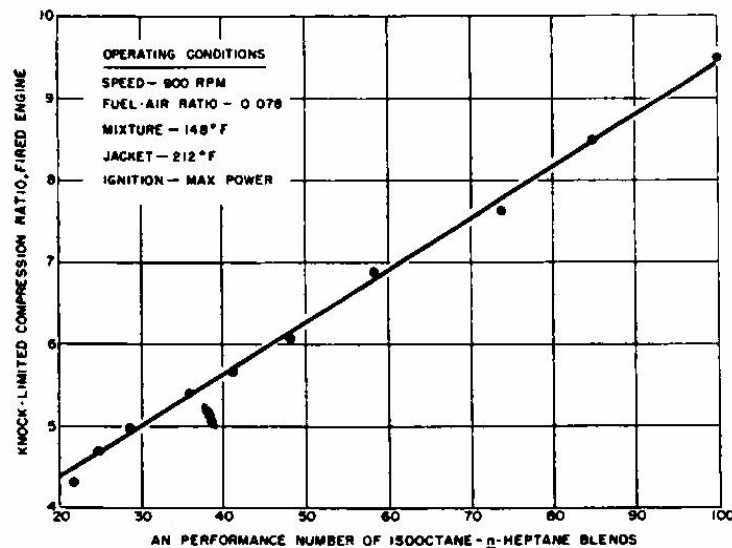


Fig. 3.9: Linear relationship between Army-Navy ('AN') Performance Number of isooctane/n-heptane blends versus critical compression ratio. (Reproduced from Mason and Hesselberg (1954), reprinted with permission from SAE Transactions, Vol. 62, pp. 141-150, © 1954 SAE International)

3.4 APPROACHES TO EXTEND THE RELEVANCE OF RON AND MON RATINGS

Kerley and Thurston (1956) use a nomographic approach to predict the response of engines and vehicles to changes in fuel composition, and report a good correlation between predicted and measured results for changes in CR, engine speed, air density, distributor tolerances and temperature. This approach demanded many baseline tests be carried out on the so-called 'S'-series reference fuels. The use of toluene blended with the PRFs, in order to create control fuels with differing RON and MON values, will be discussed again in Section 3.7.

A multi-variable approach was also taken by Douaud and Eyzat (1978), who sought to establish the constants of the Arrhenius rate equations directly (Equation 3.3). They used the results of RON and MON tests directly and also used elements of both tests to create two further octane rating methods which they term 'RON prime' and 'MON prime'. Essentially the speed of the RON test was used with the intake conditions of the MON test to create the 'RON prime' test and *vice-versa*. They used all four of these ratings to enable planar plots to be drawn and to determine the knocking behaviour of a fuel and engine at any operating point. Douaud and Eyzat (1978) claimed the accuracy of their method was within 0.5 octane units. They also observed that a fuel shows more sensitivity to temperature if the constant B in Equation 3.3 is high.

A similar multi-variable approach was taken by Kalghatgi (2001a and 2001b), who examined octane sensitivity (S), and applied a weighting factor (K) to determine the octane index (OI) of the fuel at any given condition, such that

$$S = \text{RON} - \text{MON} \qquad \text{Eqn 3.5}$$

and

$$OI = (1 - K) RON - KMON. \quad \text{Eqn 3.6}$$

Equations 3.5 and 3.6 imply that

$$OI = RON - KS. \quad \text{Eqn 3.7}$$

Of particular interest in Kalghatgi's work is that modern engines increasingly appear to require a fuel with high sensitivity, i.e. that when operated on a fuel with a given RON they have greater knock resistance if the fuel has a lower MON. In fact, in one of his papers the results suggested that K is now negative for modern engine and fuel combinations (Kalghatgi, 2001a). Kalghatgi cites Leppard (1990) in explaining the importance of fuel chemistry on the reaction of paraffinic, aromatic and olefinic fuels to the RON and MON tests, and contended that modern engine designs require fuels that are characterized by more than their RON rating to determine the 'octane appetite' of the engine, this being the minimum octane required to operate without knock throughout its speed and load range. Thus he contended that modern engine design is moving 'beyond RON'.

Kalghatgi's contention is supported by the work of Duchaussoy *et al.* (2004), in which a turbocharged engine fuelled at $\lambda = 1$ showed greater sensitivity to increasing RON over increasing MON when the other value was held constant. All of this being so, it could be argued that the fact that European fuel standards effectively constrain the MON value of a fuel to be no more than ten octane units lower than its RON value is not assisting in the development of efficient downsized engines. On this subject it should be mentioned that in the US the 'anti-knock index' quoted on forecourt pumps coincides with Kalghatgi's OI when $K = 0.5$ in Equation 3.6, and is indicative of an attempt to provide the customer with an octane number more relevant to in-vehicle use (Heywood, 1988).

Many of these fuel factors are brought together by Burluka *et al.* (2004) in a comparative study of knock with and without different types of simulated residuals. Burluka *et al.* (2004) showed that a modified Douaud and Eyzat

prediction with a compensation for the K -factor-modified octane number propounded by Kalghatgi (2001a) gave a very good correlation for different engines, fuels and operating conditions. More recently, Kalghatgi *et al.* (2005) have again shown the importance of the charge temperature to knock sensitivity at given compression pressures in SI engines and have shown that the lower the temperature, the more negative K becomes, i.e. that the octane index of the fuel increases (Equation 3.6) and it therefore becomes more knock resistant. Yates *et al.* (2005) and Viljoen *et al.* (2005) have presented modelling results which support the contention that modern engine design is moving in the direction of favouring RON testing, and that pressure-charged engines appear to have moved beyond RON in a manner similar to Kalghatgi's contention. Their work was based upon modelling of a surrogate gasoline fuel blend, being a combination of six different compounds. The general results of their investigations into fuel requirements and engine technology level are shown in Figure 3.10, which clearly supports the contention that modern downsized engine design is increasingly requiring fuel blends outside the area characterized by the RON and MON tests.

Mittal and Heywood have undertaken similar work on the relevance of RON and MON in modern engine architectures (Mittal and Heywood, 2008) and have also conducted a comprehensive review of fuel standards over the last 70 years using data gathered by the CRC, comparing this to the changes in engine technology (Mittal and Heywood, 2009). This clearly supports the work of Kalghatgi (2001a and 2005), Duchaussoy *et al.* (2004), Yates *et al.* (2005) and Viljoen *et al.* (2005).

Against this backdrop of the effect of charge temperature- and pressure-history on the knock limit for any given type of fuel, the importance of providing an effective means of reducing charge air temperature in pressure-charged SI engines becomes very apparent.

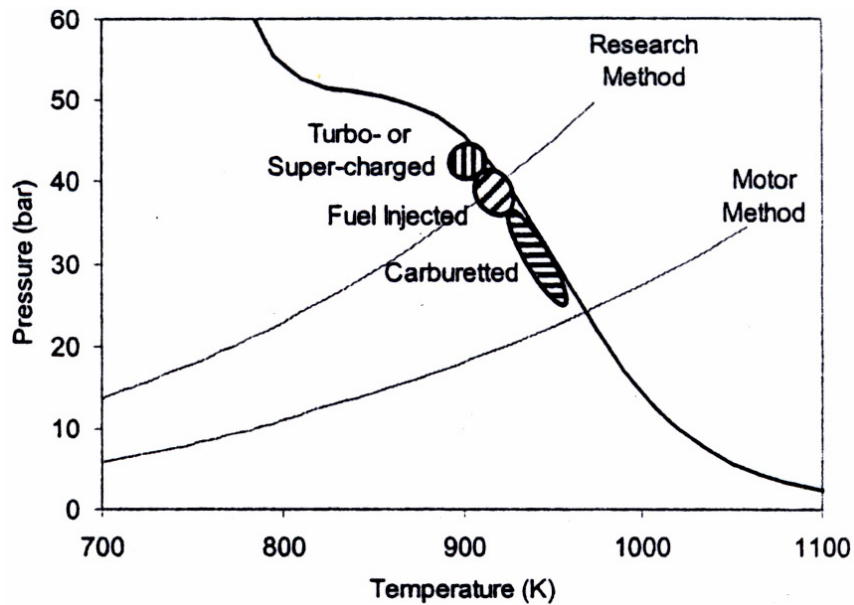


Fig. 3.10: Movement of autoignition limit for gasoline fuels with increase in technology level, showing modern pressure-charged engines to have moved 'beyond RON'. The pressure and temperature referred to on the axes are those of the charge. Solid line represents autoignition limit for a full boiling range gasoline. (Reproduced from Yates *et al.* (2005), reprinted with permission from SAE paper number 2005-01-2083, © 2005 SAE International)

3.5 OTHER FACTORS INFLUENCING THE OCCURRENCE OF KNOCK

König *et al.* (1990) pointed out that, in addition to compression and convective heating, exothermic centres (ETCs) or 'hotspots' in the combustion chamber can play a strong role in promoting autoignition. Indeed, they contended that it is probable that autoignition is initiated from such points. These ETCs can either be the result of high local surface temperatures or of inadequate mixing of hot residual gases. They give rise to thermal gradients of ~ 12.5 K/mm, leading to the developing detonation events described by Pan and Sheppard (1994). Building on the observations of Zel'dovich *et al.* (1970), Weber *et al.* (1994) show how the mixture temperature gradient and the temperature of the end gas can lead to a coupling of a hot-spot initiated pressure and combustion waves which can subsequently become a detonation wave. Equally, the pressure and combustion

waves can decouple under some circumstances, the combustion process then reverting to a deflagration wave.

Curry (1963) showed how swirl in a combustion chamber can affect the direction of flame development and hence heating of the end gas as a result of the different surface temperatures in its proximity. Schreiber *et al.* (1993 and 1994) discussed the process by which ETCs can move in the combustion chamber and initiate autoignition, and Rothe *et al.* (2006a) discussed the necessary size of an ETC to promote destructive autoignition. Maly (1994) stated that “*although autoignition is controlled by temperature, engine knock with its intensity is controlled by the properties, distribution and fluid dynamic interactions of ETCs resulting from preceding mixing processes*”.

An important factor in the magnitude of temperature inhomogeneities in the gas can be high concentrations of trapped residuals. The effect of trapped residuals on pressure-charged engine combustion has been investigated by Westin *et al.* (2000). It has also been extensively investigated by Rothe *et al.* (2006b), Zaccardi *et al.* (2009a and 2009b) and Willand *et al.* (2009) with regard to preignition leading to autoignition in heavily pressure-charged engines. Direct purging of residuals can be arranged in a DISI engine by employing large amounts of valve overlap (Klütting *et al.*, 2005 and Sauerstein *et al.*, 2009). however, this is not a route open to port fuel injected (PFI) engines where the homogeneous mixture that passes through the engine would likely combust in the exhaust system. This would create thermal durability issues for the manifold and other exhaust system components such as the turbine and catalyst.

In all pressure-charged SI engines the effect on knocking combustion of the heat energy added to the charge during the external compression stage is compounded by heat transfer from the engine structure during intake and the early stages of compression. Taitt *et al.* (2006) point this out in the modelling of a turboexpansion system fitted to an engine where, due to the increased difference between charge air temperature and engine structure due to the over-cooling of the charge air as a result of the performance of the charging system, a greater

amount of heat transfer to the air takes place. This is counter to the aims of deploying such a system and will need careful consideration in the successful application of any such system. The same will apply to reducing the charge temperature by using pre-compressor introduction of fuel as discussed by Hooker *et al.* (1941), Rosenkranz *et al.* (1986), Turner and Pearson (2001) and Turner *et al.* (2007a). In terms of its relevance to establishing the octane rating of fuels, Swarts and Yates (2007) discuss how such heat transfer effects the results obtained from the CFR engine during knock testing.

At this point, reference should be made again to the work of Bradley *et al.* (1996a and 1996b) who show that there is a 'critical radius' for a hot spot within the charge to initiate autoignition. This critical radius is of the same order as the integral length scale of turbulence in the chamber, and they show that the more reactive the mixture, the smaller this critical radius. They also show that cyclic variations of knocking behaviour can arise from cyclic variations in the burn rate.

The propensity for residuals to promote knock in engines is not only due to the thermal energy retained in the cylinder during the next cycle in general, or to the formation of inhomogeneous exothermic centres in particular (König *et al.*, 1990). There can also be an effect of certain chemically-active species in the residual gas. This has been studied in depth by employing intake systems capable of precise mixing of the two major constituents of oxides of nitrogen (NO_x) found in exhaust gas, NO and NO₂. Burluka *et al.* (2004) use such a technique to investigate the effect of intake temperature and the temperature at pre-determined pressures during the compression process. Similar research has been conducted with 'simulated air' (usually mixtures of argon in oxygen) instead of atmospheric air in order to remove the effect of nitrogen on combustion in engines (Eng *et al.*, 1997 and Kawabata *et al.*, 1999) and rapid compression machines (Griffiths *et al.*, 1997). Kawabata *et al.* (1999) reported a linear relationship between NO fraction and knock intensity. Eng *et al.* (1997) were primarily concerned with the formation of hydrocarbon emissions, although they did discuss the role of NO as a knock promoter by its helping to produce OH radicals in the low and intermediate temperature ranges in which autoignition is

promoted, thus reinforcing earlier observations made by Ricardo and Hempson (1968). Prabhu *et al.* (1996) have also investigated the effect of NO on the ignition chemistry of 1-pentene, demonstrating that the effect is very temperature dependent for some hydrocarbon compounds.

Stenlås *et al.* (2002) have similarly investigated the effect of NO concentration on knocking propensity and have also shown that while, up to a point, increasing NO increases knock, a maximum influence is reached. Here there is a clear synergy with the earlier observations of Prabhu *et al.* (1996). Stenlås *et al.* (2002) state that of the major NO_x chemicals, only NO is important as an ignition enhancer, and also observe that the mixture strength is important, such that rich conditions suppress the formation of NO directly and so delay the onset of knock while the opposite is true of lean mixtures, up to the point where very lean mixtures start to suppress NO formation and hence the knock limit starts to extend again. All of this could be considered to be in support of Kawabata *et al.* (1999), taking their investigations further, as well as the later work of Duchaussoy *et al.* (2003).

In a later paper, Stenlås *et al.* (2003) used ion current measurement to determine both the onset of knock and the influence of NO concentration and mixture strength on knock intensity. Here they found that while their new results did reinforce the conclusions from their earlier work (Stenlås *et al.*, 2002), there was no connection between intake NO concentration and the mean crank angle at which knock occurred.

Taylor *et al.* (1998) have also investigated the effect of NO addition on combustion of methanol and ethanol. They also reported that the primary promoting pathway was the formation of OH radicals due to the reaction of NO with HO₂:



They discuss a competing pathway that scavenges the NO in which:



where M is a third body facilitating the reaction. R-2 produces the stable intermediate nitrous acid, but in the case of alcohol combustion, is not favoured over R-1 due to the faster reaction rates of OH with the alcohol molecules. A slight negative temperature dependence is reported in R-2, but this only means that higher temperatures tend to favour the production of OH and subsequent reaction with the alcohol and not combination with NO.

In investigations using a motored CFR engine, Leppard (1987) has also shown an increase in heat energy due to precombustion reactions can lead to autoignition in the next cycle. This is shown in Figure 3.11, which shows pressure traces for two consecutive cycles, and in which one can see the late autoignition of the n-butane in the second cycle. The pressure trace of this second autoigniting cycle is slightly higher than the first non-autoigniting cycle from just before TDC, indicating chemical reaction occurring. After autoignition the residuals become mainly the combustion products H₂O and CO₂, changing the balance of residuals in the chamber and causing the alternating shift between non-autoigniting and autoigniting cycles.

From the observation that many of the radicals formed in combustion contribute to the initiation of low temperature chemistry in the following cycle (be they NO or fuel-based radicals) it can be concluded that any increase in CR to reduce the clearance volume of the engine would particularly be of benefit in PFI engines, since this reduces the amount of active species carried over in retained residuals. This is especially the case in turbocharged PFI engines because the cylinder cannot be purged of residuals with only fresh air during an extended valve overlap phase, as is possible when DI is employed (Wirth *et al.*, 2000, Lang *et al.*, 2005, Klütting *et al.*, 2005, Sauerstein *et al.*, 2009). However, it must be remembered that the mass of residuals trapped is a function of both pre-turbine pressure and temperature (i.e. the density of the exhaust gases) as well as the

clearance volume of the engine. The exact form of the pressure-charging system used will, therefore, have a bearing on the mass fraction of residuals retained in the cylinder as a result of the multiplication of the main exhaust system back pressure by the overall expansion ratio of the turbine stage (in the case of a conventional turbocharger-based system).

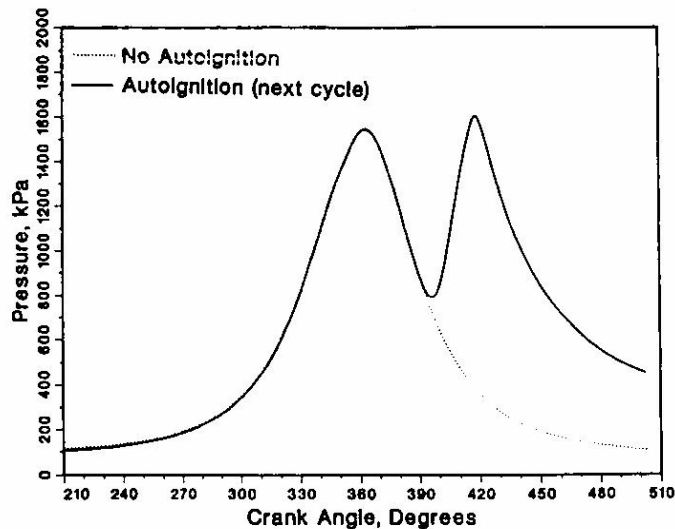


Fig. 3.11: Cylinder pressure histories for two consecutive engine cycles for a CFR engine motored at 600 rpm, fuelled with n-butane at a CR of 8.32:1 and with an intake manifold pressure of 100 kPa. The first cycle (dotted line) shows no autoignition. The second cycle (solid line) shows a pressure trace above the dotted line from $\sim 350^\circ$ CA (or 10° BTDC), with autoignition occurring from $\sim 390^\circ$ CA (or 30° ATDC). Reproduced from Leppard (1987). (Reprinted with permission from SAE paper number 872150, © 1987 SAE International)

The turbine stage can therefore have a significant bearing on the knock limit of the engine, and is one of the factors motivating the need for more efficient turbocharging systems with respect to balancing the pressures across the combustion chamber. This effect is believed to be at the root of the poor performance of the Nomad research engine with respect to its knock limit when fitted with its turboexpansion system and reported by the author and co-workers (Turner *et al.*, 2005a). This work will be discussed in detail in Chapter 4.

Compound-charged engines are now being produced partly to alleviate this problem (Krebs *et al.*, 2005a and 2005b). A comprehensive study of the effect of the turbine stage in turbocharged engines was made by Westin (2005). Sauerstein *et al.* (2009 and 2010) have investigated combinations of pulse-divided exhaust manifolds and variable turbine geometry and the use of two-stage turbocharger systems in SI engines with respect to improving the pressure differential across the engine. However, the use of 3-cylinder configurations to provide optimum pulse separation with sufficient time-area to provide good scavenging with minimal residual trapping is potentially an architectural approach which will give a closer-to-ideal solution. Investigations using such an engine will be reported later in Chapters 7 and 8.

3.6 KNOCK SUPPRESSION BY CHARGE DILUTION

The most widespread, and to some extent the most pragmatic, approach to extending the knock limit of any given engine geometry has historically been to retard the ignition and enrich the mixture (Heywood, 1988). The excess fuel slows down the combustion process by absorbing some of the heat released, while the delay in ignition timing phases the combustion event later with regard to compression. This lowers the peak cylinder pressures. Both approaches clearly increase fuel consumption, and ignition retard also causes hotter temperatures at exhaust valve opening (EVO). However, other means of providing a 'sink' in the cycle for combustion heat have been known for many years. In early work, Ricardo discussed the effect of charge conditioning both by air and by cooled exhaust gas (Ricardo 1919 and 1920 and Institution of Automobile Engineers, 1924). These approaches are being investigated currently as a means to avoid the increase of fuel consumption at high load associated with the fuel enrichment approach. Grandin and Angström (1999) and Duchaussoy *et al.* (2003) compared the effect of excess air with cooled EGR and conventional enrichment fuelling, and Grandin *et al.* (1998 and 2001) studied the cooled EGR approach in detail. Stokes *et al.* (2000) and Lake *et al.* (2004a and 2004b) proposed the use of excess air as a diluent to suppress knock, but Hiroshi *et al.* (2004) concluded that in an excess air strategy, the high ratio of specific heats of the excess air

ensures a higher temperature rise during compression of the end gas than if cooled EGR was used as a knock suppressant instead. This in turn increases, rather than reduces, the likelihood of knock occurring.

While Lake *et al.* (2004a and 2004b) were very supportive of their so-called 'lean boost' excess air approach, they also showed very nearly equivalent results with cooled EGR. De Petris *et al.* (1994) used a CFR engine to show that the knock limit of an engine fuelled on gasoline and operated at stoichiometric AFR could be usefully extended to the benefit of fuel consumption by using cooled EGR, and in related later work Diana *et al.* (1996) successfully applied the technique to a multi-cylinder vehicle engine. In two related papers, Cairns *et al.* (2006) and Hattrell *et al.* (2006) showed that cooled EGR can provide the ability to operate a turbocharged engine on gasoline at a high CR with stoichiometric fuelling at 18.8 bar BMEP. Particularly, Hattrell and co-workers showed that in terms of knock suppression, cooled EGR is preferable to operation with excess air for the same reasons as those cited by Hiroshi *et al.* (2004).

There is, therefore, a developing consensus that cooled EGR is the most effective method of suppressing knock in diluted boosting systems, particularly when it is remembered that a lean boost approach as favoured by Lake *et al.* (2004a and 2004b) will result in the requirement for a NO_x trap if it is to be used as a strategy throughout the operating range. Conversely, cooled EGR permits the use of a simple and robust three-way catalyst and would also permit a degree of the commonly-used fuel dilution if necessary without significantly effecting high-load fuel consumption. Of course, the attractiveness of any of these methods is dependent on the position of the knock limit with respect to the engine operating points in the vehicle drive cycle. Cooling the EGR also means any radicals still active in the exhaust gas should be deactivated through the EGR loop, ensuring an inert gas feed to the intake. However, stable species would still be present. Hoffmeyer *et al.* (2009) discussed a novel approach to deactivating such species, placing a catalyst in the EGR loop to fully convert the gas and ensure a maximum amount of water and CO₂ in the cooled EGR fed to the intake. Using kinetic modelling they showed that the most important species deactivated

using this approach are NO and acetylene. However, Roth *et al.* (2010a) presented results which suggested that catalysis of the EGR gas may not be beneficial. Thus the approach of catalyzing the EGR requires further investigation.

Alcohol fuels have a high octane rating in their own right, with methanol and ethanol having RON values of 106-109 (Germane, 1985 and Owen and Coley, 1995). One of the reasons for the spread in RON is that alcohol fuels can pre-ignite under some conditions (Hagen, 1977), and the design of the CFR engine used to rate fuels makes this a possibility. Note that preignition similarly makes assessing the octane rating of hydrogen problematic (Verhelst *et al.*, 2006), which could be a contributing factor in some results investigating mixtures of CO, methane and H₂ in a CFR engine (Li and Karim, 2006).

Alcohols, moreover, possess another advantage with regard to operation at high levels of EGR in that they possess a laminar flame velocity ~50% higher than that of gasoline (Metgalchi and Keck, 1982 and Neame *et al.*, 1995). Ryan and Lestz (1980) showed that, in the absence of a diluent, methanol has a significantly higher laminar burning velocity than several other hydrocarbon fuels (except, interestingly, n-heptane). They also showed that, in general, introducing 10% mass dilution reduced the laminar flame speed by ~27% for the fuels that they tested. Because alcohols initially have a much higher laminar flame speed, they can tolerate greater amounts of diluent than gasoline before the flame extinguishes. Ryan and Lestz (1980) showed that as the amount of diluent increases, the laminar flame speed of methanol becomes proportionally much higher than isooctane, and overtakes that of n-heptane as the level of dilution is increased. In general, this means that, since far greater levels of EGR can be tolerated by an alcohol, then as a result when it is cooled it can also be used to extend the knock limit further.

Employing this strategy, Brusstar *et al.* (2002) and Brusstar and Bakenhus (2005) showed that when operating a light-duty diesel engine converted to SI and PFI on

methanol and ethanol, operation at stoichiometric conditions and a CR of 19.5:1 is possible. They used up to 50% cooled EGR in the air charge mass. This strategy yielded thermal efficiencies as high as 43%, in excess of the maximum given by the same engine operating as a diesel, and indeed over a wider speed and load range. The same strategy has been proved on a medium-duty diesel engine (Brusstar and Gray, 2007). In another converted diesel engine and using supercharging, direct injection and operation on methanol, Sato *et al.* (1997) showed that reducing the degree of charge cooling of the air did not change the thermal efficiency of the engine. They also showed a high level of thermal efficiency being maintained with up to 23% EGR and further benefits (primarily in NO_x formation) when using an EGR cooler.

Clearly low-carbon-number alcohol fuels have potential for future high efficiency engines, a fact reinforced by Turner *et al.* (2007a) who showed that the full-load thermal efficiency of a high CR supercharged engine could be increased by a factor approaching 1.2 by operating on E85 (a blend of 85% ethanol and 15% gasoline) in comparison to 95 RON gasoline. The fact that ethanol and methanol can be made from renewable sources makes these fuels worthy of further research to gauge their suitability for any future mobility scenario (Hammerschlag, 2006, Pearce, 2006b, Olah *et al.*, 2006, Pearson and Turner, 2007, Turner *et al.*, 2007b and Pearson *et al.*, 2009b).

3.7 EMPLOYING THE LATENT HEAT OF VAPORIZATION OF A FUEL TO INCREASE THE KNOCK LIMIT

The effect of fuel vaporization and its ability to cool the charge when fuel is injected directly is a well-known means of increasing the knock limit (Anderson *et al.*, 1996). If the fuel is injected during the intake phase, the volumetric efficiency improves, but if injection occurs in the compression phase (i.e. post-IVC) it will cool the compressing charge and simultaneously reduce its pressure. This influences the temperature- and pressure-time histories of the end gas. The effect has been shown to be equivalent to increasing the octane rating of a gasoline-type fuel from 96 to 100 in a PFI engine by Okamoto *et al.* (2003), who

investigated the relationship between fuel delivery system, fuel octane rating and CR in a single-cylinder engine operating on fuels composed of 72% toluene with different proportions of n-heptane and isooctane to give them RON values of between 90 and 114. They showed that operation on PFI had a greater requirement for higher octane as the CR was increased. Hence the latent heat of vaporization could be disproportionately beneficial in direct-injection engines. Some fuels, notably the low-carbon-number alcohols methanol and ethanol, have significantly higher latent heats of vaporization when compared to gasoline, which can be used to the benefit of knock suppression (Germane, 1985 and Owen and Coley, 1995). Some of the properties of gasoline, ethanol and methanol, including latent heat of vaporization, are shown in Table 3.2.

Table 3.2: Properties of gasoline, ethanol and methanol. Data taken from Owen and Coley (1995), Bosch (2000) and Turner et al. (2007b)

Property	Gasoline (Typical)	Ethanol	Methanol
Chemical formula	Various	C ₂ H ₅ OH	CH ₃ OH
Density at atmospheric pressure and temperature (kg/m ³)	740	789	791
Lower heating value (MJ/kg)	42.7	26.8	19.9
Stoichiometric AFR (kg/kg)	14.7	9	6.4
Specific energy* (MJ/kg mixture)	2.905	2.978	3.062
Specific energy ratio**	1	1.025	1.054
Volumetric energy content (MJ/m ³)	31.6	21.2	15.7
Research octane number	95	109	106
Motor octane number	85	98	92
Sensitivity	10	11	14
Latent heat of vaporization (kJ/kg)	180***	930	1170
Mole ratio of products to reactants****	0.937	1.065	1.061
Oxygen content by weight (%)	0	34.8	50

*At stoichiometric conditions **Relative to gasoline ***Assumes no alcohol present
****Including atmospheric nitrogen

Apparent from Table 3.2 is that, theoretically, it takes significantly more energy to evaporate a stoichiometric mixture of the alcohols than gasoline. However, in reality, the air saturates before this can happen (see later). Hence, to gain the maximum effect but no more, only a proportion of the fuel equating to that

required to saturate it should be injected to cool the air. Tests utilizing this approach in a supercharged engine utilizing PFI are discussed in Chapter 5.

Wyszynski *et al.* (2002) discussed the internal charge cooling effect of different types of fuel blends when injecting the fuel directly, including the benefit of using only a small amount of alcohol. Brusstar *et al.* (2002) discussed the change in compression work in a port-fuel-injection engine fuelled on methanol. The characteristic high latent heat of vaporization of low-carbon-number alcohol fuels can therefore readily be used to extend the knock limit of an engine when operating on such a fuel, as shown by Bromberg and Cohn (2010) in a discussion of the limits of direct injection of alcohols in heavy-duty engines. This is in a manner complimentary to the higher octane rating and faster flame speed of the alcohol. The fact that combustible mixtures of alcohol fuels and air possess a higher specific energy and a more favourable mole ratio of products to reactants than gasoline-air mixtures also makes them more attractive as high performance engine fuels (Germane, 1985). Their lower adiabatic flame temperature also brings benefits in heat rejection and hence in thermal efficiency. However, unlike gasoline, at conditions near to stoichiometry the air saturates with alcohol fuels and therefore a proportion of the combustion occurs in the liquid phase (Price *et al.*, 2007). This could be expected to yield a tendency to create soot at higher loads, although in trying to mitigate this fact, Sato *et al.* (1997) point out that methanol has no carbon-carbon bonds, and similarly ethanol has only one.

The use of ethanol and methanol as separate, directly-injected knock suppressants in a gasoline PFI engine has been proposed by Bromberg *et al.* (2006). They showed that the majority of the effect which can be realized by using such an approach in a mainly port-injected engine is primarily from the high latent heat of vaporization of the alcohol fuel. They suggested that because of the increased boost pressure that the engine can support, its swept volume can be halved with such an approach, and consequently that its fuel economy can be improved by 30% on a drive cycle. The validity of the approach was shown by Whitaker *et al.* (2010) in a DI engine fitted with auxiliary PFI to investigate the approach. Therefore, this technology could be as beneficial as VCR, because

similar improvements in in-use fuel economy were shown using VCR systems by Drangel and Bergsten (2000), Schwaderlapp *et al.* (2002), MCE-5 (2010) and De Gooijer (2011). The complication here is that the vehicle has to carry two fuel systems (one each for gasoline and the alcohol), although in the case of ethanol, the anticipated ethanol consumption on a drive cycle was calculated by Bromberg and Cohn (2006) to be ~5% of that of gasoline. This figure was shown to be dependent on vehicle type and drive cycle in the work of Whitaker *et al.* (2010). Interestingly, because of its higher latent heat of vaporization, Bromberg and Cohn (2006) found a similar result in terms of volumetric fuel consumption for methanol, which, given the similarity of its RON and MON values to those of ethanol, indicates that latent heat of vaporization is the more important factor.

3.8 OTHER MEANS OF SUPPRESSING KNOCK

Clearly, the most pragmatic approach to suppressing knock in an engine of fixed geometry is to operate it on a fuel of higher effective octane rating. This is shown by important work by Haghgoie (1990), who operated an NA four-valves-per-cylinder (4vpc) engine on two different fuels at different intake temperatures and showed a clear extension of the knock limit with increasing RON of the fuel and also with decreasing intake temperature. These effects are illustrated in Figure 3.12.

Haghgoie (1990) showed that a 30°C reduction in charge air temperature can outweigh a 6 unit change in fuel octane rating (in Figure 3.12, compare the 91 RON, 306 K data with that for 97 RON, 366 K). This is very significant and can be compared with data from Hiereth and Withalm (1979), suggesting that the knock limit of pressure-charged engines (as inferred from increasing boost pressure) increases as the charge air temperature is reduced. However, the rate of improvement is not linear, as is shown in Figure 3.13. Heywood (1988) reproduced this data in his text book as part of a discussion of factors influencing the knock limit in pressure-charged SI engines.

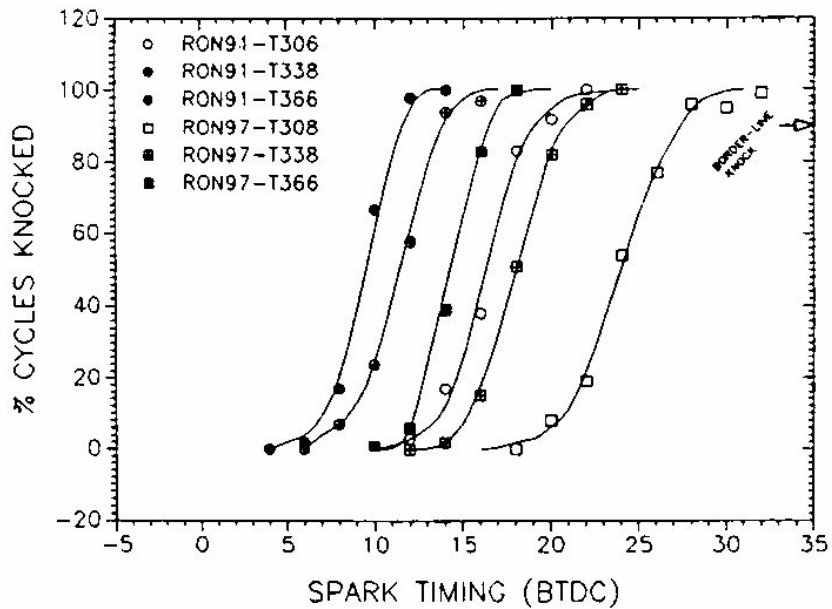


Fig. 3.12: Effect of increasing RON and decreasing charge air temperature on the knock limit in a naturally-aspirated 4vpc engine, as determined by ignition advance. Engine operated at stoichiometric AFR and at 1500 rpm. Intake temperature T in K. (Reproduced from Haghooie (1990), reprinted with permission from SAE paper number 902134, © 1990 SAE International)

Work by Tanaka *et al.* (2003) in an RCM used for the study of HCCI also shows that the ignition delay of PRF mixtures is related to initial charge temperature. Like Haghooie, Tanaka *et al.* (2003) used a constant fixed initial pressure and fixed compression ratio, but varied the temperature, i.e. in both cases the charge density changed. Figures 3.14 and 3.15 show respectively that the ignition delay varies with initial temperature, but that the burn rate (defined as the rate of pressure rise between 20 and 80% of the maximum pressure) does not correlate with the initial temperature. It is interesting to note from the results of Tanaka *et al.* (2003) in Figure 3.15 that the higher octane fuel (in this case isooctane) shows a stronger response to temperature than the lower octane fuel (a 90 ON PRF mixture). This again could be of importance in hydrocarbon fuels in relation to their RON and sensitivity as discussed by Kalghatgi (2001a and 2001b), Yates *et al.* (2005) and Viljoen *et al.*, (2005) and Mittal and Heywood (2008 and 2009).

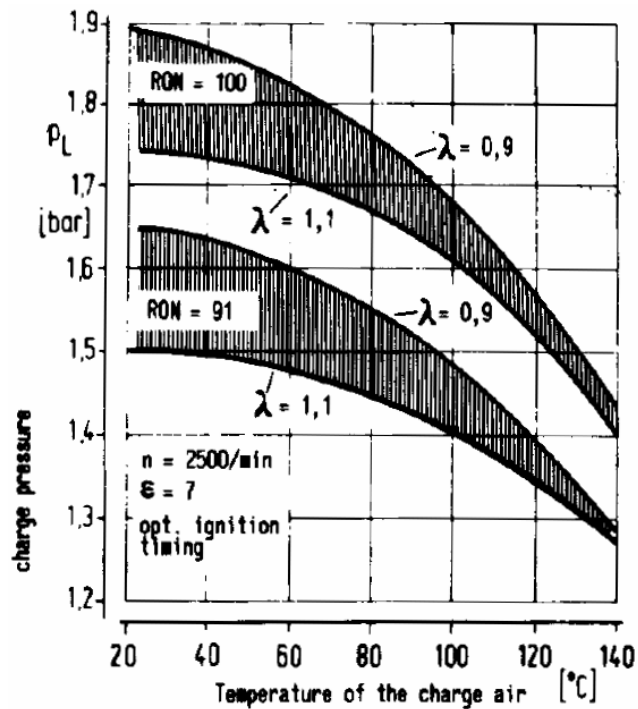


Fig. 3.13: Dependence of SI engine knock limits on charge pressure, temperature and relative AFR (λ) at an engine speed of 2500 rpm, MBT/KLSA ignition timing, and with 91 and 100 RON fuel. Engine bore 86.0 mm, stroke 78.8 mm and CR = 7. (Reproduced from Hiereth and Withalm (1979), reprinted with permission from SAE paper number 790207, © 1979 SAE International)

All of this work suggests that over-cooling the charge air, in the manner of turboexpansion system, may yield benefits in terms of extending the knock limit which could in turn be exploited by the adoption of an increased CR. There is therefore merit in investigating this effect further, and results of such an investigation are discussed in Chapter 6.

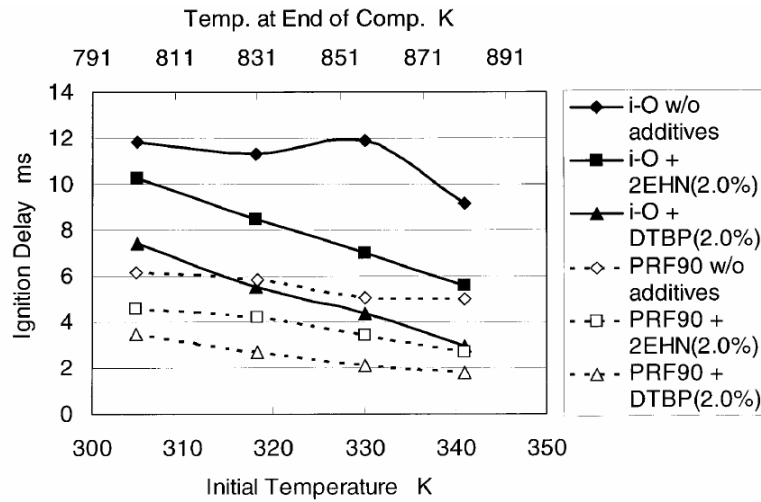


Fig. 3.14: Effect of initial temperature on ignition delay of two PRF/air mixtures with and without additives in a RCM. Equivalence ratio: 0.4. Initial pressure: 0.1 MPa. CR: 16. The end of compression temperature given is calculated from the pressure history of the charge during compression. (Reproduced from Tanaka et al. (2003), by permission of Elsevier)

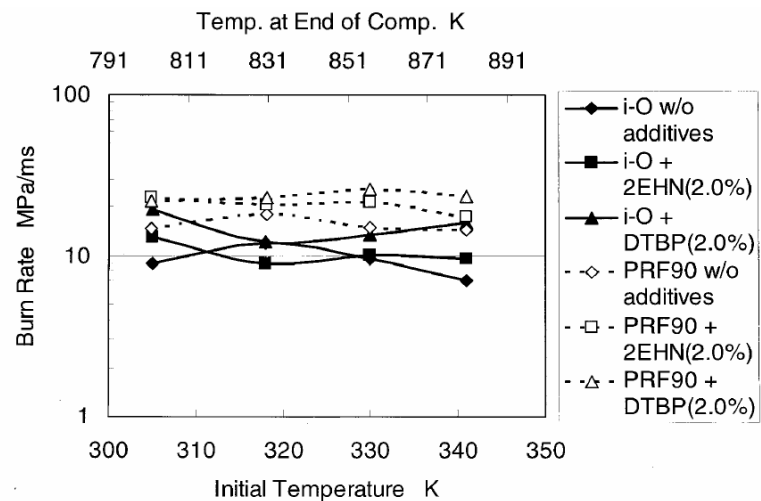


Fig. 3.15: Effect of initial temperature on burn rate of two PRF/air mixtures with and without additives in a RCM. Equivalence ratio: 0.4. Initial pressure: 0.1 MPa. CR: 16. The end of compression temperature given is calculated from the pressure history of the charge during compression. (Reproduced from Tanaka et al. (2003), by permission of Elsevier)

Apart from operating the engine on a fuel of increased octane rating, other means of suppressing knock have been investigated. More unusual means of suppressing knock have included deliberately accelerating charge air motion during the latter stages of combustion by direct injection of high-pressure air, which has allowed the minimum ignition advance for best torque (MBT) to be achieved on a 9.8:1 CR NA engine when operating on 98 RON gasoline (Hirooka *et al.*, 2004). The use of a specially-profiled piston intruder registering in a correspondingly-modified combustion chamber has also been proved to be beneficial (Ueda *et al.*, 1999 and Miyamoto *et al.*, 2006).

Approaches such as these can be seen as practical embodiments of accelerating the final stages of combustion, when the end gas is clearly most likely to autoignite. That this is especially beneficial was shown by Elmqvist *et al.* (2003) who presented data with the important finding that if knock does not occur before a certain value of MFB (in their case 93%) then it does not occur at all. Similar results, showing how small the amount of charge involved in the knock event is, have also been shown by Spicher *et al.* (1991) and in a pressure-charged DISI engine under so-called 'extreme knocking' conditions by Rothe *et al.* (2006b). Hence, accelerating the burn rate at the end of combustion such that there is insufficient end gas to knock is one way to suppress it. The findings of Elmqvist *et al.* (2003) were echoed in the previous work of Pan and Sheppard (1994), whose experiments led them to conclude that "*knock intensity is more sensitive to mean end gas temperature than to the mass of end gas available for autoignition.*"

Haghgoie (1990) linked intake temperature to the RON of the fuel and the mass of charge involved in the knocking process, as shown in Figure 3.16. Clear from this is that the highest octane and lowest intake air temperature combination delays the onset of knock for significantly longer, and *vice-versa*. In Figure 3.16, there is a factor of 10 in the proportion of the end gas involved in the knocking process, supporting the later findings of Pan and Sheppard (1994), Elmqvist *et al.* (2003) and Rothe *et al.* (2006b).

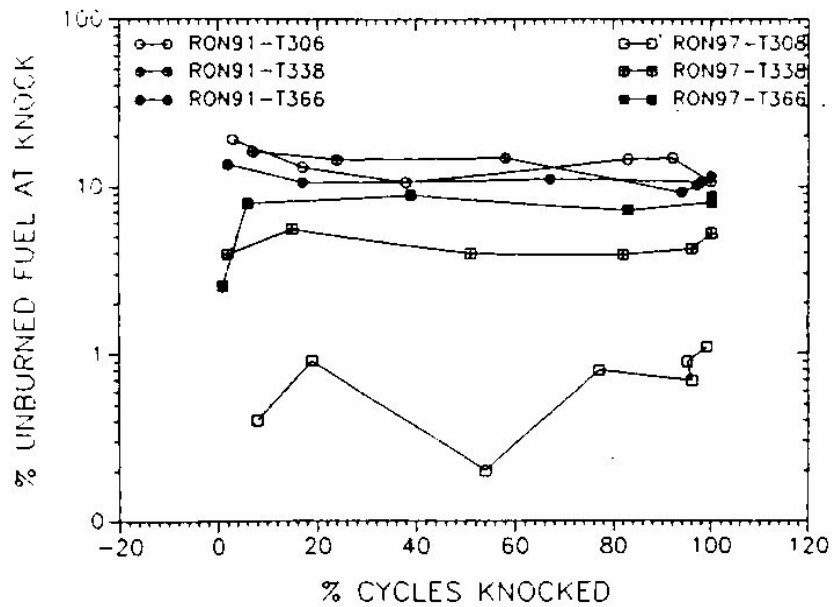


Fig. 3.16: Mass fraction of fuel unburned at the onset of knock for different RON fuels and air intake temperatures in a naturally-aspirated 4vpc engine. Engine operated at stoichiometric AFR and at 1500 rpm. Intake temperature T in K. (Reproduced from Haghgoie (1990), reprinted with permission from SAE paper number 902134, © 1990 SAE International)

More recently, 'Divided Exhaust Period' (DEP) has been proposed by researchers at Saab to improve scavenging in the combustion chamber of a 4-cylinder turbocharged engine so that residuals are purged out more fully due to a beneficial positive pressure gradient across the intake and exhaust valves during the overlap phase (Moller *et al.*, 2005). This concept is a development of a patent originally filed by the Rateau company (Patent, 1923). The configuration tested by Saab is illustrated schematically in Figure 3.17, in which it can be seen that the exhaust ports are separated, and while one is connected directly to the turbine, the other bypasses the turbine completely and instead allows exhaust gas to flow through a starter catalyst before rejoining the flow from the first port just before the main catalyst.

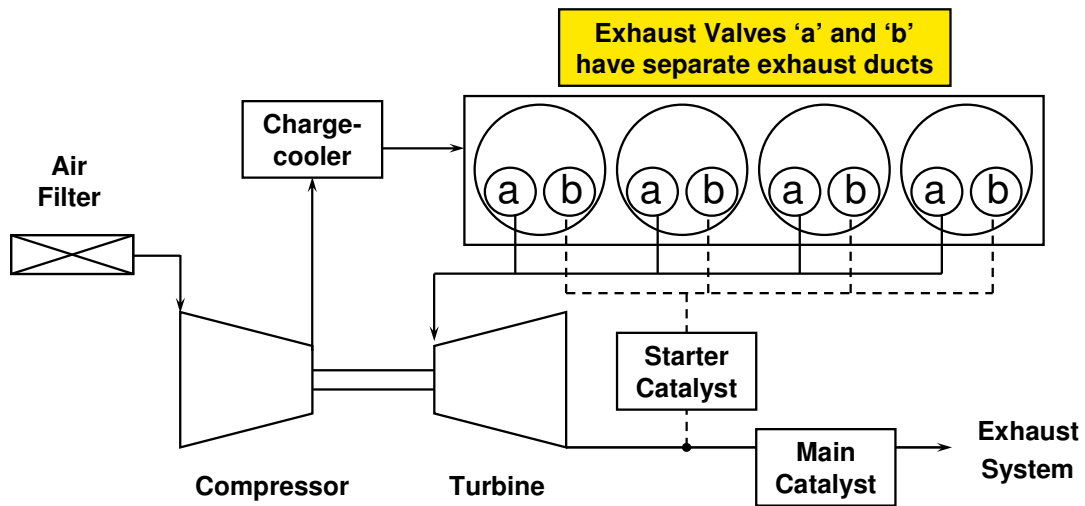


Fig. 3.17: Schematic of a 'Divided Exhaust Period' system for a turbocharged engine (adapted from Moller et al., 2005)

In the method of operation described by Moller *et al.* (2003), the 'exhaust blowdown valve' communicating with the turbine opens first at $\sim 45^\circ$ before bottom dead centre (BDC) and has a period of $\sim 180^\circ$, closing $\sim 45^\circ$ before top dead centre (TDC). The scavenging valve opens at $\sim 55^\circ$ after BDC and closes $\sim 10^\circ$ after TDC. The intake valve profiles are conventional. Because the turbine blowdown valve has a period of 180° , the high pressure before the turbine is thus mechanically isolated from the combustion chamber during valve overlap. Since the intake pressure is higher than the pressure in the scavenging valve duct, the combustion chamber can be thoroughly scavenged of residuals in a manner similar to that which can be arranged in supercharged engines, and beyond the point where boost cross-over (i.e. when the pressure in the exhaust port becomes higher than that in the intake) normally occurs in the manifolds of conventional turbocharged engines, including those with DI.

The DEP approach is unusual in that while it increases pumping work during the exhaust stroke (due to the gas flow through the exhaust valves being choked for much of the exhaust phase), overall pumping work actually reduces due to the efficient gas exchange process at TDC. It is this which scavenges the hot

residuals from the chamber, leading to an extended knock limit and the ability to advance the ignition timing to improve fuel economy. This increase in the knock limit can then be set against a higher compression ratio, further to improve part-load fuel consumption and to reduce exhaust gas temperature at a fixed EVO timing.

A further embodiment of the DEP system improves start-up emissions of the engine by employing a valve deactivation mechanism on the exhaust blowdown valve. Thus, at start-up all exhaust gas can be directed to the starter catalyst via the scavenging valve and hence the thermal inertia of the turbine is not an issue in the catalyst light-off phase. After main catalyst light-off the exhaust blowdown valve is activated and it continues to be operational until the engine is shut down. The DEP approach has also been investigated by Roth *et al.* (2010b) in a DI engine fitted with a mechanism to allow independent control of the two exhaust cam lobes. They termed it a 'Valve-Event Modulated Boost System' and the flexibility provided by their variable valve timing system has the potential to delete the turbine wastegate.

The DEP system is of particular benefit in 4-cylinder turbocharged engines with a common manifold before the turbine inlet. This is because in a conventional turbocharged engine, the blowdown pulse from one cylinder can communicate with the next cylinder in the firing order, and can thus increase the mass of residuals trapped by reverse-charging of the first cylinder. In the DEP approach, however, this cannot occur because each cylinder is mechanically isolated from the next in the firing order, as discussed. Note that in 3-cylinder 4-stroke engines the corresponding period before cylinder-to-cylinder pulse interaction occurs would be 240° , and so with typical exhaust cam profiles each cylinder is in all cases isolated from the others by a combination of exhaust valve timing and period and cylinder firing interval. With appropriate grouping, this can also be utilized in engines with multiples of three cylinders (Welter *et al.*, 2006), and even with a single turbocharger in 6-cylinder engines if the exhaust system to the turbine is pulse-divided (Klauer *et al.*, 2009).

Pulse division is also a pragmatic approach with 4-cylinder engines. In such an approach two cylinders firing 360° apart are grouped together and their exhaust pulses physically separated from the other pair of cylinders by a division of the manifold, which can be continued through the turbine housing to create a meridionally-divided dual volute. The benefits and disadvantages of this approach are discussed in Turner and Pearson (2009) and by Andriesse (2006 and 2008). Another approach is to reduce the period of the exhaust valves to ~180°, thus isolating the cylinder blowdown pulses from each other. This has been productionized by VW, and Szengel *et al.* (2007) discuss the performance of such an engine, showing that the short exhaust period limits the rate at which gas can be exhausted and causes a lower performance. To provide high power output with this approach a switching valve train can be used to move to a longer-period exhaust camshaft profile at higher engine speeds, as discussed by Wurms *et al.* (2008). The effect of this short exhaust cam period approach in 4-cylinder engines, versus the advantages of 3-cylinder groups, will be discussed in detail in Chapter 7.

Maly and Ziegler (1982) showed that increasing the turbulence in the fuel-air mixture can accelerate combustion, supporting the approaches of Ueda *et al.* (1999), Miyamoto *et al.* (2006) and Hirooka *et al.* (2004). They also discuss the mechanism of top piston ring land damage as a result of combustion chamber shape and squish flow. This and later work has also shown that this effect can be very destructive since combustion can be accelerated around the edge of the piston and shock fronts formed within the top ring land. The localized knock events contained within the small ring land volume can lead to pressures high enough to damage aluminium piston alloys (Maly and Ziegler, 1982 and Maly *et al.*, 1990). Such damage could be avoided by using strengthened piston crowns to survive knock when it occurs, and the use of a steel ring carrier in a recent turbocharged DI engine is one example of this approach (Böhme *et al.*, 2006).

Lee and Schaefer (1983) showed that coating specific areas of two of the piston crowns in a four-cylinder engine with iron made them resistant to the damage

suffered by the uncoated pistons when the engine was subsequently operated in knock. This coating was only 20 μm thick and limited to the valve recesses and top land area. Lee and Schaefer (1983) contended that the coating in these areas functioned as a hard, flexible diaphragm which protected the aluminium beneath. Klein *et al.* (1994) discussed a mechanism for the cause of the very high pressures found just beneath the surface of pistons where Rayleigh surface waves are created as a result of a blast wave from a knock event striking the surface. This explains why brittle cracking of silicon crystals in the aluminium alloy of pistons is observed, which is indicative of a mechanically-destructive effect on the surface rather than a thermal one. Their results showed that stresses just beneath the surface could exceed the ultimate tensile strength of a typical piston alloy by a factor of 2.7. Therefore, it is to be expected that thin coatings and piston ring groove inserts could in future be adopted more widely to protect components within the engine enabling it to be operated in knock, although the associated characteristic noise would, of course, still be present.

3.9 SUMMARY AND CONCLUDING REMARKS

This chapter has described the author's research into the literature of SI engine combustion knock, a phenomenon which is particularly important in that it especially limits the performance of pressure-charged engines. From the literature on the subject it is clear that SI combustion knock is a problem which has been and is being studied in great detail. It is also apparent that there are a number of ways that can improve engine knock limits.

As mentioned in Chapter 2, charge-air cooling via a heat-exchanger device (sometimes known as a chargecooler or intercooler) is the most commonly-used method to limit the charge air temperature increase in pressure-charged engines, which is a result of work done on the air in the external compression stage(s). This increase in temperature reduces the knock limit of pressure-charged engines. The effectiveness of a charge-cooling stage can be considered to be of great importance because one of the main drivers on knock initiation and propagation is the condition of the charge at the time of ignition. Ignition timing is

one of the main controls on avoiding knock in most engines, influencing as it does the phasing of combustion heat release versus the temperature change due to piston motion. The combination of the two influences the temperature- and pressure-time history of the end gas after combustion has been initiated. If the charge temperature cannot be reduced at the point in the cycle when ignition occurs, ignition must be retarded to reduce the amount of compressive and convective heating undergone by the end gas. Hence the expansion of the gas during the power stroke offsets its temperature increase due to combustion, and so lengthens the autoignition delay time, τ .

However, retarding the ignition results in an unfavourable time shift of the heat release curve and therefore it reduces engine fuel economy. Because of the retarded combustion event, it also results in higher gas temperatures at exhaust valve opening (EVO). This can mean extra fuel enrichment is necessary to reduce piston, turbine inlet or catalyst inlet temperature. The fuel enrichment reduces combustion efficiency further as well as directly increasing fuel consumption. Extending the knock limit of the engine is therefore very important when considered against the backdrop of the need to improve engine efficiency to reduce CO₂ emissions.

Although one cannot discount significant changes in gasoline fuel formulation that might occur in the future, this is unlikely to happen rapidly in the short term because of the number of SI engines in operation which do not need a significant improvement in fuel quality to operate. Therefore, new engine concepts such as turbocharged DISI and VCR are likely to be the most immediate developments. These concepts can then be more flexible with regard to likely changes in fuel quality which may occur. However, the potential widespread adoption of renewable alcohol fuels offers the possibility of a step-change to a lower effective-CO₂-output fuel which can also significantly improve engine thermal efficiency. Currently the extreme embodiment of this is the adoption of E85 in Europe and the US, a blend of 85% ethanol and 15% gasoline, the latter added primarily for reasons of cold starting of the engine. However, there is a limit on how much ethanol can be made in a renewable manner. The manufacture of

methanol by any means which reduces the carbon footprint of the fuel itself would similarly permit improvements in both well-to-tank as well as tank-to-wheel efficiency, since alcohol-fuelled engines permit greater levels of downsizing and engine efficiency due to the characteristics of the fuel discussed here. Ultimately, the potential feed stocks to manufacture methanol are almost limitless if CO₂ from the atmosphere or oceans is combined with hydrogen obtained by electrolysis of water. Improving the efficiency of such alcohol-burning engines will be very important since it permits a direct reduction in the amount of renewable energy necessary to make the fuel to supply the market in this manner.

A fuller understanding of the reaction of representative spark-ignition engine combustion systems to changes in intake charge conditions while running on modern gasoline and alcohol-based fuels would, therefore, aid greatly the understanding of the subject. It would also allow an appraisal of the potential of new concepts such as turboexpansion to assist in the reduction of fuel consumption. The interaction of intake charge conditions with engine architecture is also very important, so that a balanced approach to engine development can be undertaken. The research presented in this thesis is therefore aimed at:

1. Investigating combustion in a modern combustion system operating under a wide envelope of charge intake pressures, temperatures and densities in order to provide data to gauge the potential benefit of improved charge cooling techniques;
2. Investigating the use of fuel properties other than octane number when attempting to suppress knock;
3. Ascertaining how engine architecture and configuration can be better used to extend the knock limit in the interests of engine efficiency.

A greater understanding of all of these areas can provide valuable information for engine designers and developers which can then have a beneficial effect on

production engines in terms of fuel consumption and CO₂ emissions reduction, and so act as a means of helping to reduce climate change.

Having reviewed the literature on knock and the various means of mitigating it in this chapter, the next chapter will discuss the previous work carried out by the author in the areas relevant to the aims of the research.

Chapter 4: Previous Work

The purpose of this chapter is to discuss previous work undertaken by the author in the area of extending the performance and knock limit of pressure-charged Otto cycle engines through investigation of the interaction of charging system and fuel characteristics. This research was done primarily in the interest of being able to increase the compression ratio, with the intention of improving fuel economy when installed in a vehicle, the reasons for which were discussed in Chapters 1 and 2. Primarily, the chapter discusses:

1. General pressure-charged SI engine work with concepts designed to utilize the potential benefits of the latent heat of vaporization of SI engine fuels.
2. Work he has conducted to develop the concept of turboexpansion, including his initial attempts to prove its potential by using a bespoke 4-cylinder research engine.

4.1 PRESSURE-CHARGED ENGINE WORK UTILIZING THE BENEFITS OF THE LATENT HEAT OF SPARK-IGNITION ENGINE FUELS

The author has been involved in the area of pressure-charged spark-ignition engine development since 1992, starting with work in the area of performance development within the 'XB' IndyCar engine project at Cosworth Engineering. This was after several years' work primarily in the area of performance development of high-power-output NA engines.

This initial pressure-charged engine work led to an interest in the interaction of charging systems with combustion engines and specifically the effect of charge air cooling (by whatever means) on engine performance. In this respect, the XB engine was an unusual example because it employed a 'pre-compressor fuel injection' (PCI) system. This approach has also been termed a 'wet compressor'

technique, particularly when a carburetter is employed (Rosenkranz *et al.*, 1986). This PCI system had been developed because of the racing series regulations then in place, which forbade the use of chargecoolers. It was known that utilizing the latent heat of vaporization of the fuel to offset the increase in charge temperature due to compression in an external charging stage in SI engines could reduce intake charge temperatures in the manner discussed by Hooker *et al.* (1941).

In this particular instance methanol is an ideal fuel, since it has a very high latent heat of vaporization of 1170 kJ/kg, which is coupled to a low stoichiometric air-fuel ratio of 6.4 (Owen and Coley, 1995). Together these values ensure a very high theoretical evaporative charge cooling capability. In the case of the Cosworth XB engine, fuel delivery was optimized by splitting the amount and position of its introduction between the pre-compressor point and the intake ports. Thus only sufficient fuel to saturate the air was introduced upstream of the compressor, and the remainder was introduced in the intake ports as per the normal manner in port-fuel-injection (PFI) engines.

The system was so thoroughly developed that the absence of a chargecooler was not a performance demerit, because its optimization ensured that the compressor outlet temperature was lower than its inlet temperature. At any particular operating point, the precise proportion of the PCI fuelling rate was mapped, based on throttle position and boost pressure. During system mapping, the response of the engine to varying the percentage of fuel mass introduced at the compressor eye (so-called '% PCI loops') was the first real exposure the author had as to how engine performance could be increased with cooler charge air temperatures. Maximizing air temperature reduction without exceeding the saturation limit is especially important in an engine running on low-carbon-number alcohol fuels such as methanol and ethanol because these fuels not only have a low stoichiometric AFR but are capable of being run very rich to the benefit of the specific energy in their cylinders (Owen and Coley, 1995). Conversely the introduction of too much fuel at the compressor eye would displace air there, which is obviously an issue in a racing engine.

Later, during development work on the Lotus Type 918 V8 engine, some of the experience from the XB IndyCar engine programme was brought to bear. The Lotus V8 was turbocharged but not chargecooled, despite the fact that the in-line 4-cylinder engine it was to replace had been. Both of these engines were fitted in a mid-engined car, for which the provision of cooling air to air-to-air chargecoolers is a significant problem. In the predecessor 4-cylinder engine, a liquid chargecooling system had been employed. Such an indirect chargecooling arrangement is simpler to arrange in a mid-engined vehicle than air-to-air cooling, but is significantly more expensive. This indirect system was described by Wood and Bloomfield (1990), but was not specified on the initial V8 installation in order to offset some of the cost of the larger engine.

The fuel injectors fitted in the intake ports of the Lotus V8 were not capable of providing all of the full-load fuel requirement of the engine. This was because the requirement to maintain accurate fuel control under idle conditions meant that the maximum flow rate had to be compromised. As a consequence, the engine was provided with secondary injectors in the pipes leading from the turbocharger compressor to the plenum for each bank of cylinders. The author conducted tests to show that even in this application, using gasoline as the fuel, optimizing the fuel delivery split between the port and secondary injectors provided a useful evaporative cooling effect on the charge. In turn, this allowed the target power and torque of the engine to be achieved at a lower boost pressure and permitted re-optimization of the turbocharger specification to reduce back pressure on the cylinders. Some of these effects were discussed much later in a historical article on the engine by Crosse (2011).

In 2000 the author performed related work on a supercharged development engine, again for fitment to a mid-engined car, and again non-chargecooled. Here, following the success of the system used on the Lotus V8, the secondary injectors were positioned before the entry to the supercharger. This was a Lysholm-type device manufactured by Opcon AB. The results of this work were published by Turner and Pearson (2001), in which the effects of the PCI system

were quantified and shown to be worth up to 18% increase in torque, due to an increase in the density of the charge in the plenum and the increase in spark advance that could be sustained at the knock limit. However, because of the relatively low latent heat of vaporization and high stoichiometric air-fuel ratio of the gasoline being used, up to 80% of the fuel mass had to be introduced pre-compressor. This 80% limit was adopted because of concerns of operating with an ignitable mixture in the intake system, and not because of achieving saturation of the air⁷ (Turner and Pearson, 2001).

Thus an interest in the benefits of more fully utilising the physical characteristics of the fuel was developed by the author, and also in how such systems could be applied to road vehicles in turn to improve performance and thermal efficiency. In research presented in this thesis this concept was developed further and is reported in Chapter 5.

4.2 DEVELOPMENT OF THE TURBOEXPANSION CONCEPT AS A FUEL ECONOMY TECHNOLOGY

In 2000 the author was involved in a discussion with another ex-Cosworth employee, Chris Whelan, about the 'GB' turbocharged Formula 1 engine project, during which Whelan conducted work on an unusual charge air conditioning system termed 'turboexpansion'. In the case of the Cosworth GB engine there was a plenum chamber pressure limitation set by the governing body. However, Whelan knew of earlier work on large gas engines where turboexpansion systems had been successfully used to extend their knock limit by using excess turbine power to drive a charge-air conditioning system to reduce air intake temperature (Crooks, 1959 and Helmich, 1966). This had been done because these were conversions of diesel engines and so necessarily had high CRs, which, despite natural gas having a very high RON of 130, meant that the lean

⁷ Despite this concern, it is interesting to note that many supercharged piston aero engines habitually operated with the introduction of all of the fuel into the air before it flowed into the supercharger. Thus, engines such as the Rolls-Royce Merlin and Napier Sabre always operated with an ignitable mixture in the intake system, most of the time under supercharged conditions (Hives and Smith, 1940, Hooker *et al.*, 1941 and Sheffield, 1944).

knock limit could readily be breached. Since in Formula 1 boost pressure was defined at that time to be the pressure in the plenum immediately upstream of the engine intake, there was a possibility to use the excess turbine power available in unsilenced racing engines to drive a turboexpansion system with the intention of reducing charge-air temperature while adhering to the regulation 4 bar (absolute) plenum boost pressure limit. This would increase the charge mass flow rate flowing through the engine and therefore the theoretical power output. Thus rig work on the system was undertaken at Cosworth.

This work was, of course, not aimed at extending its knock limit, since even at that time Formula 1 engines operated at such high engine speeds that knock was rarely a problem. For example, Bamsey (1988) stated that ignition systems for these engines were specified to permit 13,000 rpm, meaning that the amount of time that they operated at rotational speeds where knock is a significant issue was minimal. The benefit of high rotational speed to permit engine downsizing in supercharged engines has also been discussed by the author and co-workers (Turner *et al.*, 2004c) and Chapter 3 has discussed the importance of time in the autoignition process. Whelan refers to his work on turboexpansion during this time in his papers (Whelan and Rogers, 2005 and 2006).

Hence the author started to investigate using such a system to 'over-cool' the charge air relative to a simple chargecooler system. This was in order to use the reduction in temperature to extend the knock limit of a gasoline engine such that its CR could usefully be increased. This is an important distinction from the Cosworth racing engine approach, instead being predicated on the belief that the dominant factor in determining the knock limit in gasoline engines was the charge temperature-time history and not the pressure-time history.

At this time, the Saab Variable Compression (SVC) engine was being presented (Drangel and Bergsten, 2000). Consequently there was much interest in variable compression ratio (VCR) engines to reduce vehicle fuel consumption. However, the apparent complexity of VCR systems in poppet-valve 4-stroke engines meant that there was attractiveness in a concept which could potentially give a

meaningful proportion of the drive cycle benefit of VCR within a conventional engine architecture. This would mean that the complexity of a VCR mechanism would not have to be accommodated within existing engine assembly lines.

Effectively turboexpansion is an embodiment of an air-cycle refrigeration system. The application of the concept to combustion engines is not new, having been the subject of patent activity since 1950 (Patents, 1950, 1977, 1984, 1982 and 1985). It has been studied with respect to both diesel and spark-ignition applications since then (Meyer and Shahed, 1991 and Whelan and Rogers, 2005 and 2006). A schematic of the system which was studied in previous work by the author and colleagues is shown in Figure 4.1 (reproduced from Turner *et al.*, 2003 and 2005a). This is similar to the system discussed earlier in Figure 2.13, except that the means of power rejection is a belt drive, which will be discussed later. The thermodynamic cycle for the schematic system shown in Figure 4.1 is the same as that given in Figure 2.14, reproduced here as Figure 4.2.

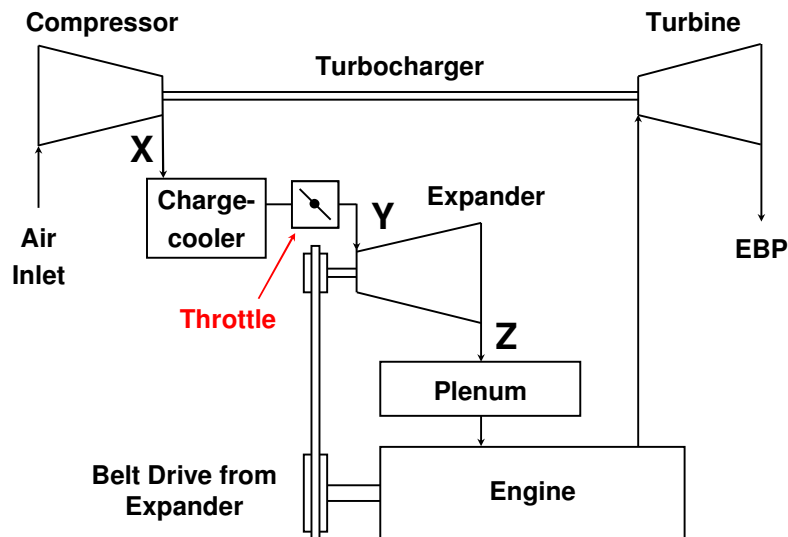


Fig. 4.1: Schematic of one possible embodiment of a turboexpansion system utilizing a belt drive to transmit power from the expander to the crankshaft (EBP = Exhaust Back Pressure). (Reproduced from Turner et al., 2005a)

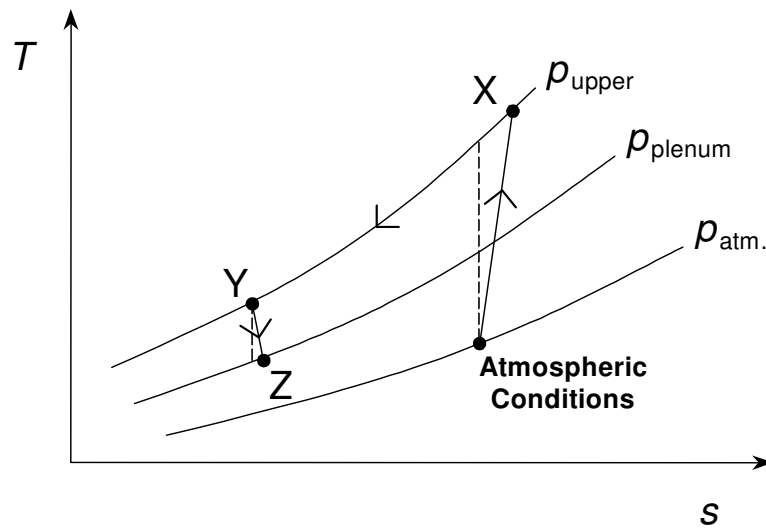


Fig. 4.2: Temperature-entropy diagram for the turboexpansion system shown schematically in Fig. 4.1

As was discussed in Chapter 2, in a turboexpansion system air is admitted to the compressor and is compressed to an upper system pressure which, importantly, is above the desired plenum pressure. It is then cooled in the chargecooler, ideally at constant pressure. The process is identical thus far to a conventional pressure charging system except that the maximum system pressure is higher. Finally, it is passed through the expander, which reduces simultaneously the pressure and temperature of the charge air. This makes it possible to achieve a given charge air density in the plenum at a temperature below that which a simple chargecooler system can deliver, with the very important rider that the individual system component efficiencies are sufficiently high.

In researching this concept, the author's first piece of work was to construct a thermodynamic model in a Microsoft Excel spreadsheet allowing the magnitude of any potential gain to be studied. This spreadsheet did not take into account pipe friction or heat losses in the charging system, but it did suggest that if a large enough pressure ratio could be engineered before the chargecooler stage, and if high adiabatic efficiencies could likewise be arranged for all of compressor and expander stages, then a high charge air density could be achieved in the plenum

chamber. This could be in excess of twice that of the atmosphere, and furthermore the charge air temperature could even be arranged to be sub-atmospheric. This, and a brief comparison with published data on the then-new SVC engine, was sufficient to procure research funds for a more comprehensive 1-D modelling study to be carried out by others in the organization. A copy of the original spreadsheet is included in Appendix I. It allowed investigation of turboexpansion systems with single- and two-stage compression, and it was data from this tool that was presented by the author at a UnICEG meeting in April 2002 (Turner and Pearson, 2002a).

In order to use what was thought to be representative combustion data for the 1-D modelling work, Saab were approached and provided combustion data from the SVC engine. Since the SVC engine had been operated at 104 kW/l (140 bhp/l) this was thought to be ideal (Drangel and Bergsten, 2000). These modelling results were encouraging and were reported in an initial SAE paper (Turner *et al.*, 2003). Consequently, funds were made available to build an engine for test fitted with the charging system modelled. This engine design took its name from an acronym arising from 'efficiency optimization married to aggressive downsizing', or η OMAD, which became 'Nomad'.

4.3 DESIGN OF THE 'NOMAD' RESEARCH ENGINE AND INITIAL TURBOEXPANSION SYSTEM DYNAMOMETER TESTING

The Nomad engine was specified by the author. As well as the initial turboexpansion work, it was also to have been used for separate test programmes investigating other technologies. It was to be capable of resisting peak cylinder pressures of 115 bar, specifically to allow design protection of the structure for turboexpansion system testing. As a result of this requirement, the choice of using the cylinder block, crankshaft and bearings from a high speed direct injection (HSDI) diesel engine was made. This was because it was known that such engines are designed to operate at higher cylinder pressures than SI engines, and it was reasoned that these components would be sufficiently robust for a high-BMEP SI application. Consequently Adam Opel AG agreed to support

the programme by supplying base donor 1.7 litre HSDI diesel engines, which had originally been engineered by Isuzu.

Thus the Nomad engine design used the cylinder block, crankshaft, bearings and pumps from the Isuzu engine, with an SI 4vpc double overhead camshaft cylinder head. It had dual port fuel injectors per cylinder, to permit the fuel flow rates sufficient for high specific outputs. Opcon AB, known for their twin-screw Lysholm-type superchargers, were also involved in the project, supplying a twin-screw expander which drove the crankshaft via a dedicated belt drive. Opcon had been independently developing their twin-screw expander technology for fuel cell engine applications, and the Nomad turboexpansion system expander was a modification of one of these units. Honeywell Charging Systems (commercially known as Garrett) supplied engineering expertise for the turbocharger, which was of a special configuration due to the requirement for a high pressure ratio compressor. The design of this engine was the subject of a paper at the SAE 2006 World Congress (Turner *et al.*, 2006b). Photographs of the completed engine with turboexpansion system fitted are shown in Figure 4.3.

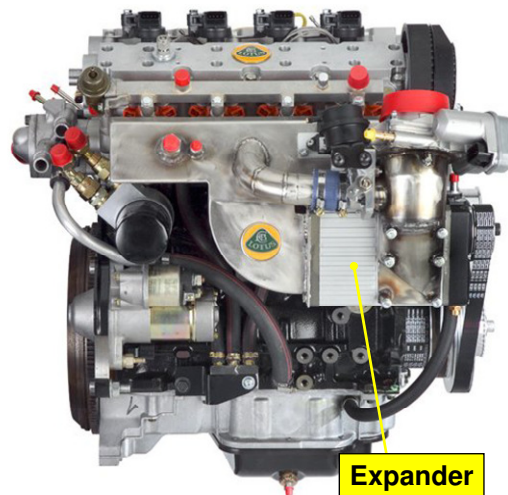


Fig. 4.3(a): Photograph of right hand (intake) side of the Nomad research engine in the form used for initial turboexpansion testing as reported by Turner et al. (2005a). Note the twin-screw expander. (Photograph courtesy Lotus Engineering)



Fig. 4.3(b): Photograph of left hand (exhaust) side of Nomad research engine in the form used for initial turboexpansion testing reported by Turner et al. (2005a). (Photograph courtesy Lotus Engineering)

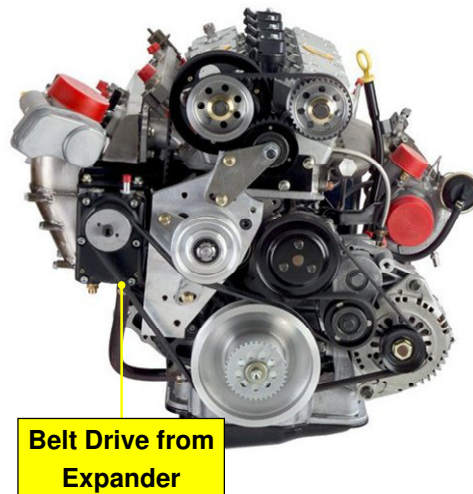


Fig. 4.3(c): Photograph of front of Nomad research engine in the form used for initial turboexpansion testing reported by Turner et al. (2005a). Note the drive belt from the expander to the crankshaft positioned in front of the other accessory drives. (Photograph courtesy Lotus Engineering)

The Nomad engine was designed and built between mid-2003 and mid-2004 and was tested with the charging system as shown in Figure 4.1. A photograph of the engine mounted on the dynamometer during this test work is shown in Figure 4.4. Despite being a brand new design, it successfully completed 70 hours of operation at ~20 bar BMEP, being removed from the test bed only at the end of the turboexpansion system test work. However, from the results it was apparent that the interaction between the engine and turboexpansion charging system was not as straightforward as had initially been hoped, because the engine was extremely knock limited.

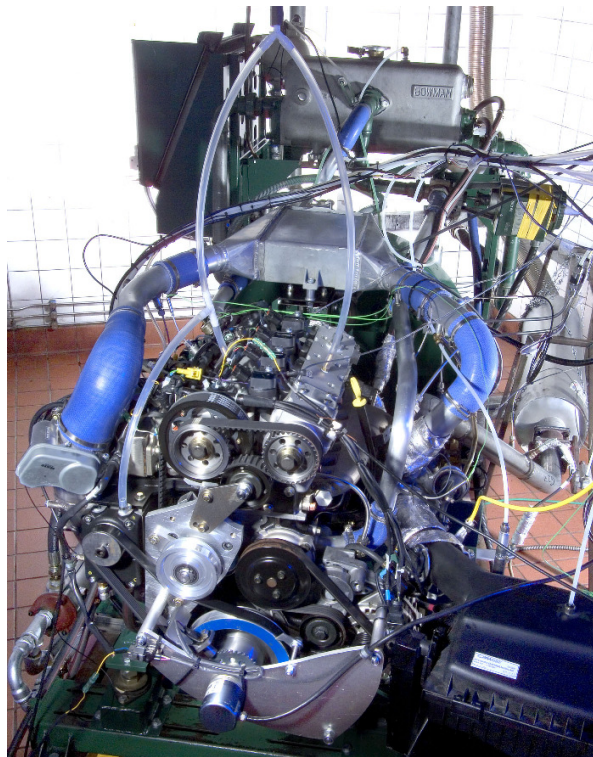


Fig. 4.4: Photograph of Nomad research engine fitted to test bed for initial turboexpansion testing reported in Turner et al. (2005a). (Photograph courtesy Lotus Engineering)

This test work was reported in an SAE paper presented in 2005 (Turner *et al.*, 2005a). In summary, from this work it appeared that requiring a turbocharger's turbine to provide all of the energy to drive the charging system was causing a

scavenging limit in the engine. This was because a very high turbine expansion ratio was necessary to provide the excess boost pressure which was subsequently recovered in the expander. This necessitated a high pre-turbine pressure, increasing the density of the hot residuals. In a 4-cylinder engine with exhaust profiles significantly longer than 240°, these residuals are either trapped in the combustion chamber or pushed back into the intake system during the valve overlap phase. The severity of this problem was illustrated by the fact that even after the camshaft timing was adjusted so that there was zero valve overlap, the engine was still significantly knock limited (Turner *et al.*, 2005a).

A 3-cylinder configuration would have provided a much better situation with regard to pulse interaction due to firing interval effects as will be discussed in Chapter 7. However, for the Nomad engine this was not an option. Even taking into account the relatively small clearance volume afforded by the high compression ratio of 10.5:1, the mass of the residuals trapped inside the combustion chamber were causing a significant reduction of the knock limit. To illustrate this, this heavily knock-limited performance was found to be the case even when operating the engine on 103 RON fuel (Turner *et al.*, 2005a).

Figures 4.5 and 4.6 show some results from this initial work, including the fact that although the expansion ratio of the expander is not very high, ~7°C could still be removed from the air passing through it. This was considered to be usefully more than could have been achieved with a simple pipe of the same length, although originally 15-20°C temperature reduction from the expander had been hoped for. Before testing commenced, it had been hoped to operate at an upper system pressure sufficiently high to force the expansion ratio of the expander up, and with it the expander isentropic efficiency. This would have allowed the charge air temperature to be reduced to the hoped-for value. However, this higher pressure could not be achieved because it was not possible to drive the engine through the knock-limited area of what was, effectively, a high part-load area of operation.

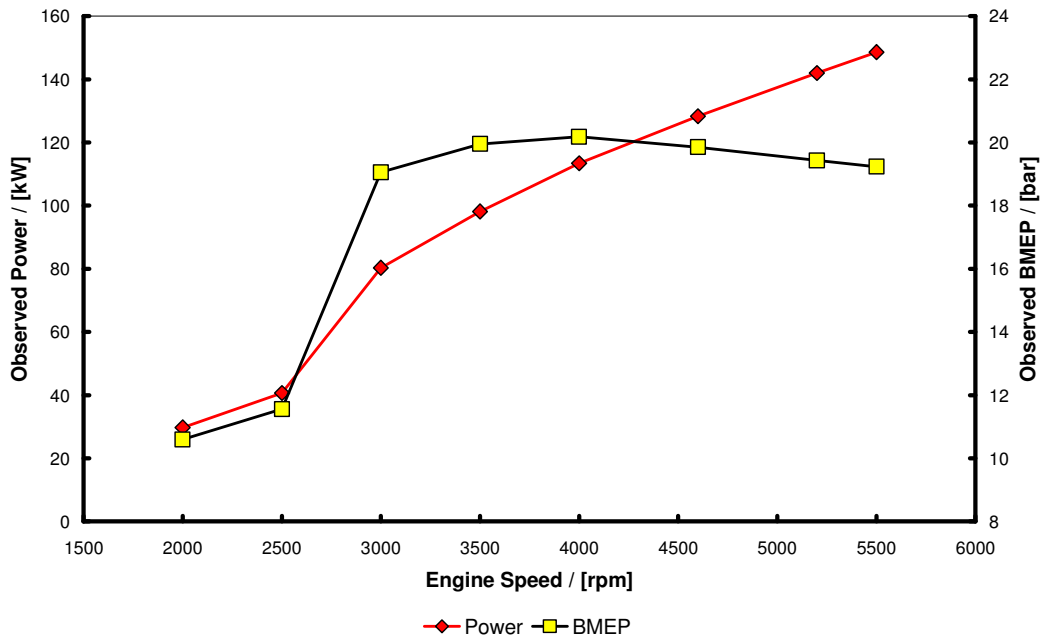


Fig. 4.5: Full-load power curve of the Nomad turboexpansion research engine when operating on 103 RON fuel. (Data from Turner et al., 2005a)

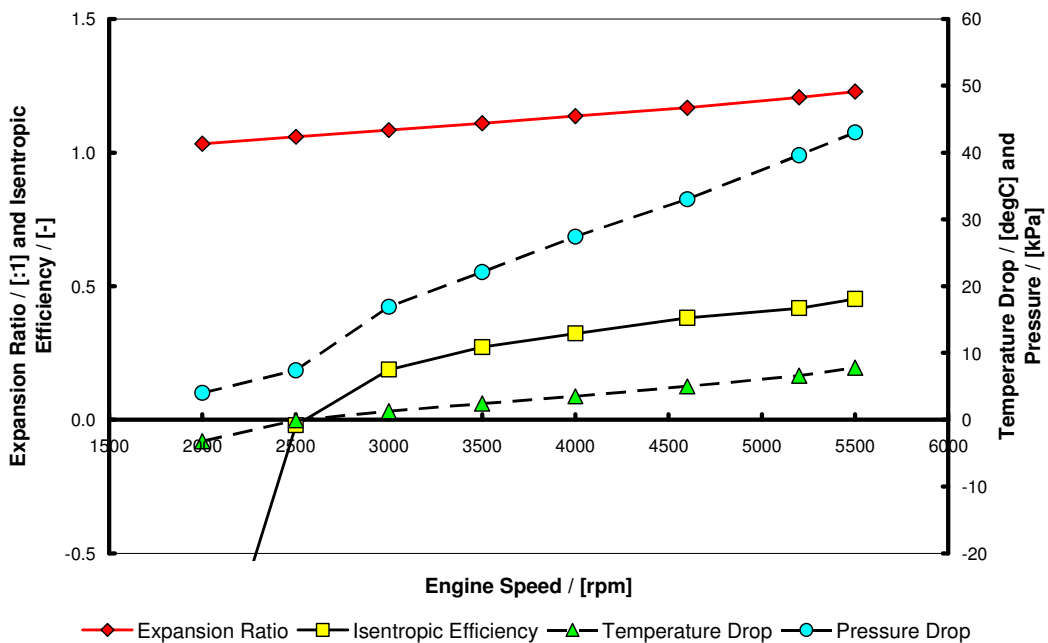


Fig. 4.6: Performance of expander during Nomad turboexpansion research engine testing. (Data from Turner et al., 2005a)

In Figure 4.6 the isentropic efficiency is calculated from the temperature drop across the expander and the measured expansion ratio, in the same manner as was discussed for turbocharger turbines in Chapter 2. Figure 4.6 shows that the isentropic efficiency was very low. Clearly this initial dynamometer work had not proved positive beyond the fact that an expander could be configured to remove some charge air temperature from the air passing through it. The results were subsequently used by David Taitt at Loughborough University to calibrate a model of the system which, in turn, suggested that a CR increase of about 0.5 should be possible for a conventional port-fuel-injected turbocharged engine with a properly configured charge air conditioning system of this form (Taitt *et al.*, 2006). Taitt *et al.* (2006) used data from the Nomad engine and also the results from some previous characterization work to arrive at this conclusion as a result of modelling using the commercial one-dimensional engine simulation code Lotus Engine Simulation (LES).

The findings of Taitt *et al.* (2005 and 2006) prioritize the order of importance of the efficiencies of the devices in a turboexpansion charging system thus:

1. Intercooler effectiveness;
2. Expander isentropic efficiency;
3. Compressor isentropic efficiency.

From Figure 4.6, at the conditions tested, the expander fitted to the Nomad engine had an isentropic efficiency of <45%. In light of the above ranking in importance of component efficiencies, it is perhaps unsurprising that the initial research engine results were disappointing.

From this initial turboexpansion work it was clear that fundamental questions concerning the combustion of highly pressure-charged gasoline engines needed to be answered. This was particularly the case with PFI where the latent heat of directly-injected fuel cannot be used to reduce the charge temperature in-

cylinder, and blow-through scavenging without fuel cannot be employed during an extended valve overlap period in order to reduce the residual rate. For PFI such questions needed to be answered in order to make an informed opinion on the value of attempting to re-engineer the charging system in order to provide the low charge air temperature which was previously thought to be the biggest factor in extending the knock limit of such engines.

At the same time, renewed interest in renewable alcohol fuels, in order to offset CO₂ from road vehicles, and the synergy of these fuels with pressure-charged engines also drove a desire to study in more detail their benefits in such engines. It also raised the potential to exploit some of their physicochemical properties in novel ways in charging systems as per the pre-compressor approach, in order to avoid having to operate SI engines at very high boost pressures to provide high levels of downsizing.

4.4 SUMMARY AND CONCLUDING REMARKS

Since 1992, the author's work has been heavily involved in pressure-charged SI engine performance, and this, coupled the global desire to reduce CO₂ emissions has led him to research engine downsizing as one means of reducing vehicle fuel consumption. The unanswered questions relating to the initial turboexpansion work reported in his two SAE papers on the subject (Turner *et al.*, 2003 and 2005a), and particularly the combustion of fuels under conditions of high levels of pressure charging, have led to a requirement to study the interaction of charging system, fuel delivery and fuel type more closely. This has resulted in the following series of investigations, connected by the desire to research interactions between charge conditioning, knock and SI engine architecture:

1. Multi-cylinder engine research work where the high latent heat of vaporization of alcohol fuel is utilized directly to reduce charge air temperature in road-legal engines (described in Chapter 5).

2. Single-cylinder variable-air-density tests to better understand the relationship between air temperature and knock when the mass flow of charge through an engine is held constant (described in Chapter 6).
3. The creation of an optimized pressure-charged engine concept drawing on the realization from the Nomad-based turboexpansion research work that both residual concentration and their temperature must be minimized (this new engine being the Sabre engine, described in Chapter 7).
4. The investigation of alternative knock-mitigation technologies to attempt to further improve the very good full-load fuel consumption of the Sabre engine (described in Chapter 8).

However, before leaving this chapter, it is pleasing to note a completeness in returning to alcohol fuels and their interaction with charging systems, a phenomenon which originally led the author to take such an interest in pressure-charged engines in 1992.

Chapter 5: Supercharged Engine Tests with Alcohol-Based Fuel

This chapter discusses research into the use of alcohol fuels in a high performance pressure-charged engine (such as is typical of the type currently being developed under the 'downsizing' banner). To illustrate this it reports modifications made to a production supercharged high-speed sports car engine to enable it to run on a high-blend ethanol-based fuel containing 85% ethanol by volume in gasoline, i.e. 'E85'. As discussed in previous chapters the ability for engines to be able to run on alcohol fuels may become very important in the future from both a climate change viewpoint and that of security of energy supply. Additionally, low-carbon-number alcohol fuels such as ethanol and methanol are attractive alternative fuels because, being liquids, they can be stored easily (unlike gaseous fuels). Also, the amount of energy that can be contained in the vehicle fuel tank, while still less than when using gasoline, is relatively high. These fuels also have a much higher octane rating than gasoline which makes them particularly attractive as a fuel for pressure-charged engines, which are frequently knock-limited in their ignition advance curves as discussed in Chapter 3.

The modifications made to the engine to record the data reported in this chapter include the reconfiguration of the fuel system to investigate making best use of the high latent heat of vaporization of high-blend alcohol fuels by injection of a proportion of the fuel mass upstream of the supercharger – the so-called 'wet compressor' technique (Rosenkranz *et al.*, 1986). With this configuration, engine performance data when operating on E85 with optimized engine management system (EMS) settings are presented and compared to the original gasoline-fuelled performance. Discussion is made of the nature of the evaporative effect of the alcohol versus oxygen displacement arising from the lower stoichiometric AFR, its effect on supercharger drive power and of the improvement of the spark advance curve as a result of the increase in octane rating of the fuel. To illustrate this response, curves when varying the percentage of fuel delivered upstream of

the supercharger are presented. Some discussion of the practical issues to be addressed on the fitment of such an engine to a vehicle is also made, together with how the wet compressor technique might be adopted with minimal impact on evaporative emissions. Conclusions as to the attractiveness of this approach in maximizing ethanol-fuelled engine performance are drawn based on the results presented and the vehicle issues listed.

5.1 ALCOHOLS AS ALTERNATIVE FUELS FOR SPARK-IGNITION ENGINES

Chapter 3 discussed some of the advantages of the low-carbon-number alcohols in terms of knock suppression. Additionally, ethanol is an attractive fuel for passenger cars because it is possible to offset some of its post-combustion CO₂ emissions by using biomass as the main feed stock in its production. This leads to a partially-closed CO₂ cycle. Methanol is also a potential energy carrier for society in the long-term future because it can be made from a wide variety of feed stocks. Ultimately, its fossil carbon intensity can be negated completely if it is synthesized directly from CO₂ removed from the atmosphere, providing a shorter CO₂ cycle than that for ethanol derived from biological sources (Olah *et al.*, 2006). Thus, with either ethanol or methanol, the net rate of release of CO₂ into the atmosphere from transport can be reduced. Indeed, theoretically, the accumulation of CO₂ in the atmosphere can be completely halted if all of the energy used in the fuel manufacturing process is renewable or nuclear.

Additionally, and somewhat unusually for 'alternative' fuels, alcohols such as ethanol and methanol have the potential to increase engine performance over that achievable with gasoline due to a combination of factors (Owen and Coley, 1995). These include: high octane ratings; a much higher latent heat of vaporization; a lower adiabatic flame temperature; and a higher mole ratio of products to reactants. The high latent heat of vaporization combines with a low stoichiometric AFR to provide a very significant charge cooling effect in comparison to gasoline. To illustrate this, a comparison of some of the pertinent

properties of gasoline, ethanol and methanol were given in Table 3.2, reproduced below as Table 5.1.

Table 5.1: Properties of gasoline, ethanol and methanol. Data taken from Owen and Coley (1995), Bosch (2000) and Turner et al. (2007b)

Property	Gasoline (Typical)	Ethanol	Methanol
Chemical formula	Various	C ₂ H ₅ OH	CH ₃ OH
Density at atmospheric pressure and temperature (kg/m ³)	740	789	791
Lower heating value (MJ/kg)	42.7	26.8	19.9
Stoichiometric AFR (kg/kg)	14.7	9	6.4
Specific energy* (MJ/kg mixture)	2.905	2.978	3.062
Specific energy ratio**	1	1.025	1.054
Volumetric energy content (MJ/m ³)	31.6	21.2	15.7
Research octane number	95	109	106
Motor octane number	85	98	92
Sensitivity	10	11	14
Latent heat of vaporization (kJ/kg)	180***	930	1170
Mole ratio of products to reactants****	0.937	1.065	1.061
Oxygen content by weight (%)	0	34.8	50

*At stoichiometric conditions **Relative to gasoline ***Assumes no alcohol present
****Including atmospheric nitrogen

From Table 5.1 it is readily apparent that alcohol fuels possess some significant attractions over gasoline when engine performance is considered. Indeed, methanol has for some time been accepted as a good fuel for turbocharged engines (Pannone and Johnson, 1989). To their high RON and MON values and high latent heat of vaporization must be added that heat rejection during combustion is reduced due to the lower adiabatic flame temperature, and that at the mixture strengths typical of those used at maximum power, ethanol and methanol generally have significantly faster burning velocities than paraffins (Gülder, 1982 and 1984 and Metghalchi and Keck, 1982). The latter can give a further benefit in reduced negative work in the cycle (i.e. less ignition advance for the same angle of maximum pressure) (Brinkman and Stebar, 1985). However, while the combustion performance of alcohol fuels is undoubtedly attractive, the low volumetric energy content caused by their partially-oxidized state has always

been perceived as a disadvantage. Nevertheless, the high octane values of these fuels means that they are often used as blend agents in gasoline, and historically had been considered as a major potential constituent of gasoline fuels, until tetraethyl lead (TEL) was developed as a means of reducing fuel consumption of the vehicle fleet (Boyd, 1950).

The data in Table 5.1 illustrates a practical problem of moving to alcohol-based fuels for the end-user, in that the volumetric energy content of these fuels is significantly lower than that of gasoline. This is perhaps one of the greatest advantages of gasoline. Figure 5.1 shows a plot of volumetric energy content for methanol- and ethanol-gasoline blends. The lower volumetric energy content results from the lower calorific (heating) value of alcohols. However, against the background of the problems of storing low-density gases on board a vehicle, whether cryogenically or under high pressure, and with that their necessarily low installed volumetric and gravimetric energy content, storage and use of alcohol fuels is perhaps a simpler problem. Both ethanol and methanol can corrode light metals and so the fuel system needs to be modified to suit, although these challenges are all well understood (Kremer and Fachetti, 2000). They can also be distributed and stored with modifications to the existing infrastructure, which is a significant advantage in their acceptance when compared to hydrogen, for example. Indeed, distribution and storage of hydrogen is a very significant problem, and indeed it is yet to be shown that this can be practically achieved in mass production and particularly on board a vehicle, despite some recent success in this area (Amaseder and Krainz, 2006).

Starting an engine in cold conditions can be problematic with alcohol fuels, due to their lower volatility than gasoline, itself a function of the hydrogen bonding phenomenon they exhibit. The hydrogen bonding is fundamental to their being a liquid at normal atmospheric conditions, this being despite their extremely low molecular weights which would ordinarily suggest they should be in the gaseous region of matter. It also leads to their high latent heat of vaporization and very high vapour pressure, particularly versus gasoline, whose volatility is a consequence of it being a mixture of different hydrocarbons with a very wide

range of boiling points. It is for startability reasons that 15% gasoline is normally blended into ethanol and methanol (to form E85 and M85, respectively) for use in port-fuel-injected engines.

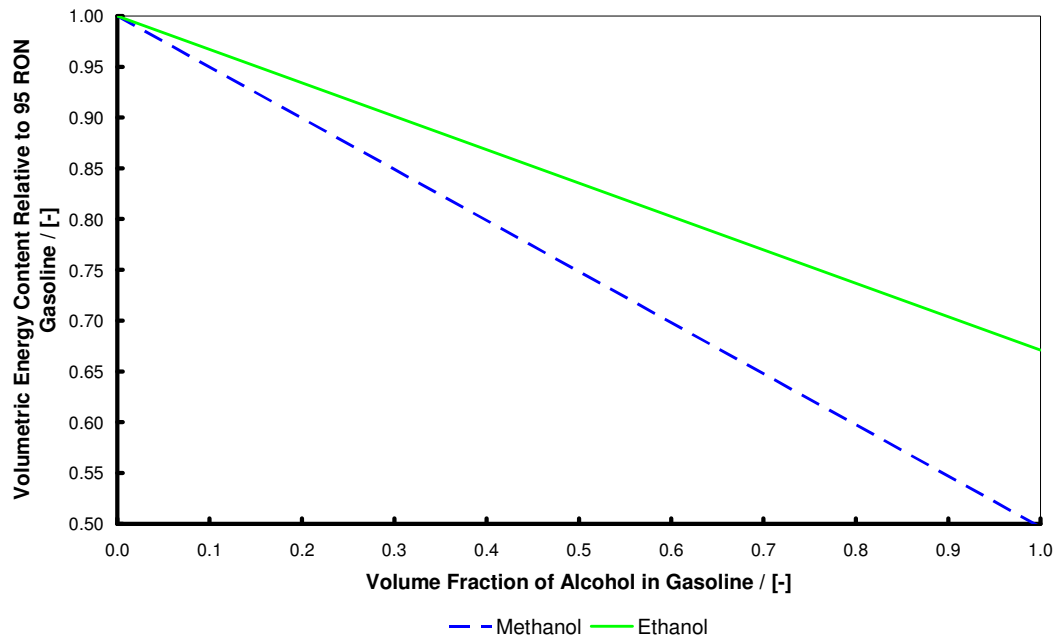


Fig. 5.1: Volumetric energy content of methanol- and ethanol-gasoline blends

The high latent heat of vaporization of alcohols means that when DI is employed, there can be increases in the volumetric efficiency in SI engines of ~12% at stoichiometric conditions (Wyszynski *et al.*, 2002), whereas ordinary gasoline gives <10%. Even 10% by volume ethanol or methanol blended in gasoline can have a similar effect to the pure alcohols (Wyszynski *et al.*, 2002). In pressure-charged engines, as an alternative to DI, introducing the fuel before the compressor can influence performance through reducing compressor work and increasing the charge-air mass flow rate due to the reduced air temperature at the intake. This ‘wet compressor’ strategy was used in aircraft engines for many years either for the introduction of all of the fuel or as an additional boost in take-off power by temporary injection of alcohols or of water/alcohol mixtures. Indeed, pre-compressor introduction of the fuel was the normal means of fuelling an

engine for many aero engine manufacturers, because even gasoline has a beneficial effect when introduced at the inlet to the compressor (Hooker *et al.*, 1941). The technique was also shown to be of benefit in supercharged engines operating on gasoline in which it has been shown that in excess of 80.5 kW/l (108 bhp/l) can be achieved without a chargecooler (Turner and Pearson, 2001). It was also investigated as an aid to improving the fuel consumption of turbocharged engines (Rosenkranz *et al.*, 1986).

In the test results presented in this chapter, E85 was used to fuel what was already a high performance port-fuel-injected gasoline engine. This fuel is in common use in parts of the world including Sweden and the US, and has been introduced to the market in the UK. There is some debate as to how best to introduce ethanol into the spark-ignition fuels market, and the reason for this research was to investigate the magnitude of the performance benefit that could be achieved in a sports car vehicle so that ethanol use could perhaps be seen as attractive to the end user. This is the approach employed by Saab in their 'Biopower' vehicles, where fuelling the car on E85 enables the customer to increase the power output of the vehicle by 20%, due to the synergy between E85 and pressure charging (Bergström *et al.*, 2007a and 2007b).

The approach of increased performance when operating on the alcohol fuel could be attractive to some premium vehicle manufacturers since it may cause ethanol fuelling to be seen as a desirable attribute by the market place and hence accelerate its uptake, rather than its being introduced piecemeal into the wider gasoline fuel pool. The contract with the vehicle customer will then take the form of balancing increased performance with higher volumetric fuel consumption, and (it could be argued) the high-performance, premium vehicle purchaser will be less affected by the higher running costs due to increased fuel consumption, should the price of the fuel not approach parity on a unit cost per unit energy scale. Although increased performance has not been afforded in the adoption of flex-fuelling of products from Bentley Motors Limited, the renewable nature of the biofuel these vehicles can operate on is seen as a potential positive attribute by some of their customers in the marketplace (Bentley Motors Limited, 2008).

The base engine employed for this work, fuelling philosophy adopted, dynamometer results gathered and some of the practical considerations in applying the approach to a vehicle are discussed in the following sections.

5.2 BASE SUPERCHARGED TEST ENGINE

The base engine used for this work was a Toyota 2ZZ-GE engine, supercharged by Lotus for sale in the 'Exige S' vehicle. The initial work in supercharging this unit for the vehicle application was reported by Turner *et al.* (2004c). The normal charging system comprised an Eaton M45 Roots-type blower with an air-to-air chargecooler fed by cooling air ducted from an intake pressurized by forward motion of the vehicle. Figure 5.2 is a photograph of the production engine and Table 5.2 lists key data of the engine when operated on 95 RON gasoline. The EMS is Lotus's T4e production system with electronic throttle actuation.

From the initial research work into supercharging the 2ZZ-GE engine for application to this vehicle, it was known that the base engine was relatively knock resistant, as is illustrated by its ability to tolerate a compression ratio of 11.5:1 when supercharged and yet still give good performance at low speed while operating on 95 RON gasoline (Turner *et al.*, 2004c). This can be seen by the production calibration spark advance curves for the NA and supercharged versions of the 2ZZ-GE engine shown in Figure 5.3. The base NA engine is not very knock limited; the supercharged engine, while becoming knock limited at full load, shows a maximum reduction in spark advance in the mid-range of 10° crank angle. The use of ethanol fuel in these tests was thus expected to allow the engine to operate substantially knock-free throughout most of its speed range.



Fig. 5.2: Production supercharged 2ZZ-GE engine. (Photograph courtesy Lotus Engineering)

Table 5.2: Base engine data of supercharged Toyota 2ZZ-GE engine as fitted to Lotus Exige S production vehicle

General Architecture	In-line 4-cylinder with chain driven DOHC and 4 valves per cylinder with VVTL-i cam profile switching mechanism
Material	All aluminium with MMC cylinder block
Bore and stroke	82.0 mm x 85.0 mm
Displacement	1796 cm ³
Compression ratio	11.5:1
Maximum power	162.5 kW (218 bhp) at 7800 rpm
Maximum torque	215 Nm (158.6 lbft) at 5500 rpm
Charging system	Eaton M45 Roots-type supercharger and air-to-air chargecooler with force-fed cooling air
Intake cam timing authority range	43°CA
Cam profile switch point at full load	4500 rpm
Maximum engine speed	8500 rpm (intermittent) 8000 rpm (continuous)
Minimum octane appetite	95 RON
Engine management system	Lotus T4e
Emissions compliance	Euro 4 / LEV

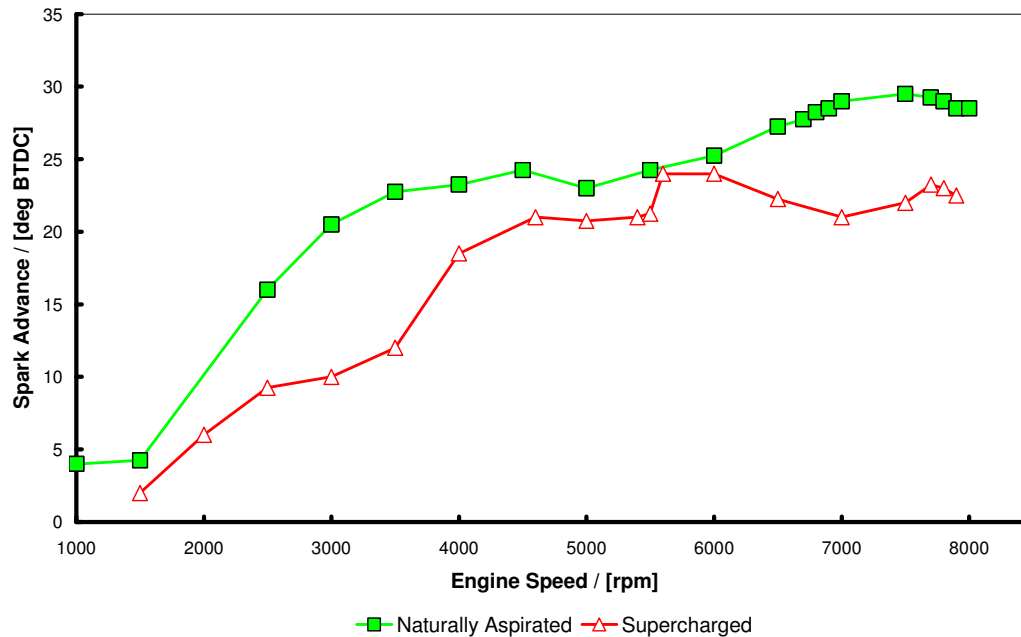


Fig. 5.3: Full load spark advance curves for naturally-aspirated and supercharged Lotus versions of the Toyota 2ZZ-GE engine

Note that since this was a production engine, the cylinders were not fitted with pressure transducers and hence cylinder pressure data was not available. In the context of this thesis, the purpose of this series of tests was to gauge the improvement in downsized engine performance that could be achieved through the use of the latent heat of vaporization of an alcohol fuel in addition to its increased octane number and sensitivity relative to gasoline. This meant that knock-limited spark advance (KLSA) was instead gauged using the production knock-sensor signal. Operation of the engine to establish the KLSA was the same for each fuel. It also meant that a novel fuel introduction system had to be engineered to maximize the effect of the latent heat of vaporization of the fuel, and to permit this investigation independently of the effect of octane number. This is discussed in the next section.

5.3 FUELLING PHILOSOPHY ADOPTED: THE USE OF PRE-SUPERCHARGER INJECTION TO MAXIMIZE THE BENEFIT OF ALCOHOL FUEL

Since it was known from the change in volumetric energy content shown in Figure 5.1 that the fuelling rates would be higher on E85 than on 95 RON gasoline, the port fuel injectors had to be changed to a higher-flow-rate specification. These upgraded injectors had a static flow rate (at 3 bar pressure) of 425 cc/min versus 300 cc/min for the standard NA 2ZZ-GE injectors, and are essentially an upgraded version of those fitted to the standard Exige S vehicle. Even with the high-flow specification chosen, it was calculated that there would be insufficient injector flow rate to run the engine entirely on only one port injector per cylinder above 6500 rpm, and thus two additional 425 cc/min injectors were added. In order to investigate the effect of the high latent heat of the fuel when operating on E85, these extra injectors were positioned in the inlet 'swan neck' between the throttle body and the supercharger entry. A schematic of the air flow path through the engine and its intake system is shown in Figure 5.4: note that the main port injectors are not specifically shown in this figure since they are in the conventional position in the intake runners. As shown in Figure 5.4, the two extra injectors were termed 'pre-compressor' (PC) injectors, despite the fact that the supercharger used had no internal compression, and the production Lotus T4e EMS used was modified to control them separately to the port fuel injectors. A photograph of the PC injectors in the swan neck is shown in Figure 5.5.

The two PC injectors were positioned such that the path of the fuel they delivered into the supercharger entry corresponded with the maximum air velocity at the exit bend in the swan neck. An additional fuel rail was fabricated and the wiring loom modified to allow the EMS to drive the PC injectors: this is also visible in Figure 5.5. Because of the high latent heat of the fuel and the fixed pulley ratio of the positive displacement supercharger, one of the primary mechanisms for increasing the power of the engine is to increase air mass flow through the supercharger by reducing the intake temperature to the rotors. This is discussed later.

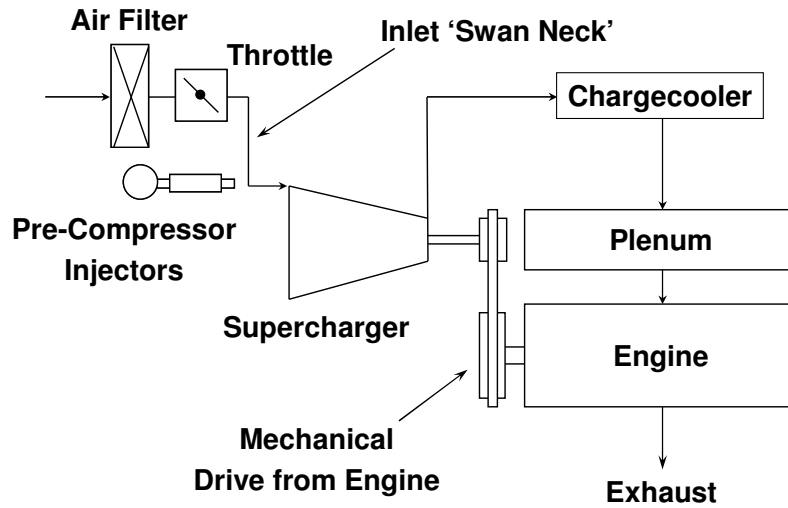


Fig. 5.4: Schematic of engine showing the position of the throttle, pre-compressor injectors and inlet swan neck in air flow path

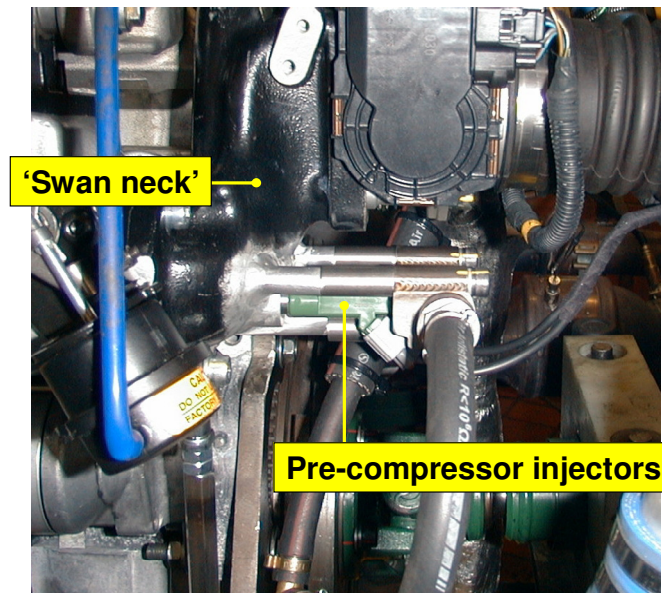


Fig. 5.5: Pre-compressor injectors in position in the intake system 'swan neck', downstream of the electronic throttle body and upstream of supercharger entry. (Photograph courtesy Lotus Engineering)

A special software program and calibration of the T4e EMS was created to drive the PC injectors independently of the port injectors; the PC injectors were timed such that one fired at the same time as the port injector of cylinder 1 and the other with that of cylinder 4, i.e. 360° CA apart in the engine firing order of 1-3-4-2. Thus, when operating on long pulse widths, there would be significant overlap of flow from these injectors. With these modifications, tests to gauge the benefit of attempting to evaporate the fuel before the supercharger could be conducted.

An operational difference between the injectors was that the PC injectors were subject to a greater pressure differential across them versus those in the intake ports (due to the lack of boost pressure on their outlet side). This allowed high rates of fuel mass to be supplied pre-supercharger despite there being half the number of injectors as at the intake ports.

Table 5.1 earlier showed that the specific energy of ethanol is about 2.5% greater than gasoline. For E85 this advantage is still above 2 per cent. The greater mole ratio of products to reactants and the faster flame speed of ethanol both provide possible further performance benefits to be obtained from E85 in the simple port fuel injection combustion system employed in this engine (i.e. without direct injection as per Whitaker *et al.* (2010) and Cruff *et al.* (2010), or the use of external cooled EGR as per Brusstar *et al.* (2002)). It is, however, the significantly higher octane index and latent heat of vaporization which separately offer the greatest potential for performance increase.

The addition of some portion of the fuel upstream of the supercharger is aimed at exploiting the latter characteristic to some extent. With a fixed drive ratio between the crankshaft and the supercharger the only way to increase the mass flow rate in a supercharged engine is to increase the charge air density upstream of it. This is not the same situation as with a turbocharger where the fluid coupling (provided by the exhaust gas turbine) permits increased boost to be applied where exhaust enthalpy is available (Bergström *et al.*, 2007a). With the arrangement shown in Figures 5.4 and 5.5 the close proximity of the fuel injectors to the supercharger will cause a significant amount of the latent heat of the fuel to

be extracted from the metal of the supercharger rotors, in turn reducing their temperature. It is also likely that there will be a gradual evaporation of the fuel as it passes through the supercharger. This makes it very difficult to make a simplistic prediction of the magnitude of the cooling effect of the fuel on the air charge without the aid of modelling. The other factors which impact on the engine performance through adding the fuel upstream of the supercharger relate to the effect on the compression work. Increasing the mass flow rate of fuel through the supercharger increases the compression work while reducing the temperature rise across it serves to reduce it (Hooker *et al.*, 1941 and Turner and Pearson, 2001). Adding fuel to the air changes its properties by increasing the specific heat capacity and lowering the value of the ratio specific heats – the former effect increases the compression work and the latter decreases it. It was shown by Turner and Pearson (2001) that even with a fuel with a relatively low latent heat of vaporization such as gasoline, the net effect of these phenomena is a decrease in the amount of work performed on the air by the supercharger. This reinforced the findings of Hooker *et al.* (1941).

5.4 DYNAMOMETER TESTING AND RESULTS

The test engine was coupled to the dynamometer and instrumented to record temperatures and pressures in the intake and exhaust system. For this research it was also fitted with a water-cooling system for the standard chargecooler matrix, to accurately control the temperature in the engine plenum chamber. The charge air side of the chargecooler was kept standard. The air inlet to the engine was held constant at 25-27°C throughout testing by the test cell conditioning system. Figure 5.6 is a photograph of the engine installed in the test cell.

Since this was a production engine taken from a vehicle and thus had not had a controlled run-in performed on it, it was decided to perform a baseline test with a vehicle calibration suitable for the upgraded port injectors used. This test was carried out without any gasoline being introduced via the PC injectors as it was not considered as advantageous when running on gasoline with a chargecooler in use at the modest boost pressures being utilized here (Turner and Pearson,

2001 and Hooker *et al.*, 1941). This effectively created a specification expected to deliver approximately 175.2 kW (235 bhp) with the opening angle of the electronic throttle limited to 74%, a characteristic of the production calibration and chosen there to avoid an excessive duty cycle on the injectors.

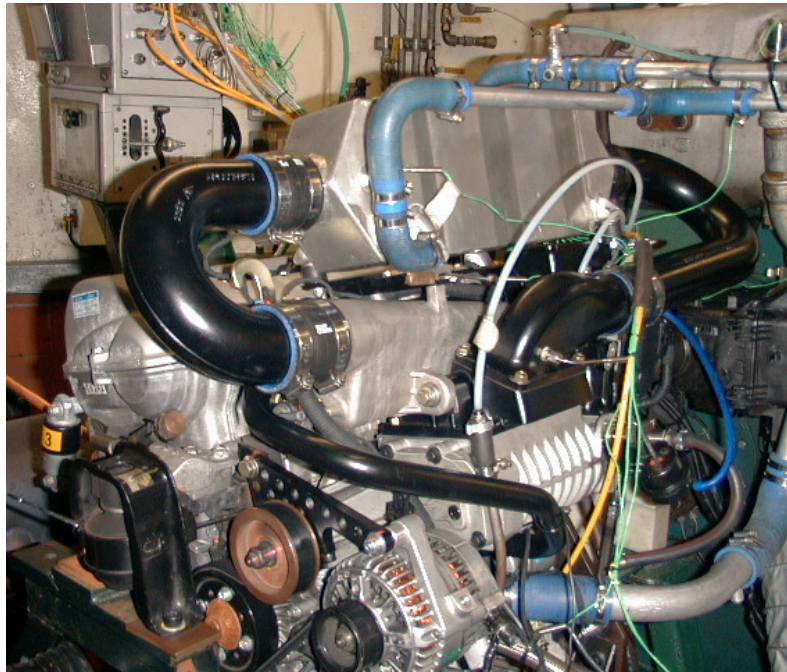


Fig. 5.6: Test engine installed in test cell. (Photograph courtesy Lotus Engineering)

Power, torque and brake specific fuel consumption (BSFC) results of this baseline test are shown in Figure 5.7. The correction factor used throughout this work was 88/195/EEC, as normally used during development testing at Lotus Engineering. In order to minimize variables, this test was performed on an ‘automatic’ calibration suitable for this injector specification; base fuelling was essentially leanest fuel for best torque (LBT) up to the cam switch point of 4500 rpm and then an air-fuel ratio (AFR) of 12.7:1 above that speed, representing $\lambda = 0.88$. Spark advance with this calibration was minimum advance for best torque (MBT) or borderline knock minus 2°, representing KLSA, whichever was reached first; this was the case for most of the speed range.

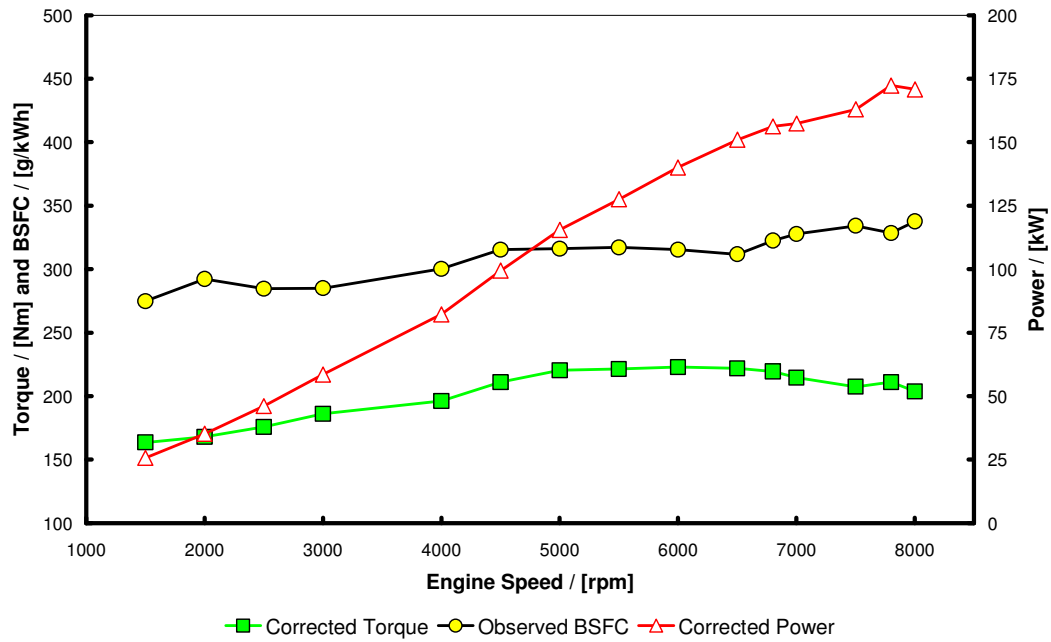


Fig. 5.7: Corrected power and torque and observed BSFC of test engine running on 95 RON gasoline with no pre-supercharger injection of fuel

Maximum power for this specification was 172.4 kW (231 bhp) at 7800 rpm and maximum torque was 223 Nm at 6000 rpm, representing a BMEP of 15.6 bar. These results were as expected from the above discussion of injector and calibration changes and so the engine was passed off for the E85 research work.

After this test the fuel system was purged of gasoline and the E85 fuel supplied to the engine.

5.4.1 Fuelling tests to investigate the effect of pre-supercharger injection of alcohol-based fuel

As stated above, a fundamental part of this piece of the research was to investigate the benefit of pre-supercharger injection of an alcohol-based fuel in the reduction of charge air temperature and its effect on engine performance. Therefore, some initial tests were conducted at fixed speed and full load, in which

the proportion of the total fuel mass being supplied by the pre-supercharger injectors was varied. The speeds investigated were 2000, 5500 and 8000 rpm, representing respectively a point commonly limited by knock at low engine speed, the maximum torque speed of the base engine and the maximum power speed. The overall AFR was kept constant at 8.7:1 for these tests, which, since E85 has a stoichiometric AFR of 9.74, represents $\lambda = 0.89$ (i.e. substantially the same as for the 95 RON gasoline test) and the spark advance criteria were the same as for gasoline. The results of the tests in terms of torque at 2000 and 5500 rpm are shown in Figure 5.8.

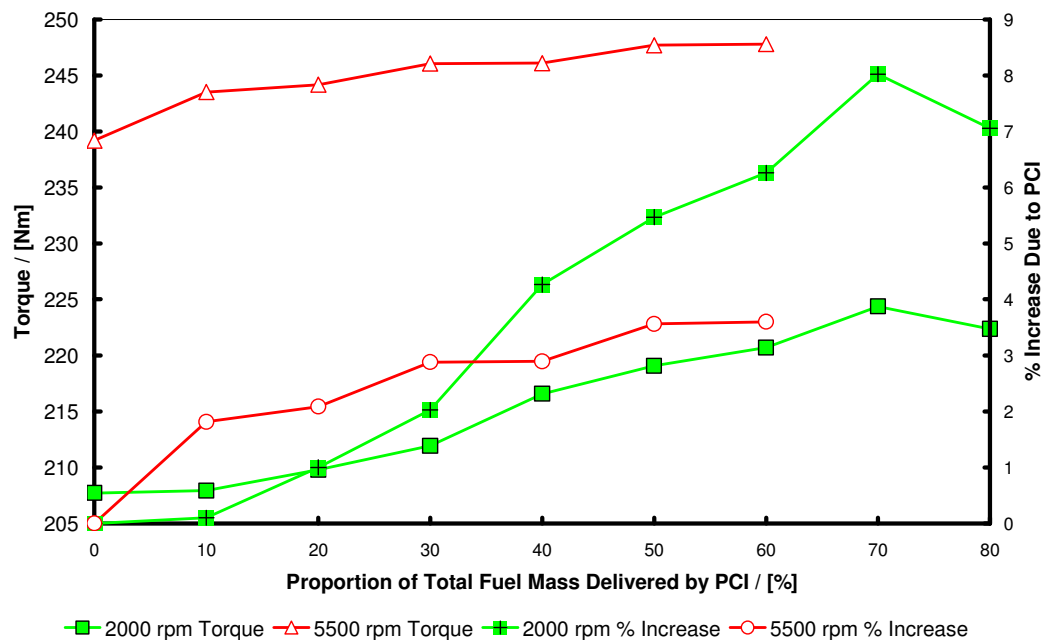


Fig. 5.8: Results of changing percentage of fuel mass delivered pre-supercharger for 2000 and 5500 rpm

For these tests, the inlet plenum temperature was held constant at 30 and 41 °C for the speeds of 2000 and 5500 rpm, respectively. These are the standard temperatures for the production engine when operating on gasoline, and were adopted to minimize the number of variables. It should be noted that for both engine speeds presented, the supercharger outlet temperature became less than

the controlled plenum temperature at 50% PCI fuelling rate. Therefore, the increase in torque above this PCI fuelling rate for both of the speeds shown in Figure 5.8 is achieved despite the water-cooled chargecooler actually heating the charge up, i.e. the charge cooling effect seen at the supercharger is not being realized at the engine inlet ports. However, the magnitude of the improvement due to PCI fuelling is such that a proportion of the increase is likely to be due to compressor work reduction in addition to the increased mass flow through the engine (Hooker *et al.*, 1941 and Turner and Pearson, 2001).

It should be mentioned that the percentage of fuel delivered by each set of injectors was not measured independently during this work. This was because the developed engine was intended to be put into a vehicle and so separate measurement of the fuel flow through the PC injectors was not possible. Instead the percentage of PCI fuelling quoted was that from a look-up table which was based on engine speed and load. The T4e EMS performed a calculation based on air flow to establish the total necessary fuel flow rate, and then split this between the port and PC injectors based upon injector 'on' time. As mentioned, the differential pressure for each set of injectors was not taken into account, and so for each of the percentage fuel loadings shown for the PC injectors, slightly increased flow rate may be expected at this position. However, because the change of flow rate with pressure for an injector is proportional to the square root of the difference in absolute pressures, 33% PC flow rate would equate to 35% with a correction applied for the 0.5 bar (gauge) boost condition, i.e. very little change. The shape of the curves in Figure 5.8 would not significantly alter, therefore, and the magnitude of the difference could be within the measurement error of most practical in-stream measurement devices.

Results are not shown at 8000 rpm because the response was flat at <0.7%. Part of the reason for this insensitivity is that, as mentioned above, the port injectors could not supply all of the fuel required to operate the engine at this point. This is illustrated in Figure 5.9, which shows the base fuel delivery required to run the engine at full load, the total that could be supplied by the port injectors, and the point at which the PC injectors had to be brought into action

because the port injectors were at their flow limit. These calculations take into account the static flow rate of the injectors together with a minimum closed period for the injectors of 500 μ s per cycle (necessary to avoid saturating their driver stages). Thus a degree of PC fuelling became necessary above 6500 rpm. It should also be pointed out that these tests were reported at 74% throttle opening, for reasons discussed in the following section, and so the air mass flow into the engine was limited at high engine speed.

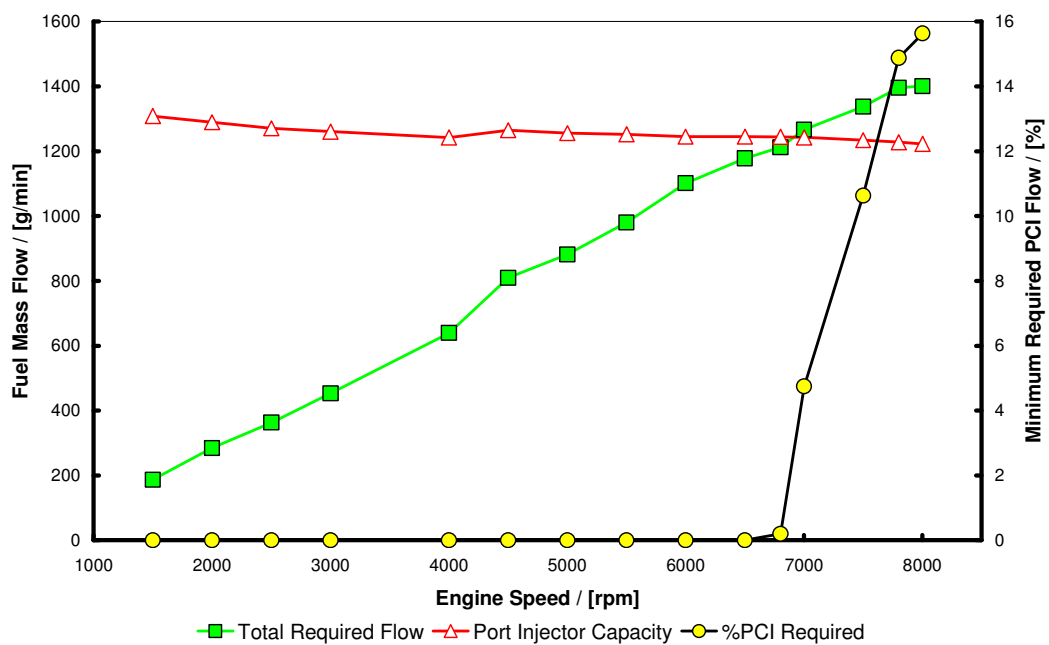


Fig. 5.9: Fuel requirement, port injector flow capacity and minimum PCI flow rate

It can be seen in Figure 5.9 that at 8000 rpm the PC injectors have to supply at least 15.6% of the total fuel mass, so some of any benefit of PCI at this point would have been present anyway. Other reasons for the reduced response to PC fuelling rate during the 8000 rpm test could be due to the fixed speed nature of the supercharger drive. On a turbocharged engine, with its variable ratio supercharger drive system (i.e. the turbine and wastegate), it is possible to make more benefit of the higher knock resistance of the ethanol-based fuel, since the boost can be increased as well as the ignition advance, subject to the limits of the

compressor map (Bergström *et al.*, 2007a). This cannot be achieved with a supercharger fixed-ratio drive system. Evidence of this effect at lower speed could perhaps be that between 2000 and 5500 rpm the benefit of introducing fuel pre-supercharger is approximately halved, from 8 to 3.5%, as is shown in Figure 5.8. This is also in line with the reduced improvement in spark advance at 5500 rpm (see later).

With 95 RON gasoline, the torque generated at 2000, 5500 and 8000 rpm was 168, 221 and 204 Nm, respectively. Performance of the engine with the different fuels and the pre-supercharger fuelling philosophy adopted is summarized in Table 5.3.

Table 5.3: Main results of the pre-compressor fuelling rate tests using E85

Engine Speed (rpm)	95 RON Torque (Nm)	E85 Torque with 0% PCI (Nm)	E85 Torque with Optimum PCI (Nm)	PCI Fuelling at Optimum (% of total)
2000	168	208	224	70
5500	221	239	248	60
8000	204	234	234	N/A

Figure 5.10 shows that the air is fully saturated by the E85 as the fuelling rate to the PC injectors reaches 40% for both the 2000 and 5500 rpm cases.

In Figure 5.8 it can be seen that the rate of torque improvement above 40% PCI fuelling is still rising slightly. The implication of Figure 5.10 is that, since the temperature increase across the supercharger effectively becomes zero from 40% PCI fuelling rate onwards, it would be possible to remove the intercooler with no reduction in power for this condition. Also, operating at rates above 40% would serve to bring the mixture in the intake system between supercharger outlet and port entry nearer to an ignitable condition. Figure 5.11 presents data for BSFC from the 2000 and 5500 rpm PCI fuelling rate tests. As the amount of PCI fuelling is increased so the BSFC falls until, in the 2000 rpm case, a

minimum is approached at 40% PCI fuelling. For the 5500 rpm case the trend is to generally decrease as the proportion of PCI fuelling increases.

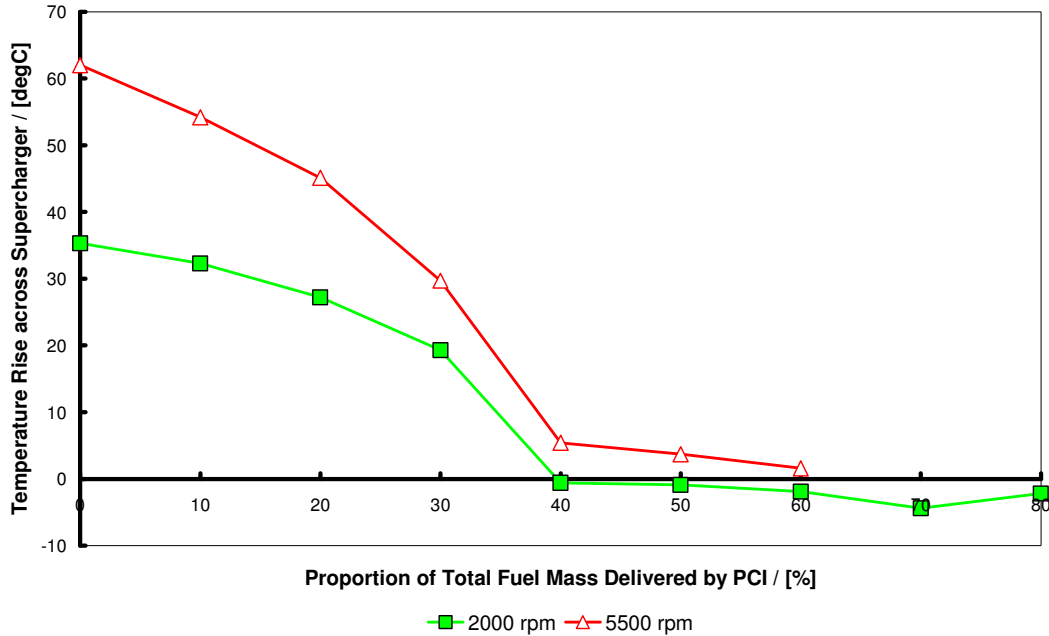


Fig. 5.10: Temperature increase across supercharger versus proportion of fuel mass delivered pre-supercharger for 2000 and 5500 rpm test points. Note that there is effectively no increase in charge temperature for this full-load condition above 40% PCI fuelling

Figure 5.12 presents data for boost pressure (expressed in gauge pressure) for the two loops. Here one can see that the boost pressure continuously rises even after the point at which there is no temperature rise across the supercharger. It must be remembered that the charge air temperature being delivered to the intake plenum from the chargecooler was being controlled to 30°C and 41°C at 2000 and 5500 rpm, respectively. The effect of this can be discerned in Figure 5.12 where there is a slight inflection for both boost pressure curves at 40% PCI fuelling rate; from this point the air is being heated and so any increase in boost pressure must be a result of the greater mass flow of air and fuel into the plenum. This is of interest since it implies that that the supercharger rotors may be being

cooled by that proportion of the E85 being delivered which is greater than that necessary to saturate the air, and so are perhaps contributing to the increase in volumetric efficiency of the supercharger which is in turn reflected in increased mass flow and hence higher boost pressure. It also means that any air displacement the extra E85 is being outweighed by the increase in bulk charge air flow into the engine. Clearly this implies that some E85 will be entering the supercharger in liquid form (to be evaporated as the air pressure increases) and this liquid may be expected to have potential implications for material durability. This will be returned to later in this chapter. These effects are believed to be the reason for the increases in torque seen beyond 40% PCI fuelling rate.

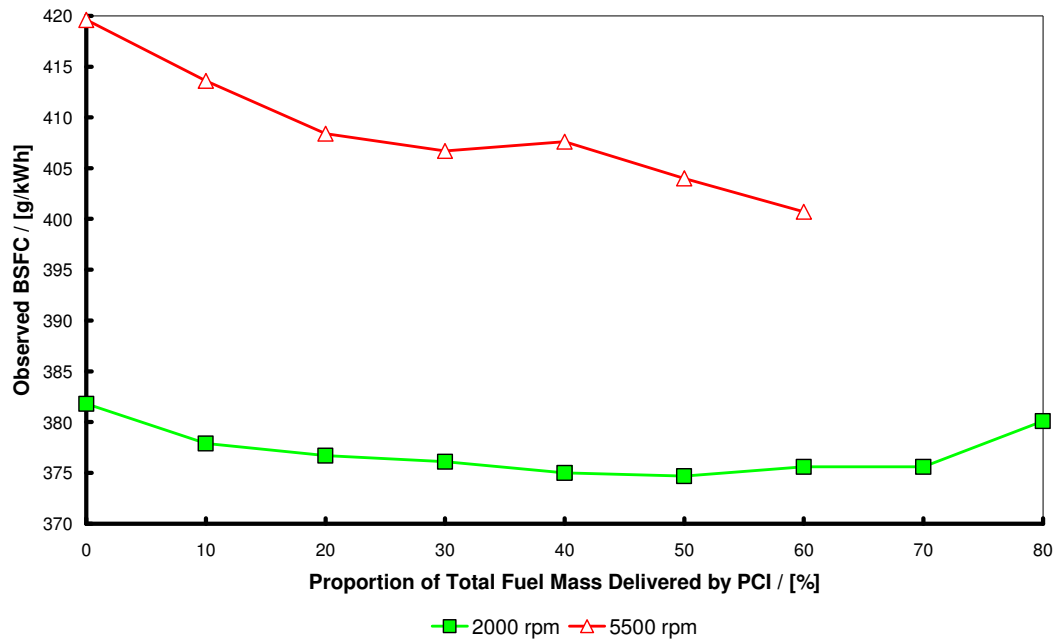


Fig. 5.11: Observed BSFC versus proportion of fuel mass delivered pre-supercharger for 2000 and 5500 rpm test points (operating torque given in Fig. 5.8)

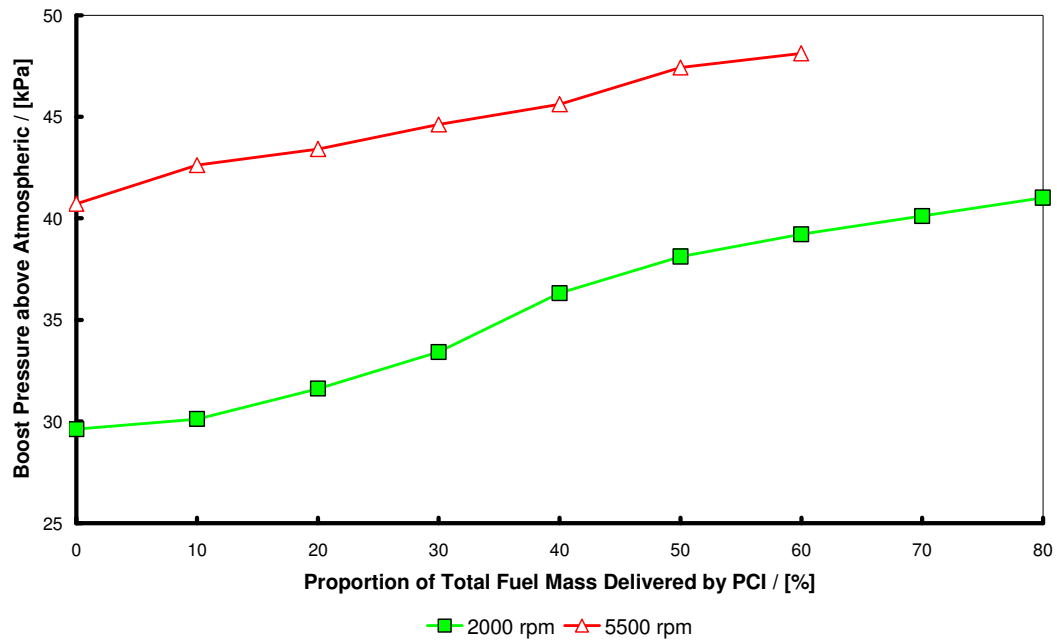


Fig. 5.12: Boost pressure above atmospheric against proportion of fuel mass delivered pre-supercharger for 2000 and 5500 rpm test points. Throttle position constant at 74% throughout test (see text)

From this work it can be concluded that for high-performance engines running on low-carbon-number alcohol fuels and with PCI, saturation of the air can readily be achieved at moderate boost pressures such that there is no net increase in charge temperature across the supercharger. The high latent heat of vaporization in turn means that mass air flow effects outweigh air displacement by the fuel. Therefore, splitting the fuelling rate between the port and the pre-supercharger location allows the maximum performance to be obtained through optimized evaporative charge cooling by the fuel.

5.4.2 Engine performance on E85 and comparison with 95 RON gasoline

A torque curve when operating on E85 was then obtained at a fixed PC fuelling rate of 30%. This figure was decided upon as a good compromise with respect to performance while avoiding operating the PC injectors on a 100% duty cycle

anywhere in the torque curve. Also, as discussed above, it was not possible to operate above 6500 rpm solely on the uprated injectors in the intake ports anyway.

As before, the throttle angle was held at the same 74% to ensure a true comparison to the gasoline baseline based on available atmospheric oxygen flow rate past the throttle and into the engine. For E85, fuelling was set to 9.1:1 at 1500 rpm and 8.7:1 AFR at all points above this (i.e. $\lambda = 0.93$ and 0.89, respectively) and, similar to the 95 RON tests, spark advance was set to MBT; this was possible because the performance was not limited by the onset of knock throughout the speed range. This approach resulted in an increase in engine power of 24.7 kW (33 bhp), the engine now producing 197.1 kW (264 bhp) at 8000 rpm (an increase of 14%) and 246 Nm at 5500 rpm, representing a BMEP of 17.2 bar and an increase in torque of 23 Nm (10%). Figure 5.13 shows the performance of the engine when operating in this manner on E85 fuel.

As discussed in the previous section, because the test cell chargecooler system effectively heated the charge up before it flowed into the engine, the major proportion of the improvement must be due to the extra spark advance made possible by the higher octane value of ethanol. Figure 5.14 shows a comparison plot of torque and power for these fixed maximum throttle position tests on the two test fuels, while Figure 5.15 compares the spark advance for the two supercharged conditions with the NA spark advance curve reproduced from Figure 5.3.

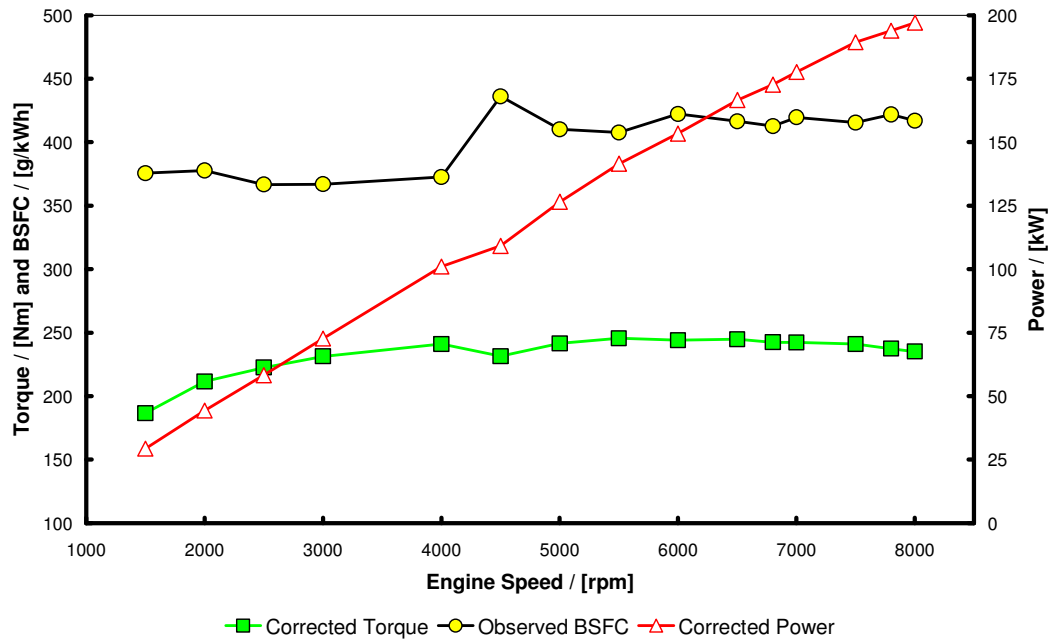


Fig. 5.13: Corrected power and torque and observed full-load BSFC of test engine when operated on E85 with a fixed 30% pre-supercharger injection of fuel mass throughout the speed range

From Figure 5.15, the increase in spark advance that can be sustained on E85 is striking: at 2000 rpm on 95 RON gasoline the maximum knock-limited spark advance was 2.5° BTDC, while on E85 the maximum spark advance (at MBT) was 16.5° BTDC, an increase of 14° crank angle (CA). This increase is typical of that obtained at the lower end of the engine speed curve, until the switch point from the low- to high-lift cam profiles at 4500 rpm. After this speed the reduced effective compression ratio due to the later intake valve closing timing and improved scavenging of residuals due to the increased angle-area presumably helps with the knock limit when operating on gasoline. Nevertheless, the improvement in spark advance due to operation on E85 is still in the region of 5-7° CA.

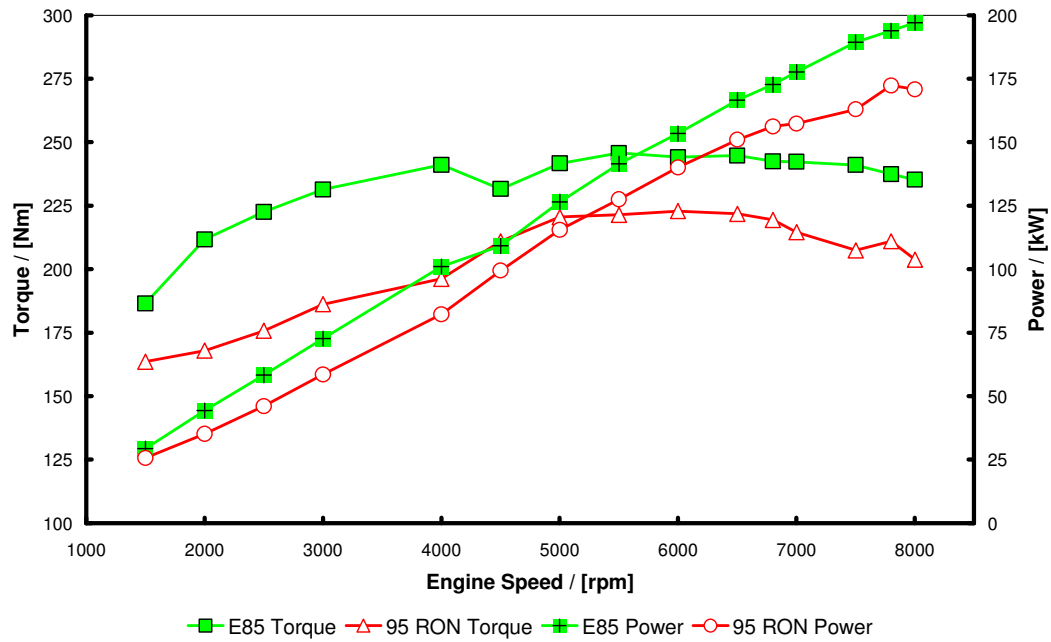


Fig. 5.14: Comparison of corrected power and torque for test engine operating on E85 and 95 RON gasoline

Figure 5.15 shows that this test engine with its slightly different injectors can support $\sim 5^\circ$ greater spark advance at 4500 rpm (the low-to-high lift cam profile switchover point in the valve system calibration, unchanged throughout this work). Furthermore, and more pertinently, as also shown on Figure 5.15, the supercharged engine when operating on E85, relative to the NA engine on 95 RON gasoline, can still support $4\text{--}5^\circ$ more spark advance through most of the speed range, and 8° more at 1500 rpm. These facts would tend to suggest a significant improvement in thermal efficiency, which will be returned to later.

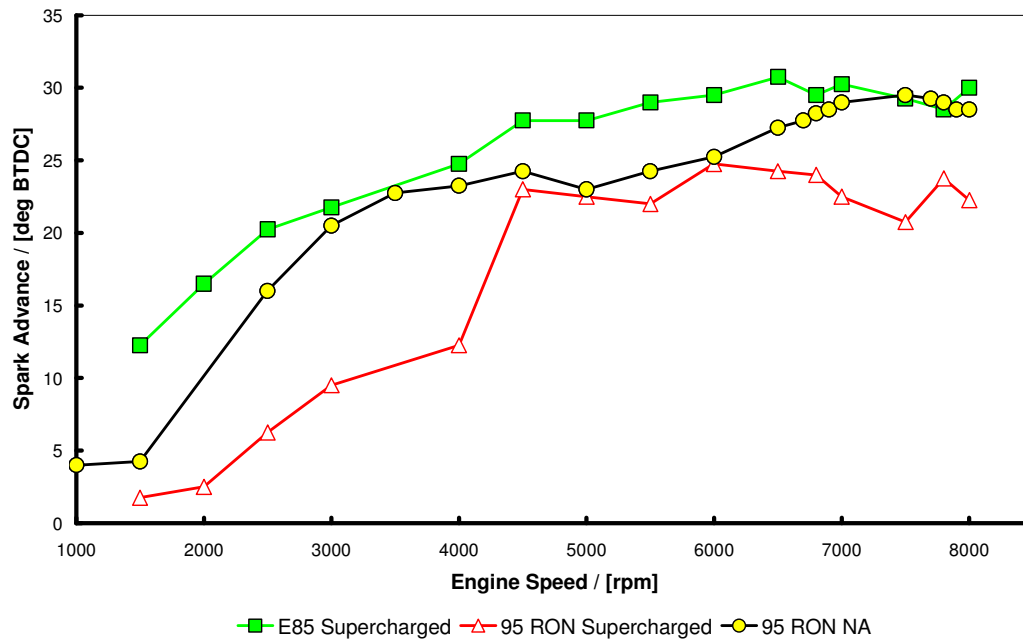


Fig. 5.15: Comparison of spark advance for test engine operating on E85 and 95 RON gasoline under supercharged conditions and 95 RON for naturally-aspirated operation

Figure 5.16 shows that operation on E85 lowered the outlet temperature from the supercharger by almost 40°C at 4500 rpm relative to gasoline. The slight increase in plenum pressure is due to the increase in overall mass flow rate. As discussed, such a detail change would not be immediately apparent if a turbocharged arrangement were tested, where the boost pressure can be individually controlled. In Figure 5.16, also note that for E85, the temperatures at 2000 and 5500 rpm tie in with those already given for the 30% PCI case in Figure 5.10.

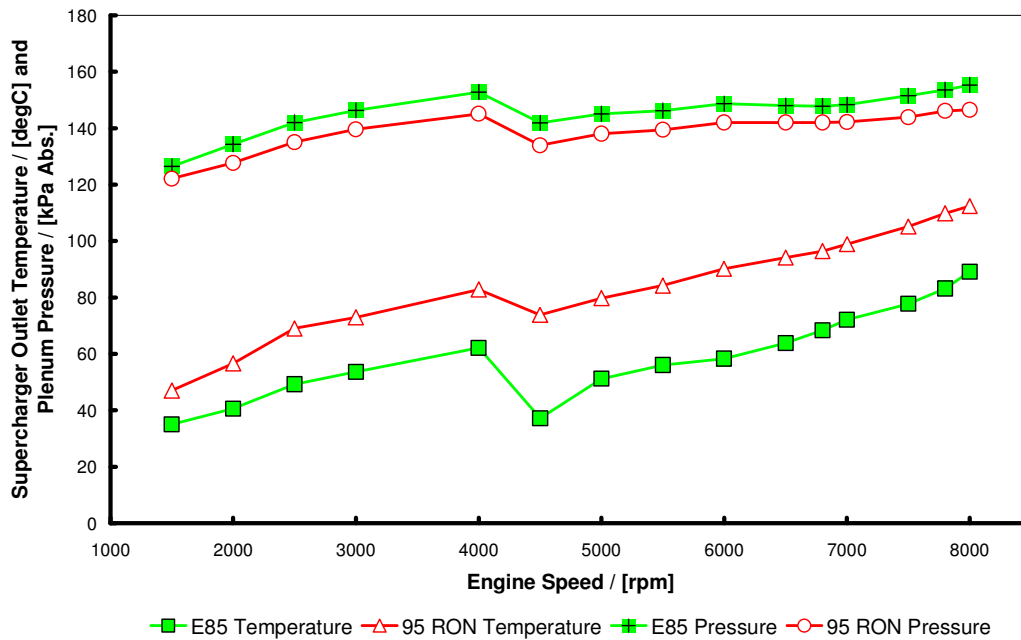


Fig. 5.16: Comparison of supercharger outlet temperature and plenum pressure for test engine operating on E85 and 95 RON gasoline

As noted above, the plenum temperature was held to a fixed relationship with respect to engine speed for all of these tests by altering the flow rate of cooling water through the chargecooler. This curve was the same as that for homologation of the Exige S vehicle and was adopted in the interest of reducing the number of test variables and simplifying the interpretation of the effects of octane number and latent heat of vaporization. A combination of the lower adiabatic flame temperature of E85, the significantly increased spark advance that its higher octane rating permits, and the higher latent heat of vaporization of any fuel passing into the exhaust during the overlap phase would however be expected to yield markedly reduced exhaust temperatures. This is shown to be the case in Figure 5.17, a plot of the temperature in the primary exhaust runner of cylinder number 3, which was the hottest for both fuel tests.

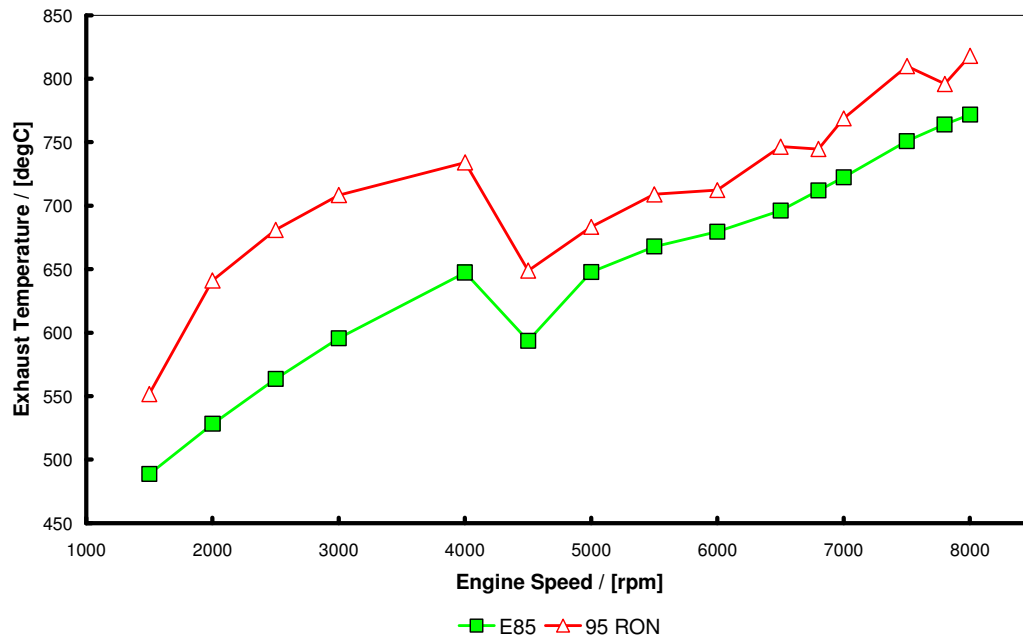


Fig. 5.17: Comparison of exhaust gas temperature in runner of cylinder 3 for test engine operating on E85 and 95 RON gasoline

In Figure 5.17, the difference in exhaust temperatures between 2000 and 4000 rpm due to operation on E85 is in the region of 100 to 150°C. After the cam profiles switch at 4500 rpm and the difference in spark advance is reduced, this difference similarly reduces to a fairly constant 50°C. Figure 5.18 shows a comparison of exhaust back pressure (EBP) for operation on the two fuels. The EBP for E85 is higher, as may be expected from the increased mass flow (inferred from higher plenum pressure and lower stoichiometric AFR) together with the higher mole ratio of products to reactants for this fuel, although the point at which the cam profiles switch is clearly discernible as well.

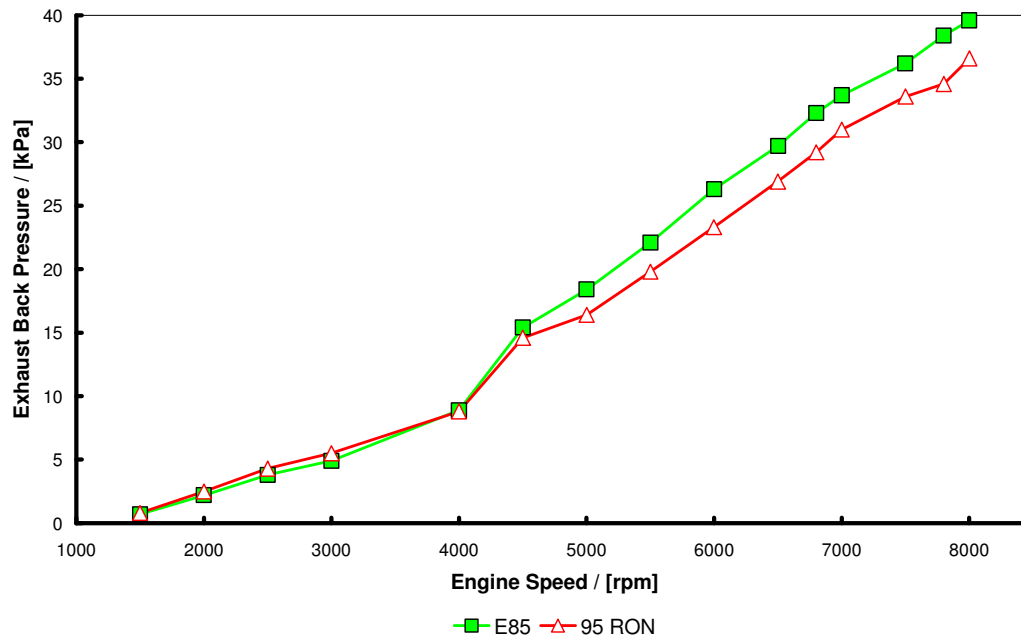


Fig. 5.18: Comparison of exhaust back pressure for test engine operating on E85 and 95 RON gasoline

5.5 DISCUSSION OF TEST RESULTS

The response of the engine to being fuelled with E85 is in line with that expected from the fuel characteristics. The 14% improvement in maximum power bears comparison with the 20% improvement found by Bergström *et al.* (2007a) for their turbocharged ‘Biopower’ engines, in which the boost pressure is increased as well. Variation of the amount of fuel introduced before the supercharger also showed the expected response at low speed, insofar as a performance benefit was seen in the tests conducted at 2000 and 5500 rpm (see Figure 5.8).

However, the pre-supercharger fuelling tests did suggest that something was restricting the performance of the engine at 8000 rpm. In order to investigate the notion that the throttle angle was becoming a restriction at 8000 rpm, a power curve was conducted with it fully open using E85 with 30% PC fuelling rate. This resulted in a maximum power of 199.9 kW (268 bhp) and maximum torque of 249

Nm. From this it was deduced that the throttle angle was not a significant restriction on performance, and that the swallowing capacity of the supercharger was likely to have been the limit. Due to the knock-free operation on E85 it was therefore recommended that the fixed drive ratio of the positive displacement blower should be altered for any future testing, in order to generate more boost and therefore to exploit the knock limit benefit of E85 further. While this was not carried out in this research, it does suggest a worthwhile future direction. Nonetheless, the fixed swallowing capacity of the engine as determined by the configuration of its charging system has allowed combustion effects to be divorced from charging system effects to an extent that operation with a turbocharger may have precluded. This has been illustrated by the increase in plenum pressure discernible in Figure 5.16 and the benefit of this approach has also been shown in the results given in the PCI fuelling loop tests.

Investigation of the fuelling tests in which the proportion of total fuel flow introduced through the PC injectors was varied (see Figure 5.8) shows that further optimization of PC fuelling would only have increased maximum torque over the power curve conducted at 30% PC fuelling rate by ~2 Nm (see Table 5.3). However, at 2000 rpm an increase of 12 Nm (to 224 Nm) could be realized through detailed optimization of PCI fuelling rate. When compared to the 168 Nm that the engine delivered on gasoline at this speed, this would be an improvement of 56 Nm, or 33%. Clearly the extension of the knock limit afforded by an increase in latent heat of vaporization of the fuel can be exploited to a significant degree in pressure-charged engines by employing alcohol-based fuels.

Figure 5.19 shows the BSFCs when operating on the two fuels, together with the ratio of the two (defined as the BSFC when operating on E85 divided by that when operating on gasoline). Figure 5.19 underlines a fundamental point when comparing the specific fuel consumption of pure hydrocarbon and alcohol-based fuels: that the disadvantage of the energy content of the alcohol fuel in volumetric terms (as was indicated in Table 5.1) can be mitigated to a degree if the engine can operate in a knock-free manner at a high compression ratio. For example,

the lower heating value of 95 RON gasoline is ~42.7 MJ/kg and that for E85 is 29.1 MJ/kg and the ratio of these values is 1.47, so that for the same combustion efficiency one might expect the BSFC of E85 to be 1.47 times higher than that on 95 RON. Figure 5.19 shows that this is not the case, which is due to the fact that one of the fuels was knock limited under these test conditions while the other could operate at MBT.

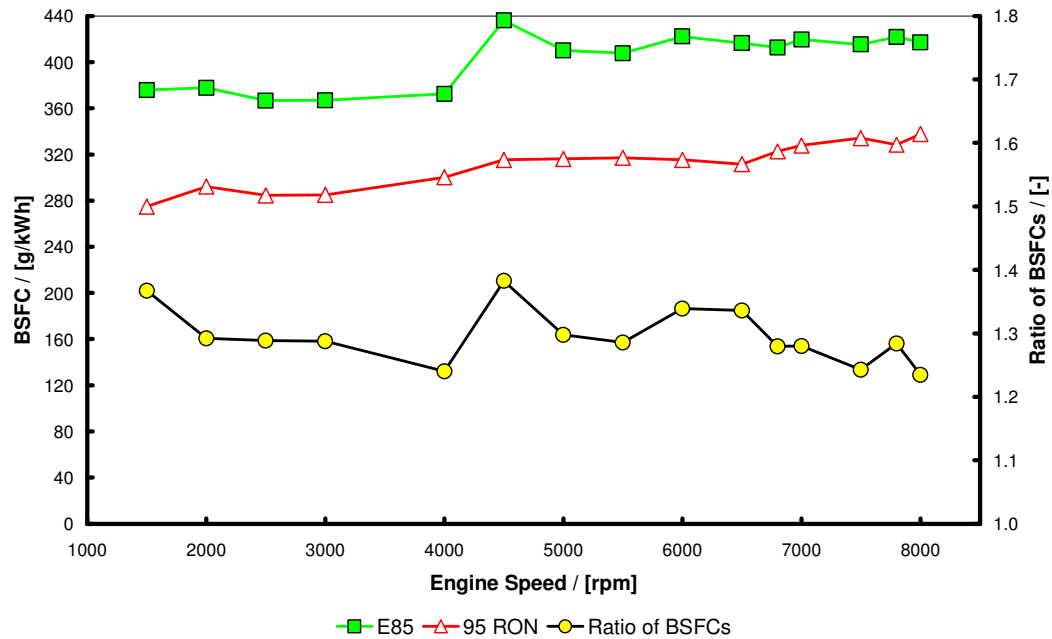


Fig. 5.19: Comparison of observed BSFC of test engine when operating on E85 and 95 RON gasoline, and ratio of the two

Clearly a far better basis for comparison of these (or any) fuels is that of thermal efficiency, enabling the degradation in performance due to operation on gasoline versus the alcohol-based fuel to be calculated quite simply. Here, the definition of fuel conversion efficiency of Heywood (1988) is used for brake thermal efficiency (BTE):

$$\eta_f = \frac{1}{\text{BSFC } Q_{\text{LHV}}} \quad \text{Eqn 5.1}$$

where η_f is the fuel conversion efficiency, BSFC is the brake specific fuel consumption and Q_{LHV} is the gravimetric lower heating value (LHV) of the fuel.

The results are shown in Figure 5.20, in which the peak BTE for E85 is shown to be 33.8% at 2500 rpm, while that for 95 RON gasoline is 30.7% at 1500 rpm, i.e. gasoline is relatively 9% worse in terms of peak thermal efficiency. More tellingly, at maximum power and maximum torque, the knock-limited nature of gasoline degrades the BTE of the engine by 12.5 and 16% respectively, although it is accepted that some of the change in performance is related to the use of the wet-compressor technique when operating on E85 in addition to the combustion effects. With physical charge-air cooling, the wet compressor technique is not believed to be especially beneficial when operating on gasoline at modest boost pressures, due to the significantly lower latent heat of vaporization (see Table 5.1, Turner and Pearson (2001) and Rosenkranz *et al.* (1986)) although this observation must be compared with the results of with Hooker *et al.* (1941) who demonstrate relevance of the wet-compressor technique at higher boost pressures when using gasoline in an aero engine.

The type of engine used in this series of tests is somewhat unusual insofar as it can be successfully operated on gasoline with a combination of a high CR and pressure charging (Turner *et al.*, 2004c), albeit in a knock-limited manner. This allows a better comparison of the efficiency benefit when operated on alcohol-based fuels. This was illustrated by the data in Figure 5.20, with the degradation in efficiency when operated on gasoline. Nevertheless, this degradation is primarily a result of the combination of characteristics chosen for the engine which preclude it being operated at MBT everywhere when operating on gasoline, while it *can* be operated knock-free at this CR on E85 above 1500 rpm, which therefore causes it to suffer a significant efficiency disadvantage when operated on 95 RON. This characteristic (i.e. that when at full load an engine operates at high efficiency when at a high knock-free CR on optimum ignition timing and an optimum air-fuel ratio) has been known for many years (Institution of Automobile Engineers, 1924).

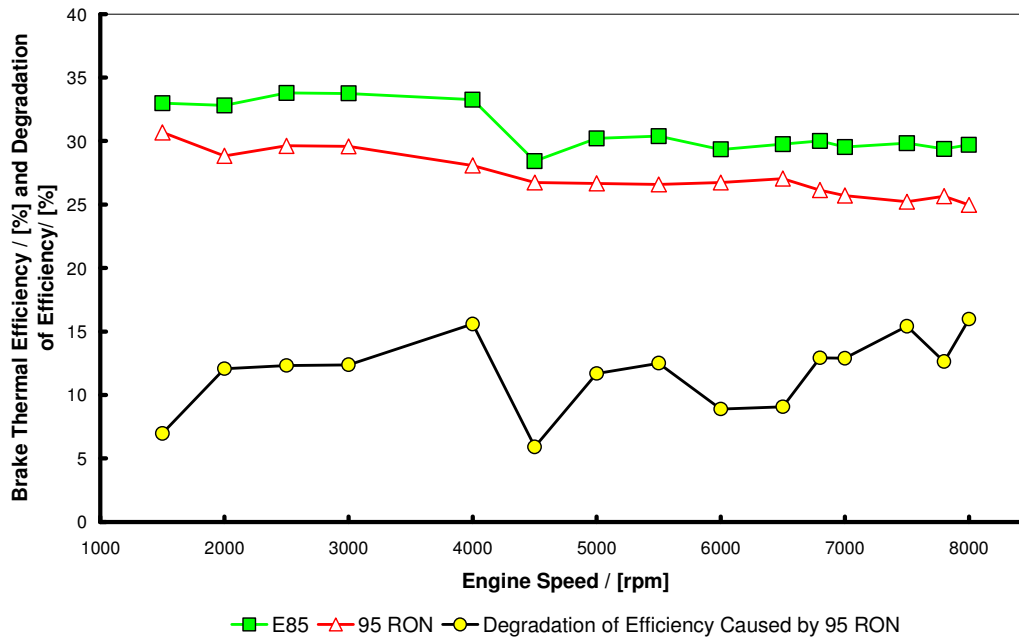


Fig. 5.20: Comparison of brake thermal efficiency of test engine when operating on E85 and 95 RON gasoline, and the relative degradation in brake thermal efficiency due to operating the engine on 95 RON gasoline

5.5.1 Practical considerations in applying a pre-supercharger injection operating strategy with E85

The basic problems of operating with a high percentage of alcohol in gasoline are well known, and have been addressed for some years in Brazil (Kremer and Fachetti, 2000). Employing a pre-supercharger injection approach for some of the fuel loading is not without further challenges. The most significant are probably evaporative emissions and the affect of ethanol being carried in the air stream on the supercharger itself.

E85 has significantly better evaporative emissions than gasoline (Benson *et al.*, 1995), although it is equally well known that the azeotrope formed by ethanol and gasoline produces a high vapour pressure below about 70% ethanol, which is

present from about 5% (Furey, 1985). This effect is because a mixture of alcohols and pure hydrocarbons does not obey Raoult's Law. For mixtures of low-carbon-number alcohols and gasoline below a certain alcohol content, therefore, there is likely to be a significant challenge in managing evaporative emissions.

As mentioned in Chapter 4, the concept of PCI had already been developed for methanol-burning IndyCar engines that the author had previously worked on. There, the amount of PC fuelling permitted was solely a function of throttle position and boost pressure, and emissions were not a concern. It was proposed for the research reported here that, for practical applications of PCI to road vehicles, the earlier approach be modified to include the proportion of alcohol in the intake air stream, and that the strategy would only be permitted above a certain level. This would minimize the amount of gasoline contained in the fuel rail spur to the PC injectors and thus limit the effect of the azeotrope. The suggested approach was utilized in related vehicle work and found to work well (Pearson *et al.*, 2009a). It is applicable to turbocharged or supercharged engines. With control of the electronic throttle as well as fuelling and ignition, this would be a prime route to compliance in this area. However, the approach would need to be studied in greater detail due to the nature of the azeotrope referred to above.

Generally, of course, evaporative emissions compliance would have to be achieved for the entire vehicle. As long as conventional fuel lines and connectors suitable for production applications are employed, this issue is unlikely to be a problem in production. It has, after all, been addressed in several countries where E85 flex-fuel vehicles are offered for sale (e.g. Sweden and the US) (Bergström *et al.*, 2007a).

The approach could also be made to function for ternary blends of gasoline, ethanol and methanol configured for the same stoichiometric air-fuel ratio. This is because any such blend of these three components will have the same

volumetric lower heating value (to within 1%), the same RON and MON values, and the same latent heat of vaporization (to within 4%) (Turner *et al.*, 2011).

Liquid ethanol (or methanol) being carried in the air stream may create a harder challenge, however, because it is aggressive in comparison to pure hydrocarbon fuels. The engine was operated for only a few hours on E85 with PC fuelling, but the rotors showed signs of removal of the abrasible coating which they carried. This is shown in Figure 5.21. However, this supercharger was relatively old when subjected to E85 operation, so the exact amount of damage due to operation on ethanol, if any, cannot be fully quantified here. In mitigation, no appreciable degradation in boost pressure was noted during this research, suggesting any damage may have been sustained before it was undertaken.

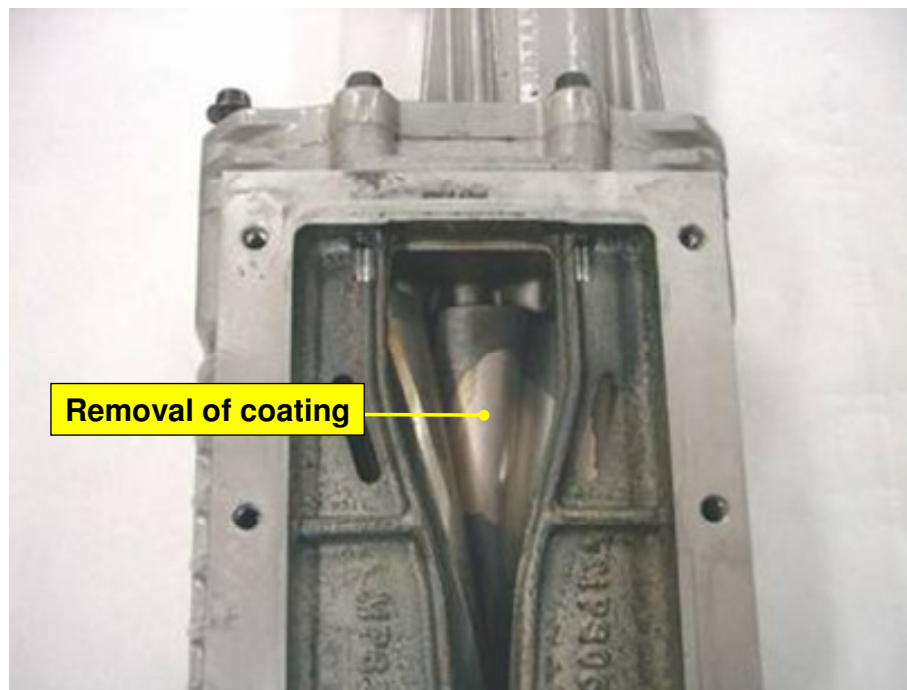


*Fig. 5.21: Removal of supercharger rotor coating noted after testing.
(Photograph courtesy Lotus Engineering)*

Coatings are typically damaged by alcohols (Hagen, 1977 and Owen and Coley, 1995), but the underlying aluminium of the rotors shown in Figure 5.21 was not

damaged. If a non-coated turbocharger compressor had been used instead, this might not have suffered the same amount of damage. Since introduction of the fuel before the compressor has been used for a long time for Indianapolis-type racing (Ludwigsen, 2001), as well as to increase the take-off performance of aircraft engines (Whitford, 2000), it is presumed that this challenge is not an insurmountable one, given that the improvements in specific output and thermal efficiency are deemed attractive enough to warrant the approach. Since this would enable further downsizing of an engine and greater reduction in throttling loss as the proportion of alcohol in the fuel is increased, there is perhaps some merit in investigating the concept further, especially since, in a turbocharged engine, this would result in lower pumping work through the reduced turbine expansion ratio required to drive the compressor. Furthermore, introducing the fuel only up to the saturation limit of the air could be expected to be beneficial, although from Figure 5.10 it is evident that the PC fuelling loops were conducted to well beyond this point. This was one of the reasons for limiting the PC fuelling rate to 30% for the power curves presented here. It could thus be that if the damage evident in Figure 5.21 was due to ethanol introduction pre-supercharger, it may have occurred only beyond a fuelling rate of 40%, and this could be relatively easily avoided in the calibration of PCI operation. Further work is warranted on this, but has not been conducted as part of the present research.

If these problems were viewed as too difficult to attempt to surmount, an alternative is to introduce the extra fuel via extra injectors positioned after the pressure-charging device. These have been arranged previously in gasoline engines where secondary injectors were necessary because of flow-range limitations of the port fuel injectors (Wood and Bloomfield, 1990 and Crosse, 2011). Introducing alcohol-based fuel at this point in the intake system will not have the same benefit in reducing compressor power, but would still allow a significant reduction in charge air temperature due to the high latent heat of vaporization of the alcohol. As noted, this could be more beneficial if a variable-speed drive was employed, as is the case in a turbocharged engine. Positioning the extra injectors here would also be expected to have a beneficial impact on evaporative emissions in the case of an engine supercharged by a positive-

displacement device, since the supercharger would form a mechanical gate to the fuel vapour when the engine is shut down.

5.6 CONCEPTS TO IMPROVE THE EFFICIENCY OF FLEX-FUEL ENGINES

This research has shown that alcohol-based fuels, with their high octane rating and high latent heat of vaporization, can permit such an extension of the knock limit and engine performance that for flex-fuel engines there is a significant compromise to be accepted if they are also required to operate on gasoline. This is especially the case within the constraints of conventional engine architectures.

Compared to operation on gasoline, alcohol-based fuels can simultaneously permit high compression ratio and high boost pressures to facilitate aggressive downsizing. This can theoretically be to a degree far higher than is currently being pursued for engines fuelled by gasoline, because gasoline is more limited by fuel autoignition considerations (be it knock or increasingly more commonly preignition (Bergström *et al.*, 2007b, Manz *et al.*, 2008, Zaccardi *et al.*, 2009 and Kalghatgi, 2009)). The effects of direct injection of alcohol would enable a significant further extension of the knock limit due to the manner in which such a fuel introduction method permits the exploitation of the latent heat of vaporization. Thus, if an engine is developed primarily for operation alcohol-based fuels, part load thermal efficiency could exceed that when it operates on gasoline, since the CR could be increased significantly to the benefit of cycle efficiency. This overall benefit would be expected to result from increased throttling loss reduction due to increased levels of downsizing, despite the fact that the higher CR works against the reduction of throttling loss. The test engine used here effectively represents one form of alcohol-optimized engine, because its high CR severely compromises gasoline operation at low engine speed (for evidence of this see the ignition advance curves in Figure 5.12).

In Section 5.4.1 the observations with regard to the reduced charge temperature rise across the compressor as the PCI fuelling rate is increased show that, for this boost level, operation without an intercooler on alcohol-based fuels would

easily be possible: a zero-degree temperature rise implies an intercooler would be redundant in an alcohol-optimized engine. This was the approach during the author's previous work with IndyCar engines mentioned to in Chapter 4. Removal of the chargecooler system would represent a significant reduction in bill-of-material (BOM) and also aerodynamic drag for a vehicle. Any flex-fuel vehicle with a bias towards operation on alcohol-based fuels could beneficially exploit this approach. Furthermore, in a synergy with other technology now being researched and introduced by the automotive industry and discussed later in this thesis (when gasoline is employed as the fuel) the latent heat of the fuel could be used to offset the thermal input to the charge when cooled EGR is deployed (Cairns *et al.*, 2006 and 2008).

The subject of cooled EGR and its use to improve fuel consumption by reducing the need to provide component thermal protection fuelling when gasoline is employed as the fuel will be returned to in Chapters 7 and 8. The concept of using alcohol fuel for evaporative cooling of EGR is discussed in more detail in Chapter 8. Put together, a simplified version of the alcohol engines developed by Brusstar and co-workers (Brusstar *et al.*, 2002, Brusstar and Bakenhus, 2005 and Brusstar and Gray, 2007) could therefore be imagined with a low BOM cost and a thermal efficiency approaching or exceeding that of a diesel engine, while still possessing the ability to operate on gasoline (albeit at reduced power levels) in circumstances when the alcohol fuel is unavailable.

The amount of degradation of thermal efficiency caused by operating on 95 RON gasoline shown in Figure 5.20 is very significant. This clearly shows that if alcohol-based fuels are to be introduced rapidly (in terms of proportion of vehicle miles fuelled on them) a new approach should be adopted to minimize the disadvantages of requiring the engine to be capable of flexible fuel operation (i.e. with gasoline as well as high-blend alcohol fuel). This will encourage greater uptake of a superior alternative fuel, the manufacture of which captures CO₂ from the atmosphere, and will drive the development of the infrastructure necessary to manufacture and distribute it. The ultimate potential of this approach is shown in Figure 5.22, where methanol is manufactured from CO₂ captured from the

atmosphere and from molecular hydrogen obtained by electrolysis of water, using renewable energy throughout. Methanol can thus be considered as a means of chemically liquefying molecular hydrogen. If this system is adopted, enabled by the value and use of methanol as transportation fuel, and some of the resulting methanol is used as a feed stock for the petrochemical industry, then there is an opportunity to influence the CO₂ concentration in the atmosphere. This is because conversion of such methanol into other products effectively sequesters the CO₂. This opportunity is not provided by a molecular hydrogen-based energy economy.

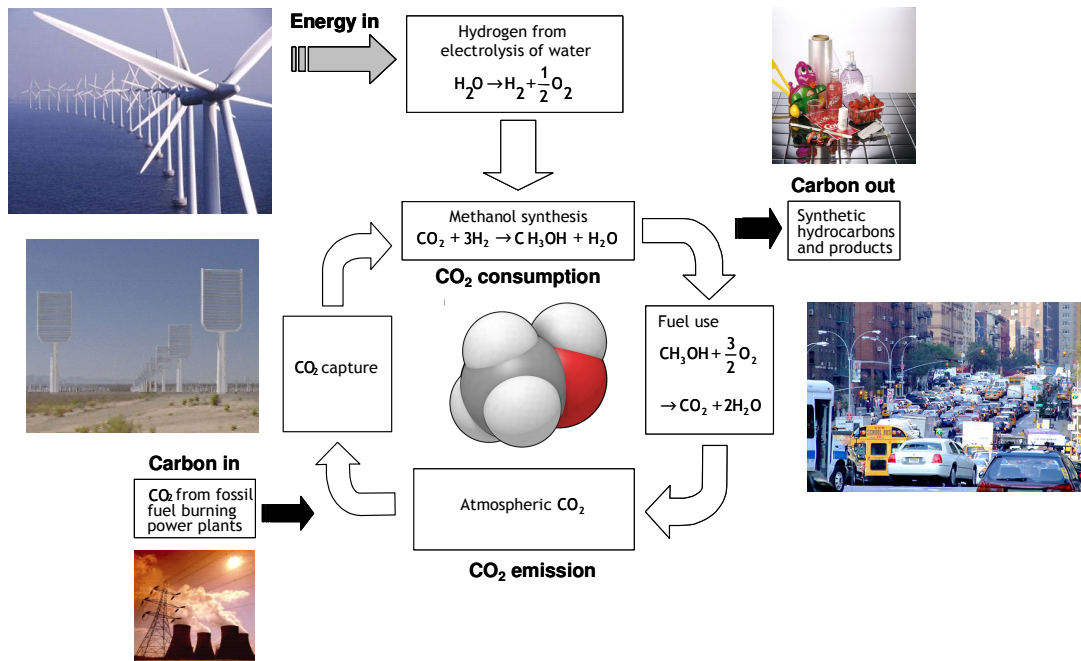


Fig. 5.22: Closed CO₂ cycle for manufacture and use of methanol as a transport fuel (adapted from Olah et al., 2006 and Lackner, 2008)

One approach to creating such an engine would be to configure it with a high compression ratio which is preferentially specified to operate most efficiently on alcohol fuels – say, with 12 or 13:1 CR – and make the engine capable of using gasoline in a lower power mode only, as alluded to in the previous section. Such an approach is readily implementable utilizing modern engine control systems with electronic throttle control, and ensures that the driver will not be left stranded

if they stray away from the alcohol-fuel infrastructure. There would also be minimal BOM impact on the vehicle, since the fuels are miscible in a single tank. However, this approach would require the end user to accept the compromise in vehicle performance brought about by the inefficiency of gasoline at the times when that fuel is used. Similar approaches are currently being studied by various researchers (Whitaker *et al.*, 2010 and Cruff *et al.*, 2010).

From the foregoing, it is to be expected that variable compression ratio (VCR) is a key technology to permit optimized operation on whatever proportion of alcohol and gasoline are used to fuel an engine. With such a system the optimum combination of boost and CR can be used for all operating conditions regardless of the fuel composition being supplied to the engine.

The part-load benefit of VCR is well known when an engine is fuelled on gasoline (Drangel and Bergsten, 2000 and Schwaderlapp *et al.*, 2002). Moving to a wider-range system than these researchers used (to cover a low setting of CR for full-load gasoline operation to a high CR for part-load operation on ethanol or methanol) would permit far higher thermal efficiency on the alcohol fuel across the engine map, and hence better volumetric fuel consumption. However, development of such a wide-range VCR mechanism will be a mechanical challenge in a typical overhead-poppet-valve 4-stroke engine due to the requirement to avoid valve-to-piston clash, an issue discussed in more detail by Turner *et al.* (2010a).

Direct injection of alcohol fuels can be exploited to increase volumetric efficiency (Wyszynski *et al.*, 2002, Bergström *et al.*, 2007b), and hence would be a good complementary technology to a VCR system for such a 'no-compromise' flexible-fuel engine, particularly at high load conditions.

5.7 SUMMARY AND CONCLUDING REMARKS

Through the operation of a test engine on a high-blend alcohol fuel, E85, together with a novel approach to charge cooling through utilizing the latent heat of

vaporization in an evaporative cooling system, and comparison of those results with the performance of the engine on its normal 95 RON gasoline fuel, the key conclusions from the work presented and discussed in this chapter are as follows:

1. The characteristics of the low-carbon-number alcohol fuels methanol and ethanol are ideally suited to use in high-compression-ratio, pressure-charged spark-ignition engines.
2. The high octane rating of an ethanol-gasoline blend, E85, has been shown significantly to extend the knock limit of a high-performance engine which, while knock-limited on gasoline, was already believed to be satisfactory in these terms.
3. Full-load thermal efficiency of this high-compression-ratio engine when operating on the ethanol blend was significantly higher than that for gasoline, primarily because of the extent to which the knock limit was increased. In this respect, it is suggested that it is better to think in terms of how much gasoline compromises the performance of an SI engine due to its lower octane rating when compared to its operation on an alcohol.
4. The high latent heat of vaporization of ethanol has been shown to be exploitable in terms of extra performance through its introduction into the air stream before a supercharger. Optimization of the proportion of the total fuel mass provided at this point in the engine intake system has been shown to increase both BMEP and thermal efficiency.
5. When operating on E85, the injection of ~40% of the total fuel mass at the supercharger entry resulted in no increase in temperature across the supercharger relative to atmospheric conditions. This was at a boost pressure of ~40-50 kPa (gauge).

6. Ethanol and methanol are both known to be corrosive to certain materials in comparison to gasoline, and to promote abrasion on rubbing surfaces. This has possibly been indicated by damage to the coating of the supercharger used in this work. However, due to the uncertain history of the supercharger used, this point is unproven. A different strategy for any production application may be needed, but an uncoated turbocharger impeller may well be unaffected.
7. Future engines can be optimized to greater thermal efficiency on alcohol fuels by increasing their compression ratio and the boost pressures at which they operate. Strategies allowing the engine to still operate on gasoline (albeit at lower performance) would then have to be developed, but are implementable using modern engine management systems.
8. Variable compression ratio would be a key technology to obtain the best performance from an SI engine expected to operate flexibly at the best possible efficiency on different pure hydrocarbon and alcohol fuels.
9. Optimizing engines to run at high efficiency on alcohol fuels would permit more rapid introduction and penetration of such fuels into the market for transport energy.

As a consequence of the work reported in this chapter it can be seen that exploitation of fuel characteristics can improve the thermal efficiency of conventional engines, and that renewable fuels can be introduced into the fuel pool readily if they share miscibility with those in common usage now. The benefit of cooled EGR has been mentioned and this will be further discussed in Chapter 8, where the possibility to further exploit the high latent heat of vaporization of alcohol fuels will also be returned to. The next chapter, however, investigates the benefit of improved charge cooling techniques and as such considers the effect of this for more conventional engine operating strategies when operating on gasoline.

Chapter 6: Single-Cylinder Engine Tests at Constant Charge Air Density

This chapter describes test work conducted to investigate the hypothesis that under conditions of fixed charge air density, the knock limit can be extended by reducing the charge air temperature while its pressure is reduced commensurately to maintain the fixed-density condition. Firstly, it describes the test equipment developed to gather the experimental data presented in the chapter. The single-cylinder engine employed, the overall design of the direct-injection combustion system of which the author specified, is described. Similarly, the 'charge air conditioning' rig used to control the air pressure and temperature in the test work is then described. The process of specifying volumes in the intake and exhaust systems is discussed and the supporting 1-D modelling work is also reported, the intention of which was to establish the size of orifice plates necessary to yield a target back pressure curve for the engine for the exact layout of the intake and exhaust system utilized. This was to make the results more representative of those that would be expected from a multi-cylinder turbocharged engine. Scoping tests to fix AFR and valve timing for the main tests are then presented. Finally, the fixed-air-density test results are reported, with some concluding observations regarding the original hypothesis on knock limit and charge air conditions.

6.1 SINGLE-CYLINDER TEST ENGINE

The engine used for the test work was a new type of single-cylinder engine designed by Lotus Engineering primarily for use in the UK Engineering and Physical Science Research Council (EPSRC)-funded collaborative project 'HOTFIRE' (Turner *et al.*, 2006a).

The engine had a bore and stroke of 88.0 mm and 82.1 mm respectively, yielding a swept volume of 499.3 cm³. The bore and stroke are those of a supercharged PFI V6 engine which was in development at Lotus Engineering at the same time,

and which donated much of its cylinder architecture and some of its parts to this programme. This 'donor' V6 engine is shown in Figure 6.1.

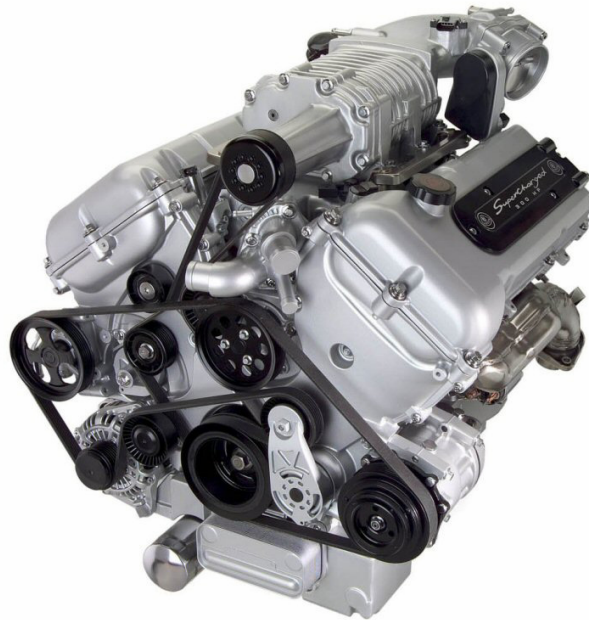


Fig. 6.1: V6 PFI supercharged engine which donated its general cylinder architecture to the test engine used in this work. (Photograph courtesy Lotus Engineering)

As well as having a PFI system configured in exactly the same way as in the donor V6, the single cylinder engine used for this work was also fitted with an 'central' or close-spaced DISI combustion system, utilising a Siemens VDO Automotive (now Continental Automotive Systems) 'XL2' 'Multistream' injector. This close-spaced arrangement was chosen to allow maximum cooling benefit to be gained from the latent heat of vaporization of the injected fuel while avoiding wetting the bore walls at a point of piston ring reversal.

The cylinder head used the same general architecture on the intake side as the donor engine, and thus had intake valves of a size so as to not be a limitation on performance. The intake port geometry was the same, too. Performance correlation back to the donor engine could therefore be carried out. However,

retention of the original intake valve sizes might have been expected to impact on the size of the exhaust valves, because the centre of the combustion chamber now had to accommodate a direct fuel injector as well as a spark plug. Consequently a 10 mm diameter spark plug was specified instead of the 14 mm diameter item in the donor engine, in order to free up space in the cylinder head for the new centrally-placed injector. Nevertheless, on the exhaust side of the cylinder head, the valve throat area had to be reduced by 10% in order to position both the spark plug and the injector into the space between the four valves. Some 1-D modelling in the design stage of the single-cylinder engine was conducted in order to show that the performance would not be adversely impacted by the reduction in exhaust throat diameter (Turner *et al.*, 2006a). The general configuration of the cylinder head can be seen in Figure 6.2, where it can be seen that the presence of the DI system did not significantly compromise the combustion chamber. The modification to the valve sizes and insertion of the injector next to the spark plug resulted in slightly different valve angles to those in the donor V6 engine, but this change was containable within the original combustion chamber shape.

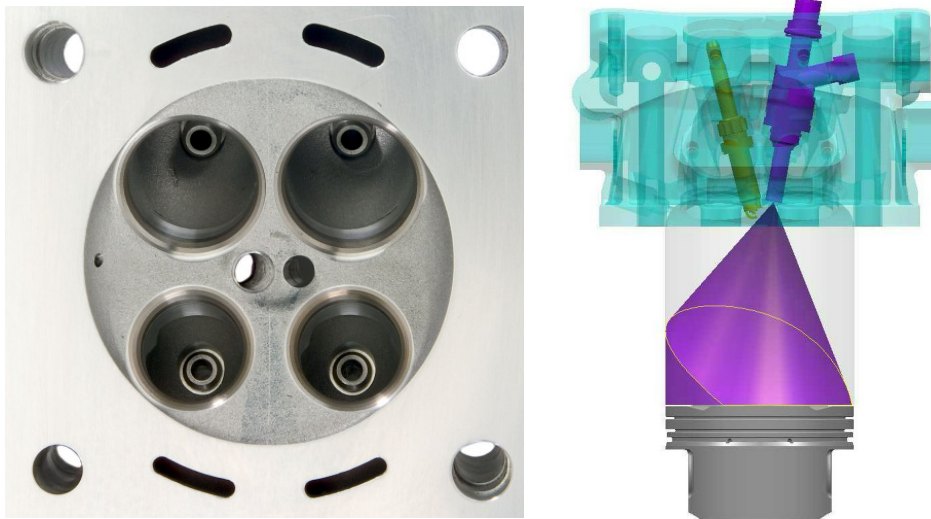


Fig. 6.2: View on fire face of cylinder head of single-cylinder test engine (left) and combustion system layout (right). (Photograph and illustration courtesy Lotus Engineering)

The compression ratio (CR) of this engine was 10.0:1, compared to 9.5:1 for the donor V6. This was because the direct injection (DI) system, when used for other test work, was expected to yield an extension to the knock limit, and it was believed that this would be shown to a greater degree by the use of a higher CR. Whilst the DI results are not reported here, this combustion system with DI was carried across largely unchanged to the Sabre demonstrator engine described in Chapter 7, which was also used to gather the cooled EGR test results presented in Chapter 8.

An unusual characteristic of the exhaust ports in this single cylinder engine is that they were separated up to the cylinder head outlet flange, and hence necessitated an external 'Y'-shaped link piece to bring them together to a single exhaust pipe. The potential functionality of this port separation was not used in this work, however, the design having been configured in this way to give flexibility for future unrelated tests when employing the Lotus Research Active Valve Train (AVT) system which was fitted to the engine.

The AVT system used electrohydraulic actuation of the poppet valves with a real-time feedback control system to provide the ability to change valve lift profiles and valve timings rapidly. This could be done while the engine was running. AVT was used primarily to investigate valve timings in one of the series of tests reported below, so that the valve events specified could be expected to yield a level of BMEP representative of a conventionally-valved engine for the test conditions investigated. The AVT system has been described in detail in other publications by the author and co-workers (e.g. Turner *et al.*, 2002b, 2004a, 2004b and 2006a).

General specifications of the engine as used in the tests described in this chapter are given in Table 6.1.

The base engine had the provision for full balancing of primary and secondary forces and could also be fitted with an optical section allowing optically-accessed operation up to 5000 rpm. In the configuration that was used here, however, only

the primary balancing system was fitted since the secondary system was really only necessary when using optical diagnostic methods. A 'ghosted' view of the general arrangement of the engine showing the primary balance shafts is shown in Figure 6.3. This view also shows the general arrangement of the AVT actuators fitted to the cylinder head.

Table 6.1: General specifications of single-cylinder test engine

General architecture	Aluminium alloy, water-cooled, 4 valve, twin primary balance shafts
Bore (mm)	88.0
Stroke (mm)	82.1
Connecting rod length (mm)	142
Swept volume (cm ³)	499.3
Compression ratio	10.0
Intake valve throat diameter (mm)	31.0
Exhaust valve throat diameter (mm)	26.0
Valve actuation system	Lotus Active Valve Train
Engine management system	Lotus 'T4' production system
Miscellaneous	External electrically-driven pumps for water and oil pressure and scavenge

6.2 CHARGE AIR CONDITIONING RIG

Fundamental to the work reported in this chapter was the ability to be able to vary charge air temperature and pressure over a relatively wide range and with significant accuracy. To this end, a dedicated charge air conditioning (CAC) rig was conceived and designed with the ability to flow sufficient air for multi-cylinder operation (as provision for possible future work to follow on from that described in this thesis). This rig had two stages of compression with two stages of water-cooled charge air cooling, one between and one after the two compression stages. A schematic of the rig is shown in Figure 6.4.

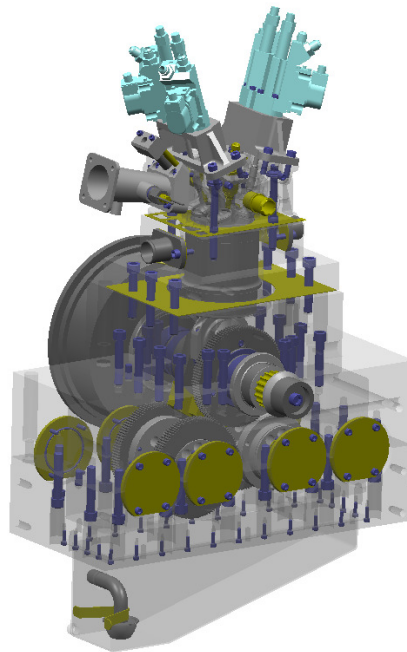


Fig. 6.3: Ghosted CAD image of test engine showing Active Valve Train system fitted to cylinder head and provision for full balancing set (primary balance system only shown) (Illustration courtesy Lotus Engineering)

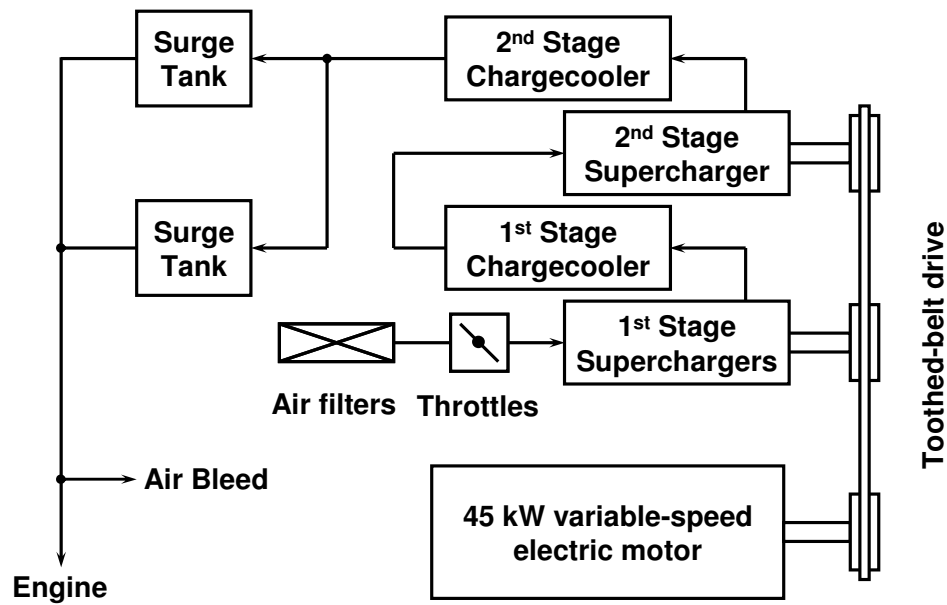


Fig. 6.4: Schematic of charge air conditioning rig

The first stage of compression consisted of two Eaton M45 superchargers in parallel (each of these had a swept volume of 45 cubic inches, or 0.74 l). A single Eaton M45 supercharger was used for the second stage. The superchargers all used the same overall gearing to the 45 kW electric motor, which was itself of a variable-speed type. This ensured that a high level of boost pressure could be achieved due to the compounding effect of the two stages, and that the air mass flow rate was variable. The use of an inter-stage water-jacketed chargecooler provided a low temperature for the air entering the second-stage supercharger. Cooling water for the chargecoolers was supplied in parallel by a single circuit from a chiller unit in the engine test cell. This system had the capability to reduce the chargecooler cooling water temperature to below 10°C in 25°C ambient air. Therefore, because of the two-stage configuration with inter-stage chargecooling and the use of the chilled water system, low outlet temperatures were possible from the rig. The superchargers were all driven by a single toothed belt taking power from the electric motor. Twin 'surge tanks' were provided in parallel downstream of the second-stage chargecooler. The purpose of these was to damp pulsations in the air flow from the rig before it was delivered to the engine.

The two first-stage superchargers were throttled via a linked throttle system with the variable-speed drive also providing a control of the flow rate. The rig, therefore, had the capability to deliver sufficient air for any size of engine up to ~330 kW (443 bhp). Clearly this level of performance was not expected from the single cylinder engine test engine but, as noted above, this specification was decided upon to provide a useful piece of test equipment for other projects. During preliminary tests a supplementary air bleed was also provided between the rig and engine so that if it had been found necessary, finer control of charge air temperature could be achieved. This air bleed is shown in the schematic in Figure 6.4. However, during preliminary tests, control of air supply was found to be so good without spilling any flow that its use was not required and it was removed. The performance of the CAC rig is discussed further in Appendix IV. A photograph of the assembled test rig is shown in Figure 6.5.

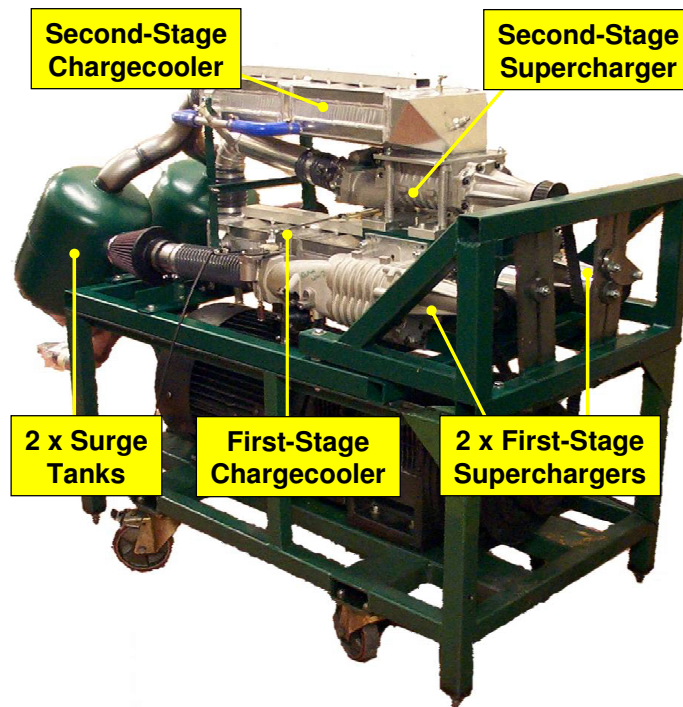


Fig. 6.5: Photograph of charge air conditioning rig. (Photograph courtesy Lotus Engineering)

6.3 TEST CELL EQUIPMENT

6.3.1 General measuring equipment

For the tests reported here a Froude Type AG30 eddy-current dynamometer was used. The engine test cell was fitted with an automated data logging system to record temperatures and pressures from non-cyclically-resolved thermocouples and transducers. Air temperature into the test cell was controlled by the standard cell air supply system to $25^{\circ}\text{C} \pm 1^{\circ}\text{C}$. Fuel consumption was recorded using an AVL gravimetric flow meter. The fuel used for the tests was commercially-available 95 RON unleaded gasoline taken from the bulk fuel tanks at Lotus Engineering.

A Kistler type 6041A water-cooled pressure transducer was mounted in the cylinder head; this can be seen fitting flush with the edge of the combustion

chamber in the photograph in the left-hand side of Figure 6.2. It was mounted in this position to place it at an anti-node of the main vibrational modes of knock and so to minimize its positional influence on knock measurements (Draper, 1938, Blunsdon and Dent, 1994 and Burgdorf and Denbratt, 1997). High-speed pressure transducers were also fitted in the intake and exhaust tracts to record pressure histories from these areas. The Kistler pressure transducer was connected via a charge amplifier to an AVL Indiset combustion analyser. The purpose of this was to use its functionality to establish a common limiting value for knock-limited spark advance (KLSA) across the testing range reported here. Since it was important that this be kept constant throughout this test programme, the default AVL knock limit algorithm was used and adhered to during all testing described in this chapter.

6.3.2 Intake and exhaust systems

The intake and exhaust systems were configured with plenum chambers in the runners to mimic the interactions found in a multi-cylinder engine. These volumes were of such a size as to be representative of the volume that pressure waves in the runners would react against in a notional multi-cylinder version of the engine. This was done so that the engine performed as much as possible as though it was one cylinder of a multi-cylinder engine. The dimensions of these volumes can be found in Table 6.2.

Table 6.2: Intake and exhaust plenum dimensions

Parameter	Intake	Exhaust
Total runner volume (including port in cylinder head) (l)	0.41	0.25
Plenum volume (l)	2.53	1.12
Plenum diameter (mm)	150	80
Plenum length (mm)	143	222

The dimensions in Table 6.2 were determined by considering a multi-cylinder engine to have a total intake plenum volume of 1.5 l and a total exhaust plenum (or 'collector') volume before the turbine of 0.5 l. Specifically, the intake volume

was the same as one half of that of the supercharged V6 donor engine as shown in Figure 6.1, i.e. suitable for a three-cylinder engine bank. To each of these intake and exhaust volumes was added 3.5 times the total runner volume (including that of the ports in the head), this being considered to be a pragmatic but workable compromise between mimicking a 3- or a 4-cylinder engine bank. The volume of the single runner was then subtracted from this total to arrive at the plenum volumes required for the installation. This approach permitted the results taken from this single-cylinder engine to be transferable to the three-cylinder research engine concept described later in Chapter 7.

On the intake side of the single-cylinder research engine, the resulting plenum was configured to have a diameter of approximately three times that of the runner into the engine, to give a large expansion for pressure waves returning from the intake valves and hence providing a basis for the reflection of those waves. The runner diameter to the engine was 49 mm and hence the plenum diameter was set to be 150 mm. Choosing this ratio also gave a practical configuration for fitment to the cell, since the length of the plenum then became only 143 mm. These dimensions gave a total volume of 2.53 l.

For the corresponding calculation for the exhaust plenum, an area ratio of 4 was chosen, which, with an exhaust runner diameter at entry to the plenum of 40 mm, meant that the plenum then had inner diameter of 80 mm as stated in Table 6.2. Its length was then 222 mm for the desired volume of 1.12 l.

Once these dimensions had been calculated and a workable exhaust system length and diameter established for the test cell, a model of the engine was constructed using the commercial engine simulation code Lotus Engine Simulation (Lotus Engineering Software, 2005). The primary purpose of this modelling work was to determine the diameter of two orifice plates which were to be used to set the mean back pressure on the engine to be representative of the pre-turbine pressure of a turbocharged multi-cylinder engine. The value of this back pressure was targeted at 2.25 bar (absolute) at the exhaust port at 6000 rpm, considered to be representative of a turbocharged multi-cylinder engine

operating with a turbine expansion ratio of 1.5 and a post-turbine exhaust back pressure (EBP) of 50 kPa (gauge). Again, this was to make the single-cylinder engine a useful research tool in the development of the three-cylinder engine discussed later in Chapter 7.

These orifice plates were to be in series and of equal diameter. They were positioned with one immediately downstream of the exhaust plenum and the other 998 mm further down the exhaust pipe (this value was measured from the test bed system *in situ*). The use of two orifice plates configured in this manner has been shown to be a more realistic representation of the actual back pressure curve applied to an engine by a turbocharger turbine by Winterbone and Pearson (1999). Also, the use of fixed orifices, instead of a simpler 'Clayton'-type adjustable butterfly valve, ensured that the back pressure was applied to the engine in a robust manner and would not be subject to variation during long-term testing.

A schematic of the engine model as used in Lotus Engine Simulation is shown in Figure 6.6. The input parameters to the engine model were all as for the test engine and test bed installation, and a heat release curve for the combustion was chosen to represent that of a supercharged port-fuel-injection base engine similar to that which the engine was based on. Gasoline was the fuel specified. A pressure and temperature of 2.012 bar absolute and 20°C respectively were applied to the inlet position marked in Figure 6.6, such that a charge air density of 2.4 kg/m³ was supplied to the engine intake. This is twice standard atmospheric density and was adopted because it was considered to be the highest density that was ever likely to be applied to the engine as a result of mimicking turboexpansion operation (Turner *et al.*, 2003 and 2005a). The diameter of the orifice plates as determined from this modelling work was 22.0 mm, and these were manufactured and inserted in the exhaust system at the two points indicated. Appendix VI contains input data used for this analysis.

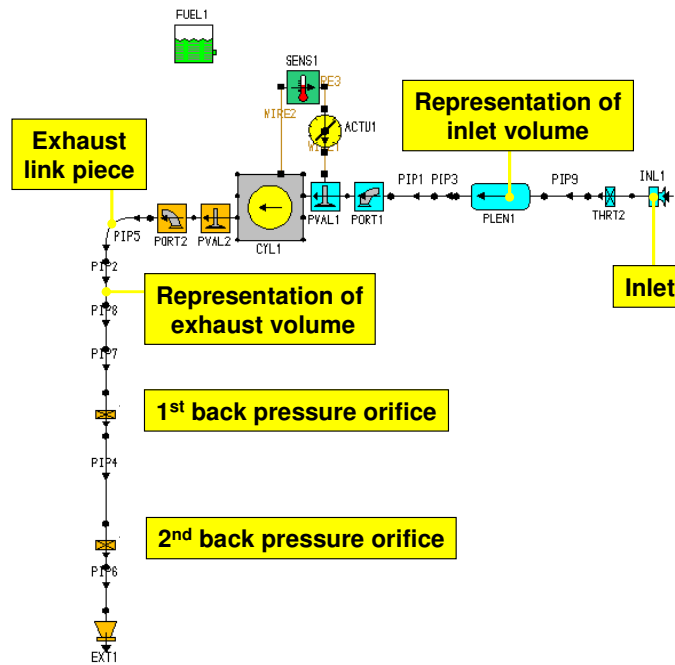


Fig. 6.6: Schematic of the Lotus Engine Simulation model of the single-cylinder engine as installed in the test cell

Silencing of the engine was achieved using a large, low back-pressure automotive silencer, fitted at the end of the exhaust run, the size of which was selected such that it had minimal effect on engine back pressure itself. Air flow was calculated from the fuel flow rate as measured by the AVL fuel flow meter and from the calculated AFR as established by Spindt's method (Spindt, 1965).

Photographs of the test equipment as configured in the test cell are shown in Figures 6.7 and 6.8.

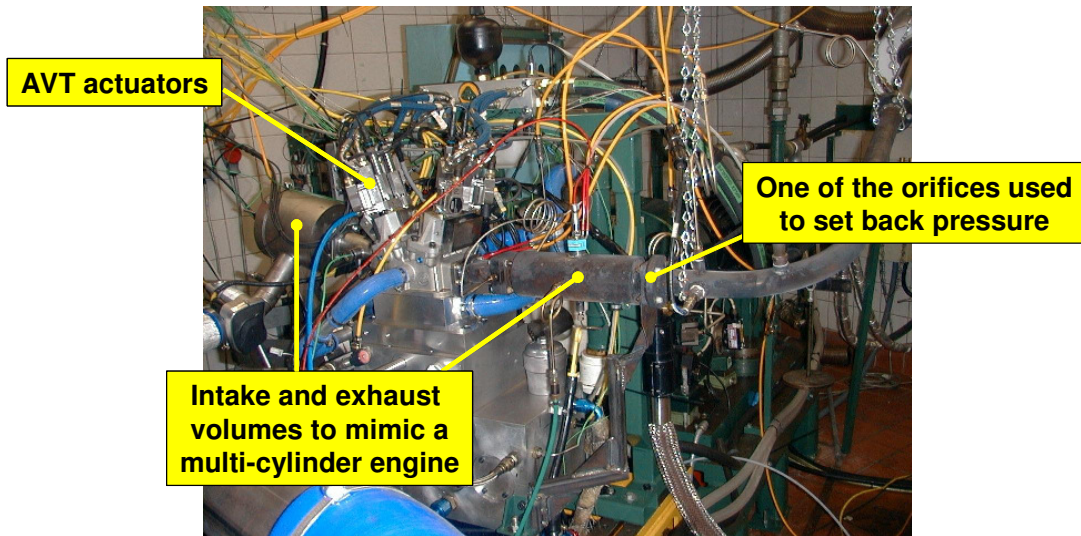


Fig. 6.7: Photograph of test engine showing Research AVT and intake and exhaust systems fitted with volumes representative of a multi-cylinder engine. The charge air conditioning rig delivers air to the throttle body seen on the left

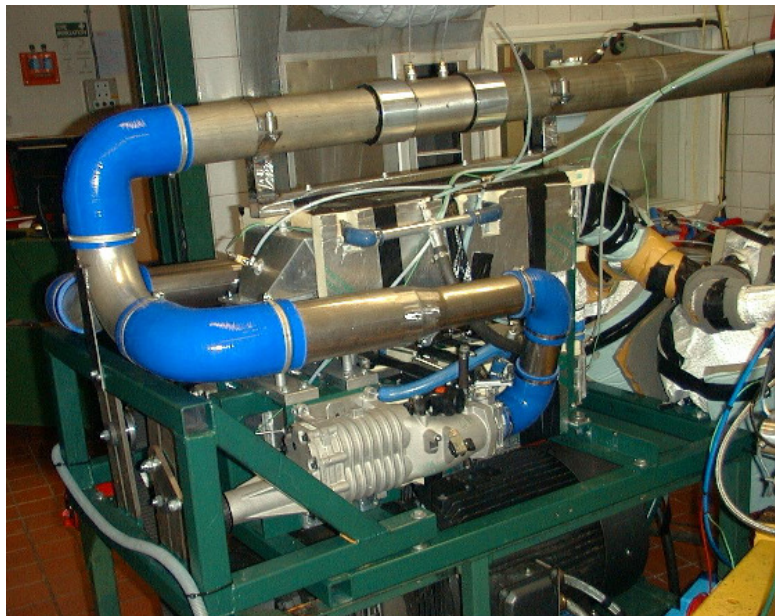


Fig. 6.8: Photograph of charge air conditioning rig when connected to test engine, with lagging fitted over the chargecoolers to retain heat

6.4 TEST RESULTS

Some initial running of all of the newly-designed and procured test equipment described in the previous sections was carried out to commission the test cell. Two sets of scoping tests were conducted to establish the sensitivity of the engine to relative air-fuel ratio (AFR) and to valve timing respectively in order to fix these parameters for the main fixed-air-density tests. All of these are described below.

6.4.1 Test conducted to determine relative air-fuel ratio for the test programme

This test was conducted to investigate the sensitivity of the engine to the relative AFR, λ , it operates at. $\lambda = 0.9$, typically used for gasoline full-load testing, is commonly found to be in the region of that for maximum performance in gasoline engines (Heywood, 1988). Metghalchi and Keck (1982) assert that this relative AFR corresponds to the maximum flame speed for many oxygenated and non-oxygenated hydrocarbons (although note that they use equivalence ratio (ϕ), the reciprocal of λ , in their work, as is common in combustion chemistry). Marshall *et al.* (2010) have also shown this to be the case for pure hydrocarbons and have also demonstrated its dependence on pressure and temperature. This finding is also reinforced by those of Gülder for alcohol fuels and their blends with paraffins (Gülder, 1982 and 1984). The value of $\lambda = 0.9$, however, is often enriched further at high engine speeds for reason of thermal protection of components in the exhaust path such as the exhaust valve(s), catalyst or turbocharger turbine, since a richer mixture than is optimum for maximum power burns less efficiently as a result of lower heat release, thus reducing gas temperatures.

As discussed in Chapters 2 and 3, this strategy of over-fuelling is also one often used to extend the knock limit of an engine since the excess fuel effectively absorbs some of the heat of combustion, cooling the end gas and extending its induction time before autoignition. The use of over-fuelling is becoming more important as engines are increasingly downsized and thus relatively highly-

boosted operation becomes more commonplace in 'real-world' conditions (Grandin, 2001, Duchaussoy *et al.*, 2003, Krebs *et al.*, 2005b, Cairns *et al.*, 2006, Hattrell *et al.*, 2006, Turner *et al.*, 2008 and 2009, Hoffmeyer *et al.*, 2009 and Taylor *et al.* 2010).

While $\lambda = 0.9$ is a convenient value to illustrate the typical fuelling rate of engines under full-load conditions (albeit in general and without component-protection fuelling), clearly all engine designs are different and it would be a simplification to believe that all would deliver best performance at the same relative AFR. Therefore, it was decided to conduct a set of 'fuel loops' to establish whether this value was near to the optimum in the case of the single-cylinder engine used here. These tests were conducted at the engine speeds of 2000, 3000 and 4000 rpm in order to gather background information on the combustion system. It had been intended to test at 1000 rpm as well, but the engine exhibited a vibrational mode at this speed and it was not considered prudent to test here. Charge air density and temperature conditions of 1.8 kg/m^3 and 40°C respectively were used in the intake plenum for these tests (which correspond to a charge air pressure of 162.8 kPa absolute), since these can be considered to be a representative level for turbocharged light-duty SI engines.

The fitment of AVT permitted a free choice of valve timing and it was decided to operate the engine at an inlet valve maximum opening point (MOP) of 95° ATDC for these relative AFR tests. Section 6.4.2 will discuss tests regarding establishment of valve timing for the fixed-air-density tests reported later in Section 6.4.3, but in general, higher levels of overlap at low engine speeds promote better scavenging of the combustion chamber and hence a better understanding of the effect of relative AFR on the combustion conditions within the chamber due to the fresh charge without the complicating effect of a high trapped residual rate.

For each engine speed, the fuelling rate was varied, and then, once the equivalence ratio was set, the KLSA was found using the knock meter of the

Indiset as previously described. The results are shown in Figure 6.9, which show that the exact value of λ for maximum performance varies slightly for each speed and $\lambda = 0.9$ is not the maximum for all cases. The response was generally flat, i.e. at the fixed-air-density test speed of 2000 rpm (see later) enriching the AFR from $\lambda = 0.9$ to 0.8 only increased the BMEP from 14.57 to 14.80 bar, or 1.6%, for a significant increase in fuel consumption.

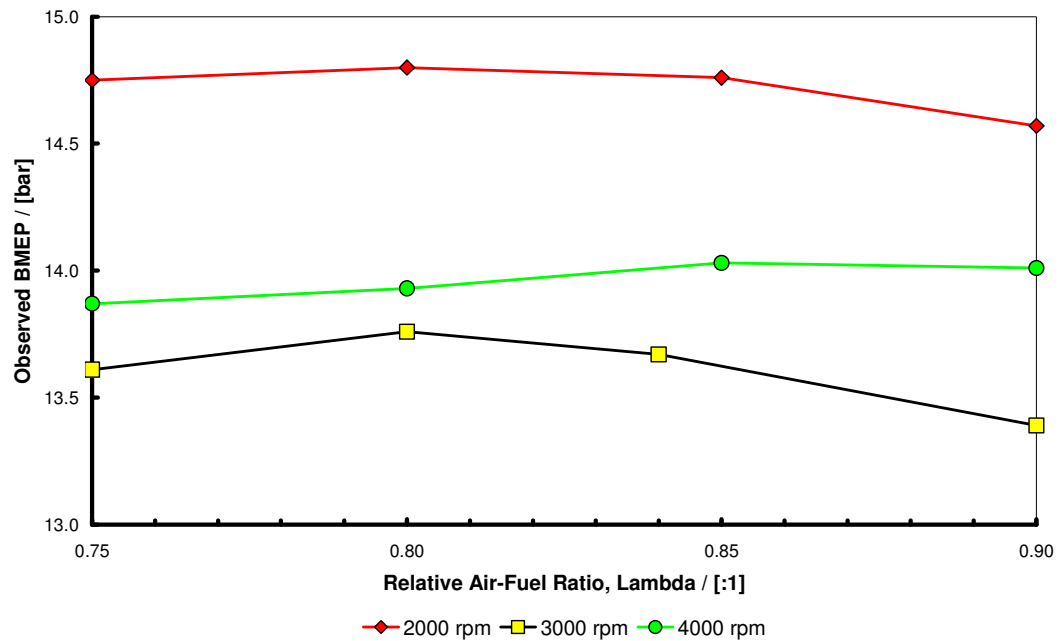


Fig. 6.9: Effect of relative AFR (λ) on observed BMEP at different engine speeds.

Intake valve timing: 95° ATDC MOP. Ignition timing: KLSA

Note that the results shown in Figure 6.9 are expressed in terms of observed BMEP, since comparative results only were required. Furthermore, the BMEP quoted was derived from the dynamometer measurement only and does not include charging system work, coolant and lubrication system work or indeed, because of the use of AVT, work necessary to drive the valve train. Also, uncorrected BMEP was exclusively used in this investigation because of the conditioned nature of the air being supplied to the engine. With the charge air conditioning rig, control and stability of charge air temperature and pressure was

extremely accurate, and so no correction factor was necessary. The subject of the accuracy of control of the charge air conditioning rig is discussed in Appendix IV.

At 3000 rpm the test was inadvertently conducted with one point at $\lambda = 0.84$ instead of 0.85. This is not believed to distort the overall shape of the results significantly, which shows the relatively flat response for all the values of λ tested. Notwithstanding the comments above, this set of results illustrate that operating this engine at $\lambda = 0.9$ would be a sensible compromise to reduce the number of test variables for both the valve timing and fixed-air-density tests which are reported below.

6.4.2 Tests conducted to determine the valve timing for the fixed-air-density tests

As mentioned above, an inherent advantage of the AVT fully-variable valve train system is the ability it provides to investigate valve timings rapidly and so to aid combustion research. The tests reported here were completed with the valve profiles depicted in Figure 6.10, essentially being those of the donor supercharged 3.0 litre PFI V6 engine albeit modified slightly to remove the 0.25 mm valve lash required in that engine. This is because, being a direct-actuation system with feedback control on position, the AVT system does not require any form of lash compensation and as a corollary of this, the beginning of an AVT valve profile corresponds to a 'top-of-ramp' profile for a mechanical valve train system.

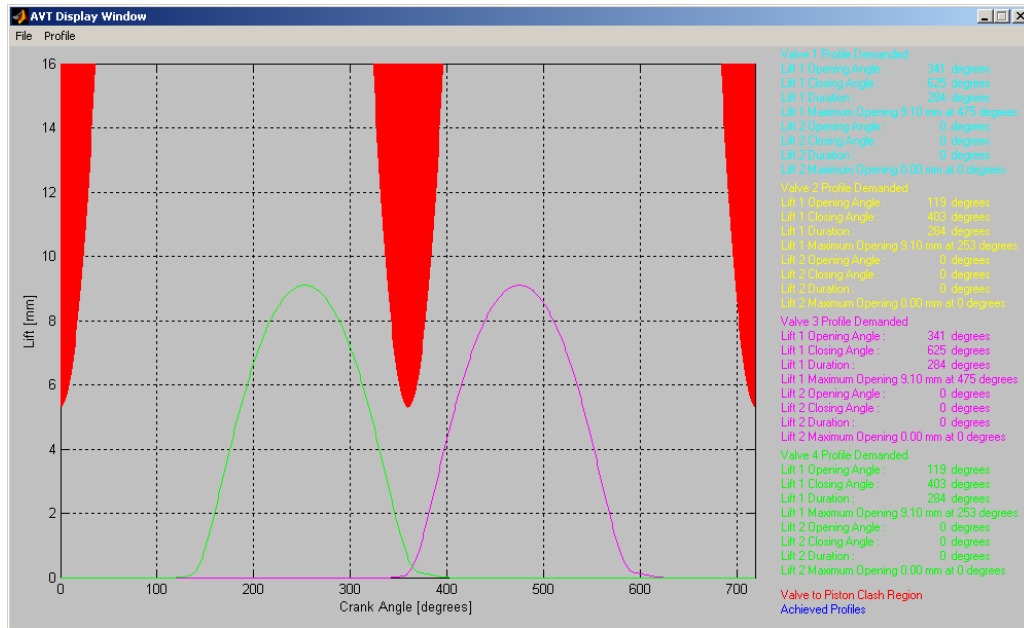


Fig. 6.10: AVT display window depicting valve events used. In this diagram, the intake valve event is depicted at 115° ATDC MOP (corresponding to 475° ATDC Firing) and the exhaust valve event at 107° BTDC MOP (corresponding to 253° ATDC Firing). Both have valve lifts of 9.1 mm (see text). Red regions depict areas of piston approach and thus areas of potential valve-to-piston clash

The intake valve timing depicted in Figure 6.10 represents the mid point of the 50° CA authority range of the continuously-variable camshaft phasing (CVCP) device fitted to the donor V6 engine. This 50° CA authority range represents a most-advanced timing of 80° ATDC maximum opening point (MOP). The donor engine had a fixed exhaust valve timing of 107° BTDC and this is shown in Figure 6.10 as well, together with the piston-approach portion of the timing diagram (in red) for which AVT has numerous interlocks to ensure avoidance of valve-to-piston contact (as well as those for valve-to-valve contact). During its initial development programme the V6 engine was habitually operated at the most-advanced condition in order to make use of charge blow-through to scavenge residuals from the chamber during the extended overlap period as briefly discussed in the previous section. However, this has always been an issue for PFI engines since fuel consumption and hydrocarbon (HC) emissions can be

expected to be high when the valve overlap is relatively large. In a DI engine, the separation of the fuelling function from the gas exchange process, of course, permits a potential 'over-scavenging' function to be very advantageous in terms of combustion chamber cooling and residual removal without the associated penalty of high fuel consumption and HC emissions, and this fact has led to the common adoption of twin camshaft phasing devices in such turbocharged DISI engines as discussed in detail by Andriessse *et al.* (2008). While there are great and intentional architectural similarities between the single-cylinder engine used here and the donor supercharged V6, it was still considered prudent to investigate intake valve timing by utilising the flexibility of the AVT system, not least because at the time of conducting this test work, full camshaft phasing tests had not been conducted within the donor V6 programme. In a manner similar to the relative AFR tests described earlier in Section 6.4.1, it was decided that this test should be conducted at different engine speeds in order to gauge the overall sensitivity of the engine to intake valve timing.

Accordingly, the single-cylinder test engine was operated at full-load at engine speeds of 1250, 2000, 3000 and 4000 rpm and the intake valve timing was advanced in 5° CA steps from 115° to 80° ATDC, corresponding to a range representing 'mid-point' to 'most-advanced' of the mechanical CVCP device on the donor V6 engine. Plenum charge air density and temperature conditions of 1.8 kg/m³ and 40°C were used for this test as for the relative AFR tests described in Section 6.4.1. Note that the lowest engine speed of 1250 rpm was used instead of 1000 rpm because of the imbalance exhibited by the engine when it was operated at this speed. For these tests, due to the known sensitivity of engine performance to valve timing (Heywood, 1988) it was considered important to gather information at the lowest engine speed which was safely achievable. This is a small operational difference to the tests described in Section 6.4.1. Following the findings already outlined in Section 6.4.1, the fuelling of the engine was set to $\lambda = 0.9$. KLSA ignition timing was used as determined by the Indiset and as discussed above, with the stipulation that no point should be run if the ignition timing had to be retarded past 4° BTDC firing to

avoid knock, in order not to damage the exhaust valves (discussed in more detail in Section 6.4.3). This limitation resulted in an incomplete series of MOP test results for the two lowest speeds, 1250 and 2000 rpm. The results of these tests are shown in Figure 6.11, and are expressed in terms of observed BMEP, for the reasons already discussed in Section 6.4.1.

These tests demonstrated that there was some advantage to be gained in terms of BMEP by advancing the intake valve timing at low engine speed. They also show that, at the intended fixed-air-density test engine speed of 2000 rpm, the effect was not significant – Figure 6.11 shows that of the speeds tested, 2000 rpm was in fact the least sensitive with a maximum change in BMEP of 2.4% as the intake valve timing was retarded from 90° to 115° ATDC.

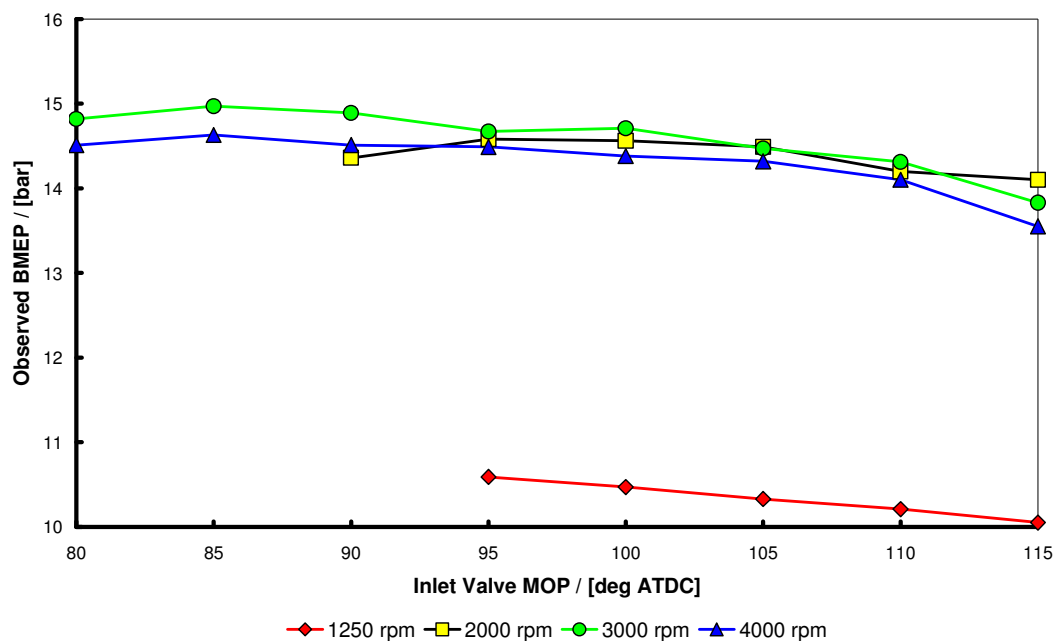


Fig. 6.11: Effect of intake valve MOP timing on observed BMEP at different engine speeds. Fuelling: $\lambda = 0.9$, ignition advance: KLSA. Exhaust valve timing fixed at 107° BTDC throughout

At the same time, as intake valve timing was retarded at 2000 rpm the BSFC decreased significantly and the benefit of increased overlap in terms of increased KLSA was not really apparent after an intake MOP of 90° ATDC. This is shown in Figure 6.12, which also shows that KLSA stays relatively constant from 95° to 115° ATDC.

As a consequence of this set of results, in order to further minimize the number of variables for the fixed-air density tests, it was decided that the intake valve timing should be 115° ATDC MOP, corresponding to the mid-point of the CVCP on the donor V6 engine.

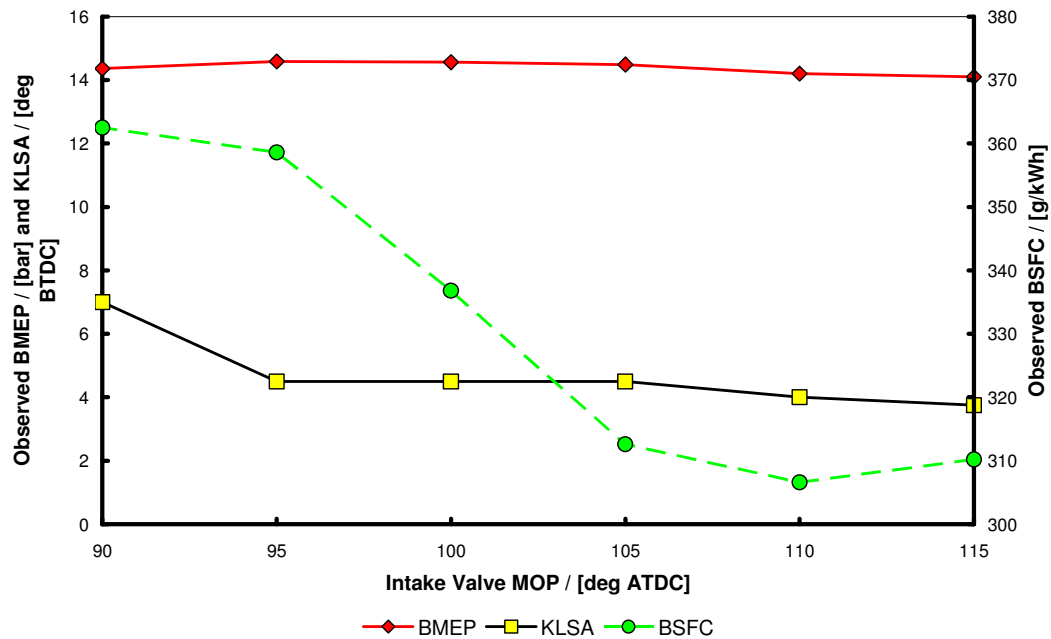


Fig. 6.12: Effect of intake valve MOP timing on knock-limited spark advance (KLSA), observed BMEP and observed BSFC. Engine speed: 2000 rpm. Fuelling: $\lambda = 0.9$. Exhaust valve timing fixed at 107° BTDC throughout

In concluding this section, the configuration of the engine valve timing and relative AFR decided upon for the fixed-air-density tests is shown in Table 6.3.

Table 6.3: Summary of valve events and relative AFR (λ) finalized by preliminary tests in order to configure the test engine for fixed-charge-air-density research work

Variable		Value
Valve duration ($^{\circ}$ CA) <i>(equivalent to top-of-ramp – see text)</i>	Intake	260
	Exhaust	260
Valve lift (mm) <i>(no lash compensation -see text)</i>	Intake	9.1
	Exhaust	9.1
Valve maximum opening point (MOP) ($^{\circ}$)	Intake	115 ATDC
	Exhaust	107 BTDC
Valve overlap ($^{\circ}$ CA)		52
Relative AFR (λ)		0.9

6.4.3 Testing at constant charge air density while varying charge inlet temperature

Having determined the test conditions in terms of λ and valve timing, a test matrix was created to investigate the main hypothesis of this part of the thesis that, for a fixed charge air density, reducing the air temperature while adjusting the pressure to compensate would improve the knock limit and would thus form the basis for justification of investigating turboexpansion-type charging systems further. The variables used for this test matrix are shown in Table 6.4.

Table 6.4: Test variables defining the test points for fixed-air-density tests

Variable	Value	No. of Sites
Plenum Density (kg/m^3)	1.2, 1.4, 1.6, 1.8	4
Plenum Temperature ($^{\circ}$ C)	20, 30, 40, 50	4

Thus there were 16 potential test sites for this investigation (at the test speed of 2000 rpm), this being considered sufficient to establish the trends anticipated if they were present and hence whether the hypothesis was valid. Operationally, in running these tests and as mentioned above, a significant limitation was decided upon for this test by using the limiting criterion that no test site should be attempted if the ignition timing for the most retarded points was later than 4°

BTDC. This was because an ignition 'hook' or 'loop' was to be run at each point comprising KLSA, then KLSA -1°, KLSA -2° and finally KLSA -4°, with the only exception to be made for conditions where it was possible to operate the engine at MBT before TDC in which case that data would have been obtained too (because MBT could theoretically be more than four degrees retarded from KLSA). This process is commonly used in industrial applications in order to verify that KLSA is on the rising part of the efficiency curve and that thermal efficiency is thus bounded by a combustion limitation.

The limitation of 'no ignition retard beyond TDC' was set in order to protect the engine from excessive thermal load and was adopted because such late ignition timings would cause such a correspondingly late shift of the heat release curve that the exhaust valve temperature would increase excessively. This limitation meant that some of the points in Table 6.4 were not achievable. Nevertheless, the approach is considered to be robust since, subjectively, the fact that a test point is unachievable because of unacceptably late ignition timing is a relevant finding within the context of understanding the combustion system and its value to the related V6 PFI engine programme. More importantly, it also served to protect the test equipment.

As discussed in the previous two sections, all of the data for the test matrix was obtained at a fixed relative AFR of $\lambda = 0.9$ and intake and exhaust MOPs of 115° ATDC and 107° BTDC, respectively. The use of the separate charge air conditioning rig together with the fact that no catalyst was fitted to the engine ensured that fuel enrichment (for component thermal protection) was not needed and therefore a true assessment of the effect of intake air conditions could be obtained without a requirement to introduce component thermal protection fuelling at any point. These test results were all gathered using the PFI system for maximum validity in light of the V6 programme. It is imagined that DI fuelling would cause an enhancement of any effect seen, although this hypothesis is unproven in the results presented below and would only hold for the same valve event timings and overlap. The avoidance of DI fuelling also removes the

complicating effects of in-cylinder air-fuel mixing phenomena to the benefit of understanding the effect of charge air temperature on combustion.

At each test point the procedure for these initial tests was to:

1. Set the CAC rig to deliver air at the desired intake density and temperature.
2. Set the relative AFR to the target value of $\lambda = 0.9$.
3. Obtain the value of KLSA using the in-built knock intensity indicator of the AVL Indiset. Record data at this condition.
4. From the KLSA position, retard the ignition in steps of 1° , 2° and 4° CA. At each of these points, log all test data.

As discussed above, if the KLSA determined in step 3 was not greater than 4° BTDC, the test point was aborted due to the criterion of the latest position of heat release and exhaust valve temperature discussed above. Note that KLSA was set by observing a limit in the rate of cylinder pressure rise of 2 bar per crank degree, considered by the algorithms in the AVL Indiset to be indicative of a borderline knock condition, and observed to further protect the test engine.

The spark loop at each test point took about one hour to complete, plus the time for the rig air temperature and pressure to stabilize.

Results from these tests, expressed in terms of the KLSA versus charge air temperature in the plenum, are shown in Figure 6.13. Note that when operating on 95 RON gasoline, none of the test points could be operated at MBT, which is a verification of the validity of the results in terms of best thermal efficiency being achieved as limited by combustion phasing and thus the knock limit.

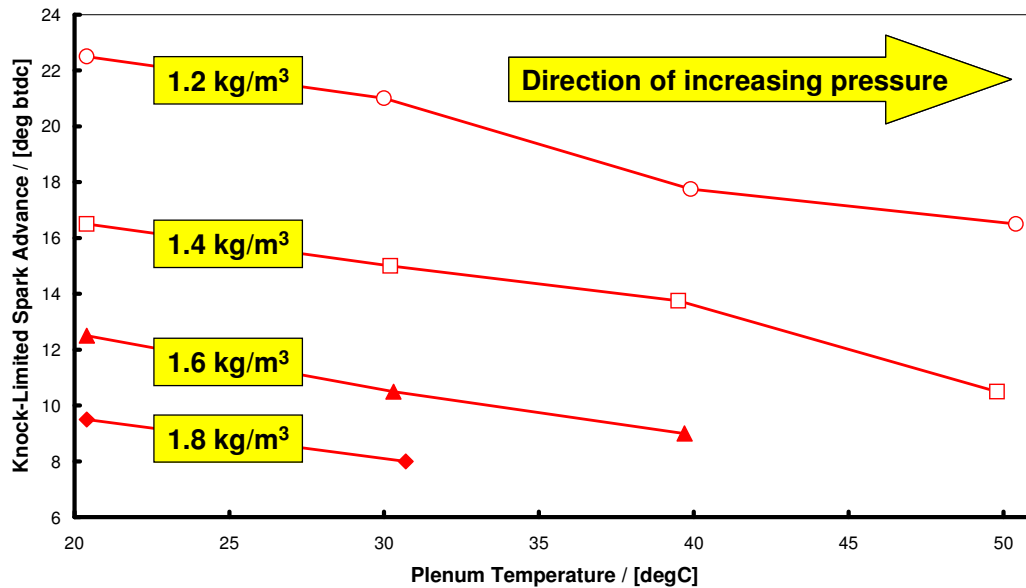


Fig. 6.13: Knock-limited spark advance (KLSA) versus charge air temperature at four different fixed values of constant plenum density for the fixed-air-density tests. Test speed: 2000 rpm. $\lambda = 0.9$ throughout

The value of this series of tests is immediately apparent because, as can be seen from Figure 6.13, for each of the tested fixed intake densities, the KLSA of the engine increased broadly linearly and monotonically with charge air temperature reduction down to the test minimum of 20°C. In the author's opinion the original hypothesis is thus borne out, and hence the turboexpansion concept discussed in Chapter 4 appears to have merit from a combustion viewpoint. Alternatively, seeking to improve the effectiveness of chargecooler systems where turboexpansion is not employed will be of much benefit. Such testing thus divorces the effects of the charging system and can be used to establish targets for that system alone. If this test work had been conducted before entering the turboexpansion research work conducted on the Nomad engine and described in Chapter 4 then a different approach to setting the targets of the charging system used there may have been adopted at that time. It also helps to illustrate why pre-compressor fuel injection, as discussed in Chapter 5, is of such benefit.

6.5 SUMMARY AND CONCLUDING REMARKS

This chapter has described the design of a single-cylinder engine and a separate charge air conditioning rig which have together been used to investigate the hypothesis that, for any fixed air density in the plenum of a engine, the knock-limited spark advance will increase as the temperature is reduced. This was the approach favoured by Crooks (1959) and Helmich (1966) and which was shown by them to work on large stationary engines operated on natural gas. The rigorous approach of using an external boosting system and fixing engine intake plenum charge density as a control variable, while adjusting temperature and pressure to suit, has not been seen by the author in the literature. In the normal process of pressure-charged engine development, the boost pressure is usually fixed (by a wastegate in a turbocharged engine) and the temperature allowed to vary under the operation of a charge air cooler, and this gives rise to a variable charge air density. Since mass air flow is a primary driver on SI engine performance with a homogeneous mixture and fixed AFR, the approach adopted in this chapter would be expected to illustrate any such combustion effects. The use of fixed λ when operating the test engine has similarly kept the fuel energy entering the engine constant and makes the results valuable.

The chapter has also described how plenum chambers were inserted into the intake and exhaust systems of the test engine to provide representative system volumes so that the single-cylinder engine would function more as though it was one of a bank of cylinders. The process by which the size and shape of these volumes were determined has been discussed. Once the dimensions of these plenum volumes were determined, a commercial engine simulation package, Lotus Engine Simulation, was used to establish the diameter of a pair of fixed orifices in the exhaust system which were employed to mimic the shape of the back pressure curve as it is applied to an engine by a turbocharger turbine. This modelling process has been discussed, together with the finding that a pair of 22 mm diameter orifices, 998 mm apart, would give the desired absolute back pressure of 2.25 bar at the modelled engine conditions.

A series of initial scoping tests was conducted to help determine the fuelling rate in terms of λ and the engine configuration in terms of intake valve timing for the main fixed-air-density test. The value of using the fully variable valve train system, Active Valve Train, in these valve timing tests was discussed. The reason for this series of tests being conducted exclusively with PFI has also been discussed; firstly this was because all of the decisions related here led to an increased relevance of the results with regard to the simultaneous V6 production engine programme which had donated its essential architecture to the single-cylinder engine, and secondly because PFI leads to increased robustness of the results by removing potential air-fuel mixing effects, had DI been employed.

The next chapter describes the design of a 3-cylinder research engine utilising the cylinder geometry of the single-cylinder engine described here. The importance of turbocharger matching together with the use of an integrated exhaust manifold (IEM) will be shown. Chapter 8 will also describe tests with the 3-cylinder engine utilising another knock-suppression strategy, cooled EGR, in order to discern the benefit of such an approach against those which accrue from the configuration of the engine architecture itself. Benefits of engine architecture cannot readily be investigated with a single-cylinder engine, even if particular care has been taken in the design and specification of the intake and exhaust systems it uses, and so a multi-cylinder engine was used for these research topics.

Chapter 7: The Sabre 3-Cylinder Downsized Demonstrator Engine Concept

This chapter describes the design of and some results from the ‘Sabre’ downsized demonstrator engine, to which the research reported in Chapter 6 contributed. The present chapter will compare the results from Sabre in its ‘Phase 1’ form with some competing technologies. This comparison will show that a combination of mutually complementary features can provide equivalent or better results than some of the advanced knock-control techniques already discussed in Chapter 3 when applied to improve full-load performance. It will thus demonstrate how a ‘clean-sheet’ approach to engine design can produce these results and describe the mechanism by which these were a result of the architectural philosophy of the engine.

7.1 THE SABRE ENGINE PROJECT

The Sabre engine project was a collaboration between Lotus Engineering and Siemens VDO Automotive (now Continental Automotive Systems) to create an advanced 4-stroke engine to act as a baseline for future spark-ignition engine technologies. This is reflected in the project name, being shorthand for ‘spark-ignition advanced baseline research engine’. Specifically, Sabre is an in-line 3-cylinder engine encompassing several technologies to realize low CO₂ in a practical automotive application. The rationale behind the adoption of a close-spaced, homogeneous, ‘second generation’ direct-injection combustion system will be described and the conscious decision not to target high BMEP as the primary route to low fuel consumption is explained. Instead, mild downsizing was adopted combined with a switching valve train to enable reductions in throttling losses and enhanced charge-air turbulence manipulation. Overall, this approach provides practical engine packaging benefits together with reduced high-load fuel consumption as a result of the lower boost requirement leading to reduced component-protection fuelling.

The basic combustion system for Sabre was taken from the EPSRC-funded 'HOTFIRE' project and is also based on the work already described in Chapter 6. The interaction of direct injection (DI) spray and air motion in the combustion system is briefly discussed in this chapter insofar as it enabled the relatively large swept volume to be used. Most of the results in the chapter are therefore concerned with full-load performance.

7.2 SABRE ENGINE DESIGN

The concept of the Sabre engine was formulated by the author following all of the research in the previous chapters. It represented an unusual approach to the problem of improving vehicle drive cycle CO₂ emissions in comparison to the then-current theme of extreme downsizing as promoted by other researchers (i.e. Kapus *et al.*, 2007b, Hancock *et al.*, 2008, Lumsden *et al.*, 2009 and Turner and Pearson, 2009). Sabre adopted a novel and synergistic combination of engine architecture, mild downsizing (as defined to be operation at ~20 bar BMEP), gasoline direct injection (DI) and variable valve train technology to realize low CO₂ with improved driveability, as evidenced by vehicle acceleration figures. These technologies were presented in a cost-effective, affordable manner.

CO₂ emissions are directly related to fuel consumption and many new technologies have been developed and are being researched with the aim of improving fuel economy. Downsizing, DI and variable valve trains have all been introduced to the market with varying degrees of success. The adoption of these technologies stem from the fact that the automotive industry remains committed to the 4-stroke Otto cycle and reducing the amount of throttling loss it suffers at part load is the primary aim of most of them. However, despite the current developmental direction for high levels of downsizing, there is still some desirability in not reducing swept volume excessively for a downsized engine because driveability and transient throttle (torque) response (so-called 'turbo lag') become an increasing challenge as the degree of downsizing increases. While DI operation can assist in the application of a downsizing, due to evaporative charge cooling and compressor map shifting, the throttling losses associated with

a larger engine will still exist if unaddressed. Furthermore, operation at $\lambda = 1$ permits simple exhaust gas after treatment (i.e. a three-way catalyst). Hence the combination of variable valve train and DI developed in the HOTFIRE programme (Turner *et al.*, 2006a and Stansfield *et al.*, 2007) was adopted for Sabre. This unlocked potential for direct reduction in throttling losses during part-load operation, with pressure charging to ~20 bar BMEP maintaining target engine power and torque. The combination of these technologies was therefore a major decision early in the specification of the engine.

The choice of a 3-cylinder architecture was unusual and was based on (a) providing a large, workable bore size for the provision of a close-spaced DI system (see Chapter 6 and below) and (b) avoiding pulse interaction in the exhaust system to ensure minimum trapped burned gas residual to extend the knock limit. This is synergistic with the lower BMEP necessary for achieving target power and torque from the larger cylinder size. Hence any degree of over-fuelling to control knock at high load could be expected to be minimized to the benefit of overall fuel consumption. Also, reducing the number of cylinders in an engine generally reduces its friction.

Knock control was further improved by the adoption of the HOTFIRE 'second generation' close-spaced DI system configured so that the evaporation of the fuel removes as much heat from the charge air as possible. This system mounts the injector centrally in the combustion chamber and thus exhibits less potential for cylinder bore washing compared to an under-port injector location. Furthermore, such a close-spaced configuration does not compromise the intake port in the same way that an under-port injector location does. It was decided that the bore should be 88 mm in order to share the cylinder architecture with the HOTFIRE single-cylinder engines. With a stroke of 82.1 mm, this provided a total engine swept volume of 1.5 litres. As described in Chapter 6, adopting a 10 mm spark plug from NGK permitted large 34 mm head diameter intake valves to be retained. This reduced flow losses and in this multi-cylinder variant could be expected to minimize the required boost pressure, to the benefit of reduced

overall pre-turbine pressure and thus provide a better balance of pressures across the combustion chamber. This will be returned to later in this chapter. All of these considerations are considered complementary. Additionally, the resulting relatively large cylinder size of 500 cm³ ensured that the combustion chamber volume to surface area ratio of the cylinder is high, to the benefit of reduced thermal losses (Heywood, 1988).

At the time that the Sabre engine concept was laid down, the only 'second generation', or close-spaced, DI systems in production used piezoelectric injectors with an associated high piece price (Lückert *et al.*, 2006, Schünemann *et al.*, 2007). Solenoid injectors are much less expensive and were specified since stratified operation was not required except at start-up, although it was accepted that effort might have to be expended to avoid nozzle coking issues. In particular this would mean full optimization of the cooling jacket and nozzle protrusion. Such injectors have since been adopted in close-spaced DI systems in production (Klauer *et al.*, 2009). The general arrangement of the injector and spark plug, together with the switching valve train concept, is shown in Figure 7.1.

By configuring the plane of the spark plug and injector to lie along the crankshaft axis, a synergy with the de-throttling provided by the valve train could be realized. This was because at part load, one valve could be fully deactivated to manipulate swirl in the chamber and improve fuel-air mixing. This so-called 'Swirl-DI' configuration gave the opportunity to investigate the valve deactivation strategy to determine which valve provided the best results, and presented a route to practical application of the research conducted as part of the HOTFIRE consortium project (Turner *et al.*, 2006a and Stansfield *et al.*, 2007). The Lotus-INA cam profile switching (CPS) tappet system was the system chosen for de-throttling and swirl manipulation. This tappet system has been put into series production by several manufacturers e.g. as reported by Bruestle *et al.* (2001) and Sandford *et al.* (2009). The results of applying the Swirl-DI system will briefly be returned to in Section 7.3.

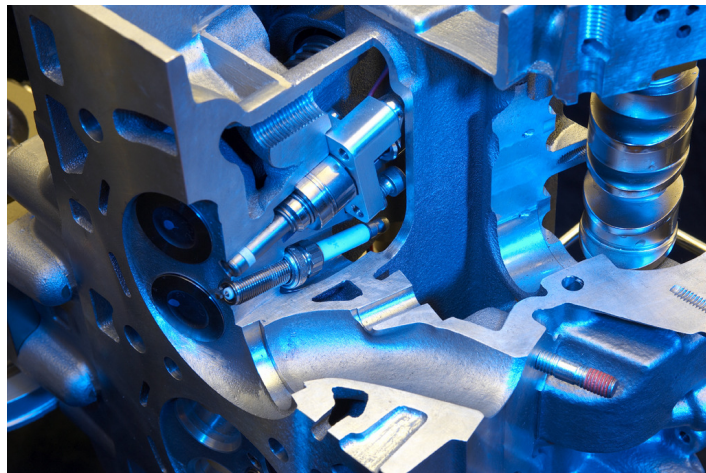
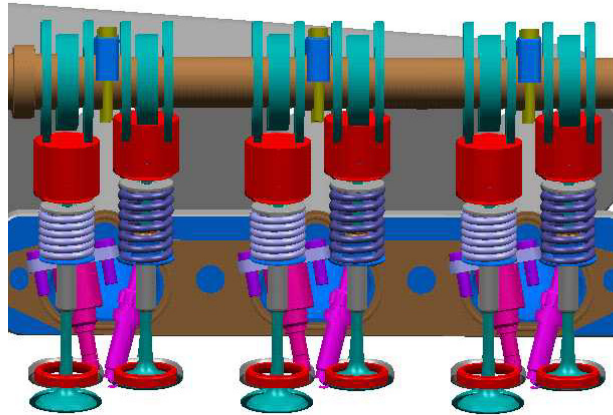


Fig. 7.1: Top: configuration of Sabre engine cylinder head showing fuel injector (orientated to left) and spark plug (to right), providing the HOTFIRE concept of swirl manipulation with a switching valve train. Bottom: photograph of sectioned Sabre cylinder head. (Illustration and photograph courtesy Lotus Engineering)

The engine also used dual continuously-variable camshaft phasing (DCVCP) devices for internal EGR control and was also design-protected for CPS tappets on the exhaust side, whose camshaft also carried the three-lobe driving cam for the DI high-pressure pump.

As discussed in Chapters 2 and 3, reducing the over-fuelling often necessary for component thermal protection (e.g. the exhaust valves, ports, manifold and

turbine system) when turbocharged engines are operated at high power levels is important with regard to real-world fuel consumption. This was addressed in Sabre by adopting a relatively large swept volume which reduced the level of boost necessary for the target power output and also by adopting an integrated exhaust manifold (IEM) built into the cylinder head. At full load, this IEM has the effect of removing some thermal energy from the exhaust gas prior to its entry to the turbocharger turbine, reducing its temperature and so removing the need for as much component thermal protection fuelling. These benefits are also discussed by Borrmann *et al.* (2008) and Kulbach *et al.* (2009). A view of the IEM as configured on Sabre is shown in Figure 7.2. This also shows the mounting arrangement of the turbocharger (which used a short spacer, or link pipe, to facilitate engine installation in the demonstrator vehicle to which the engine was later fitted). Figure 7.2 clearly shows the benefits in compactness afforded by the IEM concept.

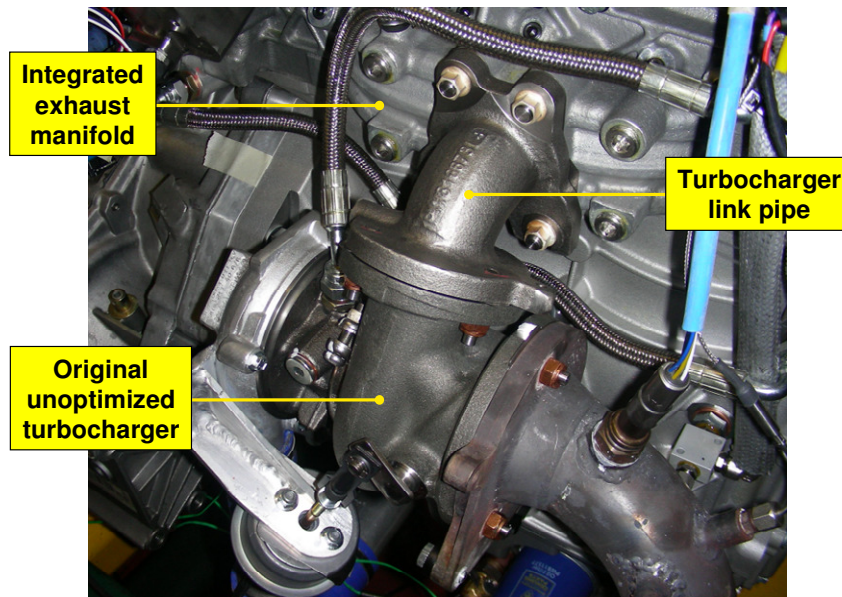


Fig. 7.2: Turbocharger mounted to IEM (via a short spacer to facilitate packaging in demonstrator vehicle). (Photograph courtesy Lotus Engineering)

Finally, a mild hybrid system was also specified as another fully-complementary technology. This comprised a 12 kW ‘pancake’ motor attached to the rear of the

crankshaft and vehicle-mounted supercapacitors. The system was designed to provide low-speed torque assistance to offset transient turbo lag, a degree of regenerative braking, and an advanced stop-at-idle function. In general such systems show clear synergies with turbocharged engines (Grebe *et al.*, 2007).

Since the architecture of large cylinder swept volume and 3-cylinders gave rise to a significant unbalanced primary couple, a particular feature of the design was the adoption of a primary balance shaft for NVH control. This was fitted with roller bearings in order to reduce friction and also carried a cylindrical shroud to minimize windage losses in the crankcase. This shaft was driven by a helical gear from the rear of the crankshaft. Roller bearings absorbed the end thrust of the drive gears, eliminating the need to adopt split gears for NVH reasons. The arrangement is illustrated in Figure 7.3, which also shows the rest of the cranktrain. The connecting rods were guided at the small end to reduce friction. Figure 7.3 shows that box-type pistons were used, providing a compression ratio of 10.2:1, with the inclusion of a shallow bowl for fuel spray containment at engine start-up. This was a detail change from the piston design for the related single-cylinder engine discussed in Chapter 6, which utilized a flat top.

A cooling system with an electric water pump and engine management system control of by-pass valves and thermostats was also applied to permit different cooling strategies to be investigated and to allow rapid warm-up of the engine. The design of the cylinder block incorporated large inter-bay breathing galleries because a 3-cylinder engine has to move a volume of crankcase gas approximately equal to one-half of a cylinder's-worth of displacement from front to back of the crankcase and *vice-versa* once per crankshaft revolution. The breather galleries also provided a 'double-skin' to stiffen the cylinder block and these are apparent in Figure 7.4. This was a design feature originally used in the production Lotus Type 918 V8 engine (Lotus Cars, unknown date and Crosse, 2011). The bedplate used a 4-bolt jointing arrangement for the main bearings and also incorporated cast-in iron inserts for bearing support. The cylinder block had ribbing on the outside for NVH control.

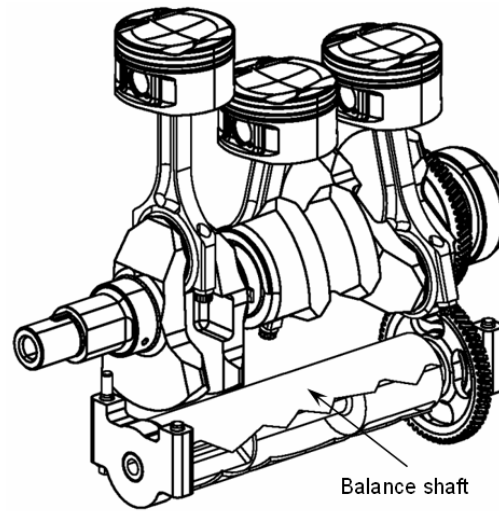


Fig. 7.3: Cranktrain and balance shaft arrangement of the Sabre engine. The shallow bowl visible in the piston crown is used for spray containment at start-up. Also visible is the shroud around the balance shaft to reduce crankcase windage. (Illustration courtesy Lotus Engineering)

The only non-electrically-driven auxiliary component on the engine was the air-conditioning compressor, which utilized an elastic belt to avoid the need for a separate belt tensioner.

Sabre was conceived with a philosophy of cost-effective, affordable technology including all of the elements required to deliver an effective technical solution to achieve low CO₂ output. Having only three cylinders, Sabre provided obvious parts count and associated cost savings over similar capacity 4-cylinder engines, but from a technological standpoint, a stratified-charge combustion system to achieve the desired fuel economy at part load would also have required an expensive NO_x trap and corresponding regeneration strategies. This requirement was avoided in the Sabre engine, which utilized relatively low-cost CPS tappets in order to permit operation on the early inlet valve closing form of the 'Miller' cycle instead. A restrictor and actuator in the oil circuit were the only items necessary to complete the system, which kept manufacturing cost and complexity to a minimum compared to other variable valve train actuation

systems (Wurms *et al.*, 2006). Also, the new exhaust-camshaft-driven single-cylinder fuel pump was designed as a low-cost component when compared to other multi-cylinder high-pressure pumps capable of delivering fuel at 200 bar.

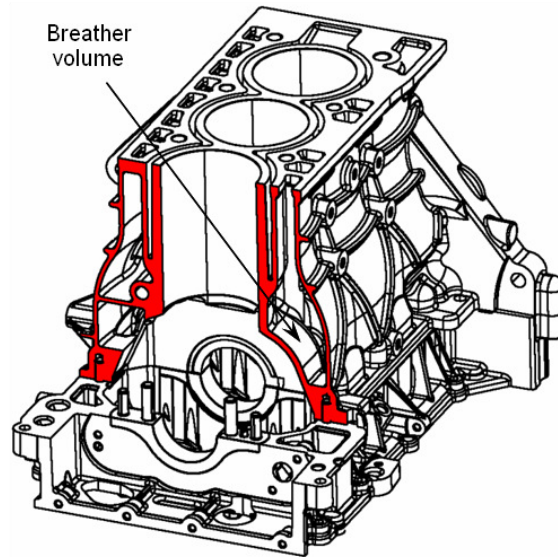


Fig. 7.4: Crankcase construction and inter-bay breather arrangement of the Sabre engine. Also visible are the four vertical bolts for each main bearing panel and associated cast iron insert in the bedplate casting. (Illustration courtesy Lotus Engineering)

The IEM, together with its thermal advantages, also had a reduced parts count in comparison to a standard manifold assembly. For a 3-cylinder engine, a standard configuration would typically comprise 28 parts (cylinder head assembly, exhaust manifold, 12 studs, 12 nuts and two gaskets), whereas the IEM design comprised 10 parts (cylinder head assembly, four studs, four nuts and one gasket). This is an 18-part reduction in bill of material (BOM) which would yield associated component cost and weight savings and reduce the cost and complexity of assembly in the manufacturing environment.

The specifications of the engine are given in Table 7.1, and photographs of the engine are shown in Figure 7.5. Coltman *et al.* (2008) describe the design of the engine in more detail.

Table 7.1: Sabre 3-cylinder downsized demonstrator engine specifications

Configuration	In-line 3-cylinder
Displacement	1.5 litres
Firing order	1-3-2
Bore x Stroke	88.0 x 82.1 mm
Compression ratio	10.2:1
Valve train	DOHC, 4 valves per cylinder, dual continuously-variable cam phasing and Lotus-INA cam profile switching tappets
Maximum power	117 kW (157 bhp) at 5000 rpm
Peak torque	240 Nm (from 2000 to 4000 rpm) (Transmission limited)
Maximum BMEP	20.1 bar
Fuel consumption at 2000 rpm, 2 bar BMEP	362 g/kWh
Maximum boost pressure	2.0 bar (absolute)
Maximum fuel pressure	200 bar
Fuel	95 RON unleaded gasoline
Exhaust manifold	Integrated into cylinder head and engine cooling system
Cooling system	Electric water pump, split cooling jacket and diverter valves

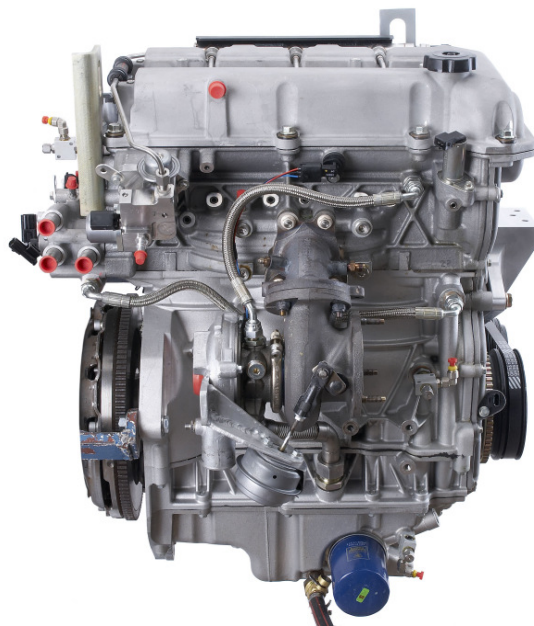


Fig. 7.5(a): Photograph of right hand (exhaust) side of Sabre 3-cylinder downsized demonstrator engine. (Photograph courtesy Lotus Engineering)



Fig. 7.5(b): Photograph of left hand (intake) side of Sabre 3-cylinder downsized demonstrator engine. (Photograph courtesy Lotus Engineering)



Fig. 7.5(c): Photograph of front of Sabre 3-cylinder downsized demonstrator engine. Note the use of a single tension belt drive for the air conditioning compressor. (Photograph courtesy Lotus Engineering)

7.3 THE CONCEPT OF SWIRL-ENHANCED COMBUSTION AND A BRIEF OVERVIEW OF PART-LOAD RESULTS

As mentioned previously, the Sabre engine employed a second-generation, close-spaced, swirl-enhanced combustion system (known as 'Swirl-DI') which positioned the injector and spark plug along an axis parallel to that of the crankshaft. This was in contrast with most other close-spaced combustion systems then in production, where the injector lay between the intake valves and the spark plug between the exhaust valves in a symmetrical arrangement (Lückert *et al.*, 2006, Schünemann *et al.*, 2007). Swirl-DI combined elements of early inlet valve closing (EIVC) operation with the manipulation of in-cylinder air motion at part load in order to improve combustion and fuel consumption. Turner and co-workers have described the operating strategy and its interaction with the cylinder architecture (Turner *et al.*, 2006a and Stansfield *et al.*, 2007). The use of DCVCP permits further optimization of the de-throttling effect. The Swirl-DI combustion performance is clearly different depending upon which intake valve is deactivated due to the asymmetric layout of the injector and spark plug. It should be noted that the asymmetric close-spaced combustion system employed in the Jaguar V8 engine described by Sandford *et al.* (2009) has many similarities with that of Sabre, except that the Jaguar engine does not manipulate swirl, using its switching tappets to provide an EIVC event only.

In all DI engines, fuel-spray targeting is very important and in a close-spaced engine there are considerable complicating effects caused by valve motion, such as direct valve/spray interaction (Zhao *et al.*, 2002 and Turner and Pearson, 2009). As a consequence of this, the Sabre engine used injectors developed specifically for the application by Continental Automotive Systems. These 'Multi-Stream Injectors' provided optimization possibilities because the individual streams could be targeted to avoid the valve heads during the injection event. Work conducted during the HOTFIRE research project was used to prove the effect of swirl-enhanced combustion in the related single-cylinder engines and to help develop the injector geometry to suit the combustion chamber. Figure 7.6 provides a comparison of spray visualisation recorded in the HOTFIRE project's

optical engine and that predicted using the Matlab-based IMPACT tool developed by Continental Automotive Systems for spray optimization. As can be seen, the spatial correlation is very good, and the IMPACT program permitted rapid development of the injector specifications for both the HOTFIRE project and the Sabre engine.

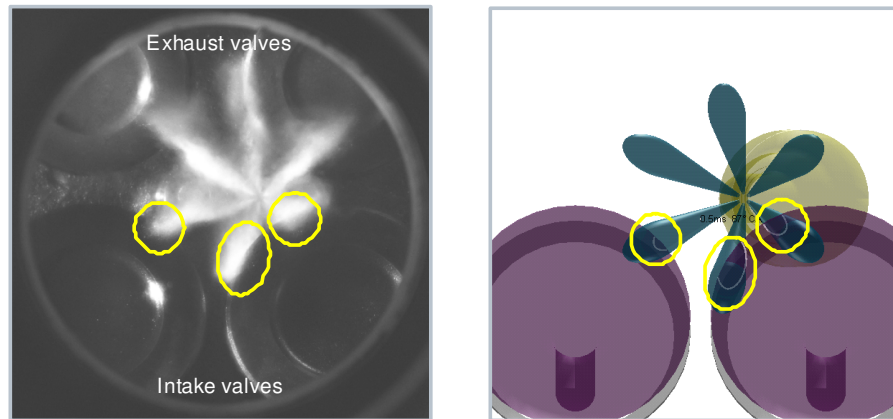


Fig. 7.6: Comparison of fuel spray results from optical engine (left) and IMPACT program (right). (Photograph courtesy Lotus Engineering)

The point at which the CPS was switched from the low- to high-lift profiles was calibrated to occur at engine speeds and loads defined to realize the best results in real-world driving. This thesis is concerned with full-load results and so it is not intended to discuss the part-load performance of the engine in detail. However, in the Sabre engine the good low-load fuel economy as a result of the Swirl-DI approach was vitally important since it permitted the use of a relatively large-swept-volume engine with moderate boost pressure to achieve target power while still providing good fuel economy when fitted in a vehicle. As an illustration of this, the BSFC at 2000 rpm, 2 bar BMEP was 362 g/kWh, which compared very favourably with contemporary downsized production engines employing homogeneous DI combustion systems, which typically gave 380-400 g/kWh at this swept volume and operating point (Coltman *et al.*, 2008, Nuglisch *et al.*, 2008 and Turner *et al.*, 2008a). It also compared well with the larger DI engine of Wurms *et al.* (2006), which utilized a two-step switching valve train system

together with a switchable oil pump and low-friction camshaft drive to give 340 g/kWh at 2000 rpm, 2 bar BMEP. Generally, up to 6% improvement in fuel economy was demonstrated on Sabre by using the Swirl-DI approach over a simpler DCVCP one with both valves operating on the high lift profiles (Coltman *et al.*, 2008).

It should also be noted that when engaged, the use of EIVC as part of Swirl-DI also permitted a reduction in transient turbo lag. This is because it ensured that, for any given torque, the intake system was at a higher pressure at part load than would be the case was conventional throttling employed instead. During a transient load change, this reduced that proportion of the time taken to achieve atmospheric pressure in the plenum.

Several prototype engines were built and all underwent dynamometer testing. Two were fitted to test vehicles (then-current GM Astra hatchback models) and vehicle calibration, including that for the hybrid system, was carried out. It is not intended to discuss vehicle-specific test results here since Nuglisch *et al.* (2008) present a full description of the results achieved, as well as the vehicle modelling work conducted to establish the combination of vehicle technologies. A photograph of one of the test vehicles is shown in Figure 7.7.

7.4 INITIAL FULL-LOAD TEST RESULTS

Full load data for what was known as Phase 1 of the Sabre engine project is shown in Figure 7.8, i.e. for the engine specification described above. This data was recorded with a turbine inlet temperature limit of 980°C using commercial 95 RON gasoline from the bulk tanks at Lotus Engineering, and was corrected using the 88/195/EEC correction factor. After running-in and turbocharger development (described below), maximum torque was found to be 245 Nm at 3000 rpm and maximum power was 117 kW (157 bhp) at 5000 rpm, corresponding to BMEPs of 20.5 and 18.6 bar, respectively. The BMEP at 1500 rpm was 16 bar and the exhaust system back pressure was 36 kPa at maximum power.



Fig. 7.7: GM Astra test vehicle fitted with Sabre downsized demonstrator engine.
(Photograph courtesy Lotus Engineering)

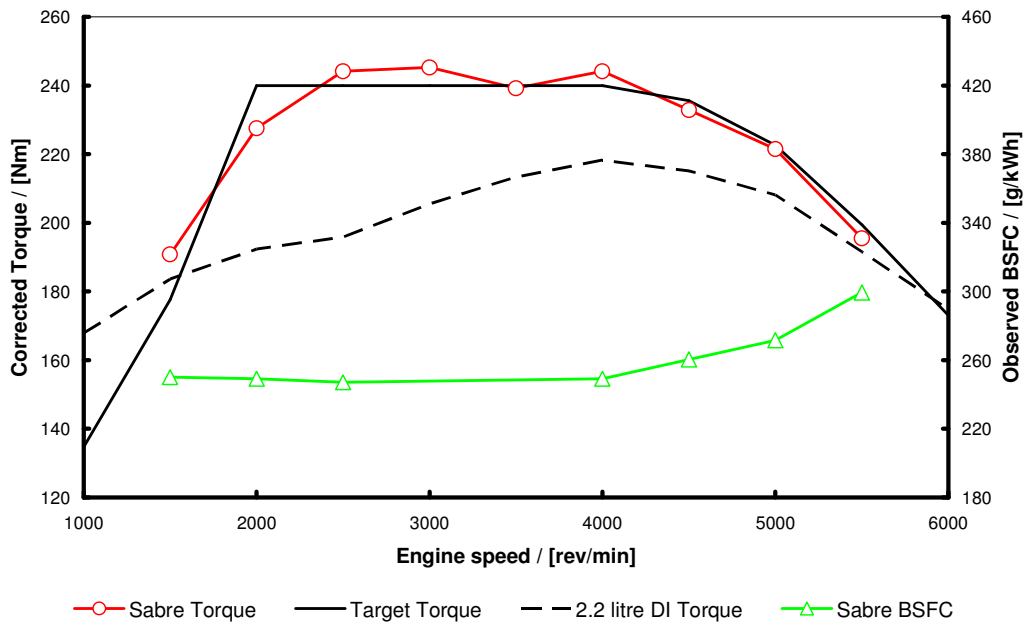


Fig. 7.8: Full load performance of Sabre engine when operating on 95 RON gasoline and comparison with the original target torque curve. A comparison curve for a typical 2.2 litre direct-injection NA engine described by Schnittger et al. (2003) is also shown

The first turbocharger used for this Phase 1 specification was, for commercial reasons, not fully optimized to the engine. During running-in of the very first build it was apparent that the turbine was too aerodynamically restrictive and was causing a significant residual retention problem in the combustion chambers as a result of a very high pre-turbine pressure. As a consequence of this, the author determined that a standard Lotus V8 turbocharger, as used on one cylinder bank on that engine (Lotus Cars, unknown date and Crosse, 2011), was of approximately the correct flow capacity and pressure ratio, and would be a better match to the engine. As a result this alternative specification of turbocharger was successfully tested and used from that point in the programme onwards as the standard 'Phase 1' turbocharger. The subject of turbocharger matching will be returned to in Chapter 8.

Figure 7.8 also includes the performance target for the engine which modelling predictions early in the programme showed was achievable with a properly-matched turbocharger. A torque curve for a 2.2 litre NA first-generation direct-injection engine, the power output of which was a target during the initial development of the Sabre engine concept, is also included for comparison. This 2.2 litre engine, which was fitted as an option to the GM Astra vehicle to which Sabre was fitted for demonstration purposes, utilized under-port injectors and is described by Schnittger *et al.* (2003). The Sabre engine in Phase 1 form gave superior torque to this engine across most of the engine speed range.

In particular in Figure 7.8, full-load BSFC is seen to be 250 g/kWh between 1500 and 4000 rpm and, as will be shown later in Section 7.6, this compares extremely favourably with more complex combustion system concepts employing excess air or cooled EGR. Sabre used neither of these in this initial Phase 1 guise. The full-power BSFC of 272 g/kWh was achieved at a specific power output of over 74.6 kW/l (100 bhp/l) and a BMEP of 18.7 bar with regular 95 RON gasoline and a relatively low turbine inlet temperature limit of 980°C⁸. The combination of the

⁸ It should be noted that the results presented here do not include electrical loads since the vehicle brake-energy recuperation system would charge the battery during vehicle operation, meaning that in most cases fuel energy would not be used directly to power the electrical system.

HOTFIRE close-spaced combustion system and the IEM enable $\lambda = 1$ fuelling up to an engine speed approaching 5000 rpm, with only modest enrichment to $\lambda = 0.9$ for component thermal protection purposes necessary above this speed. At the maximum engine speed of 5500 rpm the BSFC was 299 g/kWh. Technologies which have hitherto been suggested as necessary to support $\lambda = 1$ operation at the BMEPs of ~20 bar that the Sabre engine operated at, such as cooled EGR or separate water-cooled exhaust manifolds (Cairns *et al.*, 2006 and 2008, Kapus *et al.*, 2007b and Taylor *et al.*, 2010), have been found to be unnecessary when a rational engine design philosophy can be employed instead. These technologies will be discussed in more detail later.

Another important finding during development was that, as a result of detailed design and analysis, in over 2000 hours of diverse testing, injector coking was never found to be a problem with this engine design.

7.5 SCAVENGING ADVANTAGES OF 3-CYLINDER GROUPS IN TURBOCHARGED SPARK-IGNITION ENGINES

As mentioned above, the overall philosophy behind the Sabre concept was to offer a cost-effective engine providing excellent fuel economy from a targeted combination of technologies and attributes. The use of a 3-cylinder configuration operating at moderate BMEP was fundamental to this, since this brought the ability to operate with exhaust valve opening duration of $< 240^\circ$ CA, thus ensuring that there would be no interaction between the cylinders due to blowdown effects. Hence, with the correct valve event phasing, excellent scavenging could be achieved despite the fact that the mean pressure level in the exhaust manifold might significantly exceed that in the intake, due to the fact that during the valve overlap phase the intake port pressure could be arranged to exceed that in the exhaust.

This is considered a reasonable approach since when describing lean-operating combustion systems which require regeneration of lean-NO_x traps, e.g. spray-guided stratified combustion systems, it is not normal to apportion any fuel use necessary to ensure emissions compliance of the spray-guided combustion system to fuel consumption claims for steady state operation (Lückert *et al.*, 2006, Schünemann *et al.*, 2007).

To illustrate this, Figure 7.9 shows high-speed pressure traces taken at full load from both the intake port of cylinder number 2 and the turbocharger link pipe at two engine speeds, 2300 rpm and 5250 rpm. These engine speeds are before and after the boost cross-over point, where the mean exhaust pressure starts to exceed the mean intake pressure, and these mean pressures are also shown in the figure. The turbocharger link pipe used is shown in Figure 7.10.

Note that the results of Figure 7.9 were taken with the later 'Phase 2' turbocharger specification which will be discussed in more detail in Chapter 8. However, this fact does not change the conclusions drawn here.

Figure 7.9 clearly shows that the 3-cylinder architecture used in Sabre, coupled with optimal valve timing afforded by the DCVCP system, gives an ideal scavenging effect. Together with the ability of the DI system to retard injection until after exhaust valve closure, this means that the in-cylinder AFR will be richer than the mean exhaust system AFR. This is to the benefit of maximum load since the cylinder will be operating nearer to optimum power enrichment. Furthermore, if overall stoichiometry in the exhaust system can be achieved, there will be better exhaust emissions because the three-way catalyst will function robustly. In order to achieve a similar effect in a single-stage-turbocharged 4-cylinder engine an exhaust period of less than 180° would have to be used. This will be discussed later. The present work shows that when turbocharging an engine, adopting a 3-cylinder group makes such an approach unnecessary. Good residual scavenging is also known to be very important from the point of view of preignition of the charge (Hoffman *et al.*, 2008a, Willand *et al.*, 2009 and Zaccardi *et al.*, 2009a and 2009b), and so the adoption of the 3-cylinder configuration again provides a route to a simple solution.

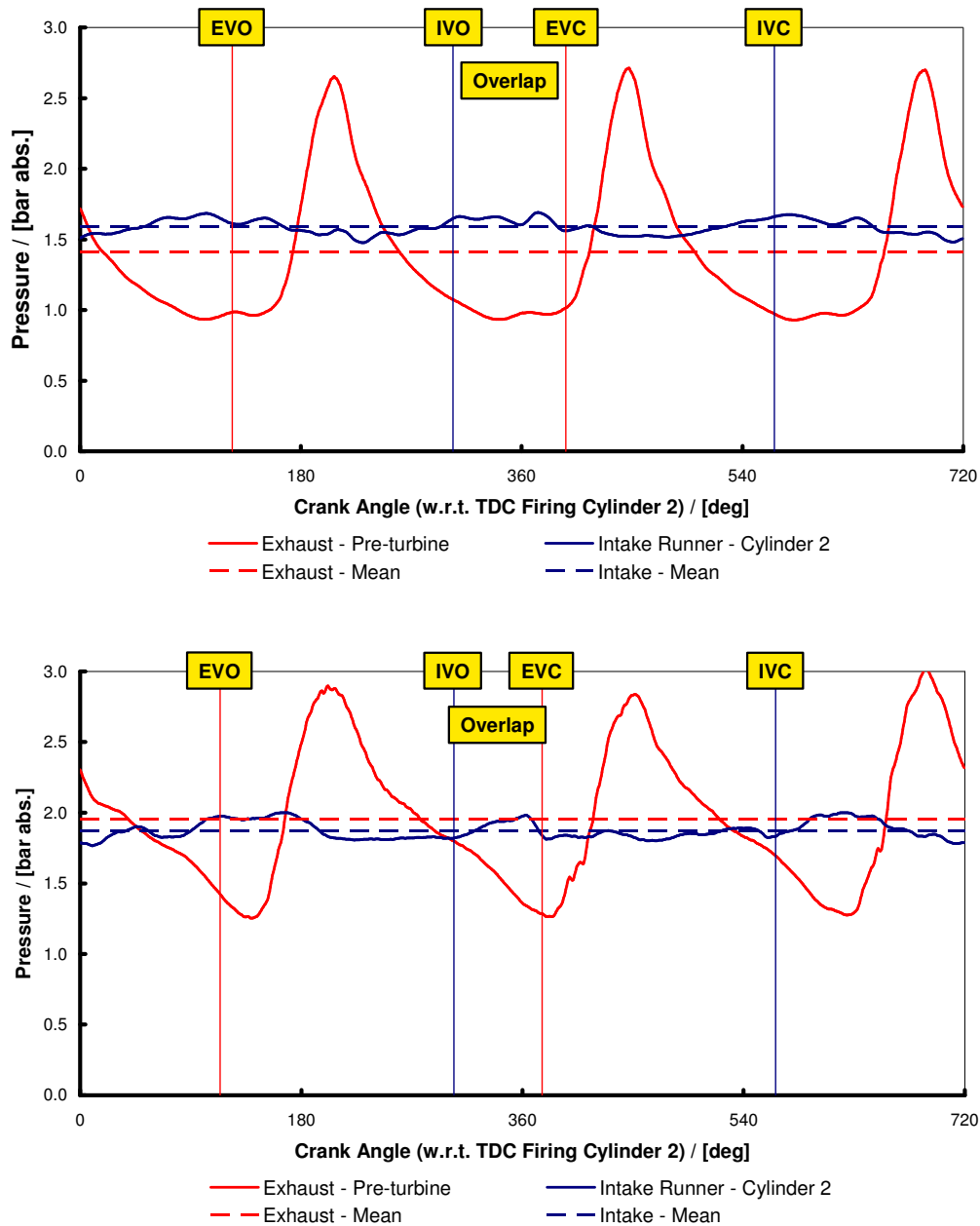


Fig. 7.9: Intake and exhaust port pressure histories at different operating conditions with intake and exhaust valve opening and closing points also shown.

Top: 2300 rpm, $\lambda = 1$, full load and before boost cross-over, i.e. the mean exhaust pressure is lower than the mean intake pressure. Bottom: 5250 rpm, $\lambda = 0.9$, full load and after boost cross-over, i.e. the mean exhaust pressure is higher than the mean intake pressure. Both traces show higher mean pressure in the intake than the exhaust during the valve overlap period

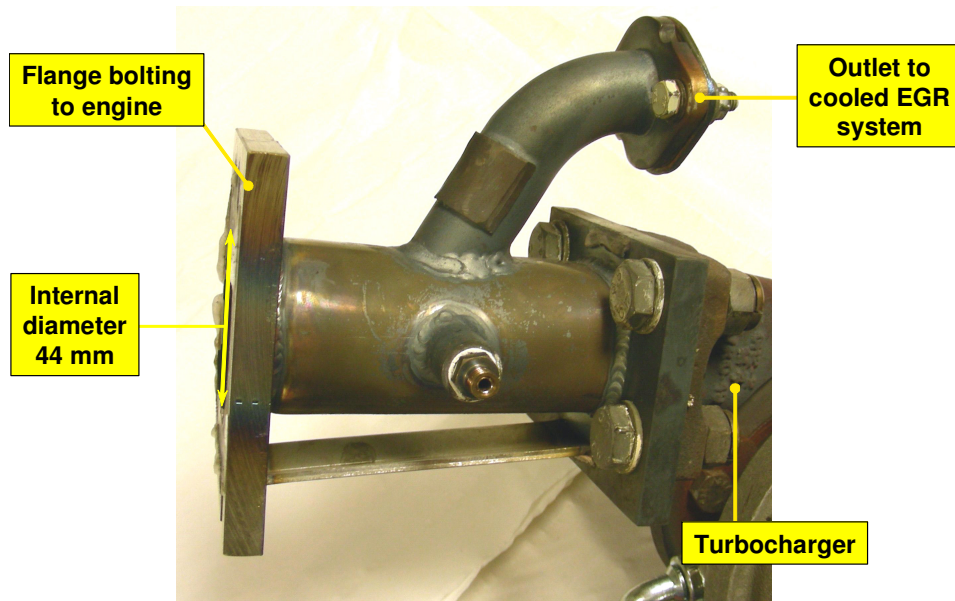


Fig. 7.10: Photograph of turbocharger link pipe. Visible are thermocouple tapings and a take-off for cooled EGR which will be discussed in Chapter 8. The high speed pressure tapping is not visible in this view. (Photograph courtesy Lotus Engineering)

7.6 SABRE ENGINE RESULTS IN COMPARISON TO COMPETING TECHNOLOGIES

The previous sections showed that the combination of features embodied in the Sabre engine allowed operation across most of the operating map at $\lambda = 1$. This section will discuss how the full-load fuel consumption of Sabre compared with some competing technologies.

7.6.1 Comparison of Sabre with compound charging systems

Having established that the Sabre engine in Phase 1 specification yielded good full-load results, comparisons will now be made with other technical solutions intended to establish a similar result. Of these, compound charging systems such as is used in the VW 'Twincharger' engine present a pragmatic solution to the changing requirements on the charging systems of 4-cylinder engines

throughout the speed range, albeit at increased BOM cost and control complexity (Krebs *et al.*, 2005a). The VW Twincharger engine was sequentially supercharged and turbocharged for good throttle response coupled with a wide BMEP range and the ability to match the turbocharger better for good high-load fuel consumption. Its maximum rated power fuel consumption is slightly better than Sabre in its Phase 1 specification but Krebs *et al.* (2005b) report that its mid-speed fuel consumption is about 10 g/kWh higher. The ability to utilize a less aerodynamically-restrictive turbine on Sabre would be expected to further improve its BSFC at maximum rated power, and this will be shown to be the case in Chapter 8.

7.6.2 Comparison of Sabre with 4-cylinder engines employing 180° CA exhaust cam period to eliminate pulse interaction

The approach of limiting the exhaust period of a 4-cylinder engine to less than 180° CA, in order to remove pulse interaction, has been used in production engines by both VW and Audi (Szenzel *et al.*, 2007, Wurms *et al.*, 2008 and Hadler *et al.*, 2009). This is analogous to the situation found in Sabre with its 240° CA exhaust period. The beneficial effect of this strategy can be seen by comparing BMEP curves between one of these engines and Sabre. The engine chosen for comparison is the Volkswagen TSI 88 kW (118 bhp) 1.4 litre in-line 4-cylinder, which employs a single-stage charging system utilizing a wastegated turbocharger, as described by Szenzel *et al.* (2007). At 62.8 kW/l (84.3 bhp/l) its specific output is slightly below that of Sabre, and some of the reason for this deficit is apparent in Figure 7.11, where it can be seen that the 180° CA exhaust cam period, which is beneficial for minimum residual carryover at low speed, causes an early limit to the gas exchange process at higher engine speed, in turn restricting air flow through the engine and limiting maximum power.

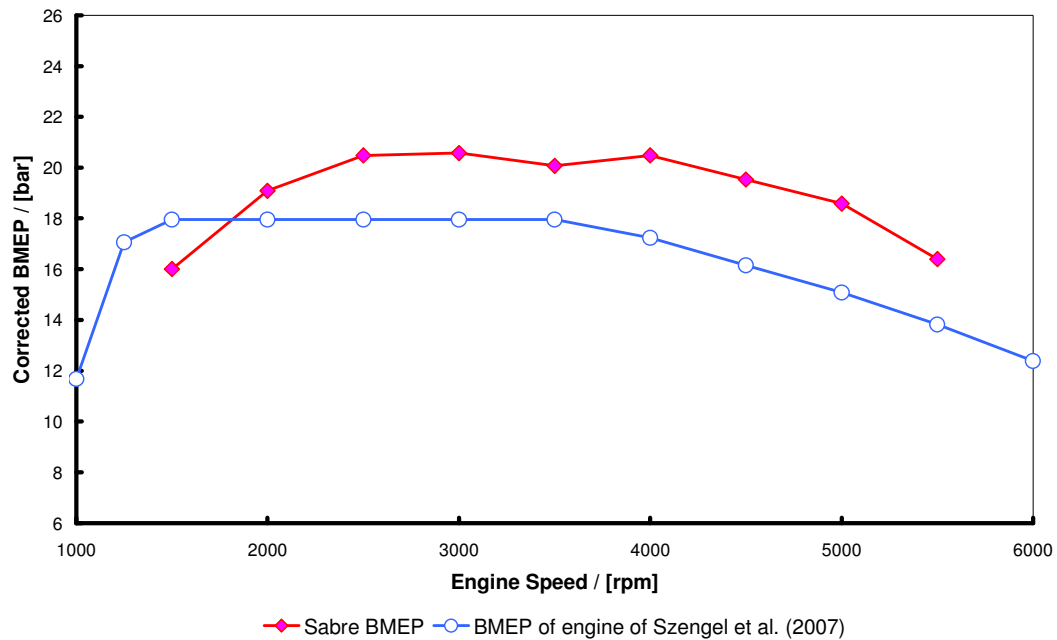


Fig. 7.11: Comparison of Sabre Phase 1 BMEP curve with that of VW 1.4 l 88 kW TSI engine described by Szengel et al. (2007)

The engine of Szengel *et al.* (2007) clearly builds up boost pressure at a lower engine speed than Sabre, but the pronounced ‘knee’ in the VW TSI BMEP curve at 3500 rpm is attributed by them to the breathing limitation caused by the 180° CA exhaust cam profile. Sabre, with its 3-cylinder layout and consequent ability to employ 240° CA without pulse interaction, suffers no such limitation to its gas exchange process, its exhaust cam profiles being capable of flowing significantly more air, as was shown in the curves for the Sabre engine in Figure 7.11.

The breathing limitation of a 180° CA exhaust cam duration in 4-cylinder engines was overcome in the engine described by Wurms *et al.* (2008) by using a two-stage switching valve train on the exhaust valves to move from a low-speed 180° CA camshaft to a longer one at higher speed. This permitted very good low speed torque together with good high speed power since, as was discussed in Chapter 3, it is possible to employ longer-duration cam profiles at higher engine

speeds where knock is less of a limitation due to the reduction in time available for autoignition to occur.

When considering limitations in air mass flow with cam duration a similar result to that reported by Szengel *et al.* (2007) was obtained during modelling for the engine of Lumsden *et al.* (2009). When utilising 240° CA camshafts in their 3-cylinder engine they found significantly reduced cylinder pressures at 3000 rpm in comparison to the alternative 276° CA items. The longer profiles were eventually chosen since they were found necessary to limit pre-turbine pressure and temperature at 6000 rpm (which was due to an exhaust-cam-profile-induced air mass flow limitation at high speed). Note that the engine of Lumsden *et al.* (2009) proves this point because the target BMEP was 30 bar at 2250 rpm with maximum power of 144 kW (193.1 bhp) at 6500 rpm, representing 22.1 bar BMEP at this condition, i.e. both significantly higher than the ~19-20 bar cases considered here.

Thus, keeping the exhaust cam period less than the firing interval in shared-manifold cylinder groups favours low-speed gas exchange and consequently combustion and performance, and it can be said that because of this, employing 3-cylinder geometry is a very pragmatic way to limit pulse interaction while permitting the use of cam periods capable of giving good maximum power. This is the case at least up to 19-20 bar BMEP.

7.6.3 Comparison of Sabre with an external water-cooled exhaust manifold

Taylor *et al.* (2010) have investigated the benefit of an external water-cooled exhaust manifold as applied to a downsized turbocharged DI engine. In their water-cooled manifold design, which they fitted to the VW Twincharger described by Krebs *et al.* (2005a and 2005b), the internal form of the exhaust duct was identical to that of the original VW engine except for the deletion of an exhaust splitter providing a degree of pulse separation up to the turbine inlet. The effect of this manifold on the engine in terms of fuel consumption and λ at full-load was

reported. For these tests the Twincharger engine was first operated without its supercharger and with a standard uncooled iron exhaust manifold. The effect of removing the supercharger on the rate of boost pressure rise with respect to engine speed is readily apparent in Figure 7.12. This also clearly shows that the turbocharger fitted to the engine of Krebs *et al.* (2005a and 2005b) is matched for low high-load fuel consumption. Figure 7.12 also shows the effect of the water-cooled exhaust manifold. At low engine speed a combination of the absence of pulse division and the reduction in temperature at the entry to the turbine caused by the water-cooling resulted in a reduction in the power the turbine could produce. This reduction in power available to drive the compressor in turn reduced the torque of the engine, and the boost versus engine speed build-up line is delayed by 500 rpm.

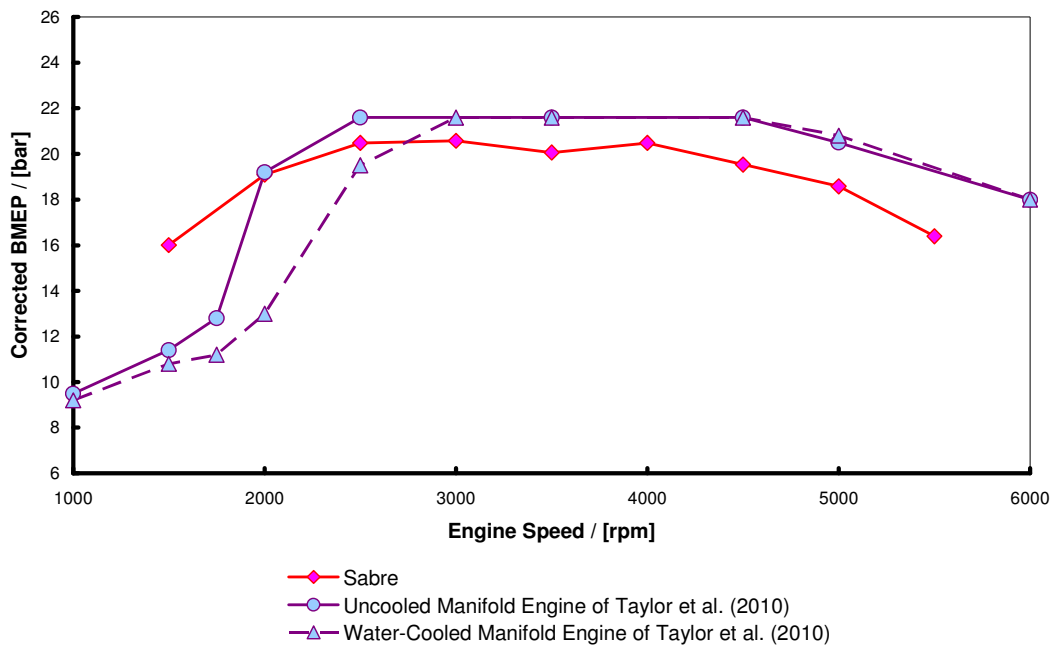


Fig. 7.12: Comparison of Sabre Phase 1 BMEP curve with those for uncooled iron and water-cooled aluminium manifold engines of Taylor et al. (2010)

Since all testing by Taylor *et al.* (2010) was conducted without the supercharger being operational, it is unknown whether the original full-load BMEP curve could have been maintained with the water-cooled exhaust manifold fitted.

Figure 7.13 shows the effect of the water-cooled manifold versus the uncooled original and results from Sabre with respect to λ . Here the ability of a water-cooled manifold to remove heat energy from the exhaust gas at high engine load and speed is seen to be especially beneficial. The uncooled exhaust manifold forces excess fuelling to be adopted for component thermal protection from 2000 rpm onwards, despite the fact that from the low-speed results of Figure 7.12 it is clear that in terms of swallowing capacity a relatively large turbocharger turbine is being used on the engine of Krebs *et al.* (2005a and 2005b). Water-cooling permits $\lambda = 1$ operation to be maintained until 3500 rpm, 500 rpm lower than Sabre. Generally Sabre is nearer to $\lambda = 1$ until 5000 rpm (its peak power speed). This is possibly partly due to operating at a BMEP 2 bar lower at these speeds.

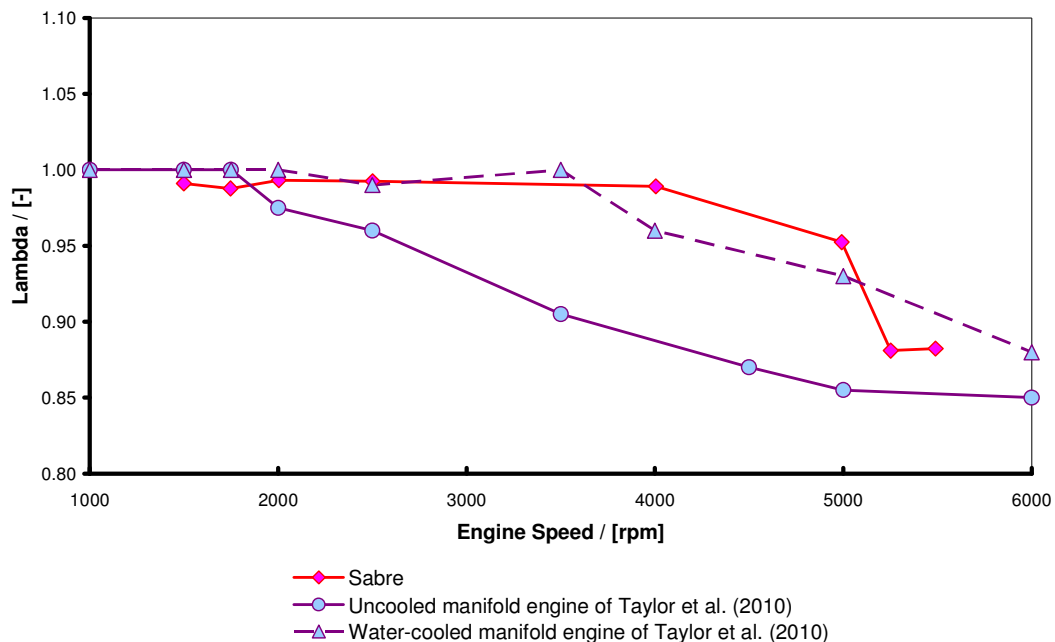


Fig. 7.13: Comparison of Sabre Phase 1 relative AFR (λ) curve with those for uncooled iron and water-cooled manifold engines of Taylor et al. (2010)

7.6.4 Comparison of Sabre with excess air combustion strategies

Another strategy that has been proposed to improve high-load fuel consumption is the so-called 'lean boost' combustion system, as discussed by Lake and co-workers (Stokes *et al.*, 2000 and Lake *et al.* 2004a and 2004b). Here excess air is used as a diluent to slow the flame speed and hence keep the end gas cooler than it would otherwise be, to the benefit of extending the knock limit. Hence it is analogous to the use of cooled EGR and, as discussed in Chapter 3, Lake and co-workers themselves found little to choose between the two approaches. Hiroshi *et al.* (2004) and Hattrell *et al.* (2006) have both raised potential concerns with the use of excess air as a diluent in pressure-charged engines since the lower ratio of specific heats of air versus EGR causes the temperature of the end gas to rise higher and can actually accelerate the autoignition process. Here, it is proposed to draw a comparison between Sabre and the excess air approach espoused by Lake and co-workers on the basis that, if the use of excess air does indeed give good high load fuel consumption, then it should be capable of at least bettering the results recorded by Sabre.

Figure 7.14 shows data taken from Lake *et al.* (2004a) in comparison to full-load data from Sabre in Phase 1 specification. The so-called lean-boost direct injection (LBDI) engine of Lake and co-workers was a 1.125 l 3-cylinder engine with direct injection and so bears some similarities to Sabre, although a significant difference was their use of a variable-geometry turbine (VGT). This was made possible because of the reduced exhaust temperature provided by the excess air and cooler combustion. Despite the potential advantages of a VGT (as discussed by Kerkau *et al.*, 2006 and Gabriel, *et al.*, 2006), the LBDI engine achieves a lower BMEP in the mid-speed range than Sabre, and has significantly worse BSFC from 2000 to 3500 rpm (nearly 20 g/kWh). From 3500 rpm onwards, the BSFC curves are similar, but the value of BMEP is ~2 bar lower for the LBDI engine.

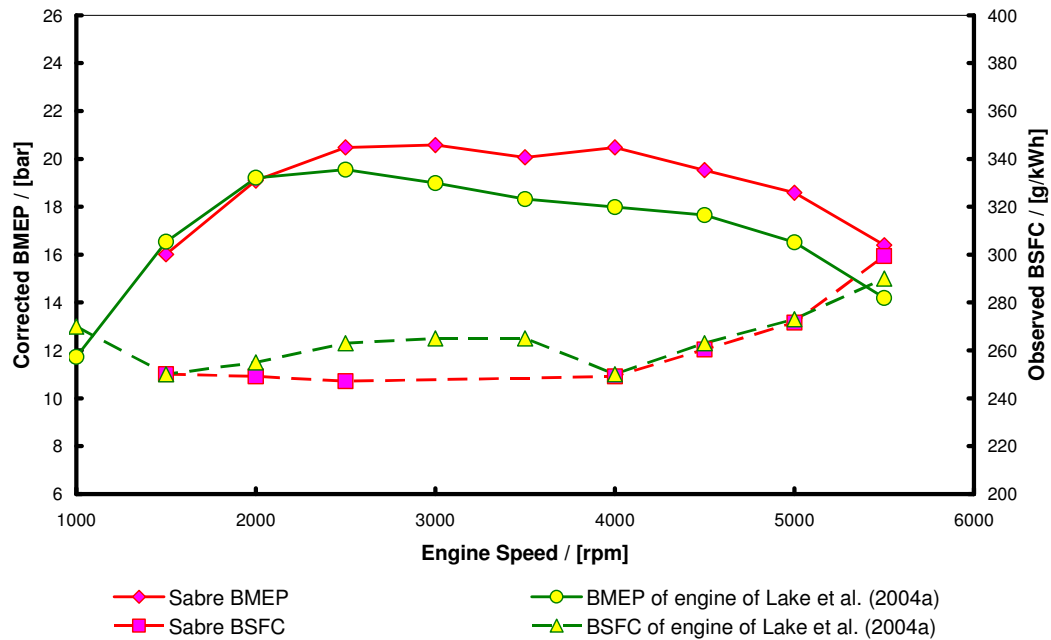


Fig. 7.14: Comparison of Sabre Phase 1 BMEP and BSFC curves with those of 'lean boost' engine of Lake et al. (2004a)

The data of Lake *et al.* (2004a) shows that with excess air operation turbine inlet temperature (TIT) was low, with a maximum of $\sim 760^{\circ}\text{C}$ versus the 980°C that Sabre was controlled to. This is the primary reason why the LBDI engine could utilize a VGT. Nevertheless, in comparison to Sabre, the anticipated VGT advantages of greater low-speed BMEP and better high-load fuel consumption are absent. This is probably due in part to the fact that the turbocharger had to supply excess air over that needed for full combustion. When remembering that the LBDI engine must use a lean-NO_x trap for exhaust after treatment at part load (instead of just a simple three-way catalyst), it is apparent that Sabre represents a very attractive alternative combination of technologies.

7.6.5 Comparison of Sabre with cooled EGR

Many researchers have pointed out the benefits of cooled EGR, ever since Ricardo initially investigated it as a means of extending the knock limit (Ricardo,

1919 and 1920, Cairns *et al.*, 2006 and 2008, Hattrell *et al.*, 2006 and Alger *et al.*, 2008). Recently Cairns and co-workers have been strong proponents and have used a 2.0 litre I4 DI engine with homogeneous fuelling to investigate the potential of the approach.

The publications of Cairns and co-workers have not stated any BSFC figures, instead quoting relative air-fuel ratio λ . This makes comparison with the results from Sabre difficult but, if one is interested in ascertaining how close one can operate an engine to $\lambda = 1$ (for the sake of simple and complete catalysis of the exhaust gas) then comparison is possible. One must remember, however, that the ability to operate at $\lambda = 1$ does not automatically result in good specific fuel consumption, a topic which shall be returned to in more detail in Chapter 8.

Figure 7.15 shows results taken from Cairns *et al.* (2006) versus those from Sabre in Phase 1 form. The results are broadly comparable in terms of TIT, since Cairns and co-workers worked to a limit of 950°C and Sabre was operated up to 980°C (which was only reached at 4500 rpm, thus causing the excursion from nominal $\lambda = 1$ fuelling rate shown at 5000 rpm). At the maximum power condition the Sabre engine is operating at ~19 bar BMEP, which is slightly lower than the 20-22 bar BMEP of the engine of Cairns *et al.* (2006) shown in Figure 7.15. Nevertheless, the results from Sabre compare extremely favourably with those obtained from applying cooled EGR to a non-optimized engine.

Comparison with the close-spaced second generation DISI engine of Lang *et al.* (2008), which was of 4-cylinder configuration and which employed piezo injectors, cooled EGR and a conventional exhaust manifold, reinforces the fact that the use of 3 cylinders and IEM is very beneficial. With their engine, Lang *et al.* (2008) showed a BSFC of 290 g/kWh at the same test condition of 5000 rpm, 18 bar BMEP as was utilized in the present work. Furthermore, the engine of Lang *et al.* (2008) appears to have been operated on 99 RON fuel to achieve the results presented in their work, whereas the gasoline used in the Sabre engine work reported here was standard 95 RON pump fuel.

For higher BMEPs, cooled EGR could still be applied to the Sabre engine, with the advantage that less mass of cooled EGR would have to be added for any given increase in BMEP in comparison with an engine of conventional configuration. This would lead to benefits in terms of combustion stability and charging system matching as well as a reduction in under-hood thermal load due to the requirement to cool the exhaust gas, a subject discussed by Alger *et al.* (2008). A series of tests designed to establish the effect of cooled EGR on the Sabre engine at the moderate BMEPs discussed here is reported in Chapter 8.

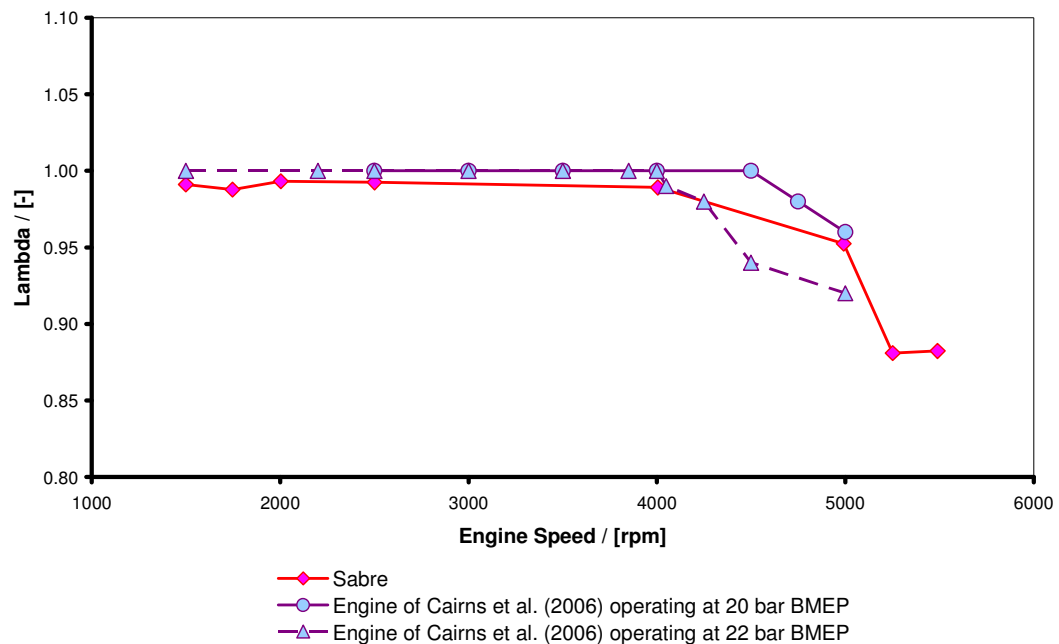


Fig. 7.15: Comparison of Sabre Phase 1 full-load relative AFR (λ) with that of cooled EGR engine of Cairns *et al.* (2006) operating at two different engine loads

7.6.6 Comparison of Sabre with higher turbine inlet temperatures

As discussed, a significant penalty often paid at high load in turbocharged engines is for component thermal protection fuelling. Since the turbine causes a

drop in the temperature of the exhaust gas before it reaches the catalyst, the turbine is often the limiting case on permissible gas temperatures.

Figure 7.16 shows results given by Kapus *et al.* (2007a) for a DISI turbocharged engine fitted with DCVCP devices and with a higher permissible TIT than was used as a limit in Sabre. The limit of 1050°C quoted by Kapus *et al.* (2007a) is more expensive to provide than the 980°C limit of Sabre, since increasing quantities of nickel need to be added to the steel of the turbine wheel and its housing in order to ensure adequate long-term durability. However, it must be noted that 1050°C is now routinely provided as a safe TIT for production turbocharged engines (Brooke, 2011). The engine of Kapus and co-workers was different to Sabre in two important characteristics: firstly it was of an I4 configuration (and thus had a shared exhaust manifold and, since they did not state otherwise, presumably a high degree of pulse interaction providing an increased exhaust residual rate) and secondly it had a conventional, uncooled exhaust manifold.

In Figure 7.16 it can be seen that the engine of Kapus and co-workers had a significantly greater BMEP at low engine speed than Sabre. This may have been the result of using a turbine with a larger expansion ratio, which one would then expect to become a limiting factor on turbine inlet temperature earlier in the engine speed range. Notwithstanding this, in the mid- to high-engine-speed range of 4000 to 5000 rpm, the increase in permissible TIT did not result in lower BSFC; in fact at the Sabre engine maximum power speed of 5000 rpm the BSFC of the engine of Kapus *et al.* (2007a) was almost 30 g/kWh (or ~9%) worse at substantially the same level of BMEP.

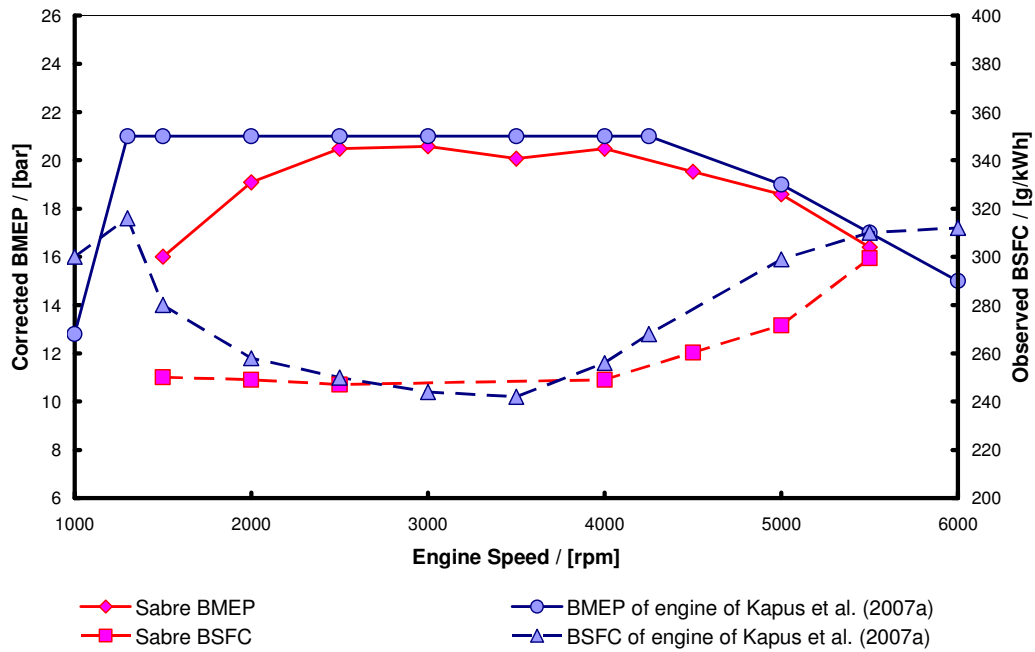


Fig. 7.16: Comparison of Sabre Phase 1 BMEP and BSFC curves with those of increased turbine inlet temperature engine of Kapus et al. (2007a)

From this it is presumed that the ability of the IEM to remove some of the heat of the exhaust gas before it is passed to the turbine, coupled with the 3-cylinder configuration, provides significant levels of reduction in that proportion of the fuel consumption which is attributable to component thermal protection fuelling. This advantage will then result in significant reductions in real-world fuel consumption at high vehicle speeds. The subject of operating the Sabre engine at higher TIT will be returned to in the next chapter.

7.6.7 Comparison of Sabre with some combinations of other technologies

Some researchers have published results for engines operating with different technologies simultaneously. In particular, Kapus and co-workers have shown various results for turbocharged DI engines with combinations of different levels of permissible TIT, water-cooled exhaust manifolds and cooled EGR (Kapus et al., 2007b). Figure 7.17 shows a comparison of their combined-technology

engine (with an undisclosed level of cooled EGR, a water-cooled exhaust manifold and a 950°C turbine inlet temperature limitation) with the alternative combination of Sabre.

The low speed BMEP of this engine was considerably higher than that of Sabre, albeit at a cost of significantly higher fuel consumption in this area of operation. This high level of BMEP at low engine speed in itself suggests that exhaust enthalpy reduction with water-cooled manifolds is not a significant issue for engines configured with such cooled manifold arrangements, be they external or IEM. However, for the added complication of an external water-cooled exhaust manifold and a cooled EGR circuit, the engine of Kapus *et al.* (2007b) did not then give any better fuel consumption than Sabre through the range of 2000-3000 rpm, and was only slightly better at higher speeds (against which it must be acknowledged that it was limited to a 30°C lower TIT).

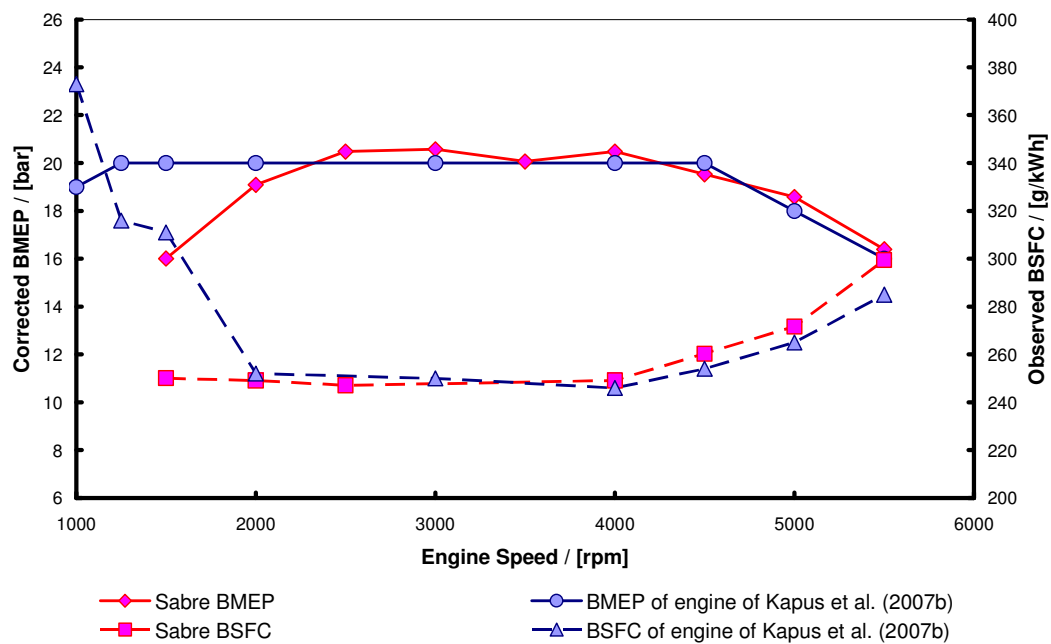


Fig. 7.17: Comparison of Sabre Phase 1 BMEP and BSFC curves with those of engine of Kapus *et al.* (2007b) employing a combination of cooled EGR and separate water-cooled exhaust manifold

A conclusion from this comparison is that at broadly-comparable BMEP a combination of technologies added to a conventionally-configured engine can improve fuel consumption to the level of Sabre, but at a penalty of significant complexity and on-cost. Conversely the Sabre engine project showed that an engine configured with a combination of complementary technologies and non-overlapping exhaust pulses could provide better high-load fuel consumption than any competing technology to date, especially when considered in isolation.

7.7 SUMMARY AND CONCLUDING REMARKS

The Sabre engine adopted a novel and synergistic combination of features and technologies to achieve a cost-effective, affordable engine with low CO₂ emissions. These include:

1. The use of a 3-cylinder configuration and 240° CA exhaust cam period to eliminate pulse interaction in the exhaust causing an increase in the trapped residual rate in sequential cylinders in the firing order;
2. Second-generation close-spaced direct injection utilizing multi-stream solenoid injectors to provide maximum homogeneity for best charge cooling and combustion;
3. An exhaust manifold integrated into the cylinder head (IEM) to accelerate catalyst light-off and reduce turbine inlet temperature at high load;
4. A relatively large swept volume to permit the use of a single-stage, fixed geometry turbocharger for best system dynamics;
5. Variable valve actuation based on switching tappets and twin camshaft phasing devices, which permitted dethrottling of the engine and in turn facilitated the use of a relatively large swept volume for a downsizing concept engine;

6. Mild electrical hybridization in order to compensate for transient turbo lag and exhaust enthalpy reduction due to the IEM when the engine is installed in a vehicle.

When operated on commercial 95 RON gasoline, the engine produced 245 Nm and 117 kW (157 bhp) (20.1 and 18.6 bar BMEP, respectively) which is similar in power and superior in torque to 2.2 litre NA engines. $\lambda = 1$ operation throughout almost the entire engine operating map was possible, except that moderate enrichment was necessary above 5000 rpm (to maintain a turbine inlet temperature limit of 980°C). Part-load fuel economy benefits of up to 6% were realized with the switchable valve train through the adoption of Swirl-DI, which simultaneously provided a degree of EIVC (Miller cycle-like) operation and manipulation of the air motion to enhance fuel-air mixing and turbulence, and so improved combustion.

The well-documented synergy between DI, turbocharging and camshaft phasing was successfully combined with the packaging, firing interval and friction benefits of a 3-cylinder configuration. The adoption of a switchable valve train, an IEM and a mild hybrid system complemented the engine design concept in a manner that enabled low fuel consumption to be achieved from mild downsizing with a relatively large swept volume. This latter feature meant that the engine was not overly reliant on the charging system dynamics to achieve good transient response.

In Phase 1 of the Sabre engine programme, the choice of engine technologies was consistent with an “affordable technology” concept. The key components were all well-understood and current-production technologies that were available at reasonable cost, and the resulting homogeneous combustion system enabled the use of conventional and robust three-way catalysis, offering a further vehicle packaging and cost benefit.

Engine testing during the programme produced results that validated both the engine design decision process and concept. In this chapter, detailed comparison with competing technologies has shown that Sabre offered class-leading levels of full-load fuel consumption, with only combinations of 'add-on' technologies able to better it in conventional engine configurations, and then only slightly. Even then, the level of improvement is not considered compelling. This realization, coupled with the significant improvement in full-load fuel economy claimed by some researchers through the application of some of the other technologies, then gave rise to a programme of research applying some of these technologies to the Sabre engine. The results of this programme are discussed in the next chapter.

Chapter 8: Experiments with Concepts to Further Improve the Full-Load Fuel Consumption of the Sabre Downsized Demonstrator Engine

This chapter describes results taken from the ‘Sabre’ downsized demonstrator engine described in Chapter 7 utilizing some technologies to further improve its full-load fuel consumption. These technologies include changing the match of the turbocharger, increasing the turbine inlet temperature, and applying cooled EGR, the latter of which was identified in Chapters 3 and 7 as a technology which has been shown to yield significant economy benefits on some turbocharged engines. When applied to Sabre, however, it will be shown that the latter approach does not produce improvements of the magnitude which other researchers have reported, and the reason for this will be discussed in some detail. Finally a new concept for evaporative cooling of EGR is developed and shown through calculation to be especially viable in alcohol-fuelled engines. A brief description of the modifications investigated and the expected results is shown in Table 8.1.

Table 8.1: Modifications investigated in study of methods to improve the full-load fuel consumption of the Sabre downsized demonstrator engine

Modification	Expected outcome
Rematched turbo-charger turbine (Section 8.1)	Improved high-speed fuel consumption and increased power output through improved high-speed air supply and reduced pumping work
Increased turbine inlet temperature (Section 8.2)	Improved full-load fuel consumption through reduced component-protection enrichment cooling
Cooled EGR (Section 8.3)	Improved full-load fuel consumption through reduced component-protection enrichment cooling

8.1 EXPERIMENTS ON THE EFFECT OF TURBOCHARGER MATCHING

As a consequence of the known sub-optimal match of the turbocharger to the Phase 1 engine which was described in Section 7.4, the decision was made to

investigate a better-matched turbocharger, within the limits of not receiving any direct support from a Tier-1 turbocharger supplier. Consequently a hybrid turbocharger was assembled by an aftermarket supplier, from components already understood by them. This new turbocharger was expected to have a significantly better turbine match although the ideal compressor characteristics were not available in a frame size to fully complement the turbine. This compressor was also different to that used in the 'normal' Phase 1 turbocharger. Nevertheless, from the initial test work described in Section 7.4, the turbine was considered to be the dominant part of the turbomachinery with regard to the standard of the overall match to the rest of the engine, because of the very high pre-turbine pressures seen with the very first turbocharger supplied for test. Hence it was decided to utilize this hybrid turbocharger to investigate potential improvements in this area with regard to fuel economy. This research was conducted with the conventional Sabre combustion system, i.e. without employing cooled EGR.

The results of the revised match (called the 'Phase 2' turbocharger specification) are shown in Figure 8.1. The correction factor for these results was 88/195/EEC, as used for all of the data presented in this chapter. Immediately apparent in Figure 8.1 is the further-improved fuel consumption at the same power condition of the Phase 1 specification. This was an operating condition of 5000 rpm, 18.4 bar BMEP, which represents 76.7 kW/l (103 bhp/l). At this point the BSFC was now <244 g/kWh. Additionally, $\lambda = 1$ fuelling was maintained up to this operating point. Gradual enrichment was necessary beyond this speed in order to limit the turbine inlet temperature to 980°C, the same limit as applied to the Phase 1 specification. This resulted in a richening of the fuelling rate to $\lambda = 0.95$ at 5500 rpm and 0.85 at 6000 rpm. Maximum power of 135.1 kW (181.2 bhp) was produced at 6000 rpm. During this work ignition timing was set to MBT or knock-limited spark advance (KLSA), whichever occurred first.

With the Phase 2 turbocharger fuel economy was better across the full speed range, although the engine was not producing as much BMEP below 2000 rpm.

Generally, between 2000 rpm and 4000 rpm the engine produced the same BMEP as it had done with the with the Phase 1 turbocharger. There was a dip in the BMEP curve at 4500 rpm but the engine produced significantly more load above 5000 rpm.

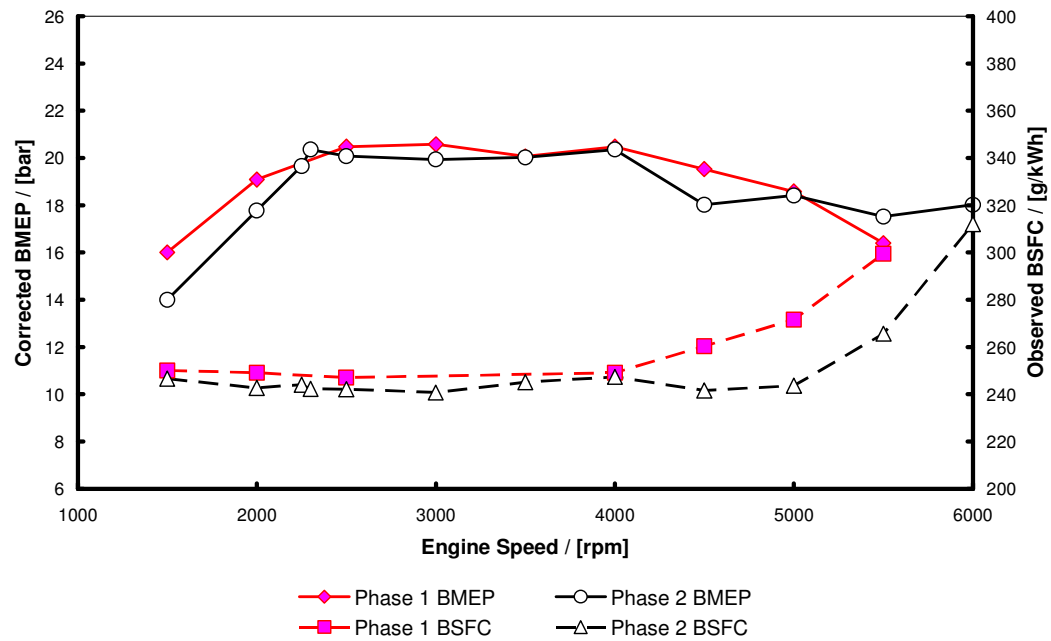


Fig. 8.1: Performance of Sabre engine 001 with different turbocharger matches – Phase 1 and Phase 2

The reduction in low-speed torque was considered acceptable because one of the intentions of the Phase 2 specification turbocharger was to increase the maximum power of the engine (i.e. providing the ability to increase the downsizing factor). In order to achieve this, the rotational speed of the engine was increase to 6000 rpm, a value similar to that adopted in the downsizing demonstrator engine of Lumsden *et al.* (2009). It was not the intention to increase BMEP since the value of 240 Nm was the torque limit of the gearbox fitted to the Opel Astra demonstrator vehicle. This higher-speed operating condition represents 90.1 kW/l (120.8 bhp/l), a similar degree of downsizing to the 1.4 litre VW ‘Twincharger’ compound-charged engine with which it now bore

some comparison since it produced approximately the same torque and power (Krebs *et al.*, 2005a and 2005b). The low-speed loss in BMEP which resulted from the adoption of the Phase 2 turbocharger was intended to be compensated for by the hybrid system in the vehicle in the manner discussed by Grebe *et al.* (2007), although it should again be noted that this turbocharger was still not one which had been fully optimized to the engine.

From the results of this investigation into turbocharger matching it was expected that employment of either a variable turbine geometry turbocharger or a compound charging system would be very beneficial in this engine, if a hybrid system was not to be employed for in-vehicle driveability reasons. This was because, from this research, fully matching a low-pressure stage to the engine would give further benefits in high-load BSFC.

8.2 EXPERIMENTS ON THE EFFECT OF INCREASING TURBINE INLET TEMPERATURE

One route to reduced high load fuel consumption in turbocharged engines is to increase the maximum turbine inlet temperature, as discussed by Watson and Janota (1986). There are two effects which arise from this: firstly it permits a direct improvement through the reduction of any component thermal protection fuelling necessary for the turbine (i.e. over-fuelling), and secondly the higher turbine inlet temperature (TIT) means that, for the same turbine isentropic efficiency and compressor characteristics, a smaller expansion ratio can potentially be used to generate the required turbocharger rotor power. This in turn reduces back pressure on the engine (pre-turbine pressure), and with it pumping work and trapped residual concentration, the latter crucial with regard to the knock limit. If the knock limit can be extended as a consequence of this, and the KLSA increased commensurately, then the TIT can be expected to further reduce, and a beneficial optimization 'spiral' is the result.

Over-fuelling for component thermal protection is essentially a form of diluent addition since the specific heat capacity of the extra fuel absorbs some of the

heat of combustion, and the lack of sufficient oxygen means that only its partial combustion is possible. There is also an effect on the cycle temperature due to the heat of vaporization of the extra fuel, which from Chapter 5 is known to be important, particularly in pressure-charged engines. The over-rich condition means that, in addition to the fuel consumption penalty, unburned hydrocarbon (UHC) and carbon monoxide (CO) emissions are typically very high, although oxides of nitrogen (NO_x) are correspondingly lower due to the lower combustion temperatures and oxygen-lean mixture. Note that a three-way catalyst will not function to convert UHC or CO at these rich conditions, although NO_x is reduced.

As a consequence of the high-load fuel consumption penalty which accompanies component thermal protection fuelling, it was decided to investigate the effect of increased TIT on the engine in Phase 1 specification, which would be achieved through the reduction in the fuelling rate provided. As discussed in Chapter 7, the Phase 1 turbocharger was normally operated with a TIT limit of 980°C, the same as it was controlled to on the Lotus V8 production engine from which it was taken (Turner, 1996). For this series of tests it was decided that this value should be raised to 1020°C as a maximum, this having been permitted during the original development test work for the Lotus V8 engine, and which had been stated by the turbocharger manufacturer as being a safe limit for short periods of operation (Turner, 1996).

The operating conditions of the engine were 5000 rpm, full load, i.e. the maximum power condition, where initial work on the Phase 1 specification engine had shown that this was where enrichment beyond $\lambda = 1$ was necessary for component thermal protection fuelling. The plenum pressure was held constant, which was achieved to within 0.5% of the starting boost pressure of 196 kPa (absolute). The plenum temperature was similarly held constant at 40°C by the water cooling system in the test cell. The spark advance was adjusted to KLSA for each of the test points. The cooled EGR tapping point utilized for the tests reported later in this chapter was present for these increased TIT tests, but it was blanked off by bolting a cover plate over the outlet.

A combustion analyzer from DSP was used to gather cylinder pressure data and so to compute coefficient of variation of indicated mean effective pressure (COV of IMEP), the crankshaft angle at which 50% mass fraction burned occurred (CA50) and the 10-90% mass fraction burned (MFB) time. These results were computed from data measured over 300 cycles using a water-cooled cylinder pressure transducer fitted to cylinder 1.

At the nominal maximum power operating point the TIT was increased by removing fuel. This was done from a starting point of 990°C up to 1020°C in nominal 10°C steps. Data logs were taken at each of the resulting four points. The results of this test are given in Figure 8.2, which shows a monotonic and essentially linear increase in λ towards stoichiometry as TIT is increased.

A curve fit to the data of Figure 8.2 suggests that $\lambda = 1$ would not in fact be achievable within the now-common current TIT limit of 1050°C for mass-production wastegated turbochargers (Brooke, 2011). Hence, if gasoline is the fuel, then to reach $\lambda = 1$, a degree of cooled EGR would have to be used as well.

Earlier it was stated that if the expansion ratio of the turbine could be reduced as a result of increased permitted TIT one might expect the KLSA to be increased. The spark advance for the test results shown in Figure 8.2 started at 16.5° BTDC for the first test point before having to be retarded very slightly to 16.1° BTDC for the subsequent points. It was thus essentially constant and this implies that any change in performance was not primarily an ignition timing issue from the first test point onwards.

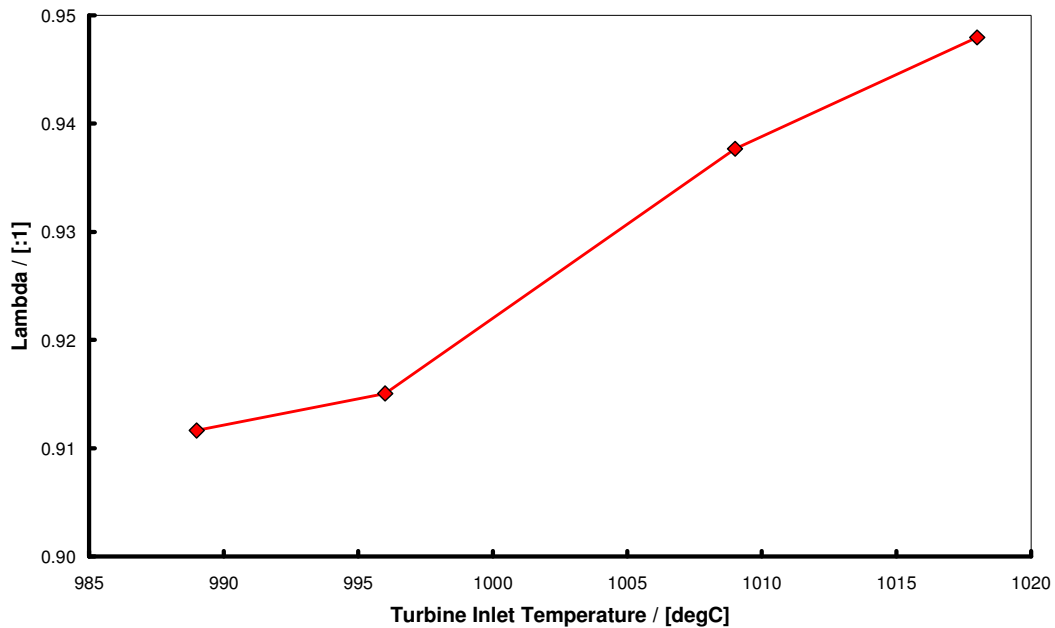


Fig. 8.2: Effect of increasing turbine inlet temperature on relative AFR (λ) at maximum rated power conditions of 5000 rpm and plenum pressure and temperature of 196 kPa (Abs.) and 40°C respectively

Generally in turbocharged SI engines, an increase in λ towards stoichiometry will yield an increase in power and simultaneously an improvement in brake specific fuel consumption (BSFC). This is certainly the case with engines which have already had to be significantly over-fuelled for component protection or for knock control. However, the BMEP and BSFC data corresponding to the results in Figure 8.2 show that while BSFC can in general be improved, the BMEP of the engine in fact degrades, even with reoptimization of the ignition timing. This effect is shown in Figures 8.3 and 8.4 respectively. Since the spark advance and air mass flow through the engine are essentially constant, the differences in measured results must be due to the manner in which the mixture burns.

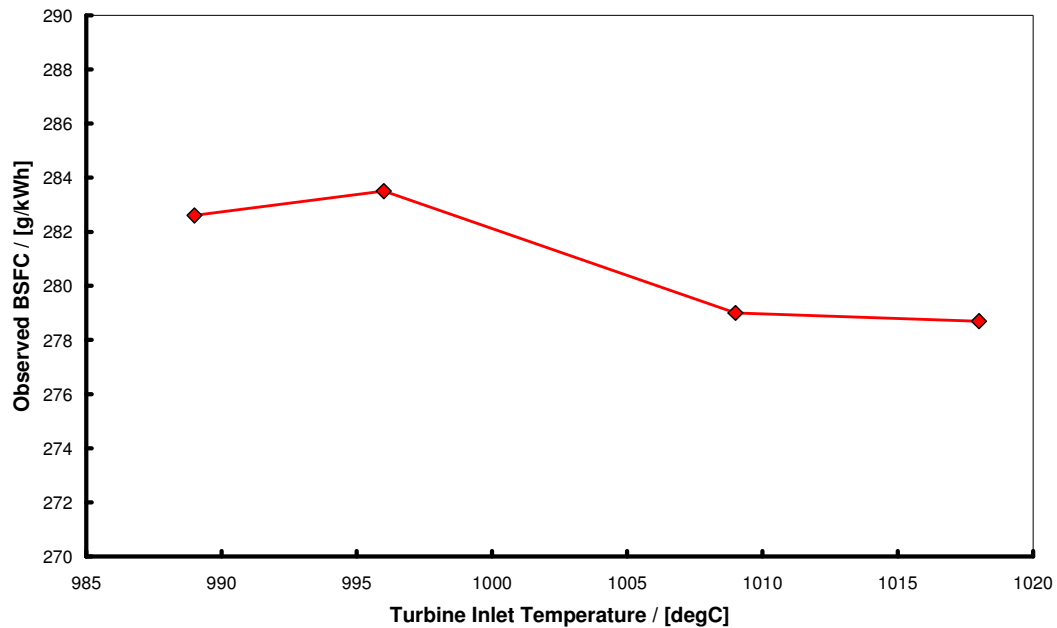


Fig. 8.3: Effect of increasing turbine inlet temperature on observed BSFC at maximum rated power of 5000 rpm and plenum pressure and temperature of 196 kPa (Abs.) and 40°C respectively

Apparent from Figures 8.3 and 8.4 is that an increase in TIT does not automatically produce a better performance from the Sabre engine (in terms of BSFC and BMEP). As noted above, the plenum pressure was held constant for this test, and Figure 8.4 clearly shows that boost pressure would have had to be increased to maintain BMEP. This suggests that, instead of improving, brake specific air consumption (BSAC) has deteriorated over the TIT range tested. This is shown in Figure 8.5.

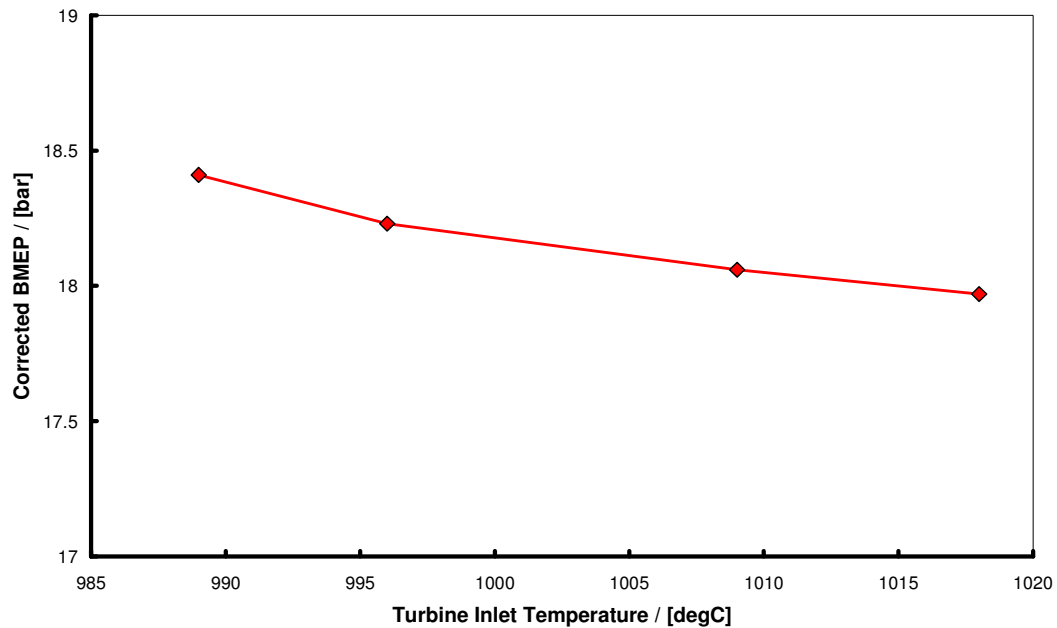


Fig. 8.4: Effect of increasing turbine inlet temperature on corrected BMEP at maximum rated power of 5000 rpm and plenum pressure and temperature of 196 kPa (Abs.) and 40°C respectively

It is clear in Figure 8.5 that the air utilization of the engine was deteriorating as the mixture was leaned off from the original fuelling condition used to generate maximum power in Phase 1 specification. From Figures 8.3 to 8.5 the Sabre engine appears to possess characteristics which permit it to behave at maximum power in a manner similar to that of an NA engine with relatively low exhaust back pressure, i.e. that when increasing TIT, the fuelling is in fact being leaned off from the maximum power condition. To underline this effect, the unburned hydrocarbon (UHC), oxides of nitrogen (NO_x) and carbon monoxide (CO) emissions performance of the engine during this TIT test is shown in Figures 8.6 and 8.7.

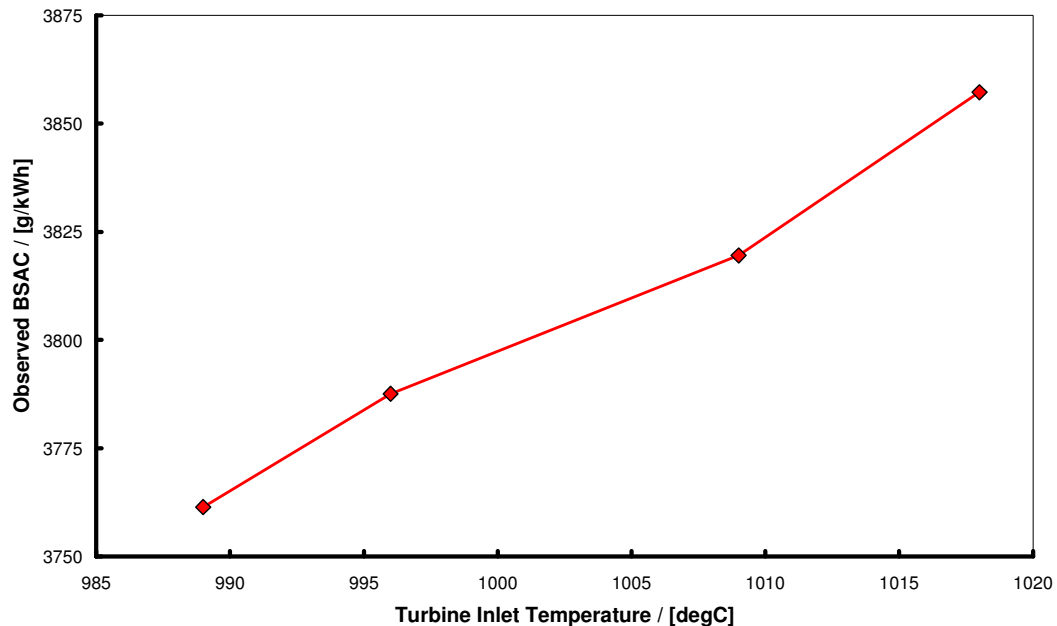


Fig. 8.5: Effect of increasing turbine inlet temperature on observed BSAC at maximum rated power of 5000 rpm and plenum pressure and temperature of 196 kPa (Abs.) and 40°C respectively

From the data, if one takes the 990°C and 1020°C nominal TIT points, the BMEP reduces by 2.4% while the BSFC has only reduced by 1.4%. Reducing the amount of enrichment fuelling appears to be the factor causing the reduction in BMEP. The effects of this are clear in both Figures 8.6 and 8.7. In Figure 8.6 NO_x is increasing while UHC is reducing as the fuelling for the engine is leaned off. Figure 8.7 shows that CO is reducing at the same time, whereas residual oxygen (O₂) is increasing slightly due to dissociation, i.e. there is insufficient fuel to ensure the consumption of all the O₂ (note that in Figure 8.7, the O₂ concentration has been multiplied by a factor of ten to scale on the axis more appropriately).

In general, at maximum power in NA engines, a CO level of 3.5-5% would be expected (Heywood, 1988), and in over-fuelled engines this would be considerably higher since there is incomplete combustion by design. At fuel-lean

conditions, CO reduces and thus one can see that the result of increasing the relative AFR is incomplete utilization of the supplied air. Thus in its combustion performance at the original Phase 1 condition of $\lambda = 0.95$ and 980°C TIT, the engine was performing as one would expect a power-enriched NA engine to behave, and (due to its lack of a requirement for significant component enrichment fuelling) significantly better than a conventional turbocharged one. As λ was increased, the engine was then being forced to operate in a condition which was 'under-enriched' for maximum power. This situation is believed to be a result of the synergistic combination of technologies adopted in the Sabre engine as discussed.

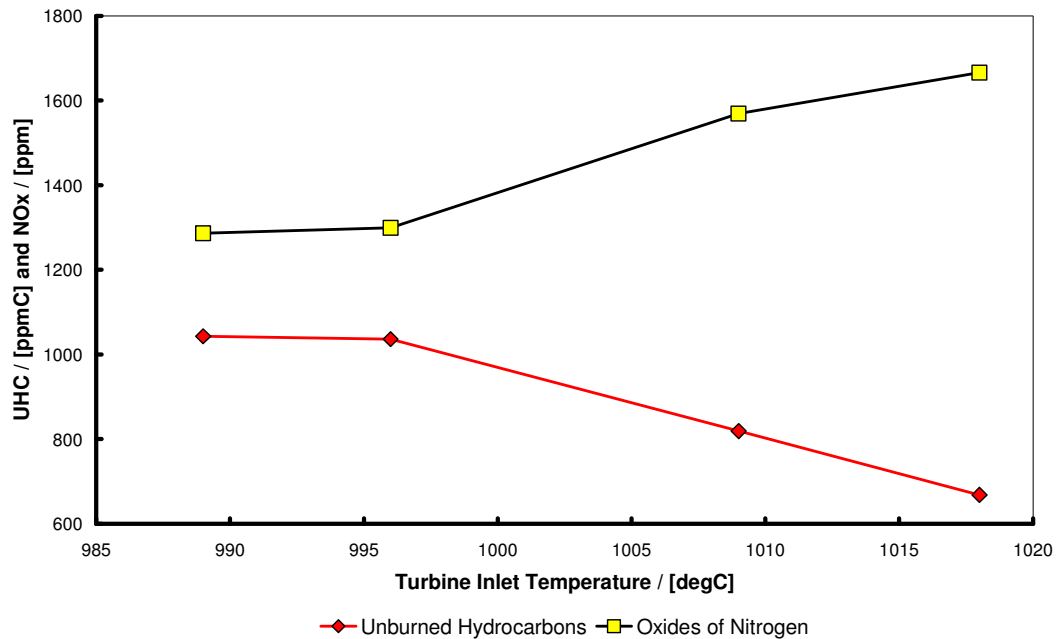


Fig. 8.6: Emissions performance of Sabre engine during TIT tests at 5000 rpm and ~18.2 bar BMEP – unburned hydrocarbons and oxides of nitrogen

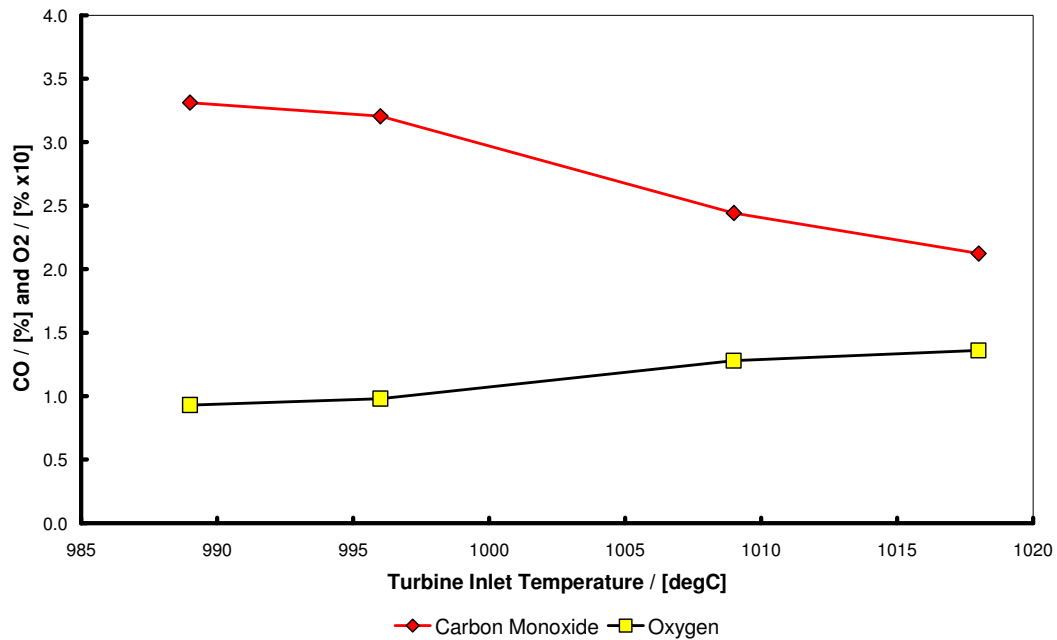


Fig. 8.7: Emissions performance of Sabre engine during TIT tests at 5000 rpm and ~18.2 bar BMEP – carbon monoxide and oxygen

Further evidence for the above observations is shown in the position of CA50, duration of 10-90% MFB, and COV of IMEP in Figure 8.8. The gradual lengthening of combustion indicated by the results for 10-90% MFB, and the effect on the COV of IMEP as fuel enrichment was removed, supports the above observations on emissions. Despite the fact that the spark advance was essentially constant, the timing of the combustion event was delayed (as shown by the retarding CA50) and this had the effect of reducing BMEP through less-favourable combustion phasing. The combustion period was increasing as a result of the reducing flame speed as the mixture was leaned away from the typically-optimum $\lambda = 0.9$ condition for maximum flame speed for hydrocarbon fuels (Metgalchi and Keck, 1982 and Westbrook and Dryer, 1980). As a consequence of these factors, the COV of IMEP increased from 4.5% up to 6.7%. A deleterious effect of both increased combustion duration and retarded CA50 is that these changes will tend to increase the temperature at exhaust valve

opening in opposition to the effect of the increasing λ . The net effect is the observed increase in TIT.

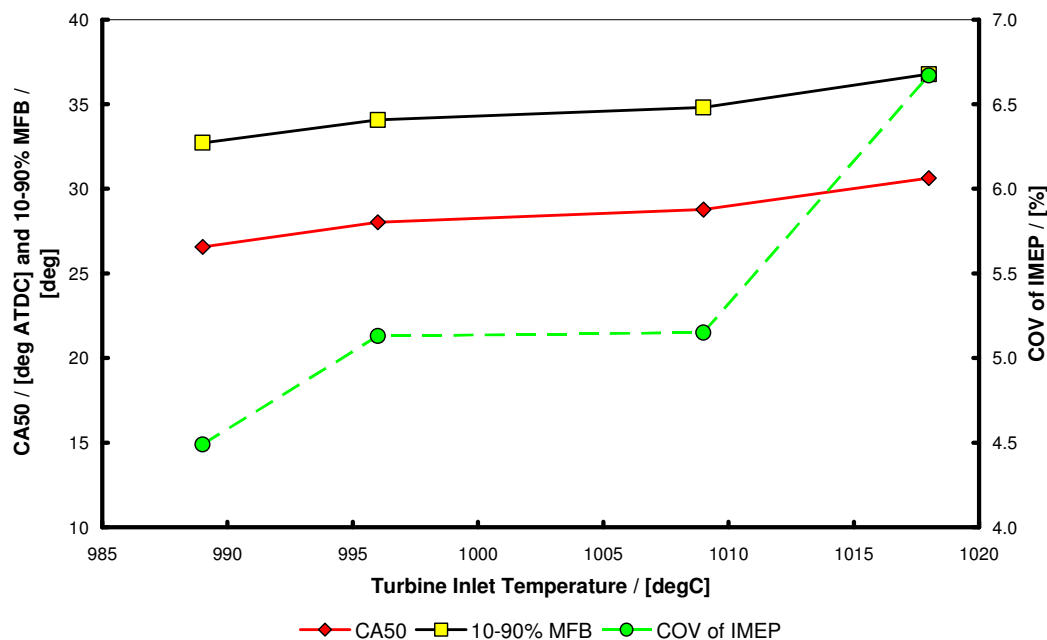


Fig. 8.8: Effect of increasing turbine inlet temperature on position of 50% MFB (CA50), 10-90% MFB and COV of IMEP

The tests suggest that the turboexpansion concept described in Chapter 4 would permit lower temperatures at exhaust valve opening due to a combination of reduced cycle temperature and the fact that, if the knock limit was successfully extended, there would be lower exhaust gas temperatures too. The fixed air density test data presented in Chapter 6 shows that, at fixed λ , the knock limit extends with reduced charge air temperature and thus improved charge cooling has an effect on the degree of enrichment fuelling necessary for component thermal protection. Finally, the tests utilizing alcohol fuel described in Chapter 5 clearly show that increasing the alcohol content can also reduce component thermal protection fuelling due to better combustion phasing through fuel octane effects, a general lowering of the cycle temperature because of the higher latent heat of vaporization, and a lowering of the adiabatic flame temperature. All of

these can be used to overcome shortcomings in the design of a pressure-charged multi-cylinder engine, but equally this section shows that an optimized combination of physical characteristics can achieve the same result at the BMEP levels typical of current production downsized engines.

8.3 EXPERIMENTS WITH COOLED EGR

A series of tests was conducted with one of the more important technologies being investigated to improve the high-load combustion of downsized engines, namely the adoption of a proportion of cooled EGR in the charge air. This section will describe these tests.

8.3.1 Modifications to the Sabre engine for cooled EGR testing

The test engine was fitted to a dynamometer and instrumented as necessary, including a tapping from the intake plenum to the exhaust analyzer so that the percentage of EGR present in the plenum could be obtained from the concentration of CO₂ in the intake air through the relationship:

$$\text{EGR} = 100 \left(\frac{V_{\text{CO}_2\text{Intake}}}{V_{\text{CO}_2\text{Exhaust}}} \right) \quad \text{Eqn 8.1}$$

where $V_{\text{CO}_2\text{Intake}}$ is the volume fraction of CO₂ in the intake air and $V_{\text{CO}_2\text{Exhaust}}$ is the volume fraction of CO₂ in the exhaust gas.

The turbocharger stub pipe, described in Chapter 7, which connected the IEM to the turbocharger and which was necessary because of vehicle installation issues, was modified to provide a take-off for exhaust gas to feed the cooled EGR system. The arrangement is shown in Figure 8.9. The turbocharger itself was again the original Phase 1 item and, as already discussed, was a non-optimized match to the engine with conventional, non-cooled-EGR, combustion.

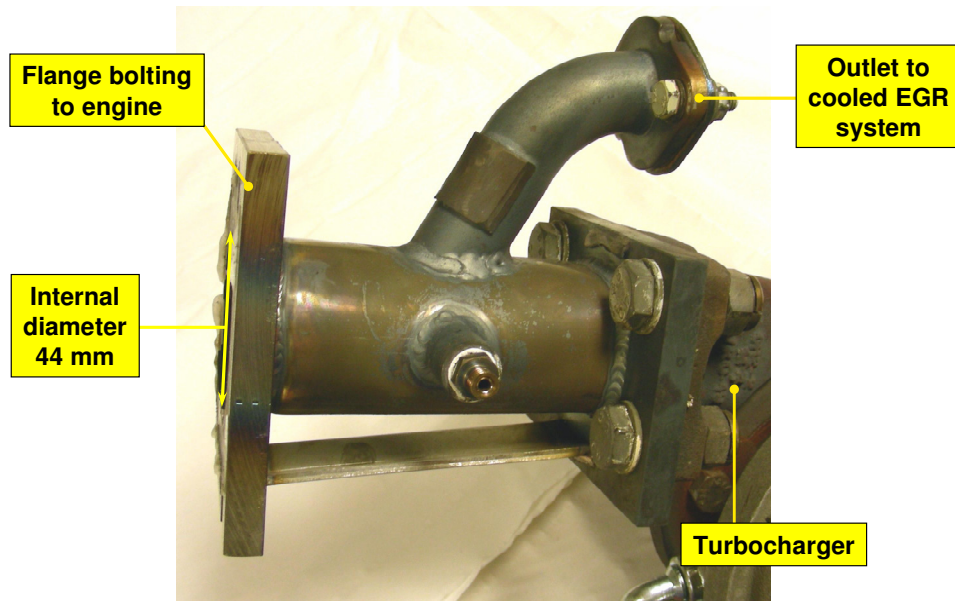


Fig. 8.9: Photograph of position of exhaust gas take-off on turbocharger stub pipe. (Photograph courtesy Lotus Engineering)

The heat exchanger used was a production diesel item and was part of an assembly provided by Continental Automotive Systems. It incorporated a flow control valve on the outlet from the cooler together with a gas bypass valve which allowed the investigation of hot EGR effects at part load. This is not discussed in this thesis (for further information and results, see Turner *et al.*, 2008b). During full-load testing the cooling element was fed with tap water in order to maximize heat removal. The necessary control for the flow rate control valve was provided by a supplementary control unit since this functionality was not provided as standard by the Continental engine management system used in the Sabre engine.

8.3.2 Effect of cooled EGR system dead volume

Before any cooled EGR was utilized on the engine, it was considered important to gauge the effect of the EGR cooler volume on performance, primarily because of the observations of other researchers concerning the effects of this (Cairns *et*

al., 2008). For this test, the cooler was set to zero flow, but all of the volume communicated with the link pipe via the stub pipe shown in Figure 8.9.

The effects of the EGR system dead volume are shown in Figure 8.10. A reduction in low-speed BMEP is evident which is in accord with the results presented by Cairns *et al.* (2008). These workers also investigated the change in performance of their 4-cylinder engine due to the fact that a pulse-divided exhaust manifold (up to, but not including, the turbine scroll) was utilized as standard, which had to be modified to provide an EGR take-off plenum such that a significant length of the pulse division was lost. They found that the removal of some pulse division had minimal impact, but inclusion of the dead volume in the circuit had a far more pronounced effect, similar to that seen in Figure 8.10. For reasons discussed in Chapter 7, the 3-cylinder configuration of Sabre removes concerns regarding pulse-division of the exhaust manifold.

Cairns *et al.* (2008) do not present a full-load BSFC curve for their engine, but for Sabre it is interesting to note that the reduction in low-speed torque is also accompanied by a reduction in BSFC which is largely in line with the change in performance. Again apparent in Figure 8.10 is the good high-load fuel consumption performance already discussed: rated power is still at 5000 rpm, at which a figure of 272 g/kWh is achieved. This suggests that further significant improvements in fuel economy are unlikely to be easily attained, as has been shown for the case of increased turbine inlet temperature earlier in this chapter.

As mentioned in the section on the increased TIT tests, the Sabre engine was found not to require significant enrichment cooling below the maximum power speed. For the same reason it was decided to restrict cooled EGR testing to this engine speed. Figure 8.10 shows there to be no significant effect on BMEP or BSFC at this engine speed due to the presence of the EGR system take off, and so any results at this condition are comparable to both the standard Phase 1 specification and the increased TIT tests already discussed.

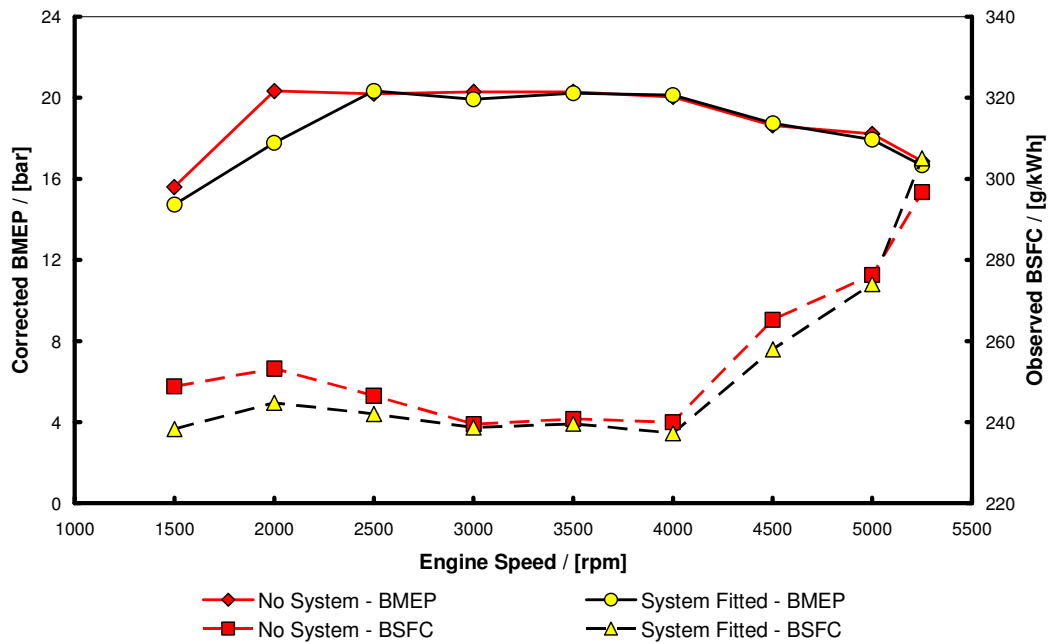


Fig. 8.10: Effect of EGR system dead volume on Sabre engine full-load performance

8.3.3 Configuration of cooled EGR system tested

There are several different configurations which can be used to introduce external cooled EGR into the combustion system of an engine at maximum power (Turner *et al.*, 2009). The three different configurations most commonly used are shown in Figure 8.11. Clearly all require a higher pressure on the exhaust side than at the intake in order to drive the EGR through the cooler and into the intake system, and thus some are more suitable for engines requiring cooled EGR before boost cross-over than others, e.g. the high-to-low- and low-pressure loops. It should also be noted that some of them are more suited to part-load operation than others: of the configurations shown, only the high-pressure loop permits the use of hot external EGR at part load and only if a switchable cooler, such as is used here, is employed.

In the work reported in this chapter, only the high-pressure route as depicted in Figure 8.11(a) was used. A broader comparison of the effects of the different configurations is given in Appendix V.

8.3.4 Means of introduction of cooled EGR into the intake air flow

Clearly, the means of feeding EGR into the intake system must ensure very good mixing. It is necessary to ensure complete mixedness in order for the CO_2 concentration in the plenum to be accurately determined, and thus Equation 8.1 to be used to ascertain the EGR rate. This could easily be arranged for the high-to-low- and low-pressure routes, where the EGR flow is introduced before the compressor and therefore could be assumed to be well mixed before it entered the plenum. This form of dynamic mixing of the EGR is not possible for the high-pressure route, however, because it was fed into the charge air after the compressor.

For the high-pressure loop tested here, this condition was achieved by positioning a radial aperture tube (RAT) mixing device after the intake throttle valve and feeding the EGR gas through it. The configuration of this device is shown in Figure 8.12. The RAT device was bulged in the middle in an attempt to keep the flow area of the intake system as constant as possible, thus reducing its effect on flow losses. It had a central feed pipe which had many radial holes drilled in it and which was blanked off at the end facing the air flow. The EGR thus flowed out into the intake air flow through jets orientated in many directions, and mixed with it prior to flowing around the right-angled bend at the entry to the plenum before subsequently being decelerated. This and previous breather system work during the Sabre project, which had already shown distribution of breather gases to be very good in the intake system, provided the necessary confidence to use single-point measurement of the intake system CO_2 concentration.

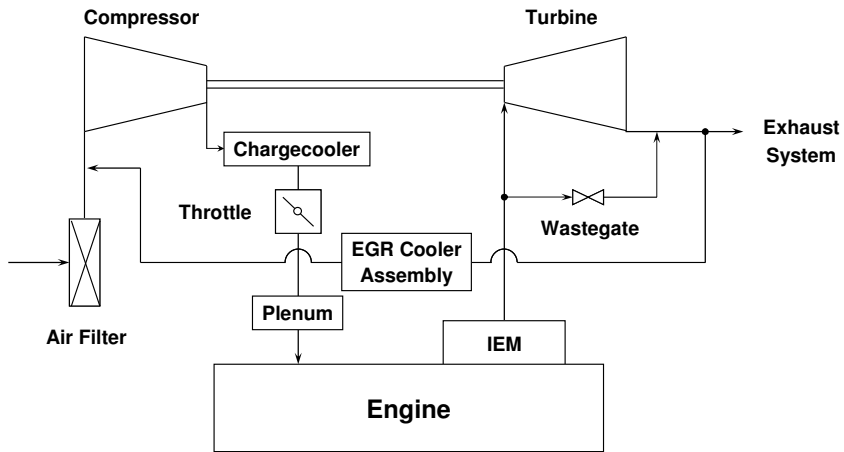
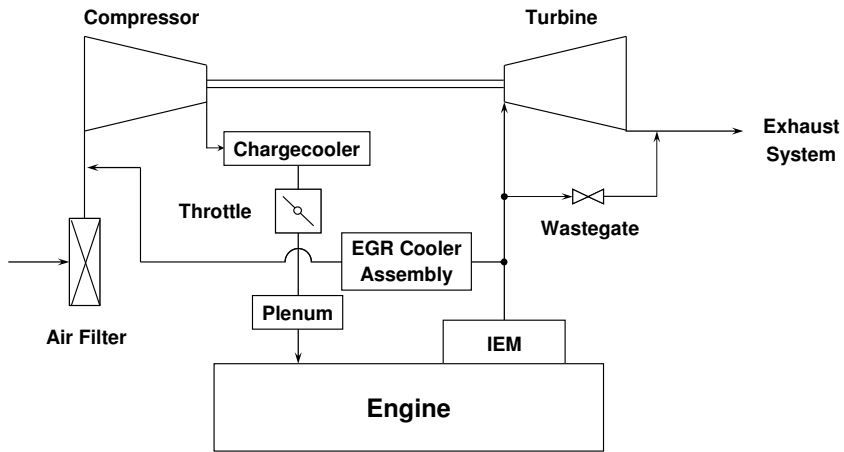
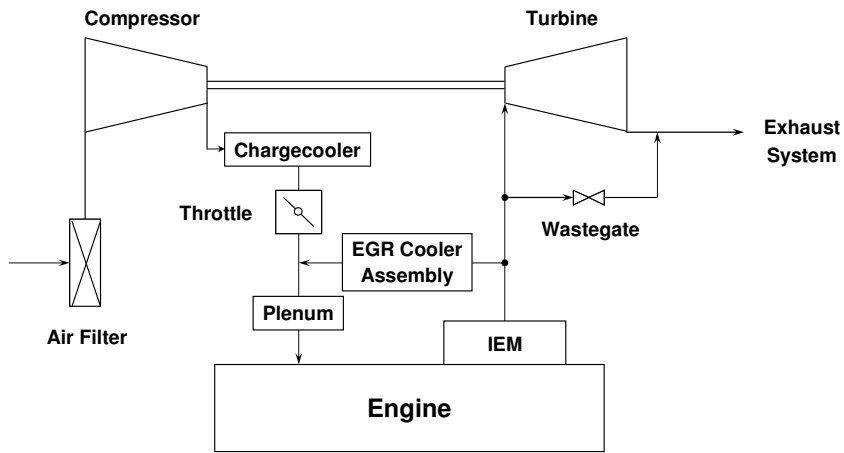


Fig. 8.11: Definition of EGR route configurations. Top: (a) short route / high-pressure loop; middle: (b) intermediate route / high-to-low-pressure loop; bottom: (c) long route / low-pressure loop

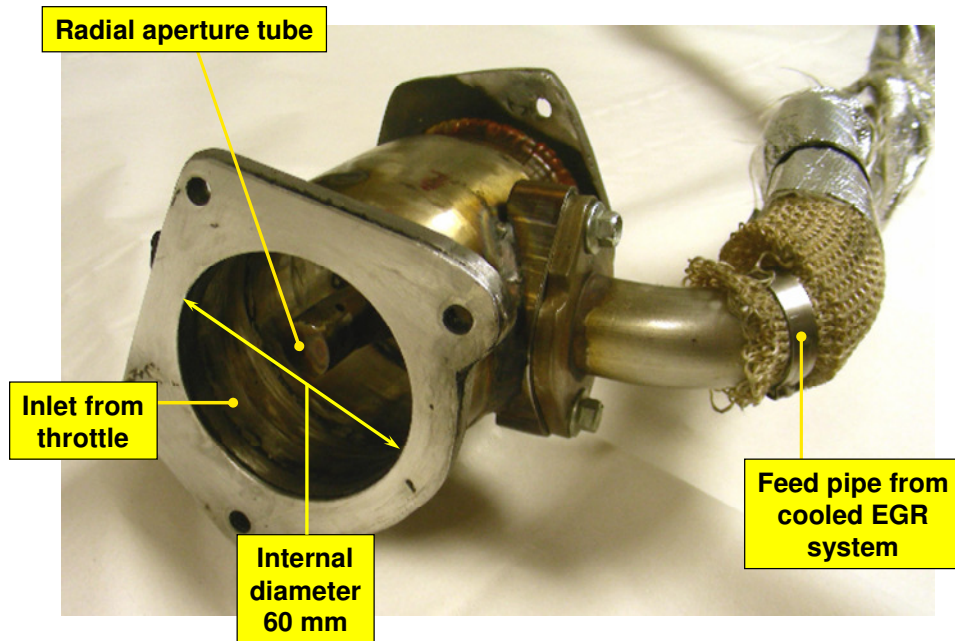


Fig. 8.12: Photograph of post-throttle mixing device with radial aperture tube (RAT) to introduce and mix EGR in the case of high-pressure loop EGR system. Flow direction is inwards at the face to the front of this photograph. (Photograph courtesy Lotus Engineering)

8.3.5 Effect of cooled EGR on SI engine combustion systems

As discussed in Chapter 3, the mechanism by which over-fuelling of the charge beyond that strictly necessary for maximum power affects the end-gas temperature and pressure histories has been understood for some time: enriched hydrocarbon vapour has a higher specific heat capacity than air, and this in turn ensures a lower increase in temperature and pressure in the end gas during the combined compression process due to piston motion and burned mixture expansion (Peletier, 1938). This reasoning can be extended to explain why cooled EGR is preferable to excess air operation as a knock-suppressant, because burned gases have a higher specific heat capacity (but lower ratio of specific heats) than air. Cooled EGR itself has also been known for many years to be a mechanism for knock mitigation (Ricardo, 1919 and 1920 and Institution of Automobile Engineers, 1924) and hence can be used to displace excess fuel

at high load in SI engines as a means of reducing the temperatures of components in the exhaust path. This is due to more-optimal combustion phasing leading to greater expansion in-cylinder and a consequent improvement in high-load fuel consumption (Cairns *et al.*, 2006 and 2008 and Hattrell *et al.*, 2006). Cooled EGR can be considered to be particularly beneficial when an SI engine is operated on gasoline which, in comparison to other SI engine fuels such as the low-carbon-number alcohols, can be considered to be a low-octane fuel, at least in its typical 'pump' form (Owen and Coley, 1995).

While there is a trade-off between the flame speed being reduced due to the presence of EGR and a consequent lengthening of the induction time in the end-gas, measurements reported in Cairns *et al.* (2006) and Alger *et al.* (2008), among others, suggested that high-load BSFC in turbocharged DISI engines operated with 10-20% cooled EGR could be reduced by on the order of 15-25%.

In Cairns *et al.* (2006), an intermediate route similar to that shown in Figure 8.11(b) was employed whereas in Alger *et al.* (2008) a high-pressure loop similar to Figure 8.11(a) was used. While Cairns and co-workers have also investigated different routes (Cairns *et al.*, 2008), apart from their cylinder count these engines differed from Sabre in one important respect: they employed a separate exhaust manifold configuration, i.e. a 'conventional' one external to the cylinder head. As discussed above, the IEM concept employed on the Sabre engine combines the exhaust manifold with the aluminium cylinder head casting and cools it directly using engine coolant. At high load this has the significant advantage that exhaust gas heat is removed between the combustion chamber and the turbine inlet, meaning that the combustion does not in itself have to be configured to provide a low TIT, i.e. that the engine can be operated at a more-optimal value of λ .

The implications of this with regard to full-load BSFC in conventional operation were discussed earlier in this chapter and in Chapter 7, and could have important ramifications for a vehicle cooling system: both Cairns *et al.* (2006) and Alger *et al.* (2008) pointed out that there is a significant increase in heat load on the vehicle cooling system when a large amount of hot EGR gas has to be cooled: for

an engine of 100-125 kW, in the region of 35-50 kW of heat energy has to be removed from the cooled EGR supplied to the intake system (Alger *et al.*, 2008). It is immediately apparent that if the IEM permits a halving of the amount of EGR required, then the EGR loop heat load to be absorbed by the vehicle system will reduce proportionally to offset the effect of the IEM. While the IEM itself clearly places an increased thermal load on the vehicle cooling system, it does have the cost advantage that it is integrated within the conventional engine cooling circuit.

Heat rejection from the exhaust gases to the cooler during the cooled EGR tests was not measured because the intention of this work was primarily to assess the potential (if any) of a cooled EGR system when used in conjunction with an IEM from the viewpoint of further fuel consumption improvement.

8.3.6 Cooled EGR test results

The Sabre engine cooled EGR tests were conducted at a condition of 5000 rpm, full load, which is similar to that used for the TIT investigation, and for similar reasons; i.e. the Sabre engine was already operating at $\lambda = 1$ with excellent fuel consumption up to just below 5000 rpm and hence there was no need to consider the application of cooled EGR below this speed. Ignition timing and fuelling rate were set to balance KLSA against leanest fuel for best torque (LBT) for all conditions; i.e. fuel was removed and torque compensated for by ignition advance if the knock limit permitted this, and if there was no reduction in torque output at the test point. Once $\lambda = 1$ was achieved, the fuelling rate was no longer reduced.

For any engine with a high-pressure take-off such as is shown in Figures 8.11(a) and 8.11(b) testing with cooled EGR is complicated by the fact that in removing mass flow from before the turbine there is a concomitant loss in boost. There is also a complicating effect on the compressor performance due to its being required to operate at an increased pressure ratio to supply the same amount of charge air (note that as this changes, in the case of the high-pressure loop so the

driving pressure through the EGR system changes too). Furthermore the turbocharger fitted to the Sabre engine had not undergone a complete matching programme to the engine either. With this in mind, the data reported in Figures 8.13 and 8.14 was all gathered at a nominal 17.25 bar +/- 0.45 bar BMEP (107.8 kW +/- 2.8 kW), with the boost pressure being increased in an effort to keep the BMEP of the engine constant. From the spread in BMEP, it can be discerned that this was only partially successful because of the effect on the charging system of employing cooled EGR already discussed.

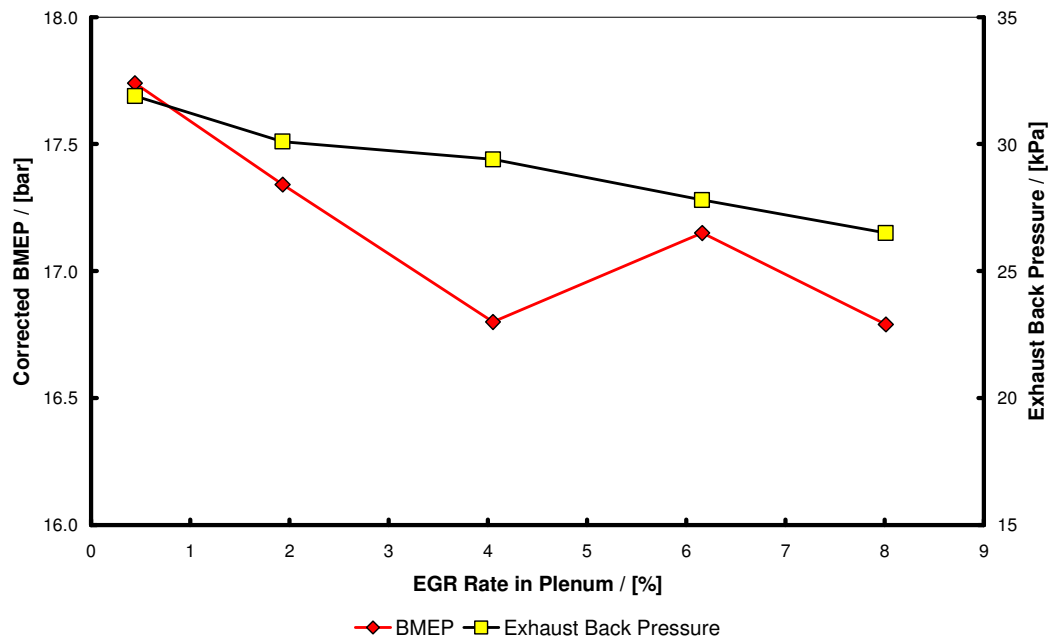


Fig. 8.13: Effect of EGR rate in plenum on BMEP and exhaust back pressure at 5000 rpm, full load

Figure 8.13 shows how BMEP and post-turbine exhaust back pressure (EBP) both reduce with increased EGR rate in the plenum. This happens because the amount of mass being recirculated is rising and the compressor cannot fully compensate for this effect despite the wastegate being closed more. Figure 8.14 shows that the BSFC and TIT both reduce as EGR rate is increased. The starting BSFC of 271.5 g/kWh is considered to be extremely good at this

condition of 110.9 kW (148.7 bhp), which is very near to 74.6 kW/l (100 bhp/l). λ at this condition was 0.95, and its variation with EGR rate is shown in Figure 8.15, together with the ignition timing used (at the KLSA condition).

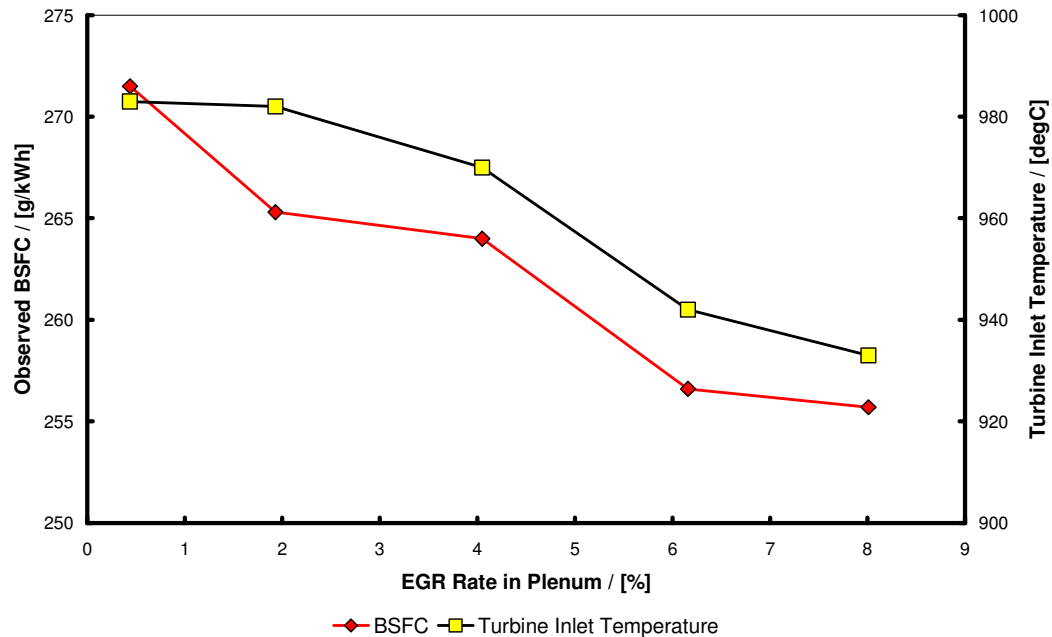


Fig. 8.14: Effect of EGR rate in plenum on BSFC and turbine inlet temperature at 5000 rpm, full load (starting at ~17.7 bar BMEP and reducing to ~16.8 bar BMEP as EGR is added)

As can be seen in Figure 8.15, $\lambda = 1$ was achieved at only 4% cooled EGR. This fact, and the effect of the adjustment in ignition timing that this permitted as shown in Figure 8.15, will be returned to in a later section.

Note that the value of λ reported throughout this thesis is that in the exhaust system, which is not the same as the in-cylinder value when DI is used and over-scavenging of the combustion chamber with air can be arranged. Figure 7.9 in Chapter 7 showed that this is likely to be the case in the Sabre engine, and so it has to be presumed that the value of λ in the cylinder is lower than unity. In terms of the discussion of the effect of removing fuel to increase λ , however, this

does not affect the results in this thesis, because the value of λ in the exhaust is the one important for exhaust gas after treatment in a three-way catalyst.

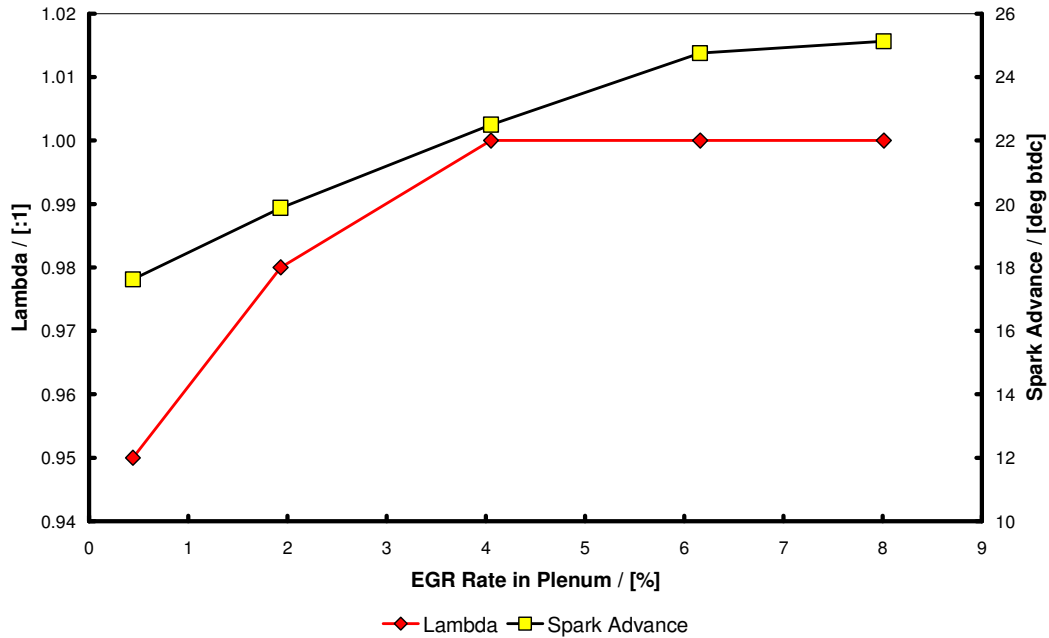


Fig. 8.15: Effect of EGR rate in plenum on λ and spark advance at 5000 rpm, full load (reducing from ~17.7 to ~16.8 bar BMEP as EGR is added)

The maximum amount of EGR gas that could be transferred by the cooler system in accordance with Equation 8.1 above was 8%. In Figure 8.16 it can be seen that as the amount of EGR recirculated was increased the pressure difference across the system started to diminish. Figure 8.13 showed that EBP reduced at the same time, as would be expected due to the increased level of recycle. This effect is believed to be at the root of why it was only possible to achieve a maximum flow rate of 8% cooled EGR, since the cooler was a production diesel item and its pipework was not optimized for the application. Figure 8.16 also shows that generally the pre-turbine pressure did not change significantly as the EGR rate was increased.

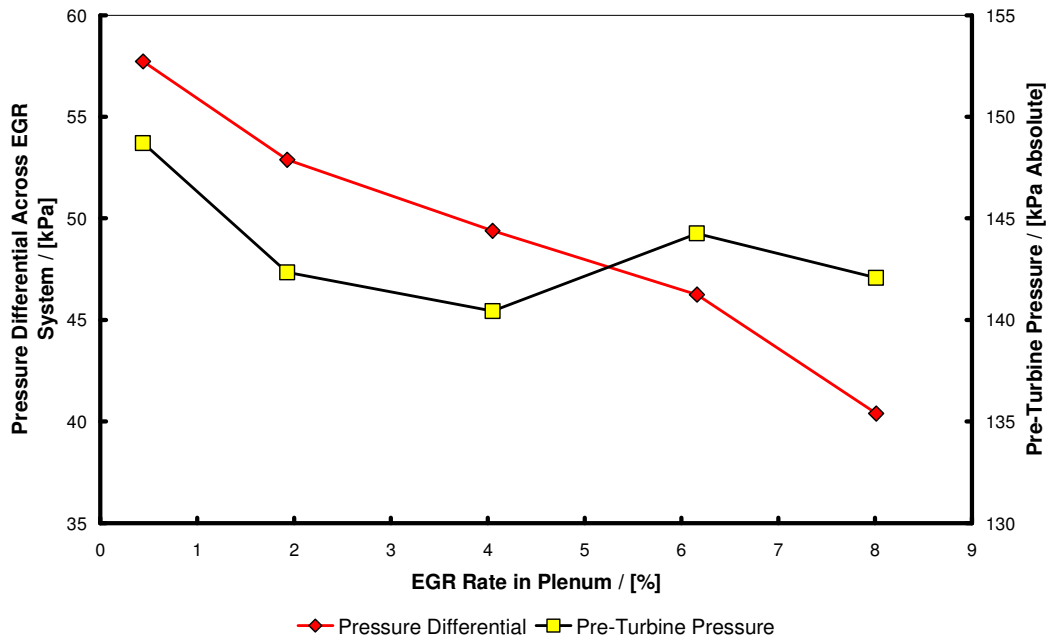


Fig. 8.16: Effect of EGR rate in plenum on the pressure differential across the EGR system and the pre-turbine pressure at 5000 rpm, full load (reducing from ~17.7 to ~16.8 bar BMEP as EGR is added)

The minimum BSFC seen in Figure 8.14 is 255.7 g/kWh. This is accompanied by a reduction in performance to 104.9 kW (140.7 bhp). At an EGR rate of 6% in the plenum the BSFC is 256.6 g/kWh, representing a reduction of 5.5% in fuel consumption for a 3.2% reduction in performance. At this operating point there is a brake thermal efficiency of nearly 33%. This result, in comparison to the increased TIT tests, will be returned to later.

Other researchers have demonstrated very significant improvements in rated power BSFC with the introduction of cooled EGR: 15-25% improvement in BSFC at 10-20% EGR rate in the area of maximum power has been reported (Cairns *et al.*, 2008 and Alger *et al.*, 2008). The data presented here does not follow these previously-reported trends in the literature. The reason for this is a subject which will be returned to in a later section.

The effect of cooled EGR on emissions is shown in Figures 8.17 and 8.18. From these it can be seen that as the EGR rate is increased, oxides of nitrogen reduce, as is to be expected. However, the UHC emissions remain broadly constant while CO reduces and O₂ increases. These effects are explained by the fact that as EGR was introduced, so λ was increased until stoichiometry was achieved. Thus oxygen utilization was not as high and combustion was more complete, meaning that HC and CO emissions did not increase despite the presence of EGR as a diluent. (Note that in Figure 8.18, as per the TIT tests, O₂ concentration is plotted at ten times the recorded result.)

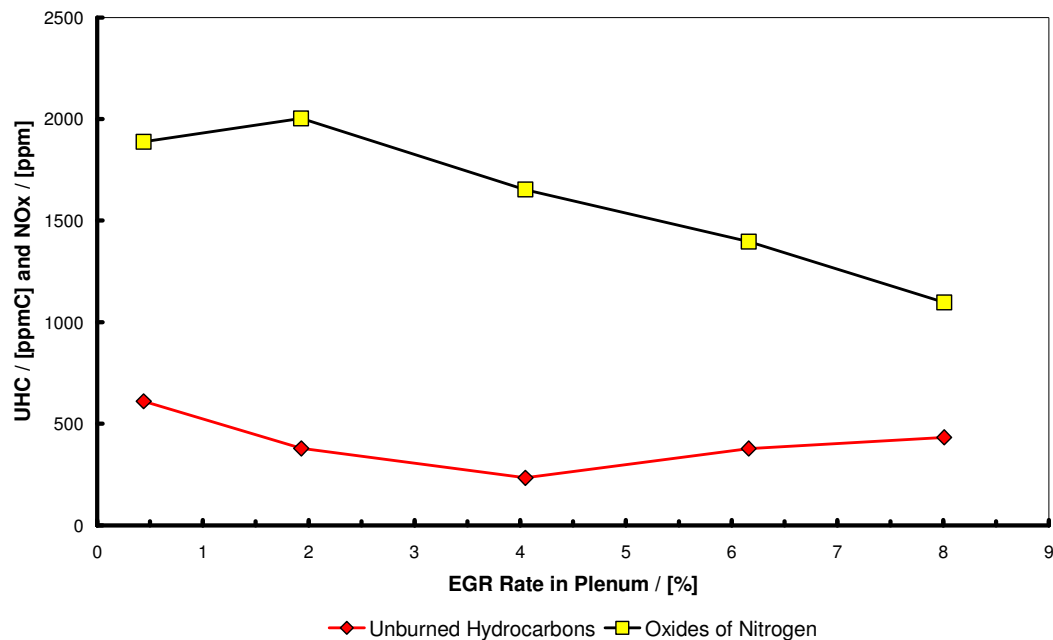


Fig. 8.17: Effect of EGR rate in plenum on unburned hydrocarbons and oxides of nitrogen at 5000 rpm, full load (reducing from ~17.7 to ~16.8 bar BMEP as EGR is added)

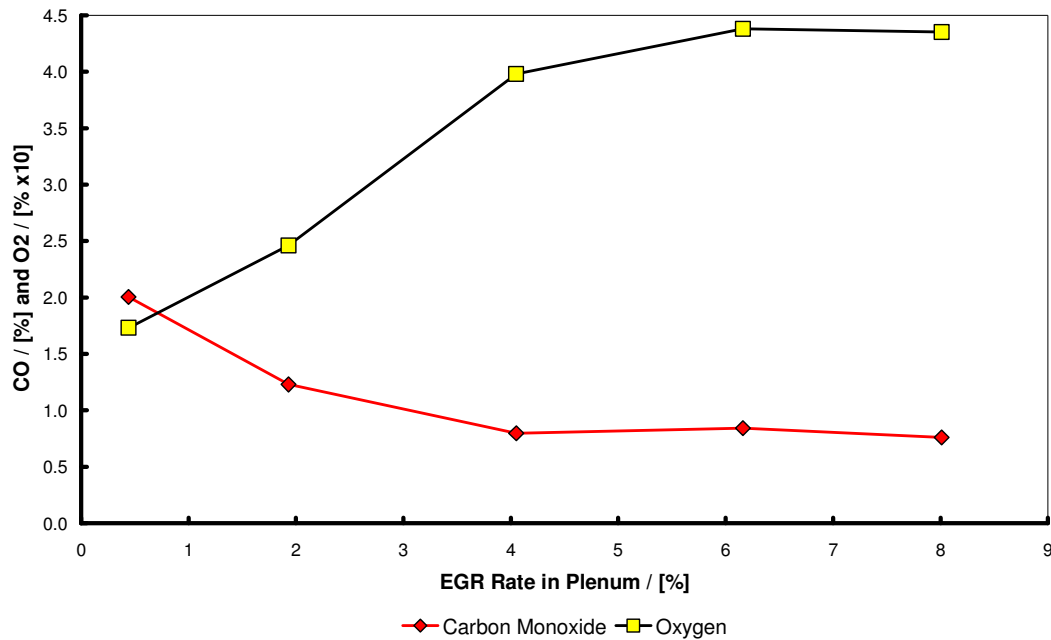


Fig. 8.18: Effect of EGR rate in plenum on carbon monoxide and oxygen at 5000 rpm, full load (reducing from ~17.7 to ~16.8 bar BMEP as EGR is added)

Figure 8.15 showed that it was possible to reach $\lambda = 1$ at 4% cooled EGR in the Sabre engine. However, for this engine, operating as it was with a mismatched Phase 1 turbocharger, the effect on combustion stability as this was done was a severe one, as shown in Figure 8.19. Combustion stability with no EGR was already borderline acceptable at just over 5% COV of IMEP; increasing the rate of cooled EGR to 4% and simultaneously removing fuel enrichment caused the COV of IMEP rapidly to deteriorate to ~9%. From the general flattening of the COV of IMEP during the increase in cooled EGR from 4 to 8%, one could surmise that the bulk of the degradation in combustion stability was due to the change in λ and not to the presence of increasing amounts of EGR. This will be returned to in a later section.

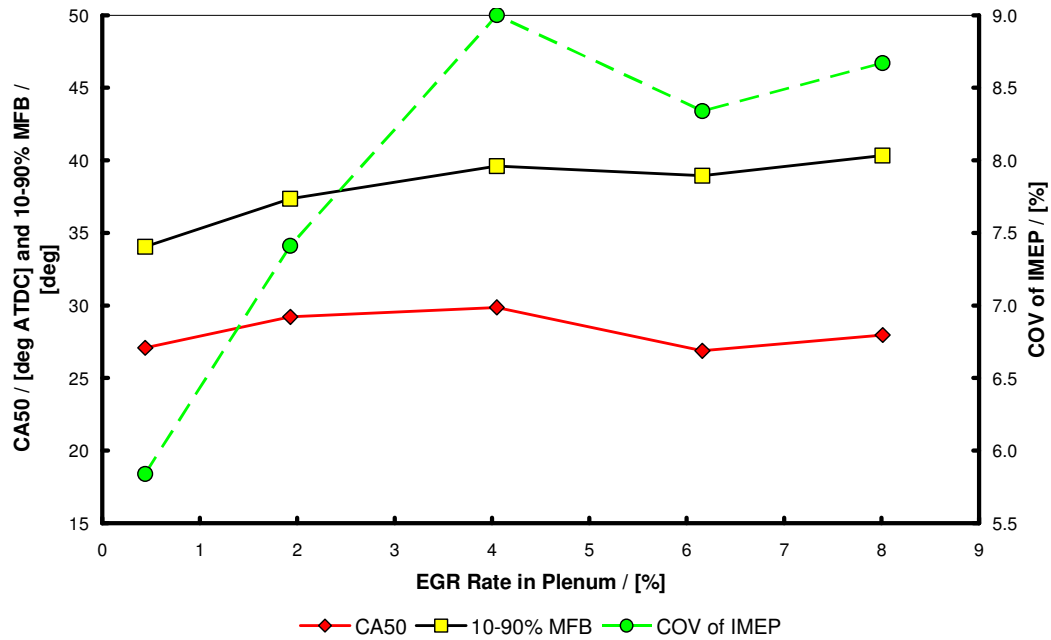


Fig. 8.19: Effect of EGR rate in plenum on position of 50% MFB (CA50), 10-90% MFB and COV of IMEP at 5000 rpm, full load (reducing from ~17.7 to ~16.8 bar BMEP as EGR is added)

The potentially complicating effect of the turbine inlet pressure on the mass of residuals trapped in the chamber is mitigated by the fact that this parameter did not change rapidly as the proportion of cooled EGR was increased (see Figure 8.16). It has also been shown in the previous chapter that, in general, due to the 3-cylinder configuration, the average pressure in the exhaust port during overlap was lower than that in the inlet port (for illustration, see Figure 7.9). From this, residual rate due to gas exchange was not believed to be a major contributor to combustion instability, and whatever was causing this at high load in the Sabre engine was compounded when cooled EGR was introduced. In fact, the fundamental no-cooled-EGR full-load combustion instability is primarily believed to be due to inadequate levels of charge motion, but that is not investigated further in this thesis. The extremely good combustion stability at part load, due to the use of valve-event governed Swirl-DI (Stansfield *et al.*, 2007, Turner *et al.*, 2008b), supports this contention, since in this case the air motion is primarily

governed by the intake valve events and not by the intake port geometry. The deterioration in COV of IMEP as cooled EGR was introduced is thus believed to be due to the increasing proportion of cooled residual in the charge, over and above the insufficient levels of charge motion during combustion specific to the Sabre engine design.

Figure 8.19 shows that the position of CA50 did not change greatly with the increase of EGR introduced into the combustion system. The spark advance, however, did increase significantly as EGR was introduced: the general rate of increase approached 1° CA per 1% EGR as shown in Figure 8.15. A consequence of this was that the combustion duration, represented by the 10-90% MFB interval, increased at a broadly monotonic rate with EGR, as shown in Figure 8.19.

These responses are well known in the literature. The smaller change in CA50 than 10-90% MFB shown in Figure 8.19 indicates a combustion event which is slowing as more EGR is introduced, which in ordinary combustion without cooled EGR would normally suggest a hotter exhaust gas temperature at the time of exhaust valve opening (EVO). The presence of EGR, however, leads to significantly cooler combustion (Hattrell *et al.*, 2006), which offsets the effect of the retarded combustion event and leads to both the reductions in TIT shown in Figure 8.14 and the reduction in NO_x shown in Figure 8.17.

From comparison with the increased TIT test results of Section 8.1, whether the extremely low level of fuel consumption achieved with cooled EGR is considered low enough in comparison to what might be achievable with a more-optimized charging system is a more difficult question. The inclusion of a cooled EGR system results in a significant BOM increase for a much smaller benefit in Sabre than can be shown in a conventional DISI engine architecture such as the 4-cylinder layout with separate, uncooled exhaust manifold. It also results in a further increase in heat rejection to the vehicle cooling system. From the results reported in this chapter, at this rating it may be that a two-stage charging system or the adoption of a VGT may be considered more cost-effective to the Sabre

engine before cooled EGR is, although as reported in Chapter 5, there is some opportunity to use the latent heat of the fuel to offset some of the cooling requirement for the EGR. This is returned to in Section 8.5.

8.4 COMPARISON OF RESULTS FOR INCREASED TURBINE INLET TEMPERATURE AND COOLED EGR

Having separately discussed the effects on combustion of increased TIT and introducing cooled EGR, this section will compare the two directly, in order to separate the effect of λ from the effect of diluent addition. A comparison in terms of λ is possible since both series of tests were conducted at similar plenum temperatures of 33-40°C. For this comparison, leaning the mixture to achieve higher TIT and increased λ is considered a means of diluent addition over the power-enriched state, since extra air is effectively being introduced into the combustion system.

Comparison between Figures 8.8 and 8.19 shows that during the increased TIT tests, CA50 was typically 33-37° CA, whereas with cooled EGR it was 34-41° CA. However, one interesting observation from comparison of Figures 8.8 and 8.19 is that, during the cooled EGR tests, CA50 levels off at 4% EGR rate. As noted above, this is point at which $\lambda = 1$ was achieved, and the fuelling was not leaned any further since this afforded the chance to provide excellent exhaust emissions under full-range operation using simple three-way catalysis. It follows that the primary reason for the deterioration of combustion quality might have been the operation at increased λ and *not* the presence of EGR in the combustion process *per se*. In order to illustrate the likelihood of this, Figures 8.20, 8.21, 8.22 and 8.23 show the spark advance employed, CA50, 10-90% MFB and COV of IMEP for both sets of tests plotted on the same abscissa in terms of λ , respectively.

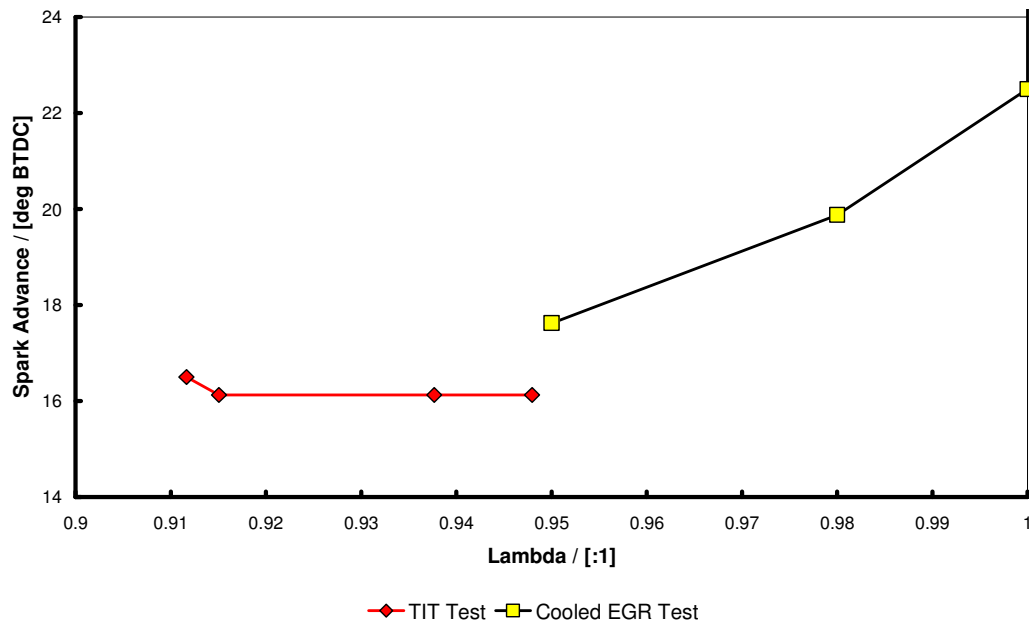


Fig. 8.20: Spark advance versus λ for turbine inlet temperature and cooled EGR sets of tests at 5000 rpm, full load (reducing from ~ 17.7 to ~ 16.8 bar BMEP as EGR is added), using the same plenum temperature ($33\text{-}40^\circ\text{C}$)

Although they were not conducted at exactly the same BMEP (as already discussed), the broadly-continuous nature of the combustion data results (with the noticeable changes occurring at $\lambda \approx 0.95$, which is the link point between the data sets at which cooled EGR is begun to be introduced) does suggest that the primary impact on combustion is probably caused by the change in AFR. This is particularly the case for spark advance, 10-90% MFB and COV of IMEP. In general it is believed that this supports the contentions of Hattrell *et al.* (2006).

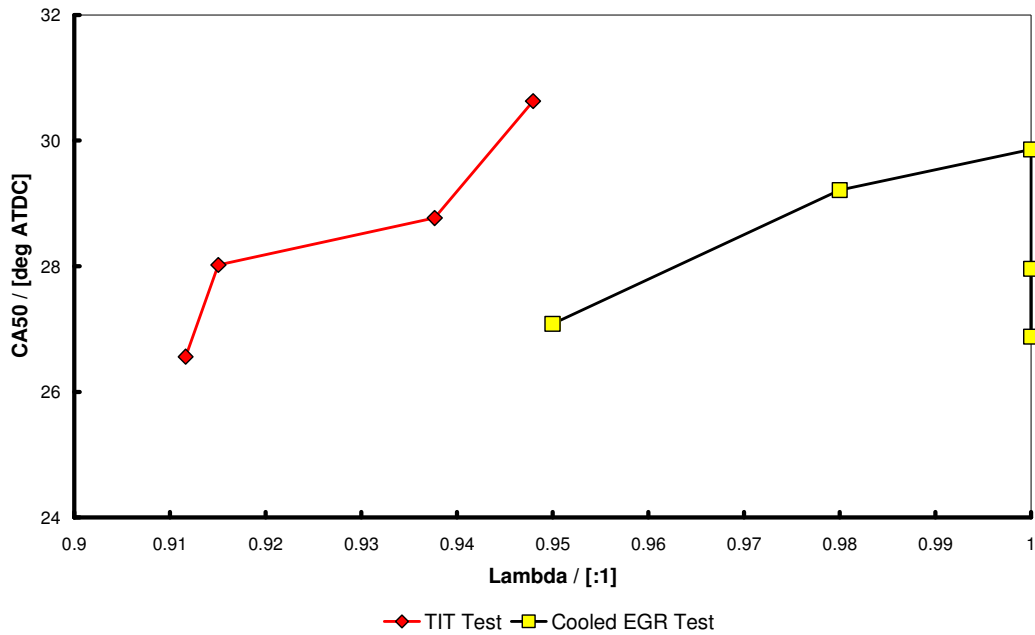


Fig. 8.21: CA50 versus λ for turbine inlet temperature and cooled EGR sets of tests at 5000 rpm, full load (reducing from ~17.7 to ~16.8 bar BMEP as EGR is added), using the same plenum temperature (33-40°C)

Overall, one can say that the response of the Sabre engine to the introduction of cooled EGR at rated power is as would be expected if the combustion system and engine configuration combination was already near some kind of optimum, especially considering its response to increased λ during the increased TIT tests. At full load, the COV of IMEP in its standard form is already high, but introducing diluents either in the form of excess air, over the fuelling level which is required for power enrichment, or as cooled EGR, made the COV of IMEP unacceptably high, i.e. approaching 10%. Furthermore, the improvement in BSFC is not significant for either approach considering that both cause a reduction in power output.

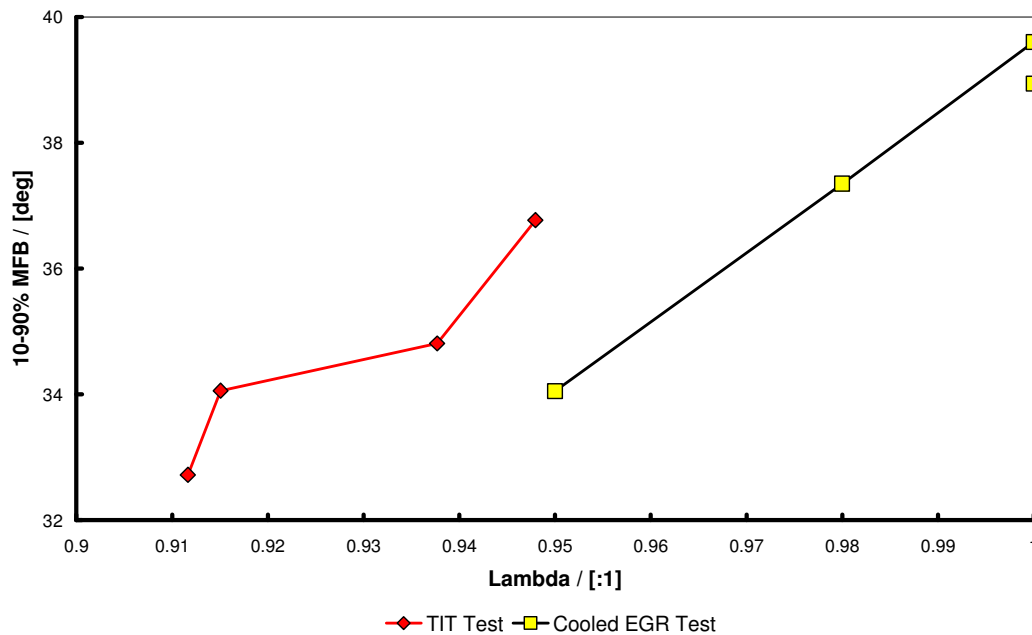


Fig. 8.22: 10-90% MFB versus λ for turbine inlet temperature and cooled EGR sets of tests at 5000 rpm, full load (reducing from ~ 17.7 to ~ 16.8 bar BMEP as EGR is added), using the same plenum temperature (33-40°C)

Issues of combustion instability apart, it is believed that far higher levels of BMEP will be required before the full-load fuel consumption of Sabre worsens to that of a typical under-port DI engine. This, it is believed, underlines the benefit of close spacing of the injector and spark plug in a 'second generation' DISI configuration over the more common first generation layout: better fuel-air mixing appears to be possible throughout the speed-load range, with less dependence on port-induced tumble. Although it is accepted that tumble itself is important to combustion rate and with it reduced combustion variability, especially in the case of diluents being present, vertical positioning of the injector suggests that good air-fuel mixing can be achieved even when combustion itself is sub-optimal. This is because the injector nozzle, and hence the fuel spray, is near-normal to the highest velocity of the intake air stream. Close-spacing thus decouples fuel-air mixing from combustion in this homogeneous combustion system. This

reinforces the validity of conducting the fixed-air-density tests discussed in Chapter 6 with port-fuel injection, since the same cylinder geometry was used.

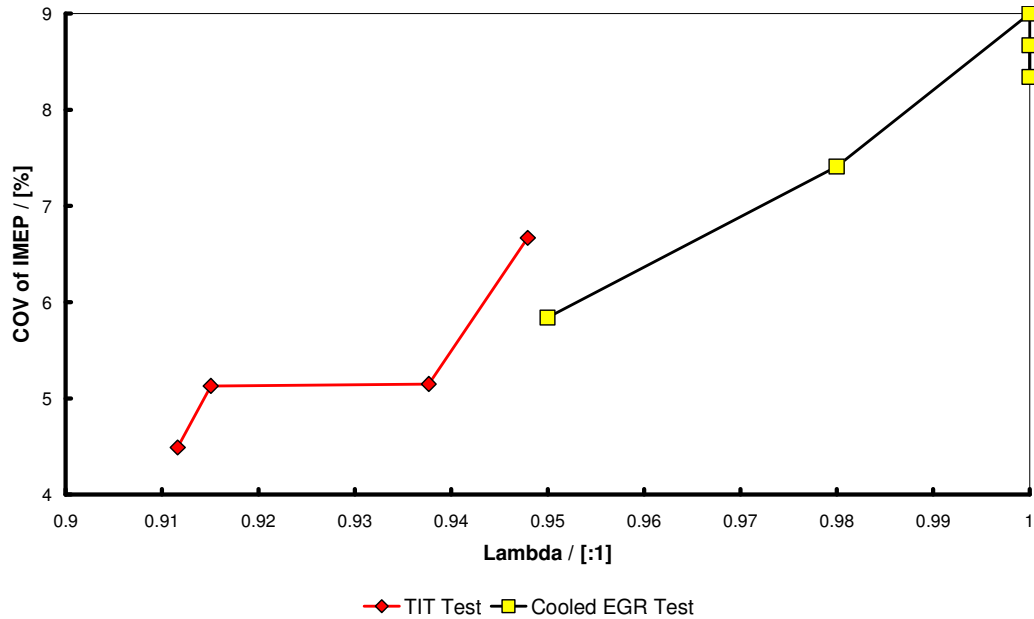


Fig. 8.23: COV of IMEP versus λ for turbine inlet temperature and cooled EGR sets of tests at 5000 rpm, full load (reducing from ~ 17.7 to ~ 16.8 bar BMEP as EGR is added), using the same plenum temperature (33-40°C)

With the introduction of EGR into the charge air there is a reduction in oxygen concomitant with the amount of EGR used, which is in part responsible for any reduction in BMEP. In order to make a qualitative comparison between the benefits of increased TIT versus cooled EGR as a strategy to improve high load fuel consumption, consider the broadly-comparable case of what happens when either the TIT is increased or sufficient EGR is introduced to reduce the BMEP of the engine by ~ 0.5 bar from the starting condition. The two quantities are respectively an increase in TIT to 1020°C or the introduction of 6% cooled EGR, as shown separately in Figures 8.4 and 8.13. For these two cases it is accepted that the starting BMEPs are not the same, being 18.4 and 17.7 bar respectively, but for discussion purposes note that the cooled EGR data in Figures 8.13 and

8.14 shows that adding EGR resulted in a 5.5% reduction in BSFC and a 3.2% reduction in BMEP for the EGR rate of 6% in the plenum. This is a more significant effect in comparison to increasing the TIT since, as already noted in Section 8.2, by doing that there was a reduction of only 1.4% in BSFC for a 2.4% reduction in BMEP.

This suggests that attempting to increase the TIT further would not be worthwhile as a strategy to reduce high-load fuel consumption. However, the absolute value of the BSFC achieved with 6% cooled EGR at an operating condition of 17.2 bar BMEP, 256.6 g/kWh, is noteworthy. Therefore, while the percentage reduction in BSFC may not be as significant as other researchers have shown, the technology is still beneficial even in this engine system, reducing as it does the TIT and affording $\lambda = 1$ operation. Note that the engine is still operating at ~ 71.5 kW/l (96 bhp/l) at this point.

Therefore, since one of the initial intentions of the research described in this chapter was to gauge the amount of cooled EGR required for significant fuel consumption improvement, and since the amount of benefit which accrues does not appear to be large, then if cooled EGR were to be adopted the important consequential effects on the vehicle cooling system would indeed be minimized. This is primarily due to the good full-load fuel consumption of the Sabre engine without cooled EGR. Only $\sim 6\%$ EGR would be needed, meaning a significantly-reduced cooling system load in comparison to the up to 25% cooled EGR other researchers have reported as necessary on engines equipped with conventional exhaust manifolds at this BMEP level. It must be remembered, though, that the IEM itself represents an increased load on the vehicle cooling system, albeit one which is acceptable in a light-duty application (Turner *et al.*, 2005c, Borrmann *et al.*, 2008). Nevertheless, if broad parity in heat rejection to the vehicle cooling pack is found between the two separate approaches of IEM or high amounts of cooled EGR, the IEM would still be preferable since it reduces the BOM cost of an engine instead of requiring another system to be added to it, which also has to be controlled. It also significantly improves warm-up times from a cold engine start (Akima *et al.*, 2006 and Kuhlbach, *et al.*, 2009).

While a maximum rated power BSFC of the order of 255-260 g/kWh is itself very attractive, the use of cooled EGR may not be compelling in this engine when the base engine specific fuel consumption is already so good. This is especially the case when considering the magnitude of the benefit against the period of time a light-duty engine operates at full load. Nevertheless, with the 95 RON fuel that this series of tests utilized, the very best cooled EGR BSFC of 255.7 g/kWh noted at 8% EGR corresponds to a thermal efficiency of 33.0% (assuming a fuel LHV of 42.7 MJ/kg (Bosch, 2000)). Considering that a modern light-duty diesel engine fitted with common rail injection will record in the region of 230 g/kWh at maximum power (Hadler *et al.*, 2007), or 36.8% thermal efficiency (assuming a fuel LHV of 42.5 MJ/kg (Bosch, 2000)), then Sabre with cooled EGR is only 3.8% worse (or relatively 10.3%). Remembering the difference in terms of CO₂ due to the amount of CO₂ produced per gram of each fuel (Coe, 2005), the diesel engine's advantage reduces slightly further at this condition. In terms of efficiency and CO₂ output at high load, then, the light-duty diesel engine appears to be under some pressure from DISI technologies in development now, very much compounded by increasingly expensive diesel exhaust gas after treatment systems.

One final observation is that while the IEM is largely responsible for the ability of the engine to operate close to $\lambda = 1$ at realistic turbine inlet temperatures and at BMEP levels of 18-19 bar, it does this in a manner that removes the need for the combustion process to be compromised (i.e. diluents do not need to be employed to achieve this). Since in the IEM concept the heat energy is removed post-combustion and specifically *outside* of the combustion chamber, there is an element of engineering purity to the approach which, however intriguing the use of cooled EGR is in a combustion science sense, gives the IEM an elegance as part of the engine system that the 'add-on' nature of cooled EGR cannot match.

8.5 A NEW CONCEPT TO REDUCE THE COMPLEXITY OF COOLED EGR SYSTEMS

The EGR cooling system used in this work comprised a single, classical heat exchanger. Cooled EGR systems have also been conceived utilizing either such a dedicated cooler, or one which splits the cooling load between a heat exchanger in the engine coolant circuit and another dedicated cooler in series with the first (Alger *et al.*, 2008 and Hancock *et al.*, 2008).

However, there are other methods of reducing the temperature of gases in addition to physical heat exchange. One such method is expansion through a turbine, which is only available with a suitable expansion ratio. This could be considered to be an element of the low-pressure loop system as described above, where the turbocharger turbine performs this function. Note that with regard to intake charge air, this concept is also the basis of the turboexpansion system discussed in Chapter 4. Another potentially significant method not seen in the literature, and briefly alluded to in Chapter 5, is to use the latent heat of vaporization of the fuel directly to reduce the temperature of the EGR gas (Patent, 2010). This is, in turn, similar to the concept of pre-compressor fuel introduction to control the temperature of intake charge air (Hooker *et al.*, 1941, Rosenkranz *et al.*, 1986, Turner and Pearson, 2001, Turner *et al.*, 2007a). A schematic of one potential arrangement is shown in Figure 8.24, in which a physical EGR cooler is placed before the evaporative fuel introduction point, here represented by a fuel injector under the control of the engine management system (EMS).

Based on this concept, some sample calculations have been conducted for various fuels being introduced directly into the EGR recirculation stream and the results of these are shown in Figures 8.25 to 8.27. The values used to generate the data in these figures are given in Table 8.2, and are those used in the Lotus Fuel Mixture Database (Lotus Engineering Software, 2009). For E85 the latent heat of vaporization was calculated using the appropriate mass ratio of gasoline and ethanol. For the purposes of illustration the specific heat capacity at

constant pressure (c_p) of exhaust gas has been assumed to be constant at 1.03 kJ/kgK, and a fuelling condition of $\lambda = 1$ has been used to generate the data used in the figures.

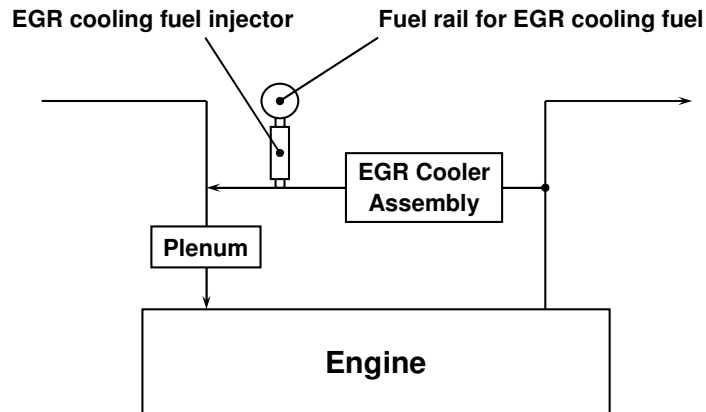


Fig. 8.24: Schematic of a possible cooled EGR system using fuel vaporization for one stage of cooling

Table 8.2: Fuel properties used to calculate results of Figures 8.25 to 8.27, taken and calculated from the Lotus Fuel Mixture Database (Lotus Engineering Software, 2009)

Fuel	Density (kg/m ³)	Latent Heat of Vaporization (kJ/kg)	Stoichiometric AFR (:1)
95 RON Gasoline	736	280	14.5
E85	781	838	9.74
Methanol	791	1170	6.4

As noted previously, in combustion systems where low proportions of cooled EGR are required, the amount of thermal load put onto the vehicle cooling system is concomitantly reduced. Using the latent heat of vaporization of the fuel promises to remove a significant proportion of the thermal load. Depending upon the evaporant used, potentially all of it can be removed. In Sabre, the data of Section 8.3 suggests that only on the order of 6% by volume of EGR would be required at nearly 74.6 kW/l (100 bhp/l). Assuming a required EGR outlet temperature of 150°C (in order to ensure that water does not condense in the

EGR system) and, from Figure 8.14, a pre-turbine temperature of 950°C with EGR in use (giving a required temperature reduction of 800°C) then if E85 was used as the evaporant the data of Figure 8.27 shows that 61% of the stoichiometric fuel mass would have to be used. If methanol was used instead, then only 29% of the input fuel would be required.

Since the examples given are based on the cooled EGR results for the Sabre engine, this analysis does not take into account changes in engine performance arising from any improvements in combustion attendant upon changing the fuel. Low-carbon-number alcohols are known to produce lower exhaust temperatures than gasoline, so if the engine used such an alcohol as its primary fuel then this would tend to reduce the amount of heat that would have to be removed from the EGR, too (see also Chapter 5 and Bergström *et al.*, 2007a and 2007b).

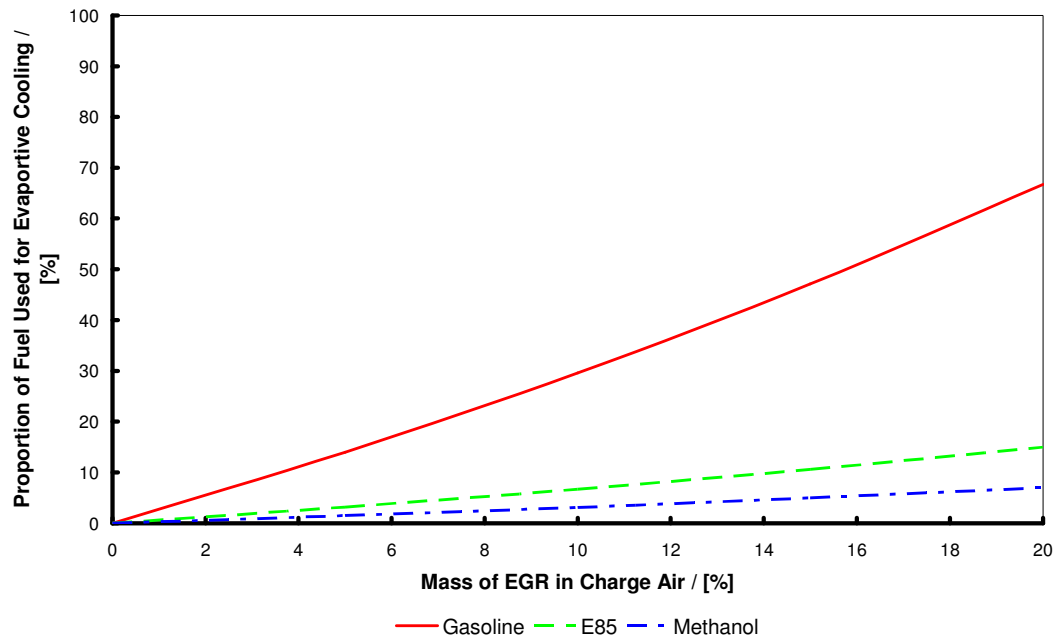


Fig. 8.25: Proportion of total fuel required to cool EGR gas by 50°C by evaporative cooling at $\lambda = 1$ for various fuels

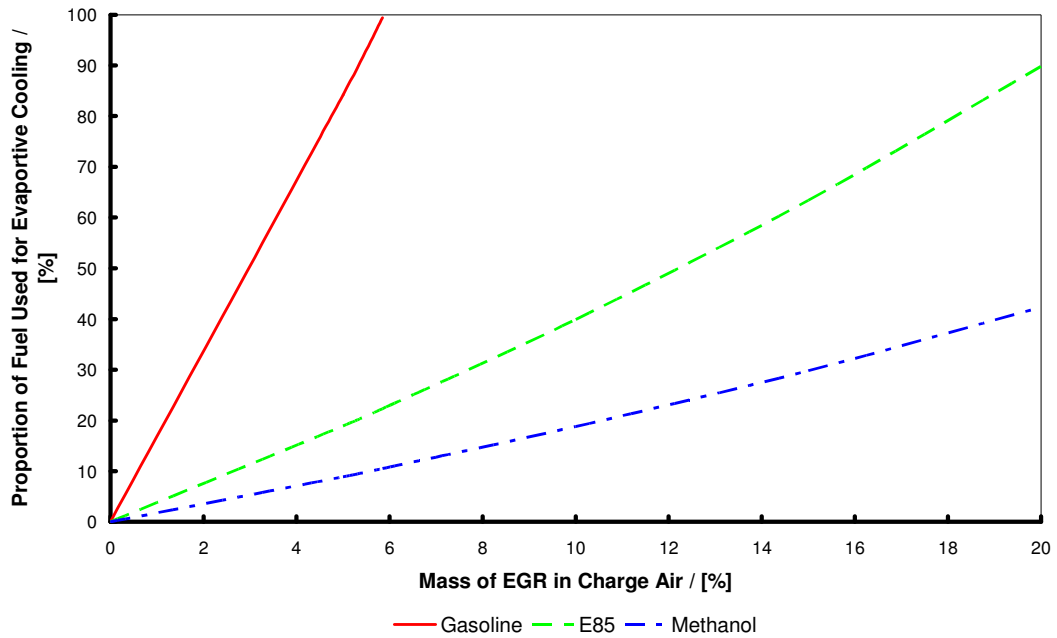


Fig. 8.26: Proportion of total fuel required to cool EGR gas by 300°C by evaporative cooling at $\lambda = 1$ for various fuels

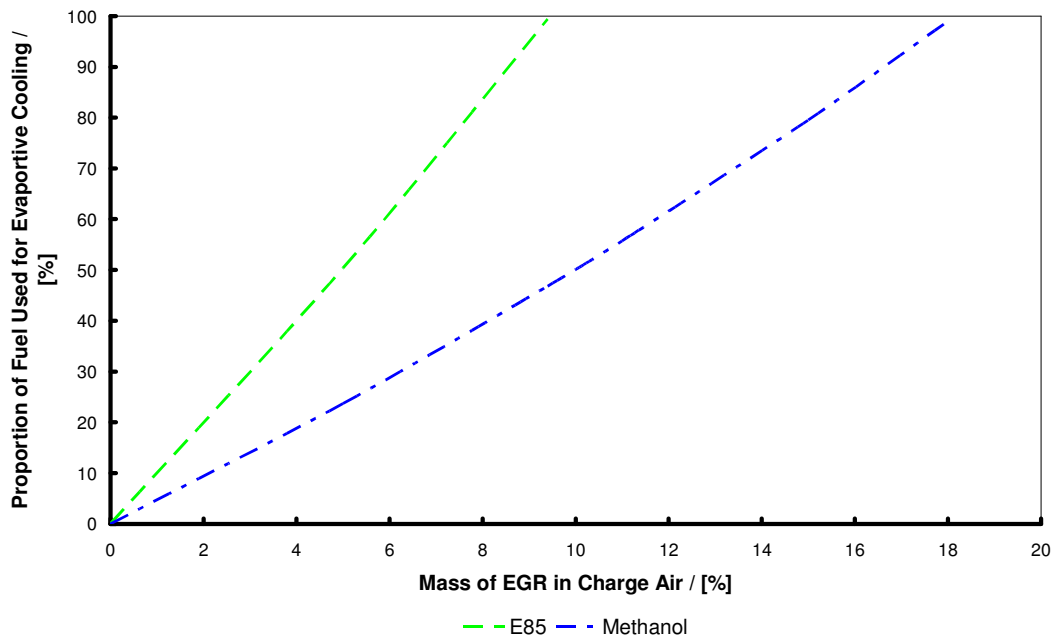


Fig. 8.27: Proportion of total fuel required to cool EGR gas by 800°C by evaporative cooling at $\lambda = 1$ for various fuels

In Figures 8.25 to 8.27, the E85 results would expect to be broadly representative of those of equivalent-stoichiometric-AFR ternary blends of gasoline, ethanol and methanol. This is because these are calculated to have the same volumetric lower heating value and latent heat of vaporization as E85 (to within 1% and 4%, respectively) (Turner *et al.*, 2011). It is imagined that the evaporant fuel flow would be controlled by the EMS based on a target plenum temperature, making for a more flexible control system for conditions where there are different blend ratios of gasoline and alcohol being supplied, as might be the case in a flex-fuel vehicle. There might then be an upper flow rate limit to avoid conditions of flammability in the intake plenum.

With a requirement for a high temperature drop the approach would not work with gasoline as the evaporant. This is due to the amount of heat to be removed, coupled to the high stoichiometric AFR and low latent heat of vaporization of gasoline, which combines to limit the maximum temperature reduction for 6% EGR to just under 300°C, where all of the fuel would be required, as can be deduced from Figure 8.26. This is considered impractical, since the mixture in the plenum would then be flammable. However, water could also be used as an evaporant due to its extremely high latent heat of 2270 kJ/kg. It would theoretically be feasible to condense this water from the exhaust gases for a gasoline-fuelled engine, although there would clearly be added complexity in the exhaust system, because the heat exchangers necessary would be relatively large. This is unlikely to prove attractive versus the use of a dedicated EGR cooler system where only 6% of the exhaust flow would need cooling.

Note that due to the relatively small amount of time that a light-duty engine such as Sabre would require cooled EGR, it would be possible to use a separate evaporant to gasoline in this approach. This is similar in concept to the direct injection of alcohol in port-fuel-injected SI engines primarily fuelled by gasoline as proposed by Bromberg *et al.* (2006) and being investigated by Whitaker *et al.* (2010) in that it would permit a degree of optimization in the use of the latent heat of an alcohol (and its increased octane number) in PFI engines, but without the added complication of direct injection.

While in the case of a separate evaporant a dedicated tank would be needed, an approach split between physical and evaporative cooling as shown in Figure 8.24 could also reduce the consumption of the evaporant, since some of the heat could be removed by a cooler in the engine coolant circuit and the rest by evaporative cooling of the EGR by fuel or water.

Overall, this invention, created from work conducted in this thesis, has led to the filing of a new patent and would be worthy of subsequent work (Patent, 2010). This is particularly the case in alcohol-fuelled engines, where part-load fuel reforming could also be conducted in such a system with the correct catalyst, to the benefit of part-load fuel consumption through a degree of exhaust heat recovery (König *et al.*, 1985 and Hoffman *et al.*, 2008b).

8.6 SUMMARY AND CONCLUDING REMARKS

This chapter has investigated various techniques to further improve the high load fuel consumption of the Sabre downsized demonstrator engine, which Chapter 7 had already shown to be very good. The principal findings and conclusions are listed below:

1. A better turbocharger match would be capable of providing improvements in fuel consumption while at the same time permitting the specific power output, and with it the downsizing ratio, to be increased. There may be some demerit in the case of low-speed BMEP, but this could be compensated for by either a compound charging system or, on a vehicle system level, through the use of a mild hybrid system.
2. Increasing the turbine inlet temperature has not shown a beneficial result: a greater percentage decrease in BMEP was found than the associated reduction in BSFC. This is believed to be due to the effect of the leaning of the charge being to take the relative AFR away from a power-enriched operating condition at which the Sabre engine operates. This is because it

requires little over-fuelling in order to protect components in the exhaust gas stream. Other reported SI engines, as they are leaned at full load, generally tend to approach optimum power enrichment because they normally operate significantly richer than optimum for reasons of component thermal protection. For such engines this then results in a power increase. The case for Sabre is the opposite.

3. Cooled EGR has been found to be beneficial at the 5000 rpm, full-load operating condition, when considered in terms of reduction in BSFC versus reduction in achievable BMEP.
4. The full-load combustion stability of the engine deteriorated rapidly as a diluent was introduced. The Sabre engine is known to have relatively poor high-load combustion since its COV of IMEP is high at this condition, but introducing a diluent rapidly causes this to exceed 5% and to approach 10% for a cooled EGR rate of 8%.
5. From the work conducted it would seem that the increase in COV of IMEP is a function of relative AFR (i.e. λ).
6. A new concept for evaporative cooling of EGR gas has been developed and initial calculations performed to show the viability of the concept. This is expected to be especially beneficial in alcohol-fuelled engines due to the high latent heat of vaporization and low stoichiometric AFR of these fuels, but for any fuel it would help to reduce heat rejection to the vehicle cooling pack. This concept is similar to that investigated on the intake side of the engine in Chapter 5.

The next chapter will summarize this thesis and will provide recommendations for future work based largely upon the results presented in this and previous chapters.

Chapter 9: Conclusions and Further Work

This chapter summarizes the work reported in this thesis. It then lists the major conclusions. Finally, some recommendations for further work are made.

9.1 SUMMARY OF THE THESIS

Chapter 1 described some of the historical background to our dependence on petroleum fuels and the co-evolution of the spark-ignition Otto cycle engine which uses gasoline as its main fuel type. It then developed the understanding of the importance of pumping losses within the Otto cycle, the similar importance of compression ratio, and in relation to this introduced the issue of controlling knock in order to set the CR as high as possible for best fuel economy.

Chapter 2 discussed the challenges of engine downsizing in more detail, and in particular the importance of charging system interactions with the reciprocating engine, as well as presenting various different charging devices and components and how they can be configured in different arrangements as systems. The impact of system efficiency, and with it charge air temperature, was discussed in relation to the knock limit of the engine and thus to its overall thermal efficiency.

Chapter 3 presented a literature review of spark-ignition combustion knock and various aspects of how it arises and the methods used to suppress it in pressure-charged engines. These included fuel characteristics, the use of diluents to suppress knock and the use of alternative charging systems to assist in controlling the onset of autoignition. These techniques are used so that all of the charge can be burnt before the autoignition reactions in the end gas (which commence as soon as the fuel is introduced to the engine) can proceed to runaway conditions. Of the various diluents (i.e. fuel, air and EGR) cooled EGR was shown to have the most potential in reducing fuel consumption because using fuel clearly does nothing to reduce it and excess air causes the temperature in the end gas to increase at a higher rate than does cooled EGR.

This effect is due to the higher ratio of specific heats of air compared to the predominantly triatomic molecules which, beside nitrogen, comprise cooled EGR (i.e., carbon dioxide and water). That this is the diluent of choice was demonstrated later in Chapter 8 using the Sabre engine design which arose out of this work.

Chapter 4 discussed relevant previous work by the author both with alcohol fuels in a racing engine and with an advanced charging system intended to prove the benefit of increased charge cooling in helping to suppress knock in a highly-pressure-charged SI combustion system. The design of that engine, the so-called 'Nomad' research engine, and its specific turboexpansion charging system was discussed, as well as the failure of the combined configuration to deliver an improvement. The chapter also discussed the belief that the original Nomad project aim of building a self-contained engine from the start was itself too ambitious, and that more-controlled single-cylinder engine test work would have been a better starting point. This was needed to check the veracity of the original hypothesis that, for a fixed charge air density, reducing its temperature would automatically lead to an improvement in the knock limit. The desirability of this single-cylinder approach was made even more apparent by the results of a parallel modelling study by Taitt *et al.* (2005 and 2006), which suggested that, while some improvement in knock limit was possible through adopting a turboexpansion system, it would be very difficult to convert it to a real benefit in vehicle fuel consumption. These tests were subsequently carried out as part of the work submitted in this thesis and discussed in Chapter 6.

Chapter 5 reported research which, instead of looking to develop a new charging system as the sole means to improve the performance of the engine, investigated the improvement in engine efficiency which could be expected when the fuel characteristics were changed instead. Here, in addition to a 95 RON gasoline baseline, the fuel used was E85, the octane number of which is significantly greater than gasoline but for which, more importantly, the latent heat is much greater. This permitted the use of controlled pre-supercharger introduction of a portion of the fuel to remove the requirement for an intercooler, and the fact that

this is beneficial up to the saturation point of the charge flowing into the supercharger was shown. The use of increased alcohol content in fuels is likely, given the potentially-renewable nature of ethanol and methanol production, and investigation of its beneficial effects in engines is important if it can improve their utilization rate as transport fuels.

Chapter 6 reported fixed air density tests using a single-cylinder test engine, the initial specification of which was laid down for the HOTFIRE research programme. These tests were essentially those which should have been conducted before embarking on the full Nomad turboexpansion programme. Here, the tests were conducted with port-fuel injection of gasoline under boosted conditions and at a fixed engine speed of 2000 rpm, important for comparison of fuel consumption improvement concepts. The test methodology was to hold the charge air density constant and adjust the air temperature and pressure accordingly, as discussed in Chapter 4. A one-dimensional engine model code was also used to design an exhaust system to make the test results more representative of a multi-cylinder engine with a turbocharger turbine in the exhaust path. The results obtained clearly demonstrated a linear relationship between knock-limited spark advance and air temperature for any given charge air density over the range tested. Within the limits of the test this is an important finding which has not been found in the literature and would be worthy of considerable further research. As such it is considered to be a major contribution to knowledge.

Chapter 7 described the design and rationale behind the Sabre 3-cylinder research engine, the prime beneficiary of the research work conducted in this thesis in terms of knock suppression and combustion system development. Its response to charging system optimization was described together with its results in its initial form. The benefits of choosing a 3-cylinder configuration were demonstrated with the use of high-speed pressure transducers in the exhaust and intake system. This engine configuration was then compared to other technologies being researched as means of improving fuel consumption, and it was shown that, due to its synergistic conception, Sabre has better fuel

consumption than most additive technologies for existing engines. The fact that an engine can be intelligently configured in the manner of Sabre, and that its features can be mutually complimentary to the degree that outstanding high-load fuel consumption can be achieved, is another contribution to knowledge.

Chapter 8 described how the Sabre engine platform was used to investigate the full-load effects of some of the various technologies other researchers have been investigating with regard to high-load engine efficiency in the pursuit of greater downsizing of the SI engine. These included increased turbine inlet temperature (TIT) and the use of cooled EGR. While increased TIT did not show a benefit, there is some potential in cooled EGR, although not to the degree of improvement shown by other researchers in less-optimized engine configurations. A new scheme to utilize the latent heat of vaporization of the fuel to cool the EGR, instead of a dedicated classical heat exchanger, was proposed. One of the outcomes of research presented in this thesis was the application for a patent to use evaporative cooling of EGR in order to reduce the thermal load on the vehicle cooling system.

9.2 MAJOR CONCLUSIONS

Through a structured approach to the challenge of mitigating knock in a spark-ignition combustion system (to the benefit of improving thermal efficiency through compression ratio increase), which has led to a succession of new engine designs with more-optimized configurations, this research has made the following contributions to knowledge:

1. Within the limits tested here, at fixed charge air density the relationship between knock-limited spark advance and air temperature is linear. This has been established for a port-fuel-injection homogeneous combustion system and there is no reason to suppose that the same relationship will not be seen for a direct-injection one, since the intent of such systems is likewise to fully homogenize the charge at full load and thus to maximize air utilization. This approach has not been seen anywhere else in the

literature and is believed to be unique, with particularly important ramifications for the design of future SI engine charging systems.

2. Through a combination of an optimized direct-injection combustion system, an exhaust manifold integrated into the cylinder head and a 3-cylinder configuration, an engine with extremely high full-load thermal efficiency can be created. This is because these characteristics are all synergistic. The high-load efficiency of this configuration as demonstrated by the Sabre engine is such that the brake specific fuel consumption at maximum power is better than has been demonstrated in the literature for other practical, self-contained engines with efficiency-enhancing technologies.
3. Against the baseline of such an engine, other technologies such as excess air operation and the use of cooled EGR offer little improvement. In the Sabre engine cooled EGR *will* increase efficiency, but at the cost of some significant extra complication and to nowhere near the level reported by other researchers utilizing more-compromised engine concepts for their research. As the maximum BMEP of the engine increases, however, this situation may change.
4. Although the effect has been seen used in racing engines for some time, when operating a pressure-charged engine on alcohol fuels, the latent heat of vaporization can be utilized in reducing supercharger (or compressor) outlet temperatures through controlled use of pre-compressor injection. The presence of a clearly-defined proportion of the fuel mass beyond which there is no benefit in introducing a greater amount at the entry to the supercharger was demonstrated. New control strategies to reduce the amount and occurrence of pre-compressor injection based on alcohol content, boost pressure and throttle position have been suggested.
5. The latent heat of the fuel can be used beneficially in engines employing cooled EGR by injecting a proportion of the fuel charge into the EGR gas directly. Such evaporative cooling would help to reduce the amount of

physical cooling of the EGR gas that would have to be performed, to the benefit of reduced thermal load on the vehicle cooling system. It has been shown that, in a manner similar to their suitability for pre-compressor injection in pressure-charged engines, the low-carbon-number alcohols, ethanol and methanol, offer a significant opportunity in this area.

9.3 RECOMMENDATIONS FOR FURTHER WORK

The findings of this thesis regarding the linear relationship of the knock limit with charge air temperature for conditions of fixed charge air density are considered to be worthy of further investigation. The absence of results in the literature where the charge air density is fixed is considered surprising considering its fundamental value and importance. Further experimental and modelling work would be extremely useful to the engine development community. In order to maximize the benefit of doing this work with regards to the future direction of engines outlined above, tests with both a real gasoline and a surrogate should be performed. Tests with high alcohol content would yield data potentially of great interest to future engine designs. These tests should be structured along the lines set out in this thesis and expanded to investigate whether the effect follows engine speed (and thus autoignition induction time) as well. A comparison of port fuel injection and direct injection would be useful to test the contention that fuel introduction method is relatively unimportant when homogeneous charge is used (while accepting that direct injection can still in itself extend the knock limit due to latent heat effects). All of this data can also support combustion modelling work. After this has been done a revisit of the engine and charging system modelling work of Taitt *et al.* (2005 and 2006) should be carried out.

Finally, a development of the cooled EGR work with the Sabre engine should be conducted, investigating higher BMEP operation with both an active and inert catalyst in the high-pressure cooled EGR loop in the manner of Hoffmeyer *et al.* (2009), together with an attempt to investigate its interaction with the integrated exhaust manifold, thus verifying or otherwise the recent work of Taylor *et al.* (2010) and Roth *et al.* (2010a). Engine tests investigating the evaporative

cooling system for EGR invention described in Chapter 8 should also be conducted, with particular emphasis on quantifying the benefit of the approach with regard to reducing the thermal load on the vehicle cooling system.

References

ACEA (2005), "Monitoring of ACEA's Commitment on CO₂ Emission Reductions from Passenger Cars (2003) - Final Report 05.10.2004", Brussels, March 2005.

Akima, K., Seko, K., Taga, W., Torii, K. and Nakamura, S. (2006), "Development of New Low Fuel Consumption 1.8L I-VTEC Gasoline Engine with Delayed Intake Valve Closing", SAE paper number 2006-01-0192, SAE 2006 World Congress, Detroit, Michigan, USA, April 2006.

Alger, T., Chauvet, T. and Dimitrova, Z. (2008), "Synergies between High EGR Operation and GDI Systems", SAE paper number 2008-01-0134, SAE 2008 World Congress, Detroit, Michigan, USA, April 2008.

Allard, A. (1982), Turbocharging and Supercharging, Patrick Stephens Limited, Cambridge, CB3 8EL, UK, 1982, ISBN 0-85059-494-4.

Amaseder, F. and Krainz, G. (2006), "Liquid Hydrogen Storage Systems developed and manufactured for the first time for Customer Cars", SAE paper number 2006-01-0432, SAE 2006 World Congress, Detroit, Michigan, USA, April 2006.

Anderson, W., Yang, J., Brehob, D. D., Vallance, J.K. and Whiteaker, R.M. (1996), "Understanding the Thermodynamics of Direct Injection Spark Ignition (DISI) Combustion Systems: An Analytical and Experimental Investigation", SAE paper number 962018.

Andriesse, D., Cazzolato, F., Marangoni, A., Oreggioni, A. and Quinto, S. (2006), "A New Generation of High Efficiency DI Gasoline Engines - Serious Competition for the DI Diesel Engine?", 18th International AVL Congress "Engine and Environment", Graz, Austria, 7th-8th September, 2006.

Andriesse, D., Comignaghi, E., Lucignano, G., Oreggioni, A., Quinto, S. and Sacco, D. (2008), "The New 1.8 I DI Turbo-Jet Gasoline Engine from Fiat Powertrain Technologies", 17th Aachen Colloquium, Aachen, Germany, 6th-8th October, 2008, pp. 563-590.

ASTM International (2007a), "Standard Test Method for Research Octane Number of Spark-Ignition Engine Fuel - Designation: D 2699-07", ASTM

International, 100 Barr Harbor Drive, PO Box C700, West Conshohocken, PA 19428-2959, United States, 2007.

ASTM International (2007b), “Standard Test Method for Motor Octane Number of Spark-Ignition Engine Fuel - Designation: D 2700-07a”, ASTM International, 100 Barr Harbor Drive, PO Box C700, West Conshohocken, PA 19428-2959, United States, 2007.

Ball, G.A. (1955), “Photographic Studies of Cool Flames and Knock in an Engine”, Fifth Symposium (International) on Combustion/The Combustion Institute, pp. 366-372, 1955.

Ballinger, P.R. and Ryason. P.R. (1971), “Isolated Stable Cool Flames of Hydrocarbons”, Thirteenth Symposium (International) on Combustion/The Combustion Institute, pp. 271-277, 1971.

Bamsey, I. (1988), The 1000 bhp Grand Prix Cars, Haynes Publishing Group, Sparkford, Yeovil, Somerset, BA22 7JJ, UK, 1988, ISBN 0-85429-617-4.

Bandel, W., Fraidl, G.K., Kapus, P., Sikinger, H. and Cowland, C.N. (2006), “The Turbocharged GDI Engine: Boosted Synergies for High Fuel Economy Plus Ultra-low Emissions”, SAE paper number 2006-01-1266.

Bassett, M.D., Brooks, T., Fraser, N.A.J., Hall, J.M., Thatcher, I. and Taylor, G.M. (2010), “A Study of Fuel Converter Requirements for an Extended-Range Electric Vehicle”, SAE paper number 2010-01-0832, SAE 2010 World Congress, Detroit, Michigan, USA, 13th-15th April, 2010.

Baxter, I. and Yeo, B. (unknown date), “An International Historic Mechanical Engineering Landmark - The Waukesha CFR Fuel Research Engine”, available at: <http://files.asme.org/ASMEORG/Communities/History/Landmarks/5519.pdf>, last accessed 6th April, 2011.

Benson, J.D., Koehl, W.J., Burns, V.R., Hochhauser, A.M., Knepper, J.C., Leppard, W.R., Painter, L.J., Rapp, L.A., Reuter, R.M., J.D., Rippon, B. and Rutherford, J.A. (1995), “Emissions with E85 and Gasolines in Flexible/Variable Fuel Vehicles - The Auto/Oil Air Quality Improvement Research Program”. SAE paper number 952508, also in SAE 1995 Transactions, Vol. 104 Sec. 4 pp. 1799-1816.

Bentley Motors Limited (2008), “Bentley and the future of biofuels”, 2008, available at:

http://www.bentleymotors.com/media/med/Libraries/1/Bentley_and_the_future_of_biofuels.pdf, last accessed 6th April, 2011.

Bergström, K., Melin, S.-A. and Jones, C.C. (2007a), “The New ECOTEC Turbo BioPower Engine from GM Powertrain - Utilizing the Power of Nature's resources”, 28th International Vienna Motor Symposium, Vienna, 26th-27th April 2007.

Bergström, K. ac, Nordin, H., Königstein, A., Marriott, C.D. and Wiles, M.A. (2007b), “ABC - Alcohol Based Combustion Engines - Challenges and Opportunities”, 16th Aachen Colloquium, Aachen, Germany, October 2007 pp. 1031-1071.

Blunsdon, C.A. and Dent, J.C. (1994), “The Simulation of Autoignition and Knock in a Spark Ignition Engine with Disk Geometry”, SAE paper number 940524.

Böhme, J., Jung, M., Fröhlich, G., Pfannerer, D., Märkle, T. and Felsmann, C. (2006), “The New 1.8 l Four Cylinder T-FSI Engine by Audi Part 1: Construction and Mechanics”, MTZ 10/2006 Volume 67, October 2006.

Bonello, M.J., Caldwell, D.M., Pigott, J.A., Prior, G.P. and Schag, T.M. (2005), “The Supercharged Northstar DOHC 4.4L Engine for Cadillac”, SAE paper number 2005-01-1854.

Borrman, D., Kuhlbach, K., Friedfeldt, R., Mehring, J. and Fritsche, R. (2008), “Cylinder Head Integrated Exhaust Manifold IEM Applied for Gasoline Downsizing Concepts”, 17th Aachen Colloquium, Aachen, Germany, 6th-8th October 2008, pp. 1001-1017.

Bosch (2000), Bosch Automotive Handbook, 5th Ed., 2000. ISBN 0-7680-0669-4.

Boyd, T.A. (1950), “Pathfinding in Fuels and Engines”, SAE Quarterly Transactions Vol. 4, pp. 182-195.

Bradley, D., Kalghatgi, G.T. and Golombok, M. (1996a), “Fuel Blend and Mixture Strength Effects on Autoignition Heat Release Rates and Knock Intensity in S.I. Engines”, SAE paper number 962105.

Bradley, D., Kalghatgi, G.T., Golombok, M. and Yeo, J. (1996b), “Heat release rates due to autoignition and their relationship to knock intensity in spark ignition

engines”, Twenty-Sixth Symposium (International) on Combustion/The Combustion Institute, pp. 2653-2660, 1996.

Brinkman, N.D. and Stebar, R.F. (1985), “A Comparison of Methanol and Dissociated Methanol Illustrating Effects of Fuel Properties on Engine Efficiency - Experiments and Thermodynamic Analyses”, SAE paper number 850217 and SAE 1985 Transactions, Vol. 94, Sec. 3, pp. 62-85.

Bromberg, L., Cohn, D.R. and Heywood, J.B. (2006), “Calculations of Knock Suppression in Highly Turbocharged Gasoline/Ethanol Engines using Direct Ethanol Injection”, MIT report PSFC/JA-06-02, MIT Plasma Science and Fusion Centre, 5th May, 2006.

Bromberg, L. and Cohn, D. (2010), “Alcohol Fueled Heavy Duty Vehicles Using Clean, High Efficiency Engines”, SAE paper number 2010-01-2199, SAE Powertrains, Fuels and Lubricants Meeting, San Diego, California, USA, 25th-27th October, 2010.

Bromnick, P.A., Pearson, R.J. and Winterbone, D.E. (1998), “Intercooler model for unsteady flows in engine manifolds”, Proc. Instn Mech. Engrs Vol 212 Part D.

Brooke, L. (2011), “EcoBoost offensive shifts to four cylinders”, Automotive Engineering International, pp. 24-25, February 2011.

Bruestle, C. and Hemmerlein, N. (1994), “Exhaust gas turbocharged SI engines and their ability of meeting future demands”, Inst. Mech. Engrs paper number C484/039/94, 1994.

Bruestle, C. and Schwarzenthal, D. (2001), “VarioCam Plus - A Highlight of the Porsche 911 Turbo Engine”, SAE paper number 2001-01-0245, SAE 2001 World Congress, Detroit, Michigan, USA, March 2001.

Brusstar, M., Stuhldreher, M., Swain, D. and Pidgeon, W. (2002), “High Efficiency and Low Emissions from a Port-Injected Engine with Neat Alcohol Fuels”, SAE paper number 2002-01-2743.

Brusstar, M. and Bakenhus, M. (2005), “Economical, High-Efficiency Engine Technologies for Alcohol Fuels”, 15th International Symposium on Alternative Fuels, San Diego, California, USA, October 2005.

Brusstar, M.J. and Gray, C.L. (2007), "High Efficiency with Future Alcohol Fuels in a Stoichiometric Medium Duty Spark Ignition Engine", SAE paper number 2007-01-3993.

Buchholz, K. (2006), "Super-turbo pairing", Automotive Engineering International, May 2006, p.70.

Burluka, A.A., Liu, K., Sheppard, C.G.W., Smallbone, A.J. and Woolley, R. (2004), "The Influence of Simulated Residual and NO Concentrations on Knock Onset for PRFs and Gasolines", SAE paper number 2004-01-2998.

Burgdorf, K. and Denbratt, I. (1997), "Comparison of Cylinder Pressure Based Knock Detection Methods", SAE paper number 972932, SAE International Fuels & Lubricants Meeting & Exposition, Tulsa, Oklahoma, USA, October, 1997.

Cairns, A., Blaxill, H. and Irlam, G. (2006), "Exhaust Gas Recirculation for Improved Part and Full Load Fuel Economy in a Turbocharged Gasoline Engine", SAE paper number 2006-01-0047, SAE 2006 World Congress, Detroit, Michigan, April 2006.

Cairns, A., Fraser, N. and Blaxill, H. (2008), "Pre Versus Post Compressor Supply of Cooled EGR for Full Load Fuel Economy in Turbocharged Gasoline Engines", SAE paper number 2008-01-0425, SAE 2008 World Congress, Detroit, Michigan, USA, April 2008.

Campbell, J.M., Lovell, W.G. and Boyd, T.A. (1930), "Detonation Characteristics of Some of the Fuels Suggested as Standards of Antiknock Quality", SAE Transactions, 1930, Vol. 25, pp. 126-131.

Carre, J. (1987), "The Screw Type Supercharger for Engine Boosting", SAE paper number 870705.

Chatterton, E. (1956), "The Napier Deltic Diesel Engine", SAE 1956 Transactions, Vol. 64, pp.408-425.

Clerk, D. (1926), "Explosive Reactions considered in reference to Internal Combustion Engines", Transactions of the Faraday Society, pp. 338-340, 1926.

Coe, E. (2005), "Emission Facts: Average Carbon Dioxide Emissions Resulting from Gasoline and Diesel Fuel", US EPA Office of Transportation and Air Quality Factsheet Number EPA420-F-05-001, February 2005.

Coltman, D., Turner, J.W.G., Curtis, R., Blake, D., Holland, B., Pearson, R.J., Arden., A. and Nuglisch, H. (2008), "Project Sabre: A Close-Spaced Direct

Injection 3-Cylinder Engine with Synergistic Technologies to achieve Low CO₂ Output”, SAE paper number 2008-01-0138, SAE 2008 World Congress, Detroit, Michigan, USA, April 2008.

Cornelius, W. and Caplan, J.D. (1952), “Some Effects of Fuel Structure, Tetraethyl Lead, and Engine Deposits On Precombustion Reactions on a Firing Engine”, SAE Transactions, Vol. 6, pp. 488-510, 1952.

Crooks, W.R. (1959), “Combustion air conditioning boosts output 50 per cent”, CIMAC Vol. 15 pp. 475-494, 1959.

Crosse, J. (2011), “Engines that moved us: Lotus 918 V8 - Twice as nice”, Classic Cars magazine, pp. 54-67, March 2011.

Cruff, L., Kaiser, M., Krause, S., Harris, R., Krueger, U. and Williams, M. (2010), “EBDI - Application of a Fully Flexible High BMEP Downsized Spark Ignited Engine”, SAE paper number 2010-01-0587, SAE 2010 World Congress, Detroit, Michigan, USA, April 2010.

Curran, H.J., Gaffuri, P., Pitz., W.J., Westbrook, C.K. and Leppard, W.R. (1995), “Autoignition Chemistry of the Hexane Isomers: An Experimental and Kinetic Modeling Study”, SAE paper number 952406 and SAE 1995 Transactions, Vol. 104, pp. 1184-1195.

Curran, H.J., Gaffuri, P., Pitz., W.J., Westbrook, C.K. and Leppard, W.R. (1996), “Autoignition chemistry in a motored engine: an experimental and kinetic modelling study”, Twenty-Sixth Symposium (International) on Combustion/The Combustion Institute, pp. 2669-2677, 1996.

Curran, H.J., Gaffuri, P., Pitz., W.J. and Westbrook, C.K. (1998), “A Comprehensive Modeling Study of n-Heptane Oxidation”, Combustion and Flame Vol. 114, pp. 149-177, 1998.

Curran, H.J., Gaffuri, P., Pitz., W.J., Westbrook and C.K. (2002), “A Comprehensive Modeling Study of iso-Octane Oxidation”, Combustion and Flame Vol. 129, pp. 253-280, 2002.

Curry, S. (1963), “A Three-Dimensional Study of Flame Propagation in a Spark Ignition Engine”, SAE paper number 630487 and SAE 1963 Transactions, pp. 628-650.

De Gooijer, B. (2011), “VCR validation”, Engine Technology International, pp. 70-71, January 2011.

De Petris, C., Diana, S., Giglio, V. and Police, G. (1994), "High Efficiency Stoichiometric Spark Ignition Engines", SAE paper number 941933, SAE International Fuels and Lubricants Meeting and Exposition, Baltimore, Maryland, USA, October, 1994.

Diana, S., Giglio, V., Iorio, B. and Police, G. (1996), "A Strategy to Improve the Efficiency of Stoichiometric Spark Ignition Engines", SAE paper number 961953, SAE International Fuels and Lubricants Meeting and Exposition, San Antonio, Texas, October, 1996.

Dickinson, H.C. (1929), "The Cooperative Fuel Research and Its Results". SAE Transactions, 1929, Vol. 24, pp. 262-265.

Doble, I.M. (1987), "Supercharging with an Axial Compressor", SAE paper number 870722.

Dorn, P. and Mourao, A.M. (1984), "The Properties and Performance of Modern Automotive Fuels", SAE paper number 841210 and SAE 1984 Transactions, Vol. 93, Sec. 5, pp. 469-485.

Douaud, A. and Eyzat, P. (1978), "Four-Octane-Number Method for Predicting the Anti-Knock Behaviour of Fuels and Engines", SAE paper number 780080.

Drangel, H. and Bergsten, L. (2000), "The new Saab SVC Engine – An Interaction of Variable Compression Ratio, High Pressure Supercharging and Downsizing for Considerably Reduced Fuel Consumption", 9th Aachen Colloquium, Aachen, Germany, October 2000.

Draper, C.S. (1938), "Pressure Waves Accompanying Detonation in the Internal Combustion Engine", J. Aero. Sci., Vol. 5, No.6, pp. 219-226, April 1938.

Drell, I.L. and Branstetter, J.R. (1950), "Knock-Limited Performance of Fuel Blends containing Ethers", National Advisory Committee for Aeronautics Technical Note 2070, 1950.

DresserWaukesha (2003), "CFR Operation and Maintenance Manual Form 847", 2nd Edition, pp. 2.10-4 and 2.10-5, 2003.

Duchaussoy, Y., Lefebvre, A. and Bonetto, R. (2003), "Dilution Interest on Turbocharged SI Engine Combustion", SAE paper number 2003-01-0629.

Duchaussoy, Y., Barbier, P. and Schmerzle, P. (2004), "Impact of Gasoline RON and MON on a Turbocharged MPI SI Engine Performances", SAE paper

number 2004-01-2001, SAE Fuels & Lubricants Meeting & Exhibition, Toulouse, France, June 2004.

EC (2010), "Progress report on implementation of the Community's integrated approach to reduce CO₂ emissions from light-duty vehicles", European Commission, November 2010, available at: <http://eur-lex.europa.eu/LexUriServ/LexUriServ.do?uri=COM:2010:0656:FIN:EN:PDF>, last accessed 6th April, 2011.

Edgar, G. (1927), "Measurement of Knock Characteristics of Gasoline in Terms of a Standard Fuel", Ind. Eng. Chem. Vol. 19, No. 1, pp. 145-146, January 1927.

Elmqvist, C., Lindström, F., Angström, H.-E., Grandin, B. and Kalghatgi, G. (2003), "Optimising Engine Concepts by using a Simple Model for Knock Prediction", SAE paper number 2003-01-3123, SAE Powertrain & Fluid Systems Conference & Exhibition, Pittsburgh, Pennsylvania, USA, October 2003.

Emmenthal, K.-D. and Manz, P.W. (1982), "Experimental results with turbocharged small displacement four stroke gasoline engines", Inst. Mech. Engrs paper number C52/82, The Second International Conference on Turbocharging and Turbochargers, London, UK, 1982, ISBN 9780852984918.

Eng, J.A., Leppard, W.R., Najt, P.M. and Dryer, F.L. (1997), "The Interaction Between Nitric Oxide and Hydrocarbon Oxidation Chemistry in a Spark Ignition Engine", SAE paper number 972889, SAE International Fuels & Lubricants Meeting & Exposition, Tulsa, Oklahoma, USA, October 1997.

Esch, H.-J. and Zickwolf, P. (1986), "Comparison of different exhaust gas turbocharging procedures on Porsche engines", Inst. Mech. Engrs paper number C112/86, The Third International Conference on Turbocharging and Turbochargers, London, UK, 6th-8th May, 1986, ISBN 0852985908.

Fieweger, K., Blumenthal, R. and Adomeit, G. (1997), "Self-Ignition of S.I. Engine Model Fuels: A Shock Tube Investigation at High Pressure", Combustion and Flame Vol. 109, pp. 599-619, 1997.

Fitton, J. and Nates, R. (1996), "Knock Erosion in Spark-Ignition Engines", SAE paper number 962102.

Fitzen, M., Hatz, W., Eiser, A., Heiduk, T. and Riegner, J. (2008), "The Audi 3.0l TFSI - the new top-of-the-range V6 engine", 29th International Vienna Motor Symposium, Year 2008 Series 12 No./Vol. 672-2 No. 8, Vienna, Austria, 24th-25th April, 2008.

Fraidl, G.K., Kapus, P. and Piock, W. (2005), "The Turbocharged GDI - The Competitor to the Diesel Engine?", 26th International Vienna Motor Symposium, Vienna, Austria, 28th-29th April 2005.

Furey, R.L. (1985), "Volatility Characteristics of Gasoline-Alcohol and Gasoline-Ether Fuel Blends", SAE paper number 852116 and SAE 1985 Transactions, Vol. 94, Sec. 7, pp. 777-788.

Gabriel, H., Jacob, S., Munkel, U., Rodenhäuser, H. and Schmalzl, H.-P. (2007), "The Turbocharger with Variable Turbine Geometry for Gasoline Engines", MTZ 02/2007 Volume 68, pp. 96-103, February 2007.

Germane, G.J. (1985), "A Technical Review of Automotive Racing Fuels", SAE paper number 852129.

Gibbs, L.M. (1990), "Gasoline Additives - When and Why", SAE paper number 902104 and SAE Transactions, 1990, Vol. 99, Sec. 4, pp. 618-638.

Gibbs, L.M. (1993), "How Gasoline Has Changed", SAE paper number 932828 and SAE 1993 Transactions, Vol. 102, Sec. 4, pp. 1832-1849.

Gibbs, L.M. (1996), "Gasoline specifications, regulations, and properties", Automotive Engineering, October 1996, pp. 35-40.

Goto, T., Hatamura, K., Takizawa, S., Hayama, N., Abe, H. and Kanesaka, H. (1984), "Development of V6 Miller Cycle Gasoline Engine", SAE paper number 940198.

Grandin, B. (2001), "Knock in Gasoline Engines – the effects of mixture composition on knock onset and heat transfer", Ph.D. Thesis, Chalmers University of Technology, Göteborg, Sweden, 2001.

Grandin, B., Angström, H.-E., Stalhammar, P. and Olofsson, E. (1998), "Knock Suppression in a Turbocharged SI Engine by Using Cooled EGR", SAE paper number 982476.

Grandin, B. and Angström, H.-E. (1999), "Replacing Fuel Enrichment in a Turbo Charged SI Engine: Lean Burn and Cooled EGR", SAE paper number 1999-01-3505.

Grebe, U.D., Larsson, P.-I., Wu, K.-J. (2007), "Comparison of Charging Systems for Spark Ignition Engines", 28th International Vienna Motor Symposium, Vienna, Austria, 26th-27th April, 2007.

- Green, R.M., Cernansky, N.P., Pitz, W.J. and Westbrook, C.K. (1987)**, "The Role of Low Temperature Chemistry in the Autoignition of N-Butane", SAE paper number 872108 and SAE 1987 Transactions, vol. 96, pp. 575-591.
- Griffiths, J.F. and Barnard, J.A. (1995)**, Flame and Combustion, Blackie Academic & Professional, 3rd Edition, 1995, ISBN 0-7514-0199-4.
- Griffiths, J.F., Halford-Maw, P.A. and Mohamed, C. (1997)**, "Spontaneous Ignition Delays as a Diagnostic of the Propensity of Alkanes to Cause Engine Knock", *Combustion and Flame* Vol. 111, pp. 327-337, 1997.
- Gülder, Ö.L. (1982)**, "Laminar Burning Velocities of Methanol, Ethanol and Isooctane-Air Mixtures", Nineteenth Symposium (International) on Combustion/The Combustion Institute, pp. 275-281, 1982.
- Gülder, Ö.L. (1984)**, "Burning Velocities of Ethanol-Isooctane Blends", *Combustion and Flame* Vol. 56, pp. 261-268, 1984.
- Gunston, B. (1995)**, World Encyclopaedia of Aero Engines, Patrick Stephens Limited, Sparkford, Yeoville, Somerset, BA22 7JJ, UK, 1995, 3rd Edition, ISBN 1-85260-509-X.
- Guzzella, L., Wenger, U. and Martin, R. (2000)**, "IC-Engine Downsizing and Pressure-Wave Supercharging for Fuel Economy", SAE paper number 2000-01-1019.
- Hadler, J., Rudolph, F., Engler, H.-J. and Röpke, S. (2007)**, "The New 2.0-l-4V-TDI Engine with Common Rail - Modern Diesel Technology from Volkswagen", *MTZ* 11/2007 Volume 68, pp. 914-923, November 2007.
- Hadler, J., Szengel, R., Middendorf, H., Kuphal, A., Siebert, W. and Hentschel, L. (2009)**, "Minimum consumption - maximum force: TSI technology in the new 1.2l engine from Volkswagen", 30th International Vienna Motor Symposium, Year 2009 Series 12 No./Vol. 697-2 No. 7, Vienna, Austria, 7th-8th May 2009.
- Hagen, D.L. (1977)**, "Methanol as a Fuel: A Review with Bibliography", SAE paper number 770792 and SAE 1977 Transactions, Sec. 4, pp. 2764-2796.
- Haghgooe, M. (1990)**, "Effects of Fuel Octane Number and Inlet Air Temperature on Knock Characteristics of a Single Cylinder Engine", SAE paper number 902134, SAE Fuels and Lubricants Meeting and Exposition, Tulsa, Oklahoma, USA, October 22-25, 1990.

Hammerschlag, R. (2006), "Ethanol's Energy Return on Investment: A Survey of the Literature 1990-Present", *Environmental Science & Technology* Vol. 40, No.6, pp. 1744-1750, 2006.

Hamori, F. and Watson, H.C. (2006), "Hydrogen Assisted Jet Ignition for the Hydrogen Fuelled SI Engine", 16th World Hydrogen Energy Conference, Lyon, France, 13th-16th June, 2006.

Hancock, D., Fraser, N., Jeremy, M., Sykes, R. and Blaxill, H. (2008), "A New 3 Cylinder 1.2l Advanced Downsizing Technology Demonstrator Engine", SAE paper number 2008-01-0611, SAE 2008 World Congress, Detroit, Michigan, USA, April, 2008.

Harvey-Bailey, A. and Piggott D.J. (1993), The Merlin 100 Series – The Ultimate Military Development, Rolls-Royce Heritage Trust Historical Series No. 19, Derby, 1997, ISBN 187292204X.

Hattrell, T., Sheppard, C.G.W., Burluka, A.A., Neumeister, J. and Cairns, A. (2006), "Burn Rate Implications of Alternative Knock Reduction Strategies for Turbocharged SI Engines", SAE paper number 2006-01-1110, SAE 2006 World Congress, Detroit, Michigan, April 2006.

Helmich, M.J. (1966), "Development of Combustion Air Refrigeration System Enabling Reliable Operation at 220psi bmep for a Large Four-Cycle Spark-Ignited Gas Engine", ASME 66-DGEP-7, April 24-28, 1966.

Heywood, J.B. (1988), Internal Combustion Engine Fundamentals, McGraw-Hill Book Company, New York, USA, 1988, ISBN 0-07-028637-X.

Hiereth, H. and Withalm, G. (1979), "Some Special Features of the Turbocharged Gasoline Engine", SAE paper number 790207, SAE 1979 World Congress, Detroit, Michigan, USA, February-March 1979.

Hiroshi, M., Makoto, K., Tetsunori, S. and Shinji, K. (2004), "The Potential of Lean Boost Combustion", FISITA paper number F2004V219, FISITA Conference 2004, Barcelona, Spain.

Hirooka, H., Mori, S. and Shimizu, R. (2004), "Effects of High Turbulence Flow on Knock Characteristics", SAE paper number 2004-01-0977.

Hives, E.W. and Smith, F. LI. (1940), "High Output Aircraft Engines", SAE Transactions, Vol. 46, No. 3, pp. 106-118, March 1940.

Hofmann, P., Kieberger, M., Geringer, B., Willand, J. and Jelitto, C. (2008a), "Release Mechanisms and Influencing Variables on Preignition Phenomena of Highly Boosted SI Engines", 17th Aachen Colloquium, Aachen, Germany, 6th-8th October, 2008, pp. 1019-1038.

Hoffman, W., Wong, V.W., Cheng, W.K. and Morgenstern, D.A. (2008b), " A New Approach to Ethanol Utilization: High Efficiency and Low NO_x in an Engine Operating on Simulated Reformed Ethanol", SAE paper number 2008-01-2415, SAE Powertrains, Fuels and Lubricants Meeting, Rosemont, Illinois, USA, October 2008.

Hoffmeyer, H., Montefrancesco, E., Beck, L., Willand, J., Ziebart, F. and Mauss, F. (2009), "CARE - CAlytic Reformed Exhaust Gases in Turbocharged DISI-Engines", SAE paper number 2009-01-0503, SAE 2009 World Congress, Detroit, Michigan, April 2009.

Hooker, S., Reed, H. and Yarker, A. (1941), The Performance of a Supercharged Aero Engine, Rolls-Royce Limited, Derby, 1941, reprinted by Rolls-Royce Heritage Trust, Derby, 1997, ISBN 1 872 922 11 2.

Hooker, S. (2002), Not much of an Engineer, Airline Publishing, The Crowood Press Ltd, Ramsbury, Marlborough, Wiltshire, SN8 2HR, UK, 2002, ISBN 978 1 85310 285 1.

Horning, H.L. (1931), "The Cooperative Fuel-Research Committee Engine", SAE Transactions, 1931, Vol. 26, pp. 436-440.

Institution of Automobile Engineers (1924), "Report of the Empire Motor Fuels Committee", Volume XVIII, Part I, Session 1923-1924.

Joos, K., Giese, J., Heil, B., Weining, K., Muerwald, M. and Lueckert, P. (2000), "Fortschritt durch Evolution: Neue 4-Zylinder-Ottomotoren von Mercedes-Benz auf Basis des M111", 9th Aachen Colloquium, Aachen, Germany, October 2000.

Joyce, M.J. (1994), "Jaguar's supercharged 6-cylinder engine", Inst. Mech. Engrs paper number C484/054, 1994.

Kalghatgi, G.T. (1990), " Deposits in Gasoline Engines - A Literature Review", SAE paper number 902105 and SAE 1990 Transactions, Vol. 99, Sec. 4, pp. 639-667.

Kalghatgi, G.T. (2001a), "Fuel Anti-Knock Quality - Part I, Engine Studies", SAE paper number 2001-01-3584.

Kalghatgi, G.T. (2001b), "Fuel Anti-Knock Quality - Part II, Vehicle Studies - How Relevant is Motor Octane Number (MON) in Modern Engines?", SAE paper number 2001-01-3585.

Kalghatgi, G.T., Nakata, K. and Mogi, K. (2005), "Octane Appetite Studies in Direct Injection Spark Ignition (DISI) Engines", SAE paper number 2005-01-0244.

Kalghatgi, G.T., Bradley, D., Andrae, J. and Harrison, A.J. (2009), "The nature of "superknock" and its origins in SI engines", IMechE Internal Combustion Engines: Performance, Fuel Economy and Emissions, London, UK, 8th-9th December, 2009.

Kapus, P.E., Fraidl, G.K., Prevedel, K. and Fuerhapter, A. (2007a), "GDI Turbo - The Next Steps", JSAE paper number 20075355 and JSAE 2007 Proceedings No. 84-07, pp.13-16, Yokohama, Japan, 23rd-25th May, 2007.

Kapus, P.E., Fraidl, G.K. and Neubauer, M. (2007b), "Low CO₂ and Fun to Drive - a Contradiction?", 16th Aachen Colloquium, Aachen, Germany, October 2007, pp. 1151-1176.

Kato, S., Nakamura, N., Kato, K. & Ohnaka, H. (1986), "High Efficiency Supercharger Increases Engine Output, Reduces Fuel Consumption Through Computer Control", SAE paper number 861392.

Kawabata, Y., Sakonji, T. and Amano, T. (1999), "The Effect of NO_x on Knock in Spark-Ignition Engines", SAE paper number 1999-01-0572.

Kawahara, N., Tomita, E. and Sakata, Y. (2006), "Visualization of Auto-ignited Kernel during Knocking Combustion in an SI Engine", JSAE 20065192 and JSAE 2006 Proceedings No. 3-06, pp.1-4.

Kemble, E. (1921a), "The Calculated Performance of Airplanes Equipped with Supercharging Engines, Part I: The calculation of performance curves for an airplane engine fitted with a supercharging centrifugal compressor". National Advisory Committee for Aeronautics Report Number 101 Part I, 1921.

Kemble, E. (1921b), "The Calculated Performance of Airplanes Equipped with Supercharging Engines, Part II: The calculation of airplane performance from the estimated performance curves of engine and compressor". National Advisory Committee for Aeronautics Report Number 101 Part II, 1921.

Kerkau, M., Knirsch, S. and Neußer, H.-J. (2006), "The New Six-Cylinder Bi-Turbo Engine with Variable Turbine Geometry for the Porsche 911 Turbo". 27th Vienna Motor Symposium, Vienna, Austria, April 2006.

Kerley, R.V. and Thurston K.W. (1956), "Knocking Behaviour of Fuels and Engines", SAE Transactions, vol. 64, pp. 555-569, 1956.

Kiefer, W., Klauer, N., Krauss, M., Mährle, W. and Schünemann, E. (2004), "The New BMW Inline Six-Cylinder Spark-Ignition Engine Part 2: Thermodynamics and Functional Properties", MTZ worldwide, December 2004, pp. 22-25.

Klauer, N., Klütung, M., Steinparzer, F. and Kretschmer, J. (2009), "Innovative Turbocharging, Variable Valvetrains and 8-Speed Transmissions - A New Generation of Drivetrains", 18th Aachen Colloquium, Aachen, Germany, 5th-7th October, 2009, pp. 1025-1039.

Kleeberg, H., Tomazic, D., Lang, O. and Habermann, K. (2006), "Future Potential and Development Methods for High Output Turbocharged Direct Injected Gasoline Engines", SAE paper number 2006-01-0046.

Klein, R., Breitbach, H., Geratz, K.J. and Senger, W. (1994), "Surface Erosion by High-Speed Combustion Waves", Twenty-Fifth Symposium (International) on Combustion/The Combustion Institute, pp. 95-102, 1994.

Klütting, M., Missy, S. and Schwarz, C. (2005), "Turbocharging of a spray-guided gasoline direct injection combustion system - a good fit?", JSAE paper number 20055412, Yokohama, Japan, May 2005.

Kociba, R. and Parr, M.D. (1991), "The General Motors Supercharged 3800 Engine", SAE paper number 910685.

König, A., Ellinger, K.-W. and Korbel, K. (1985), "Engine Operation on Partially Dissociated Methanol", SAE paper number 850573, SAE 1985 World Congress, Detroit, Michigan, USA, 25th February - 1st March, 1985.

König G., Maly, R.R., Bradley, D., Lau, A.K.C. and Sheppard C.G.W. (1990), "Role of Exothermic Centres on Knock Initiation and Knock Damage", SAE paper number 902136, SAE International Fuels & Lubricants Meeting, Tulsa, Oklahoma, USA, October 1990.

König, G. and Sheppard C.G.W. (1990), "End Gas Autoignition and Knock in a Spark Ignition Engine", SAE paper number 902135, SAE International Fuels & Lubricants Meeting, Tulsa, Oklahoma, USA, October 1990.

Krebs, R., Boehme, J., Dornhoefer, R., Wurms, R., Friedmann, K., Helbig, J. and Hatz, W. (2004), "The New Audi 2.0T FSI Engine - The First Direct Injection Turbo-Gasoline-Engine from Audi", 25th Vienna Motor Symposium, Vienna, Austria, April 2004.

Krebs, R., Szengel, R., Middendorf, H., Fleiß, M., Laumann, A. and Voeltz, S. (2005a), "The New Dual-Charged FSI Petrol Engine by Volkswagen Part 1: Design", MTZ 11/2005 Volume 66, pp. 2-7, November, 2005.

Krebs, R., Szengel, R., Middendorf, H., Sperling, H., Siebert, W., Theobald, J. and Michels, K. (2005b), "The New Dual-Charged FSI Petrol Engine by Volkswagen Part 2: Thermodynamics", MTZ 12/2005 Volume 66, pp. 23-26, December, 2005.

Kremer, F.G. and Fachetti, A. (2000), "Alcohol as Automotive Fuel - Brazilian Experience", SAE paper number 2000-01-1965, CEC/SAE International Spring Fuels & Lubricants Meeting & Exposition, Paris, France, 19th-22nd June, 2000.

Kuhlbach, K., Mehring, J., Borrmann, D. and Friedfeldt, R. (2009), "Cylinder Head with Integrated Exhaust Manifold for Downsizing Concepts", MTZ Vol. 70 pp. 12-17, April 2009.

Lackner, K.S. (2008), "Options for capturing carbon dioxide from the air", 2nd US-China Symposium on CO₂ Emissions Control Science and Technology, Hangzhou, China, 28th-30th May, 2008.

Lake, T., Stokes, J., Murphy, R., Osborne, R. and Schamel, A. (2004a), "Turbocharging Concepts for Downsized DI Gasoline Engines", SAE paper number 2004-01-0036.

Lake, T., Stokes, J. and Murphy, R. (2004b), "Downsized DI Gasoline Engines for Low CO₂" I.Mech.E. Fuel Economy and Engine Downsizing Seminar, London, UK, 13th May, 2004.

Lang, O., Geiger, J., Haberman, K. and Wittler, M. (2005), "Boosting and Direct Injection - Synergies for Future Gasoline Engines", SAE paper number 2005-01-1144.

Lang, O., Habermann, K., Krebber-Hortmann, K., Sehr, A., Thewes, M., Kleeberg, H., Tomasic, D. (2008), "Potential of the Spray-guided Combustion System in Combination with Turbocharging", SAE paper number 2008-01-0139, SAE 2008 World Congress, Detroit, Michigan, USA, 14th-17th April, 2008.

Lee, W. and Schaefer, H.J. (1983), "Analysis of Local Pressures, Surface Temperatures and Engine Damages under Knock Conditions", SAE paper number 830508 and SAE 1983 Transactions, Vol. 92, Sec. 2, pp. 511-523.

Leppard, W.R. (1987), "The Autoignition Chemistry of n-Butane: An Experimental Study", SAE paper number 872150 and SAE 1987 Transactions, Vol. 96, Sec. 7, pp. 934-957.

Leppard, W.R. (1988), "The Autoignition Chemistry of Isobutane: A Motored Engine Study", SAE paper number 881606 and SAE 1988 Transactions, Vol. 97, Sec. 3, pp. 658-680.

Leppard, W.R. (1989), "A Comparison of Olefin and Paraffin Autoignition Chemistries: A Motored-Engine Study", SAE paper number 892081 and SAE 1989 Transactions, Vol. 98, Sec. 4, pp. 879-904.

Leppard, W.R. (1990), "The chemical origin of fuel octane sensitivity", SAE paper number 902137.

Leppard, W.R. (1991), "The Autoignition Chemistries of Octane-Enhancing Ethers and Cyclic Ethers: A Motored Engine Study", SAE paper number 912313 and SAE 1991 Transactions, Vol. 100, Sec. 4, pp. 589-604.

Leppard, W.R. (1992), "The Autoignition Chemistries of Primary Reference Fuels, Olefin/Paraffin Binary Mixtures, and Non-Linear Octane Blending", SAE paper number 922325 and SAE 1992 Transactions, Vol. 101, Sec. 4, pp. 1683-1705.

Levedahl, W.J. (1955), "Multistage Autoignition of Engine Fuels", Fifth Symposium (International) on Combustion/The Combustion Institute, pp. 372-385, 1955.

Li, H., Prabhu, S.K., Miller, D.L. and Cernansky, N.P. (1994a), "The Effects of Octane Enhancing Ethers on the Reactivity of a Primary Reference Fuel Blend in a Motored Engine", SAE paper number 940478.

Li, H., Prabhu, S.K., Miller, D.L. and Cernansky, N.P. (1994b), "Autoignition Chemistry Studies on Primary Reference Fuels in a Motored Engine", SAE paper number 942062.

Li, H. and Karim, G.A. (2006), "Experimental investigation of the knock and combustion characteristics of CH₄, H₂, CO, and some of their mixtures", Proc.

Instn Mech. Engrs Journal of Power and Energy, vol. 220, part A, no. 5, pp. 459-471, 2006.

Lichty, L.C. (1939), "Internal Combustion Engines", McGraw-Hill Book Company, Inc., New York and London, Fifth Edition, Third Impression, 1939.

Lignola, P.G. and Reverchon, E. (1987), "Cool Flames". Prog. Energy Combust. Sci. Vol. 13 pp. 75-96 (1987).

Livengood, J.C. and Wu, P.C. (1955), "Correlation of Autoignition Phenomena in Internal Combustion Engines and Rapid Compression Machines", Fifth Symposium (International) on Combustion/The Combustion Institute, pp. 347-356, 1955.

Lotus Engineering (unknown date), "Lotus Engines - V8", Lotus Engineering, Potash Lane, Hethel, Norwich, Norfolk NR14 8EZ, UK.

Lotus Engineering Software (2005), Lotus Engine Simulation 5.06, current version available at: <http://www.lotuscars.com/engineering/en/lotus-engineering-software>, last accessed 6th April, 2011.

Lotus Engineering Software (2009), "Fuel Mixture Database", proprietary software of Lotus Engineering.

Louis, J.J.J. (2001), "Well-to-Wheel Energy Use and Greenhouse Gas Emissions for Various Vehicle Technologies", SAE paper number 2001-01-1343 and SAE 2001 Transactions, Vol. 110, Sec. 3, pp. 1682-1689.

Lovell, W.G. (1948), "Knocking Characteristics of Hydrocarbons", Ind. Eng. Chem., Vol. 40, pp. 2388-2438, 1948.

Lückert, P., Waltner, A., Rau, E., Vent, G. and Schaupp, U. (2006), "The New V6 Gasoline Engine with Direct Injection by Mercedes-Benz", MTZ 11/2006, Volume 67, pp. 830-840, November 2006.

Ludvigsen, K. (2001), Classic Racing Engines, Haynes Publishing, Sparkford, Somerset, UK, 2001, ISBN 1-85960-649-0.

Lumsden, G., OudeNijeweme, D., Fraser, N. and Blaxill, H. (2009), "Development of a Turbocharged Direct Injection Downsizing Demonstrator Engine", SAE paper number 2009-01-1503, SAE 2009 World Congress, Detroit, Michigan, April 2009.

Lysholm, A.J.R. (1942), "A New Rotary Compressor", Proc. Instn Mech. Engrs Vol. 148, April, 1942.

Maly, R.R., Klein, R., Peters, N. and König, G. (1990), "Theoretical and Experimental Investigations of Knock Induced Surface Destructions", SAE paper number 900025.

Maly, R.R. (1994), "State of the Art and Future Needs in S.I. Engine Combustion", Proceedings of the Twenty-Fifth Symposium (International) on Combustion/The Combustion Institute, pp. 111-124, 1994.

Maly, R. R. and Ziegler, G. (1982), "Thermal Combustion Modeling - Theoretical and Experimental Investigation of the Knocking Process", SAE paper number 820759 and SAE 1982 Transactions, Vol. 91, Sec. 1, pp. 2569-2602.

Manz, P.-W., Daniel, M., Jippa, K.-N. and Willand, J. (2008), "Pre-ignition in highly-charged turbo-charged engines. Analysis procedure and results", AVL 8th International Symposium on Internal Combustion Diagnostics pp. 51-62, Baden-Baden, Germany, June 2008.

Marshall, S.P., Stone, R., Hegheş, C., Davies, T.D. and Cracknell, R.F. (2010), "High pressure laminar burning velocity measurements and modelling of methane and n-butane", Combustion Theory and Modelling Vol. 14, No. 4, pp. 519-540, 2010.

Mason, J.M. and Hesselberg, H.E. (1954), "Engine Knock as Influenced by Precombustion Reactions", SAE Transactions, Vol. 62 pp. 141-150, 1954.

MCE-5 (2010), "MCE-5 VCRi: Pushing back the fuel consumption limits", available at: http://www.mce-5.com/english/key_results.html, last accessed 6th April, 2011.

Metghalchi, M. and Keck, J.C. (1982), "Burning Velocities of Mixtures of Air with Methanol, Isooctane, and Indolene at High Pressure and Temperature", Combustion and Flame Vol. 48, pp. 191-210, 1982.

Meyer, R. (2005), "Turbo Charging BMW's Spray Guided DI-Combustion System - Benefits and Challenges", Global Powertrain Congress, Ann Arbor, Michigan, September, 2005.

Meyer, R.C. and Shahed, S.M. (1991), "An Intake Charge Cooling System for Application to Diesel, Gasoline and Natural Gas Engines", SAE paper number 910420.

Mezger, H. (1978), "Turbocharging Engines for Racing and Passenger Cars", SAE paper number 780718.

Middendorf, H., Krebs, R., Szengel, R., Pott, E., Fleiss, M. and Hagelstein, D. (2005), "Volkswagen introduces the world's first double charge air direct injection petrol engine", 14th Aachen Colloquium, Aachen, Germany, October 2005, pp. 961-986.

Mittal, V. and Heywood, J.B. (2008), "The Relevance of Fuel RON and MON to Knock Onset in Modern SI Engines", SAE paper number 2008-01-2414, SAE Powertrains, Fuels and Lubricants Meeting, Rosemont, Illinois, USA, 7th-9th October, 2008.

Mittal, V. and Heywood, J.B. (2009), "The Shift in Relevance of Fuel RON and MON to Knock Onset in Modern SI Engines Over the Last 70 Years", SAE paper number 2009-01-2622, San Antonio, Texas, USA, November, 2009.

Miyamoto, K., Hoshiba, Y., Hosono, K. and Hirao, S. (2006), "Enhancement of Combustion by Means of Squish Pistons", Mitsubishi Motors Technical Review, No. 18, pp. 32-41, 2006.

Moller, C.E., Johansson, P., Grandin, B. and Lindström, F. (2005), "Divided Exhaust Period - A Gas Exchange System for Turbocharged SI Engines", SAE paper number 2005-01-1150.

Nahum, A., Foster-Pegg, R.W. and Birch, D. (1994), The Rolls-Royce Crecy, Rolls-Royce Heritage Trust, Derby, 1994, ISBN 1-872922-05-8.

Nates, R.J. and Yates, A.D.B. (1994), "Knock Damage Mechanisms in Spark-Ignition Engines", SAE paper number 942064.

Neame, G.R., Gardiner, D.P., Mallory, R.W., Rao, V.K., Bardon, M.F. and Battista, V. (1995), "Improving the Fuel Economy of Stochiometrically Fuelled S.I. Engines by Means of EGR and Enhanced Ignition - A Comparison of Gasoline, Methanol and Natural Gas", SAE paper number 952376, SAE Fuels and Lubricants Meeting and Exposition, Toronto, Canada, October 1995.

Nuglisch, H., Dupont, H., Crenne, D., Krebs, S., Curtis, R., Turner, J. and Coltman, D. (2008), "System Concept Car for CO₂ Reduction Measures", 17th Aachen Colloquium, Aachen, Germany, 6th-8th October 2008, pp. 235-259.

Ohkubo, M., Tashima, S., Shimizu, R., Fuse, S. and Ebino, H., "Developed Technologies of the New Rotary Engine (RENESIS)", SAE paper number 2004-01-1790.

Okamoto, K., Ichikawa, T., Saitoh, K., Oyama, K., Hiraya, K. and Urushihara, T. (2003), "Study of Antiknock Performance Under Various Octane Numbers and Compression Ratios in a DISI Engine", JSAE paper number 20030008 and SAE paper number 2003-01-1804.

Olah, G.A., Goepfert, A. and Prakash, G.K.S. (2006), Beyond Oil and Gas: The Methanol Economy, Wiley-VCH Verlag GmbH & Co. KGaA, Weinheim, Germany, March 2006, ISBN 3-527-31275-7.

Onishi, S., Jo, S.H., Shoda, K., Jo, P.D. and Kato, S. (1979), "Active Thermo-Atmosphere Combustion (ATAC) - A New Combustion Process for Internal Combustion Engines", SAE paper number 790501, SAE 1979 World Congress, Detroit, Michigan, USA, February-March 1979.

Oppenheim, A.K. (1984), "The Knock Syndrome - Its Cures and Its Victims", SAE paper number 841339 and SAE 1984 Transactions, Vol. 92, Sec. 5 pp. 874-883.

Overington, M. T. and de Boer, C.D. (1984), "Vehicle Fuel Economy - High Compression Ratio and Supercharging Compared", SAE paper number 840242.

Owen, K. and Coley, T. (1995), Automotive Fuels Reference Book, Society of Automotive Engineers, Warrendale, PA, 1995, ISBN 1560915897.

Pallotti, P., Torella, E., New, J., Criddle, M. and Brown, J. (2003), "Application of an Electric Boosting System to a Small, Four-Cylinder S.I. Engine", SAE paper number 2003-32-0039.

Pan, J. and Sheppard, C. G. W. (1994), "A Theroetical and Experimental Study of the Modes of End Gas Autoignition Leading to Knock in SI Engines", SAE paper number 942060.

Pannone, G.M. and Johnson R.T. (1989), "Methanol as a Fuel for a Lean Turbocharged Spark Ignition Engine", SAE paper number 890435.

Pastell, D.L. (1950), "Precombustion Reactions in a Motored Engine", SAE Quarterly Transactions, Vol. 4, No. 4 pp. 571-587, 1950.

Patent (1905), "Combustion machine consisting of a compressor (turbine compressor), a piston engine, and a turbine in sequential arrangement", Büchi, A., Winterthur, Switzerland, German patent number 204630, 16th November, 1905.

Patent (1923), "Improvements in or relating to Internal Combustion Engines", Societe Rateau, Paris, France, UK patent number GB179926, 1923.

Patent (1950), "Improvements in or relating to means for supplying air to internal combustion engines for combustion purposes", Bone, G. W., UK patent number UK693688, 1950.

Patent (1977), "Turbocharged Engine After Cooling System and Method", McInerney, C.E., US patent number US4010613, 1977.

Patent (1984), "Supercharger system for an internal combustion engine", Surace, F., UK patent number GB2129055 A, 1984.

Patent (1982), "Method and Device for Intake in Supercharged Engine", Kurihara, N. and Watase, J., Japanese patent number JP58155221 A, 1982.

Patent (1985), "Internal combustion engine", Tosa, Y and Shimoda, K., Japanese patent number JP61234224, 1985.

Patent (2010), "Processing of fuel and recirculated exhaust gas", Turner, J.W.G., UK Patent Application Number 1017229.4, 2010.

Pearce, F. (2006a), "Worst case global warming scenario revealed", New Scientist, 18th February, 2006, pp. 36-41.

Pearce, F. (2006b), "Fuels Gold", New Scientist, 23rd September, 2006, pp. 36-41.

Pearson, R.J. and Turner, J.W.G. (2007), "Exploitation of Energy Resources and Future Automotive Fuels", SAE paper number 2007-01-0034, SAE Fuels and Emissions Conference, Cape Town, South Africa, January 2007.

Pearson, R.J., Turner, J.W.G. and Peck, A.J. (2009a), "Gasoline-ethanol-methanol tri-fuel vehicle development and its role in expediting sustainable organic fuels for transport", 2009 I.Mech.E. Low Carbon Vehicles Conference, London, UK, 20th-21st May, 2009.

Pearson, R.J. Turner, J.W.G., Eisaman, M.D. and Littau, K.A. (2009b), "Extending the Supply of Alcohol Fuels for Energy Security and Carbon Reduction", SAE paper number 2009-01-2764, SAE Powertrain, Fuels and Lubricants Meeting, San Antonio, Texas, USA, 2nd-4th November, 2009.

Peletier, L.A. (1938), "Effect of Air-Fuel Ratio on Detonation in Gasoline Engines", National Advisory Committee for Aeronautics Technical Memorandum

No. 853, Washington, USA, March 1938 (originally published in French at the Second World Petroleum Congress, Paris, June, 1937).

Petitjean, D., Bernardini, L., Middlemass, C. and Shahed, S.M. (2004), "Advanced Gasoline Engine Turbocharging Technology for Fuel Economy Improvements", SAE paper number 2004-01-0988.

Pitz, W.J., Westbrook, C.K. and Leppard, W.R. (1988), "Autoignition Chemistry of N-Butane in a Motored Engine: A Comparison of Experimental and Modeling Results", SAE paper number 881605 and SAE 1988 Transactions, Vol. 97 Sec. 3 pp. 648-657.

Pomeroy, L. (unknown date), "The Background, Layout and Performance of the B.R.M. Engine", Reprinted extracts from The Motor.

Prabhu, S.K., Bhat, R.K., Miller, D.L. and Cernansky, N.P. (1996), "1-Pentene Oxidation and Its Interaction with Nitric Oxide in the Low and Negative Temperature Coefficient Regions", Combustion and Flame Vol. 104, pp. 377-390, 1996.

Price, P., Twiney, B., Stone, R., Kar, K. and Walmsley, H. (2007), "Particulate and Hydrocarbon Emissions Measurements from a Spray Guided Direct Injection Engine with Oxygenate Fuel Blends", SAE paper number 2007-01-0472, SAE 2007 World Congress, Detroit, Michigan, USA, April 2007.

Puzinauskas, P.V. (1992), "Examination of Methods Used to Characterize Engine Knock", SAE paper number 920808.

Quader, A.A. (1976), "What Limits Lean Operation in Spark Ignition Engines - Flame Initiation or Propagation?", SAE paper number 760760 and SAE 1976 Transactions Vol. 85, Sec. 4, pp. 2374-2387, 1976.

Ranini, A. and Monnier, G. (2001), "Turbocharging a Gasoline Direct Injection Engine", SAE paper number 2001-01-0736.

Rassweiler, G.M. and Withrow, L. (1935), "Flame Temperatures Vary with Knock and Combustion-Chamber Position", SAE Transactions, 1935, Vol. 36, No. 4, pp. 125-133.

Rassweiler, G.M. and Withrow, L. (1938), "Motion Pictures of Engine Flames Correlated with Pressure Cards", SAE Transactions, 1938, Vol. 42 pp. 185-204.

Ricardo, H.R. (1919), "Paraffin as Fuel", The Automobile Engineer, Vol. 9, pp. 2-5.

Ricardo, H.R. (1920), "Some possible lines of development in aircraft engines", *Flight & Aircraft Engineer & Mechanic*, pp. 1311-1316, 30th December, 1920.

Ricardo, H.R. and Hempson, J.G.G. (1968), The High-Speed Internal-Combustion Engine, Blackie & Son Limited, 5th Edition, 1968, reprinted by Ricardo plc, Shoreham-by-Sea, 2004.

Richardson, W.L., Barusch, M.R., Kautsky, G.J. and Steinke, R.E. (1961a), "An Improved Gasoline Antidetonant", *Ind. Eng. Chem. Vol. 53, No. 4*, p.305, 1961.

Richardson, W.L., Barusch, M.R., Stewart, W.T. and Kautsky, G.J. (1961b), "Extenders for Tetraethyllead", *Ind. Eng. Chem. Vol. 53, No. 4*, p.306, 1961.

Richardson, W.L., Ryason, P.R., Kautsky, G.J. and Barusch, M.R. (1963), "Organolead Antiknock Agents - Their Performance and Mode of Operation ", Ninth Symposium (International) on Combustion/The Combustion Institute pp. 1023-1033 (1963).

Richter H. and Hemmerlein, N. (1990), "Experiences with supercharging the Porsche 944 engine", *Inst. Mech. Engrs paper number C405/057*, 1990.

Roberts, M. (2003), "Benefits and Challenges of Variable Compression Ratio (VCR)", SAE paper number 2003-01-0398, SAE 2003 World Congress, Detroit, Michigan, USA, March 2003.

Robinson, S., Blunsdon, C.A., Dent, J.C. and Garner, C.P. (1991), "CCD Camera-Computer analysis of flame propagation in a spark ignition engine, and some comparisons with a CFD model", Institution of Mechanical Engineers International Conference on Computers in Engine Technology, Robinson College, Cambridge, UK, 10-12 September, 1991.

Robson, G. (1986), Rallying - The Four-Wheel Drive Revolution, Haynes Publishing, Yeoville, Somerset, UK, 1986, pp. 109-130, ISBN 0854297235.

Rosenkranz, H.G., Watson, H.C., Bryce, W. and Lewis, A. (1986), "Driveability, fuel consumption and emissions of a 1.3 litre turbocharged spark ignition engine developed as a replacement for a 2.0 litre naturally aspirated engine", *Inst. Mech. Engrs paper number C118/86*, 1986.

Roth, D., Sauerstein, R., Becker, M. and Meilinger, R. (2010a), "Application of hybrid EGR systems to turbocharged GDI engines", *MTZ 4/2010, Volume 71*, pp. 12-16, April 2010.

Roth, D., Keller, P. and Sisson, J. (2010b), "Valve-Event Modulated Boost System", SAE paper number 2010-01-1222, SAE 2010 World Congress, Detroit, Michigan, USA, April 2010.

Rothe, M., Heidenreich, T., Spicher, U. and Schubert, A. (2006a), "Knock Behaviour of SI-Engines: Thermodynamic Analysis of Knock Onset Locations and Knock Intensities", SAE paper number 2006-01-0225, SAE 2006 World Congress, Detroit, Michigan, 3rd-6th April, 2006.

Rothe, M., Han, K.-M. and Spicher, U. (2006b), "Investigations on the origin of extreme knocking in SI-engines with direct injection", 15th Aachen Colloquium, Aachen, Germany, October 2006.

Rubbra, A.A. (1990), Rolls-Royce Piston Aero Engines - a designer remembers, Rolls-Royce Heritage Trust, Historical Series No. 16, Derby, 1990, ISBN 1 872922 00 7.

Ryan, T.W. and Lestz, S.S. (1980), "The Laminar Burning Velocity of Isooctane, N-Heptane, Methanol, Methane and Propane at Elevated Temperature and Pressures in the Presence of a Diluent", SAE paper number 800103 and SAE 1980 Transactions, Vol. 89, Sec. 1, pp. 652-664.

Sahetchian, K.A., Blin, N., Rigny, R., Seydi, A. and Murat, M. (1990), "The Oxidation of n-Butane and n-Heptane in a CFR Engine. Isomerization Reactions and Delay of Autoignition", Combustion and Flame Vol. 79, pp. 242-249, 1990.

Sahetchian, K.A., Rigny, R. and Circan, S. (1991), "Identification of the Hydroperoxide Formed by Isomerization Reactions During the Oxidation of n-Heptane in a Reactor and CFR Engine", Combustion and Flame Vol. 85, pp. 511-514, 1991.

Sammons, H. and Chatterton, E. (1955), "The Napier Nomad Aircraft Diesel Engine", SAE 1955 Transactions, Vol. 63, No. 107 pp. 107-131.

Sato, Y., Noda, A. and Sakamoto, T. (1997), "Combustion and NO_x Emission Characteristics in a DI Methanol Engine Using Supercharging with EGR", SAE paper number 971647 and SAE 1997 Transactions, Vol. 106, Sec. 3, pp. 1810-1819.

Sandford, M., Page, G. and Crawford, P. (2009), "The All New AJV8", SAE paper number 2009-01-1060, SAE 2009 World Congress, Detroit, Michigan, USA, 20th-23rd April 2009.

Sauerstein, R., Dabrowski, R., Becker, M., Schmalzl, H.-P. and Christmann, R. (2009), "The Dual-Volute-VTG from BorgWarner - A New Boosting Concept for DI-SI engines", BorgWarner Turbo Systems, 2009.

Sauerstein, R., Becker, M., Bullmer, W. and Dabrowski, R. (2010), "Regulated Two-Stage Turbocharging for gasoline Engines - Matching, Control Strategy and Operating Behaviour", 31st Vienna Motor Symposium, Vienna, Austria, April 2010.

Schausberger, C., Bachmann, P., Borgmann, K., Hofmann, R., and Lieble, J. (2001), "The New BMW Otto Engine Generation", 10th Aachen Colloquium, Aachen, Germany, October 2001.

Schmid, A., Grill, M., Berner, H.-J. and Bargende, M. (2010), "Transient simulation with scavenging in the turbo spark-ignition engine", MTZ 10/2010, Volume 71, pp. 10-15, October 2010.

Schmidt, G.K. and Forster, E.J. (1984), "Modern Refining for Today's Fuels and Lubricants", SAE paper number 841206 and SAE 1984 Transactions, Vol. 93, Sec. 5, pp. 447-456.

Schnittger, W., Konigstein, A., Pritze, S., Popperl, M., Rothenberger, P. and Samstag, M. (2003), "Ecotec 2.2 Direct, New Otto Engine with Direct Injection from Opel", MTZ 12/2003 Volume 64, pp. 1010-1019, 2003.

Schreiber, M., Sadat Sakak, A., Poppe, C., Griffiths, J.F., Halford-Maw, P. and Rose, D.J. (1993), "Spatial Structure in End-Gas Autoignition", SAE paper number 932758 and SAE 1993 Transactions Vol. 102, Sec. 4, pp. 1502-1514.

Schreiber, M., Sadat Sakak, A., Lingens, A. and Griffiths, J.F. (1994), "A Reduced Thermokinetic Model for the Autoignition of Fuels with Variable Octane Ratings", Twenty-Fifth Symposium (International) on Combustion/The Combustion Institute, pp. 933-940, 1994.

Schünemann, E., Langen, P., Missy, S. and Schwarz, C. (2007), "New BMW 6- and 4-Cylinder Petrol Engines with High Precision Injection and Stratified Combustion", JSAE 20075363 and JSAE 2007 Proceedings No. 84-07, pp.1-6, Yokohama, Japan, 23rd-25th May, 2007.

Schwaderlapp, M., Habermann, K. and Yapici, K.I. (2002), "Variable Compression Ratio - A Design Solution for Fuel Economy Concepts", SAE paper number 2002-01-1103.

Sheppard, C.G.W., Tolegano, S. and Woolley, R. (2002), "On the Nature of Autoignition Leading to Knock in HCCI Engines", SAE paper number 2002-01-2831, SAE 2002 World Congress, Detroit, Michigan, USA, February, 2002.

Sheffield, F.C. (1944), "Napier Sabre II", Flight, 23rd March, 1944.

SMMT (2011), "New Car CO2 report 2011 – The 10th Report", March 2011, available at: <https://www.smmt.co.uk/shop/new-car-co2-report-mar-2011/>, last accessed 6th April, 2011.

Spicher, U., Kröger, H. and Ganser, J. (1991), "Detection of Knocking Combustion Using Simultaneously High-Speed Schlieren Cinematography and Multi Optical Fiber Technique", SAE paper number 912312 and SAE 1991 Transactions, Vol. 100, Section 4, pp. 569-588.

Spindt, R.S. (1965), "Air-Fuel Ratios from Exhaust Gas Analysis", SAE paper number 650507 and SAE 1966 Transactions, Vol. 74, Papers 650236-650530, pp. 788-793.

Stansfield, P.A., Wigley, G., Garner, C.P., Patel, R., Ladommatos, N., Pitcher, G., Turner, J.W.G., Nuglisch, H. and Helie, J. (2007), "Unthrottled Engine Operation using Variable Valve Actuation: The Impact on the Flow Field, Mixing and Combustion", SAE paper number 2007-01-1414, SAE 2007 World Congress, Detroit, Michigan, USA, April 2007.

Steinparzer, F., Kratochwill, H., Mattes, W. and Stuetz, W. (2004), "Two Stage Turbocharging for the BMW 3.0 Litre 6-Cylinder Diesel Engine", 13th Aachen Colloquium, Aachen, Germany, October 2004.

Stenlåås, O., Gogan, A., Egnell, R., Sundén, B. and Mauss, F. (2002), "The Influence of Nitric Oxide on the Occurrence of Autoignition in the End Gas of Spark Ignition Engines", SAE paper number 2002-01-2699, SAE Powertrain & Fluid Systems Conference & Exhibition, San Diego, California, USA, October 2002.

Stenlåås, O., Einewall, P., Egnell, R. and Johansson, B. (2003), "Measurement of Knock and Ion Current in a Spark Ignition Engine With and Without NO Addition to the Intake Air", SAE paper number 2003-01-0639.

Stosic, N., Smith, I.K. and Kovacevic, A. (2003), "Opportunities for innovation with screw compressors", Proc. Instn Mech. Engrs Vol. 217 Part E, 2003.

Stokes, J., Lake, T.H. and Osborne, R.J. (2000), "A Gasoline Engine Concept for Improved Fuel Economy - The Lean Boost System", SAE paper number 2000-01-2902, SAE International Fuels and Lubricants Meeting and Exposition, Baltimore, Maryland, October 2000.

Swarts, A., Yates, A., Viljoen, C. and Coetzer, R. (2005), "A Further Study of Inconsistencies between Autoignition and Knock Intensity in the CFR Octane Rating Engine", SAE paper number 2005-01-2081 and SAE 2005 Transactions Vol. 114, Sec. 4, pp. 702-720.

Swarts, A. (2006), "Insights relating to octane rating and the underlying role of autoignition", Ph.D. thesis, University of Cape Town, February 2006.

Swarts, A. and Yates, A.D.B. (2007), "Insights into the role of autoignition during octane rating", SAE paper number 2007-01-0008, SAE Fuels and Emissions Conference, Cape Town, South Africa, January 2007.

Sweetland, P. and Grissom, T. (2003), "Regulated 2-Stage (R2S) Charging Systems for Future Passenger Car and LDV Diesel Engines". Global Powertrain Congress, Ann Arbor, Michigan, US, September 2003.

Szengel, R., Middendorf, H., Pott, E., Theobald, J., Etzrodt, T. and Krebs, R. (2007), "The TSI with 88 kW - the expansion of the Volkswagen family of fuel-efficient gasoline engines", 28th International Vienna Motor Symposium, Vienna, Austria, 26th-27th April, 2007.

Taitt, D.W., Garner, C.P., Swain, E., Pearson, R.J., Bassett, M.D., and Turner, J.W.G. (2005), "An Automotive Engine Charge-Air Intake Conditioner System: 1st Law Thermodynamic Analysis of Performance Characteristics", Proc. Instn Mech. Engrs Journal of Automotive Engineering, Vol. 219, Part D, no. 6, pp. 389-404, 2005.

Taitt, D.W., Garner, C.P., Swain, E., Blundell, D., Pearson, R.J. and Turner, J.W.G. (2006), "An Automotive Engine Charge-Air Intake Conditioner System: Analysis of Fuel Economy Benefits in a Gasoline Engine Application", Proc. Instn Mech. Engrs Journal of Automotive Engineering, Vol. 220, Part D, no. 9, pp. 1293-1307, 2006, ISSN: 0954-4070.

Tanaka, S., Ayala, F., Keck, J.C. and Heywood, J.B. (2003), "Two-stage ignition in HCCI combustion and HCCI control by fuels and additives", Combustion and Flame Vol. 132, pp. 219-239 (2003).

Tashima, S., Okimoto, H., Fujimoto, Y. and Nakao, M. (1994), "Sequential Twin Turbocharged Rotary Engine of the Latest RX-7", SAE paper number 941030.

Taylor, D.R. (1999), Boxkite to Jet - the remarkable career of Frank B Halford, Rolls-Royce Heritage Trust Historical Series No. 28, Derby, UK, 1999, ISBN 1 872922 16 3.

Taylor, P.H., Cheng, L. and Dellinger, B. (1998), "The Influence of Nitric Oxide on the Oxidation of Methanol and Ethanol", *Combustion and Flame* Vol. 115, pp. 561-567, 1998.

Taylor, J., Fraser, N. and Wieske, P. (2010), "Water Cooled Exhaust Manifold and Full Load EGR Technology applied to a Downsized Direct Injection Spark Ignition Engine", SAE paper number 2010-01-0356, SAE 2010 World Congress, Detroit, Michigan, USA, April 2010.

Thomson, W. (1978), Fundamentals of Automotive Engine Balance, Mechanical Engineering Publishing Ltd, London, UK, 1978, ISBN 0-85298-409-X.

Tizard, H.T. and Pye, D.R. (1922), "Experiments on the Ignition of Gases by Sudden Compression", *Philosophical Magazine* Vol. 44, pp. 79-121, 1922.

Torella, E., Fiorenza, R., Durante, D., Pirelli, M. and Roffina, G. (2001), "FIRE 1.2l 16V Turbo: A downsizing concept for reducing fuel consumption", Paper number 01A5008, ATA High Performance Engines Seminar, Stresa, Italy, October 2001.

Turner, J.W.G. (1996), Lotus V8 development notes, proprietary to Lotus Engineering.

Turner, J.W.G. and Pearson, R.J. (2001), "High Output Supercharging without Intercooling: Theory and Results", Paper number 01A5006, ATA High Performance Engines Seminar, Stresa, Italy, October 2001.

Turner, J.W.G. and Pearson R.J. (2002a), "Improving Fuel Consumption through Turboexpansion", Presentation to the Universities Internal Combustion Engines Group (UnICEG) at the Motor Industry Research Association, Hinckley, Leicestershire, UK, 17th April, 2002.

Turner, J.W.G. and Pearson R.J. (2009), "The turbocharged direct-injection spark-ignition engine", in Zhao. H. (ed.), Direct injection combustion engines for automotive applications: Science and technology. Part 1: Spark-ignition engines,

Woodhead Publishing Limited, Cambridge CB21 6AH, UK, 2009, ISBN 1-84569-389-2.

Turner J.W.G., Blundell D.W., Bassett M.D., Pearson R.J. and Chen R. (2002b), "The Impact on Engine Performance of Controlled Auto Ignition versus Spark Ignition with Two Methods of Load Control", Global Powertrain Congress, Ann Arbor, Michigan, September 2002.

Turner, J.W.G., Pearson, R.J., Bassett, M.D. and Oscarsson, J. (2003), "Performance and Fuel Economy Enhancement of Pressure Charged SI Engines through Turboexpansion – An Initial Study", SAE paper number 2003-01-0401 and SAE 2003 Transactions, June 2004.

Turner, J.W.G., Bassett, M.D., Pearson, R.J., Pitcher, G.F., and Douglas, K. (2004a), "New Operating Strategies Afforded by Fully Variable Valve Trains", SAE paper number 2004-01-1386 and SAE 2004 Transactions, July 2005.

Turner, J.W.G., Kenchington, S.A. and Stretch, D.A. (2004b), "Production AVT Development: Lotus and Eaton's Electrohydraulic Closed-Loop Fully Variable Valve Train System", 25th Vienna Motor Symposium, Vienna, Austria, April 2004.

Turner, J.W.G., Pearson, R.J. and Parrott, A. (2004c), "The Performance of a High Compression Ratio, High Speed Supercharged Engine", Global Powertrain Congress, Dearborn, Detroit, Michigan, September 2004.

Turner, J.W.G., Pearson, R.J., Bassett, M.D., Blundell, D.W. and Taitt, D.W. (2005a), "The Turboexpansion Concept - Initial Dynamometer Results", SAE paper number 2005-01-1853.

Turner, J.W.G., Pearson, R.J. and Kenchington, S.A. (2005b), "Concepts for Improved Fuel Economy from Gasoline Engines", JER03504, Int. J. Engine Res. Vol. 6, 2005.

Turner, J.W.G., Burke, P., Balding, A. and Osborne, K. (2005c), "Concepts to Reduce Architectural Complexity and Mass in Reciprocating Engines", 6th Lean Weight Vehicle Conference, Warwick, UK, December 2005.

Turner, J.W.G., Pitcher, G., Burke, P., Garner, C.P., Wigley, G., Stansfield, P., Nuglisch, H., Ladommatos, N., Patel, R. and Williams, P. (2006a), "The HOTFIRE Homogeneous GDI and Fully Variable Valve Train Project - An Initial Report", SAE paper number 2006-01-1260.

Turner, J.W.G., Kalafatis, A. and Atkins, C. (2006b), "The Design of the NOMAD Advanced Concepts Research Engine", SAE paper number 2006-01-0193, SAE 2006 World Congress, Detroit, Michigan, USA, April 2006.

Turner, J.W.G., Pearson, R.J., Milovanovic, N. and Taitt, D. (2006c), "Extending the knock limit of a turbocharged gasoline engine via turboexpansion", 8th I.Mech.E. Conference on Turbochargers and Turbocharging, London, May 2006.

Turner, J.W.G., Pearson, R.J. and Milovanovic, N. (2006d), "Reducing the Octane Appetite of Pressure-Charged Gasoline Engines using Charge Air Conditioning Systems", JSAE paper number 20065414, Yokohama, Japan, May 2006 and JSAE Transactions No. 3-06, pp.11-16.

Turner, J.W.G., Pearson, R.J., Holland, B. and Peck, B. (2007a), "Alcohol-Based Fuels in High Performance Engines", SAE paper number 2007-01-0056, SAE Fuels and Emissions Conference, Cape Town, South Africa, January 2007.

Turner, J.W.G., Peck, B. and Pearson, R.J. (2007b), "Flex-Fuel Vehicle Development to Promote Synthetic Alcohols as the Basis of a Potential Negative-CO₂ Energy Economy", SAE paper number 2007-01-3618, 14th Asia-Pacific Automotive Engineering Conference, Los Angeles, California, USA, August 2007.

Turner, J.W.G., Coltman, D., Curtis, R., Blake, D., Holland, B., Pearson, R.J., Arden., A. and Nuglisch, H. (2008a), "Sabre: A Direct Injection 3-Cylinder Engine with Close-Spaced Direct Injection, Swirl-Enhanced Combustion and Complementary Technologies", JSAE paper number 20085014 and JSAE 2008 Proceedings No. 79-08, pp.5-10, ISSN 0919-1364, JSAE 2008 Congress, Yokohama, Japan, 21st-23rd May 2008.

Turner, J.W.G., Pearson, R.J., Curtis, R. and Holland B. (2008b), "Improving Fuel Economy in a Turbocharged DISI Engine Already Employing Integrated Exhaust Manifold Technology and Variable Valve Timing", SAE paper number 2008-01-2449, SAE International Powertrains, Fuels and Lubricants Meeting, Rosemont, Illinois, USA, October 2008.

Turner, J.W.G., Pearson, R.J., Curtis, R. and Holland B. (2009), "Effects of Cooled EGR Routing on a Second-Generation DISI Turbocharged Engine employing an Integrated Exhaust Manifold", SAE paper number 2009-01-1487, SAE 2009 World Congress, Detroit, Michigan, USA, April 2009.

Turner, J.W.G., Blundell, D.W., Pearson, R.J., Patel, R., Larkman, D.B., Burke, P., Richardson, S., Green, N.M., Brewster, S., Kenny R.G., and Kee R.J. (2010a), "Project Omnivore: A Variable Compression Ratio ATAC 2-Stroke Engine for Ultra-Wide-Range HCCI Operation on a Variety of Fuels", SAE paper number 2010-01-1249, SAE 2010 World Congress, Detroit, Michigan, USA, April 2010.

Turner, J.W.G., Blake, D., Moore, J., Burke, P., Pearson, R.J., Patel, R., Blundell, D.W., Chandrashekar, R.B., Matteucci, L., Barker, P. and Card, C.A. (2010b), "The Lotus Range Extender Engine", SAE paper number 2010-01-2208, SAE Powertrains, Fuels and Lubricants Meeting, San Diego, California, USA, 25th-27th October, 2010.

Turner, J.W.G., Pearson, R.J., Purvis, R., Dekker, E., Johansson, K. and Bergström, K. ac (2011), "GEM Ternary Blends: Removing the Biomass Limit by using Iso-Stoichiometric mixtures of Gasoline, Ethanol and Methanol", SAE paper number 2011-24-0113, The 10th International Conference on Engines and Vehicles, Capri, Naples, Italy, 11th-16th September, 2011.

Tuttle, J.H. (1980), "Controlling Engine Load by Means of Late Intake-Valve Closing", SAE paper number 800794.

Tuttle, J.H. (1982), "Controlling Engine Load by Means of Early Intake-Valve Closing", SAE paper number 820408.

Ueda, T., Okumura, T., Sugiura, S. and Kojima, S. (1999), "Effects of Squish Area Shape on Knocking in a Four-Valve Spark Ignition Engine", SAE paper number 1999-01-1494, SAE International Fuels & Lubricants Meeting & Exposition, Dearborn, Michigan, USA, May 1999.

Unknown Author (1958), "Latham Supercharger", Automobile Engineer, January 1958.

Uthoff, L.H. and Yakimow, J.W. (1987), "Supercharger versus Turbocharger in Vehicle Applications", SAE paper number 870704.

Vancoillie, J., Verhelst, S. and Demuyneck, J. (2011), "Laminar burning velocity correlations for methanol-air and ethanol-air mixtures valid at SI engine conditions", SAE paper number 2011-01-0846, SAE 2011 World Congress, Detroit, Michigan, USA, 12th-14th April, 2011.

- Vandeman, J.E. and Heinecke. O.H. (1945)**, “Effect of Water-Alcohol Injection and Maximum-Economy Spark Advance on Knock-Limited Performance and Fuel Economy of a Large Air-Cooled Cylinder”, National Advisory Committee for Aeronautics Report Number E-264, originally issued as Memorandum Report No. E5H12, August 1945.
- Verhelst, S., Sierens, R. and Verstraeten, S. (2006)**, “A Critical Review of Experimental Research on Hydrogen Fueled SI Engines”, SAE paper number 2006-01-0430, SAE 2006 World Congress, Detroit, Michigan, April 2006.
- Viljoen, C.L., Yates, A.D.B., Swarts, A., Balfour, G. and Möller, K. (2005)**, “An Investigation of the Ignition Delay Character of Different Fuel Components and an Assessment of Various Autoignition Modelling Approaches”, SAE paper number 2005-01-2084 and SAE 2005 Transactions, Vol. 114, Sec. 4, pp. 748-763.
- Viljoen, C.L., Yates, A.D.B., and Coetzer, R.L.F. (2007)**, “A Molecular Investigation of Selected Gasoline Molecules to Relate Oxidation Pathways to their Autoignition Behaviour”, SAE paper number 2007-01-0005, SAE Fuels and Emissions Conference, Cape Town, South Africa, January 2007.
- Walzer, P. (2001)**, “Future Power Plants for Cars”, SAE paper number 2001-01-3192, SAE Automotive and Transportation Technology Congress and Exposition, Barcelona, Spain, 2001.
- Watson, N. and Janota, M.S. (1986)**, Turbocharging the Internal Combustion Engine, MacMillan Education Ltd, Basingstoke, Hampshire, UK, 1986, ISBN 0-333-24290-4.
- Weber, H.-J., Mack, A. and Roth, P. (1994)**, “Combustion and Pressure Wave Interaction in Enclosed Mixtures Initiated by Temperature Nonuniformities”, *Combustion and Flame*, Vol. 97, pp. 281-295.
- Website (2002)**, <http://www.arb.ca.gov/cc/ccms/documents/ab1493.pdf>, last accessed 6th April, 2011.
- Website (2006a)**, http://science.nasa.gov/headlines/y2004/05mar_arctic.htm, last accessed 6th April, 2011.
- Website (2006b)**, http://unfccc.int/kyoto_protocol/items/2830.php, last accessed 6th April, 2011.

Website (2011a), <http://www.scania.com/products-services/trucks/main-components/engines/engine-technology/turbocompound/index.aspx>, last accessed 6th April, 2011.

Website (2011b), http://www.dresserwaukesha.com/documents/1262_1009.pdf, last accessed 6th April, 2011.

Westbrook, C.K. (2000), "Chemical Kinetics of Hydrocarbon Ignition in Practical Combustion Systems", Proceedings of the Combustion Institute, Vol. 28, pp. 1563-1577, 2000.

Westbrook, C.K. and Dryer, F.L. (1980), "Prediction of Laminar Flame Properties of Methanol-Air Mixtures", Combustion and Flame Vol. 37, pp. 171-192, 1980.

Westbrook, C.K., Warnatz, J. and Pitz, W.J. (1988), "A Detailed Chemical Kinetic Reaction Mechanism for the Oxidation of Iso-Octane and n-Heptane Over an Extended Temperature Range and Its Application to Analysis of Engine Knock", Twenty-Second Symposium (International) on Combustion/The Combustion Institute (1988), pp. 893-901, 1988.

Westbrook, C.K., Pitz, W.J. and Leppard, W.R. (1991), "The Autoignition Chemistry of Paraffinic Fuels and Pro-Knock and Anti-Knock Additives: A Detailed Chemical Kinetic Study", SAE paper number 912314 and SAE 1991 Transactions, Vol. 100, Sec. 4, pp. 605-622.

Westin, F. (2005), "Simulation of turbocharged SI-engines - with focus on the turbine", Ph.D. Thesis, KTH School of Industrial Engineering and Management, Sweden, 2005.

Westin, F., Grandin, B. and Angström H.-E. (2000), "The Influence of Residual Gases on Knock in Turbocharged SI-Engines", SAE paper number 2000-01-2840.

Welter, A., Unger, H., Hoyer, U., Brüner, T. and Kiefer, W. (2006), "The new turbocharged BMW six cylinder inline petrol engine", 15th Aachen Colloquium, Aachen, Germany, October 2006.

Whelan, C. D. and Rogers, R. A. (2005), "Turbo-Cooling Applied to Light Duty Vehicle Engines", Polish Scientific Society of Combustion Engines Congress 2005, Bielsko-Biala, Poland, 25-28 September, 2005.

Whelan, C. D. and Rogers, R. A. (2006), "Turbo-cooling applied to light duty vehicle engines", 8th I.Mech.E. Conference on Turbochargers and Turbocharging, London, May 2006.

Whitaker, P., Shen, Y., Spanner, C., Fuchs, H., Agarwal, A. and Byrd, K. (2010), "Development of the Combustion System for a V8 Flexible Fuel Turbocharged Direct Injection Engine", SAE paper number 2010-01-0585, SAE 2010 World Congress, Detroit, Michigan, USA, April 2010.

Whitford, R. (2000), Fundamentals of Fighter Design, Airlife Publishing Ltd, Shrewsbury, SY3 9EB, UK, 2000, ISBN 1-84037-112-9.

Willand, J., Daniel, M., Montefrancesco, E., Geringer, B., Hofmann, P. and Kieberger, M. (2009), "Limits on Downsizing in Spark Ignition Engines due to Pre-ignition", MTZ Vol. 70, pp. 56-61, May 2009.

Winterbone, D.E. and Pearson, R.J. (1999), Design Techniques for Engine Manifolds: Wave Action Methods for IC Engines, Professional Engineering Publishing Limited, Northgate Avenue, Bury St Edmunds, IP32 6BW, UK, 1999, ISBN 1 86058 179 X.

Wirth, M., Mayerhofer, U., Piock, W. and Fraidl, G. (2000), "Turbocharging the DI Gasoline Engine", SAE paper number 2000-01-0251.

Wood, S.P. and Bloomfield, J.H. (1990), "Clean Power - Lotus 2.2 Lt Chargecooled Engine", SAE paper number 900269.

Wurms, R., Grigo, M. and Hatz, W. (2003), "Audi FSI Technology - Improved performance and reduced fuel consumption", ATA Vol. 56 no. 3 / 4 March-April 2003.

Wurms, R., Kuhn, M., Zeilbeck, A., Adam, S., Krebs, R. and Hatz, W. (2004), "The Audi Turbo FSI Technology", 13th Aachen Colloquium, Aachen, Germany, October 2004.

Wurms, R., Dengler, S., Budack, R., Mendl, G. Dicke, T. and Eiser, A. (2006), "Audi Valvelift System - A New Innovative Valve Train System Designed by Audi", 15th Aachen Colloquium, Aachen, Germany, October 2006, pp. 1069-1093.

Wurms, R., Budack, R., Böhme, J., Dornhöfer, R., Eiser, A. and Hatz, W. (2008), "The New 2.0L TFSI with the Audi Valvelift System for the Audi A4 - The Next Generation of the Audi TFSI Technology", 17th Aachen Colloquium, Aachen, Germany, 6th-8th October, 2008, pp. 1067-1089.

Wyszynski, L.P., Stone, C.R. and Kalghatgi, G.T. (2002), "The Volumetric Efficiency of Direct and Port Injection Gasoline Engines with Different Fuels", SAE paper number 2002-01-0839.

Yamamoto, K., Rotary Engine, Sankaido Publishing Co. Ltd., 1st Ed., Tokyo, 1981.

Yates, A.D.B., Viljoen, C.L. and Swarts, A. (2004), "Understanding the Relation Between Cetane Number and Combustion Bomb Ignition Delay Measurements", SAE paper number 2004-01-2017.

Yates, A.D.B., Swarts, A. and Viljoen, C.L. (2005), "Correlating Auto-Ignition Delays And Knock-Limited Spark-Advance Data For Different Types of Fuel", SAE paper number 2005-01-2083 and SAE 2005 Transactions, Vol. 114, Sec. 4, pp. 735-747.

Yates, A.D.B., Viljoen, C. and Metcalf, O. (2007), "An Accurate Determination of the Cetane Number Value of GTL Diesel", SAE paper number 2007-01-0026, SAE Fuels and Emissions Conference, Cape Town, South Africa, 23-25 January, 2007.

Zaccardi, J.-M., Duval, L. and Pagot, A. (2009a), "Development of Specific Tools for Analysis and Quantification of Pre-ignition in a Boosted SI Engine", SAE paper number 2009-01-1795, SAE International Powertrains, Fuels and Lubricants Meeting, Florance, Italy, June 2009.

Zaccardi, J.-M., Lecompte, M., Duval, L. and Pagot, A. (2009b), "Pre-ignition in Highly Charged Spark Ignition Engines - Visualisation and Analysis", MTZ Vol. 70, pp. 40-47, December 2009.

Zel'dovich, Y.B., Librovich, V.B., Makhviladze, G.M. and Sivashinsky, G.I. (1970), "On the development of detonation in a non-uniformly preheated gas", *Astronautica Acta*, Vol. 15, Issue 5-6, pp. 313-321, November 1970.

Zhao, F., Harrington, D. L. and Lai, M.-C. (2002), Automotive Gasoline Direct-Injection Engines, Society of Automotive Engines, Inc., Warrendale, Pennsylvania, USA, 2002, ISBN 0-7680-0882-4.

Zhao, H. (ed.) (2007), HCCI and CAI engines for the automotive industry, Woodhead Publishing Limited, Cambridge CB21 6AH, UK, 2007, ISBN 978-1-84569-128-8.

Appendix I: Original Spreadsheet for Turboexpansion Concept

Figure A1.1 is a reproduction of the original spreadsheet thermodynamic model constructed in Microsoft Excel and used to calculate plenum conditions that may be expected when a turboexpansion system is used. This spreadsheet was fundamental in persuading management to invest in the Nomad research engine.

Spreadsheet to Calculate the Effect of Turboexpansion		
General		
Atmospheric Temperature:	20 degC =	293 K
Atmospheric Pressure:	100 kPa	
Atmospheric Density:	1.18 kg/m3	
Compressor Isentropic Efficiency:	0.7	
Pressure after Compression Stage (Gauge):	200 kPa	
Pressure Ratio of Compression Stage:	3.00	
Desired Boost at Engine (Gauge):	125 kPa	
Expansion Ratio:	1.33 (1 = No Expander)	
Expander Isentropic Efficiency:	0.65	
Intercooler Effectiveness:	0.9	0.9 = Chargecooler Assumed
Cp for Air:	1.01 kJ/kgK	
Gamma for Air:	1.4	
Specific Gas Constant:	288.6 J/kgK	
Expander Mechanical Efficiency:	0.98	
Mass Airflow	0.2 g/s	
Conditions After Compression		
Isentropic Outlet Temperature:	128.0 degC =	401.0 K
Actual Outlet Temperature:	174.3 degC =	447.3 K
Actual Outlet Density:	2.32 kg/m3	
Compressor Power:	155.9 kW per unit mass air flow	
Conditions After Intercooling		
Temperature Post-Intercooler:	35.4 degC =	308.4 K
Post-Intercooler Density:	3.37 kg/m3	
Temperature Drop through Intercooler:	138.9 degC	
Conditions After Expansion		
Isentropic Outlet Temperature:	11.1 degC =	284.1 K
Actual Outlet Temperature:	19.6 degC =	292.6 K
Temperature Drop through Expander:	15.8 degC	
Actual Outlet Density:	2.66 kg/m3	
Expander Power:	16.0 kW per unit mass air flow	
	3.2 kW	4.3 bhp
Actual Outlet Density:	2.66 kg/m3	
Net Compression Work:	140.2 kW per unit mass air flow	
Key Facts for this Case:		
Plenum Temperature	19.6 degC	
Plenum Density	2.66 kg/m3	
Density Ratio	2.25 :1	
Difference between Expansion and Compression Stage Work (-ve means turbine needs assistance)	-140.2 kW per unit mass air flow	
Power input required:	-28.0 kW	-37.6 bhp

Fig. A1.1: Original turboexpansion spreadsheet written in Excel

Appendix II: Notes on Accuracy of Results

All of the results reported in this thesis were gathered in the test cells of Lotus Engineering. As such they are all subject to the normal Lotus quality procedures, which includes frequent calibration of the various pieces of test equipment to ensure that traceable accuracy is maintained to ISO 9001:2008. There follows some details on the accuracy of the individual pieces of equipment used:

Supplier: Froude Consine

Dynamometers: Torque Calibration for AG30 Dynamometer: ± 0.3 Nm
Torque Calibration for AG150 HS Dynamometer: ± 1.25 Nm (AG150 HS torque range 500 Nm)

Thermocouples: K-type with a range of 0 to 300°C: $\pm 0.05\%$
K-type with a range of 0 to 1000°C: $\pm 0.2\%$

Pressure gauges: $\pm 0.1\%$ of full scale (ranges supplied: 0 to 150, 250, 500, 1000 kPa)

Supplier: ECM

Air-fuel ratio meter: ECM AFRecorder 2400 unit: ± 0.1 in the range of 10 to 18 for air-fuel ratio, spark angle accuracy: ± 1 degree

Supplier: Maywood

Load cell: Accurate to 0.03% of full scale deflection

Supplier: Lab Facility

Thermocouples: K-Type (Class A): accurate to $\pm 1.5^\circ\text{C}$ in the -40 to 1000°C range

Supplier: Micro Cal

Calibration unit: $\pm 0.2^\circ\text{C}$ for a range of 0 to 960°C

Supplier: Eurotherm

Calibration unit: 0.1% of full scale deflection

Supplier: Druck

Pressure transducers: DPI 610: +/- 0.025% of full-scale deflection for 1 to 10000 psi (0.069 to 689 bar)

DPI 601: +/- 0.05% of full-scale deflection for 35 to 70 bar ranges and +/- 0.01% for 35 to 700 bar ranges

Supplier: AVL

Fuel weighers: Type 733 and 733s: +/- 0.12% of the measured value

Supplier: Vaisala

Humidity probe: +/- 2%

Calibration unit: HMI 41 and probe: +/- 2%

As an example of the effect of the above component accuracies on the results given in this thesis, consider the case of the operation of the Sabre engine at its best operating condition with cooled EGR delivered via the high-pressure loop. From Chapter 8 this was 255.7 g/kWh with 8% EGR. At this condition the BMEP was 16.8 bar and the torque consequently 200.4 Nm. A Froude Consine AG150 HS dynamometer was used, with a manufacturer-quoted accuracy of +/- 1.5 Nm, meaning a maximum over- or under-reading of the torque value of 0.75%. Combined with the +/- 0.12% accuracy of the AVL fuel weighers this implies a maximum error in BSFC of +/- 0.87%. Thus the maximum range on BSFC is 2.2 g/kWh, ~20% of the improvement shown in Figure 8.14.

Appendix III: Further Details of the CFR Fuels Testing Engine

As discussed in Chapter 3, the CFR™ engine is the standard test engine for fuels testing. It was originally designed in 1928 to a specification laid down by the Cooperative Fuels Research committee, after which it takes its name (Baxter and Yeo, unknown date). The engine is manufactured by the DresserWaukesha division of Dresser, Inc., and has remained largely standard since it was presented on 14th January 1929 at the Society of Automotive Engineers's annual meeting.

For interest, various specifications and illustrations of the engine are included in this appendix, all kindly provided compliments of DresserWaukesha. Table A3.1 shows general specifications as given in the CFR Operation and Maintenance Manual (DresserWaukesha, 2003). The engine has a swept volume of 37.33 cubic inches (611.7 cm³). It has two overhead valves and a side-mounted spark plug, giving a long flame travel and a significant volume of end gas a long distance from the point of ignition. As such, it can immediately be seen that, in general architectural terms, the CFR engine has little in common with modern SI engines.

One of the key characteristics of the engine is that the compression ratio is continuously variable and that, as it is being adjusted, the valve timing stays constant. The manner in which this is achieved is discernible in Figure A3.1. Figure A3.2 shows the dial gauge indicator used to read the position of the cylinder barrel and hence determine the compression ratio. Another unusual feature of the engine is that it is of monoblock construction, with the barrel and head constructed in one piece, i.e. it does not have a separate cylinder head gasket and attendant cylinder head bolts. Also, another key difference to modern engines is that it has an evaporative cooling system.

Table A3.1: General specifications of the CFR™ fuels rating engine. (Information kindly supplied compliments of DresserWaukesha)

Item	Description
Crankcase type and material	Model CFR-48D, cast iron
Cylinder type and material	Flat combustion surface, integral cooling jacket, cast iron
Bore	3.250 inches (82.55 mm)
Stroke	4.500 inches (114.30 mm)
Swept volume	37.33 cubic inches (611.7 cm ³)
Compression ratio	Continuously variable between 4:1 and 18:1
Compression ratio adjustment mechanism	Cranked worm shaft with worm wheel drive in cylinder clamping sleeve
Valvetrain	Overhead valve
Valve mechanism	Pushrod with open rocker assembly and linkage for constant valve clearance and timing as CR is adjusted
Intake valve	Stellite faced with 180° shroud and anti-rotation pin
Exhaust valve	Stellite faced without shroud
Ring pack	Top: chrome plated, straight sided 2 nd , 3 rd and 4 th compression rings: ferrous, straight sided Oil control: one-piece slotted cast iron
Camshaft overlap:	5°CA
Fuel system	Single-jet carburetter with vertical jet and adjustable float chamber level to vary AFR; graduated sight glass for fuel level observation
Carburetter venturi diameters	F1 specification (RON test): 9/16 inch F2 specification (MON test): dependent on altitude: 9/16 inch from sea level to 1600 feet, 19/32 inch for 1600 to 3300 feet, ¾ inch over 3300 feet
Ignition system	Electronic capacitive discharge
Ignition timing	F1 specification (RON test): 13° BTDC F2 specification (MON test): variable (see Figure 3.7); basic setting 26° BTDC at 5:1 CR
Intake air humidity	Controlled by ice tower or refrigeration
Intake mixture heating	F1 specification (RON test): none F2 specification (MON test): electrical heater in intake manifold

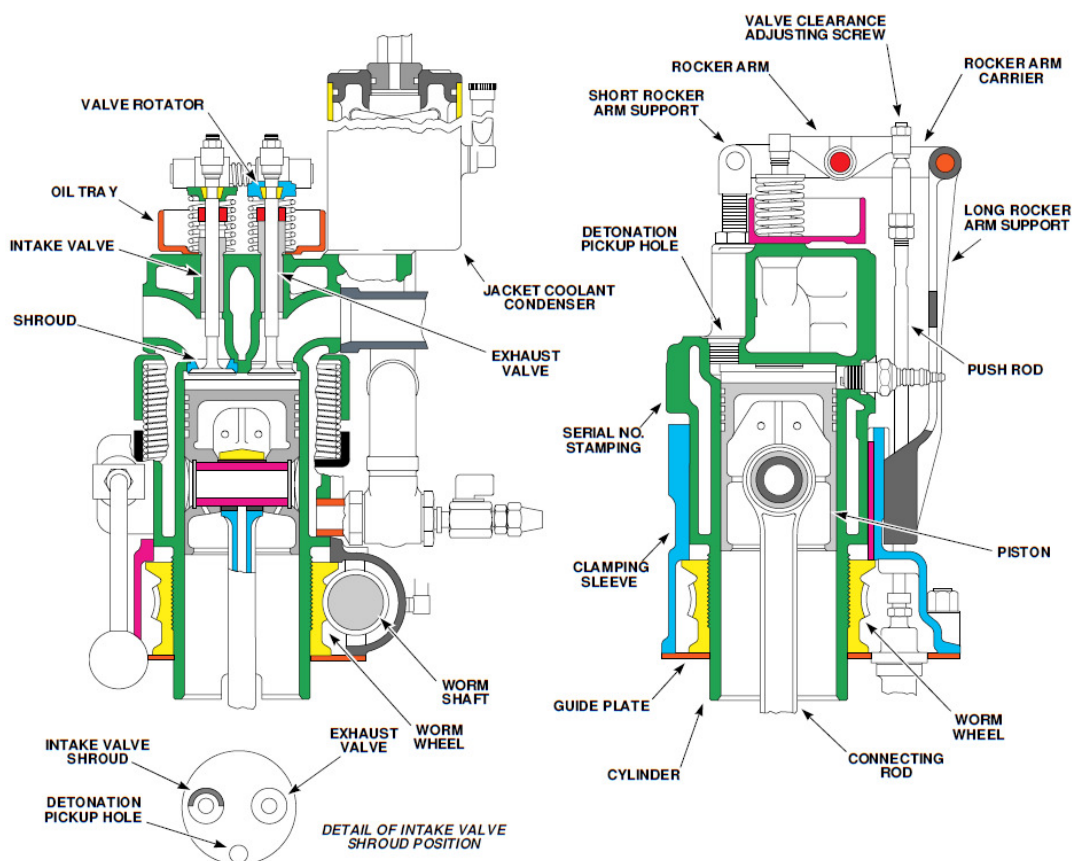


Fig A3.1: Sections of the CFR™ fuels rating engine in F1/F2 specification for RON and MON testing. (Illustration provided compliments of DresserWaukesha)

Horning (1931) describes the engine in its original form and also some of the early modifications to improve its fitness for purpose. Importantly, these relate to the mechanical specification, and the combustion chamber, ports, valve timing etc. have been kept constant, meaning that results from one engine over the last 80+ years should be comparable to any other over the same period. The 'F1/F2' specification is currently available for octane testing (to the ASTM D-2699 Research and ASTM D-2700 Motor methods, respectively) (ASTM International, 2007a and 2007b) with another 'F5' specification currently available for the rating of diesel fuels. Although new techniques are being investigated for this latter purpose (Yates *et al.*, 2004), it is unlikely that the CFR engine in F1/F2 specification will be usurped in the near future because of amount of use it has

seen across the globe for rating SI engine fuels. There is also equipment for the 'F3' 'ASTM Aviation' and the 'F4' 'ASTM Supercharge' methods but, as was mentioned in Chapter 3, with the usurpation of the high-performance aircraft piston engine by the gas turbine, these are no longer widely used.

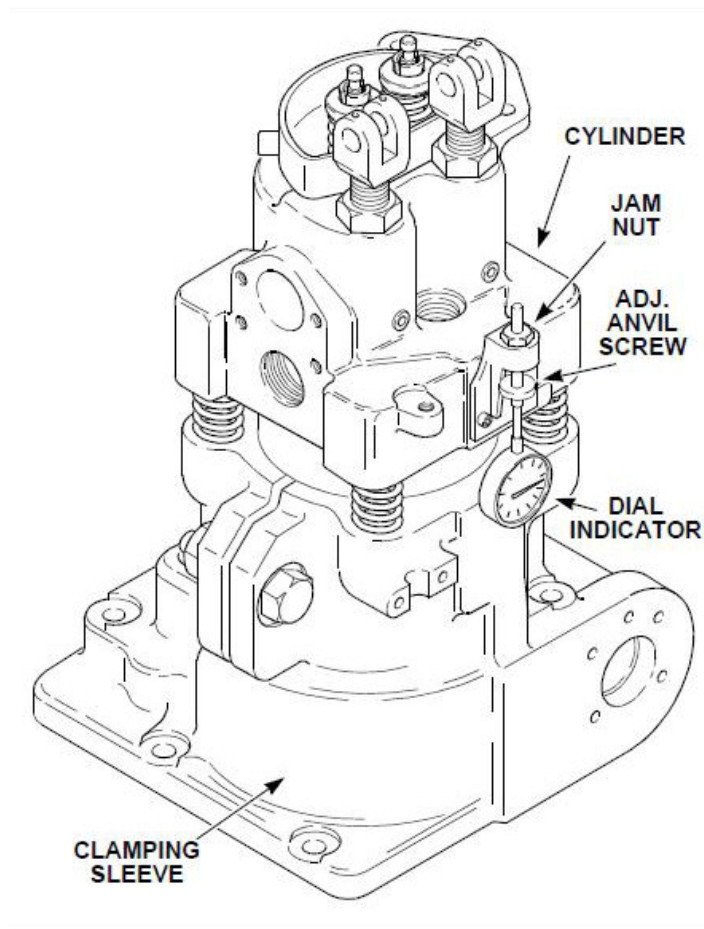


Fig A3.2: Drawing of the moveable-height cylinder of the CFR™ fuels rating engine, in F1/F2 specification for RON and MON testing. The dial indicator shown measures the vertical cylinder position in order to allow determination of the compression ratio. (Illustration provided compliments of DresserWaukesha)

As discussed by Swarts (2006), the engine has some peculiarities in the way that autoignition occurs within it and how it is detected, but there can be no doubt that, for all its differences to modern engine architectures, it must surely still be the

most important engine ever designed and built. This contention is made because it enabled standardization of fuel specifications across the globe, therefore enabling fuels and vehicles to be developed simultaneously so that the vehicle customer could be confident that there would be no issues with regard to their use in the field.

The creation of the CFR engine also provided a standard base for scientific research into combustion in general and the autoignition phenomenon in particular. Notable research using the engine in standard and modified form has been conducted by Quader (1976), Leppard (1987, 1988, 1989, 1991, 1992 and 1993), Pitz *et al.* (1998), Sahetchian *et al.* (1990), Curran *et al.* (1996), Swarts *et al.* (2005, 2006 and 2007), Eng *et al.* (1997) and Westbrook *et al.* (1988 and 1991). Perhaps one of the most extraordinary early uses of the engine is reported by Leary and Livengood in the discussion to Pastell (1950), where they describe using the CFR engine to investigate a form of autoignition combustion which appears to be a form of homogeneous charge compression ignition (HCCI). This predates what is widely taken to be the first publication on this subject by Onishi *et al.* (1979) by 29 years.

All of the above merely underlines the importance of the CFR engine, and with retrospect makes it even more extraordinary to note that, when it was first designed, it was expected that no more than 75 would be required “*to satisfy the entire needs of the industry*” (Baxter and Yeo, unknown date). This number was exceeded in the first year of production. During the year it was accepted into the ASME International Historic Mechanical Engineering Landmark series, Waukesha were expecting to manufacture the 5000th engine, and were still making them at a rate of 85 per year (Baxter and Yeo, unknown date). Updates continue to be made in order to make the engine simpler to use, and recently the ‘XCP Digital Octane Panel’ has been offered to enable more rapid and robust determination of octane numbers, and to bring the process of octane testing into the 21st century (Website, 2011b). A photograph of the now-superseded analogue control panel, with the knock meter readout above it, is shown in Figure A3.3.



Fig. A3.3: Analogue control panel for the CFR™ fuels rating engine in F1/F2 specification for RON and MON testing. The knockmeter readout is positioned at the top. This control panel has just been superseded by the XCP Digital Octane Panel (Website, 2011b). (Photograph provided compliments of DresserWaukesha)

Appendix IV: Notes on the Performance of the Charge Air Conditioning Rig

Regarding the performance of the specially-constructed charge air conditioning rig during the tests described in Chapter 6, it is worthy of note that for the 13 points depicted in Figure 6.13 and reproduced here as Figure A4.1, analysis of the density in the plenum showed that the maximum deviation from the desired value was only 0.7%. 70% of test points showed a deviation of less than $\pm 0.3\%$.

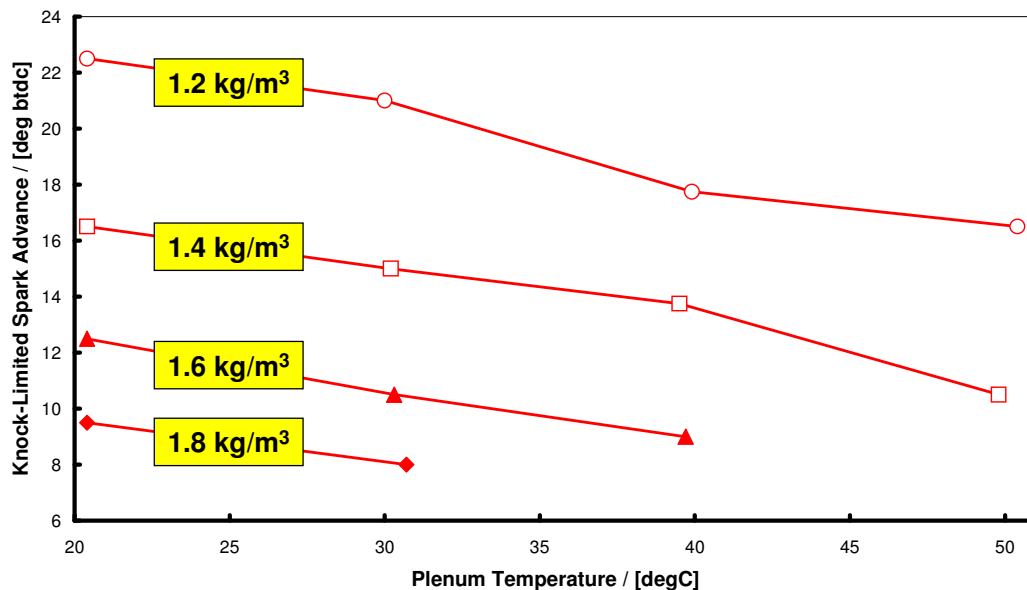


Fig. A4.1: Knock-limited spark advance (KLSA) versus charge air temperature at four different values of constant density in the plenum for the fixed-air-density tests. Test speed: 2000 rpm, relative AFR $\lambda = 0.9$ throughout

This is an excellent result when one considers the maximum air flow capability of the rig and the relatively small air consumption of the single-cylinder test engine: the two first-stage superchargers were taken from a production engine with a brake power output of 149 kW (200 bhp), meaning that the rig would be capable of delivering sufficient air for a gross engine output of ~ 330 kW (443 bhp). In turn, the performance of the rig also validates the decision to use uncorrected BMEP as the comparator for the different conditions described in Chapter 6.

Appendix V: Comparison of the Effects of Different EGR Routes on the Sabre Downsized Demonstrator Engine

As part of the investigation into the effect of cooled EGR when applied to the Sabre engine, different EGR routes were investigated. The different configurations possible for EGR routes were briefly discussed in Chapter 8, before the results for the high-pressure loop configuration were used to illustrate the effect of cooled EGR in general. This configuration was chosen for comparison purposes because the intake conditions and engine loads were similar to those used for the increased turbine inlet temperature (TIT) tests, and further comparisons were drawn with that technology. This appendix reports the results of the route comparison in more detail for completeness. Figure 8.11, which shows the different routes possible, is reproduced as Figure A5.1.

The testing of the various different routes was considered important since, if any one of them had a better interaction with the charging system, or provided the same results with a lower requirement for EGR mass flow, there could be important ramifications for the engine installation, particularly for a vehicle cooling system. In particular, of the routes illustrated in Figure A5.1, the long-route configuration might allow significant exhaust gas thermal energy to be removed because of the effect of the turbine expansion ratio: if 100°C could be removed from the gas by the turbine, then this would theoretically reduce the heat rejection required in the cooled EGR loop. Furthermore, if the performance of the IEM meant that the amount of EGR required was low, then there would be the opportunity to trade off any driveability impacts due to the individual systems because of the synergies between them.

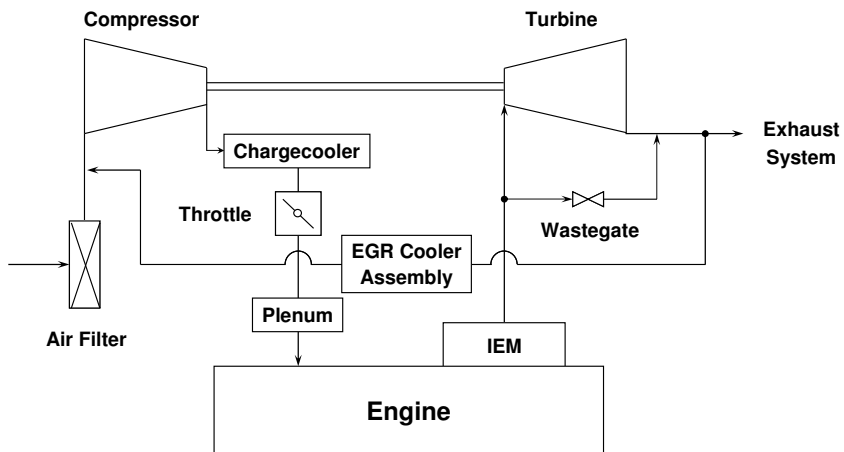
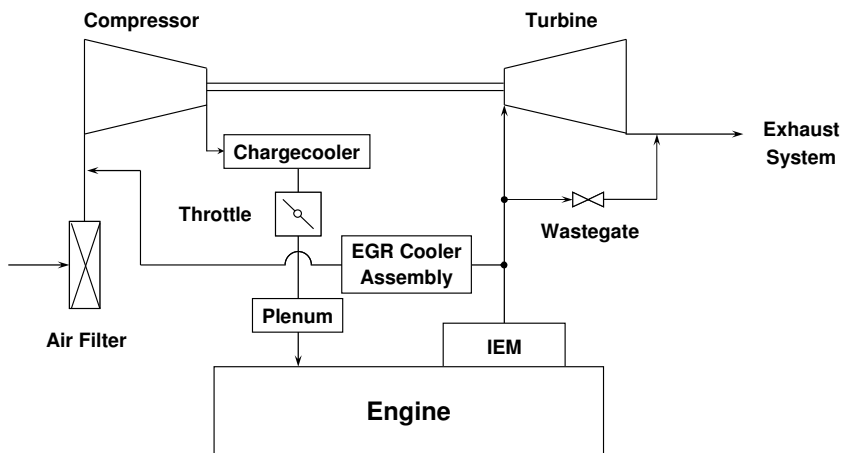
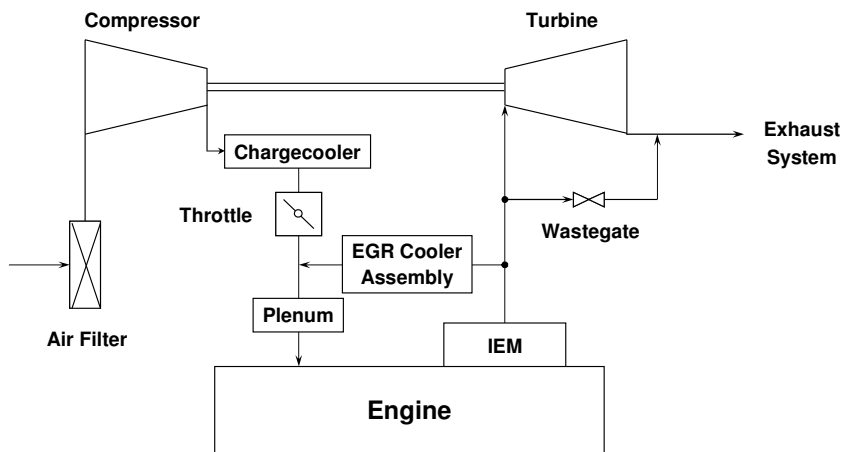


Fig. A5.1: Definition of EGR routing configurations used in this appendix. Top: (a) short route / high-pressure loop; middle: (b) intermediate route / high-to-low-pressure loop; bottom: (c) long route / low-pressure loop

A5.1 EFFECT OF EGR ROUTE ON THE PERFORMANCE OF THE CHARGING SYSTEM OF THE SABRE ENGINE

In a similar manner to the earlier-reported results for TIT testing and the high-pressure loop EGR test, the other EGR route tests were conducted at a condition of 5000 rpm, full load. This was because the Sabre engine was already operating at $\lambda = 1$ up to just below 5000 rpm and was giving excellent fuel consumption in this range. Again, as per the earlier tests, ignition timing and fuelling were set to balance knock-limited spark advance (KLSA) against leanest fuel for best torque (LBT) for all conditions; i.e. fuel was removed and if possible torque recovered by ignition advance if this was permitted by the knock limit. This was done as λ increased towards unity, but not beyond, since the advantages of operation at stoichiometric conditions in terms of exhaust after treatment were then available. Once $\lambda = 1$ had been achieved, this was held constant, and more cooled EGR was added if it could be supported, in order to gauge the effect on fuel consumption. This is the same as the procedure already described in Chapter 8.

The same test equipment was used for these tests, with only the connection points into the intake and from the exhaust system varying. The pre-compressor feed of EGR into the entry of the turbocharger compressor for the high-to-low and low-pressure loops was the same simple pipework, but did not include the RAT device discussed in Chapter 8 since it was reasoned that the compressor would perform the function of adequately mixing the cooled EGR flow with the fresh charge air. As per the work in Chapter 8, heat rejection from the exhaust gases to the cooler during the cooled EGR tests was not measured, for the same reasons as were outlined there. The high-pressure route data is the same as that already presented in Chapter 8, and is used here for comparison purposes; again, the correction factor used throughout this work was 88/195/EEC.

The impact on charging system matching of the three different EGR routes is presented in Figure A5.2, which is a comparison of BMEP for different levels of

EGR in the intake plenum as calculated using Equation 8.1. Note that it was not possible to introduce more than 8% EGR into the plenum with either the high-pressure loop or the high-to-low-pressure loop, whereas for the low-pressure loop only 6% was the maximum that could be supported. Nevertheless, the results of this section are believed to be sufficient to show the general effects of the different routes on engine performance.

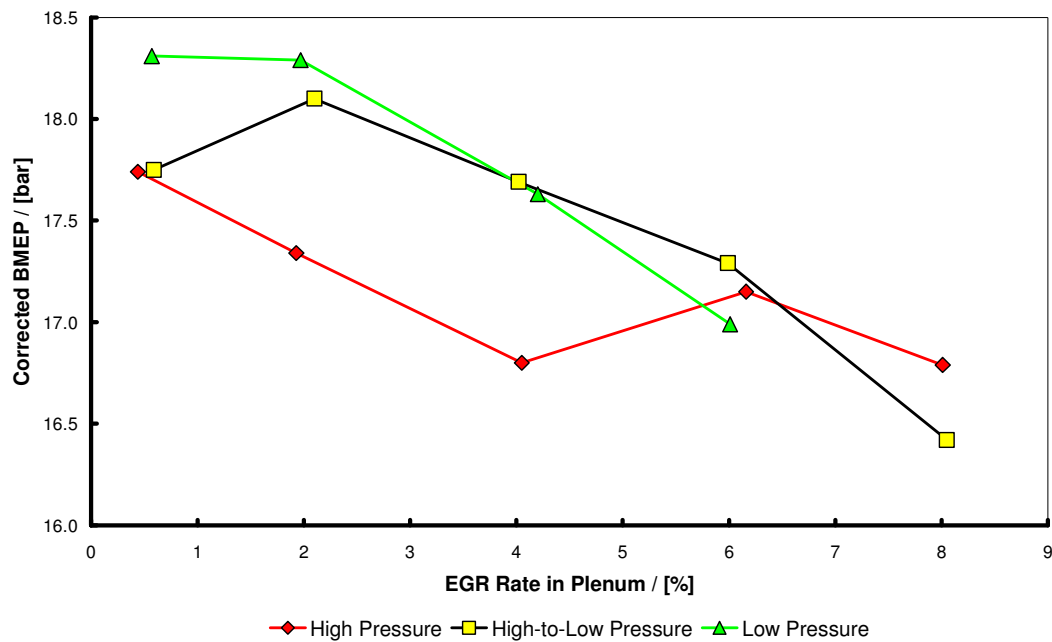


Fig. A5.2: Effect of EGR route on BMEP of Sabre engine at 5000 rpm, full load

The limit to the achievable flow is believed to be due to a combination of the available pressures to drive the EGR into the plenum and the unoptimized nature of the pipework and cooler. The available pressure difference for each system is illustrated in Figure A5.3, where it can be seen that, in theory, the high-to-low-pressure route should be capable of flowing the most EGR. The fact that this was not the case suggests a restriction in the proprietary EGR cooler which was used. The high- and high-to-low-pressure systems show a monotonic reduction in available pressure to drive flow in the system as the amount of flow bypassed around the EGR system was increased. The low-pressure route does not show

such an effect because the intake depression and exhaust back pressure was effectively constant, these measurement points being on the system boundary.

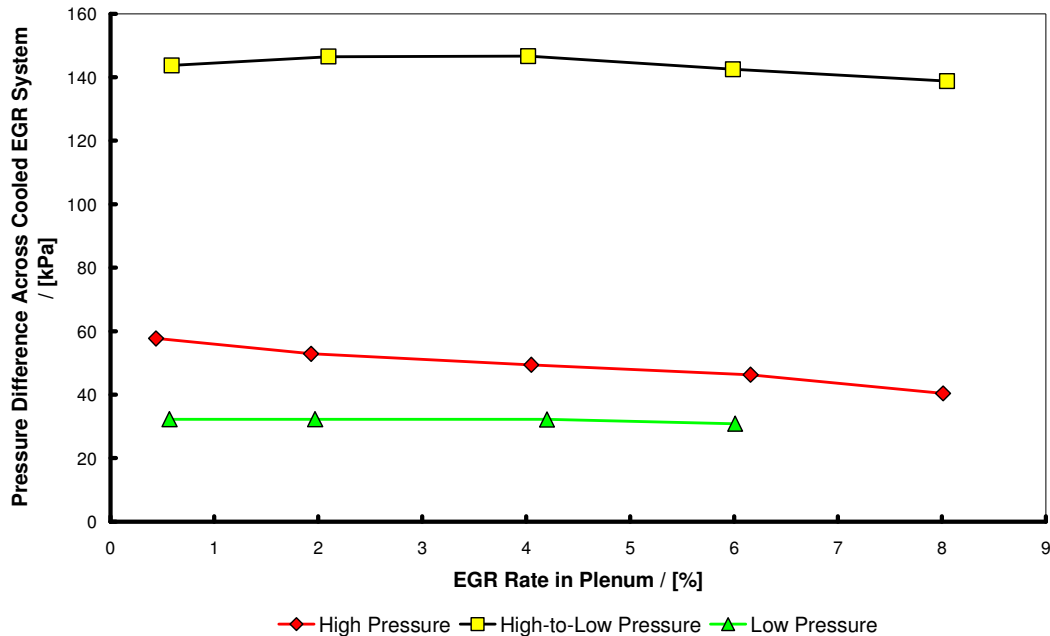


Fig. A5.3: Pressure difference across cooled EGR system available to drive gas flow from exhaust to intake for the three different cooled EGR systems tested on the Sabre engine at 5000 rpm, full load (starting at ~18.0 bar BMEP and reducing to ~16.5 bar BMEP as EGR is added)

Figure A5.4 shows that the total charge density in the plenum changes more for the high-pressure loop data than for the other two. This is partly due to a slight change in methodology during the tests. For the high-pressure route, as mentioned, it had been attempted to hold the BMEP constant, but as Figure A5.2 shows, this was unsuccessful. Instead, for the high-to-low-pressure and low-pressure route tests it was decided to fix plenum density in order to control one more variable. However, note that for all cases, plenum temperature was controlled to 33-40°C.

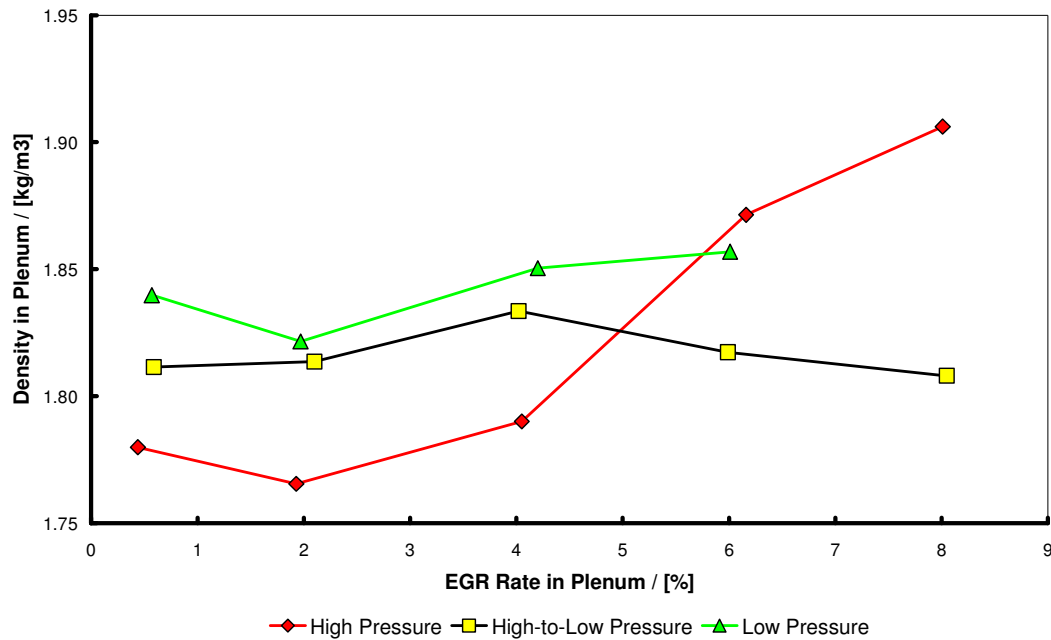


Fig. A5.4: Effect of EGR route on plenum density of Sabre engine at 5000 rpm, full load (reducing from ~18.0 to ~16.5 bar BMEP as EGR is added)

In general the lower plenum density in Figure A5.4 is reflected in lower BMEP in Figure A5.2, and at the point where the densities are most similar (i.e. 6% EGR rate) the engine produced substantially the same BMEP regardless of the route employed. This suggests that the combustion system is largely insensitive to EGR route, as one might expect. This subject will be returned to later.

From the above, except at an EGR rate of 6%, there is a small density effect in the data presented, with comparisons between high-to-low-pressure and low-pressure loops being more robust than for either of these with the high-pressure configuration. This does not impact on the comparisons between the high-pressure route and TIT, but is the reason why the comparison of the different routes is not included in the main body of this thesis.

Figure A5.5 presents the effect of EGR system routing on BSFC at the 5000 rpm test point. All start from the same good, nominally-zero-EGR, value of ~272

g/kWh, as already discussed in Chapters 7 and 8. However, the low-pressure loop shows the slowest response to increasing EGR rate, with the best response being for the high-to-low-pressure loop, at least for EGR rates below 6%, where it also delivered good BMEP (see Figure A5.2). Eventually the high-pressure route is better at the 8% point, and this corresponds to a slightly higher BMEP at this EGR rate versus the high-to-low-pressure route (again, see Figure A5.2). Generally, however, for the high- and high-to-low-pressure routes, 6% EGR would appear to be an optimum, since a good trade-off in BMEP and BSFC is achieved at this level for both.

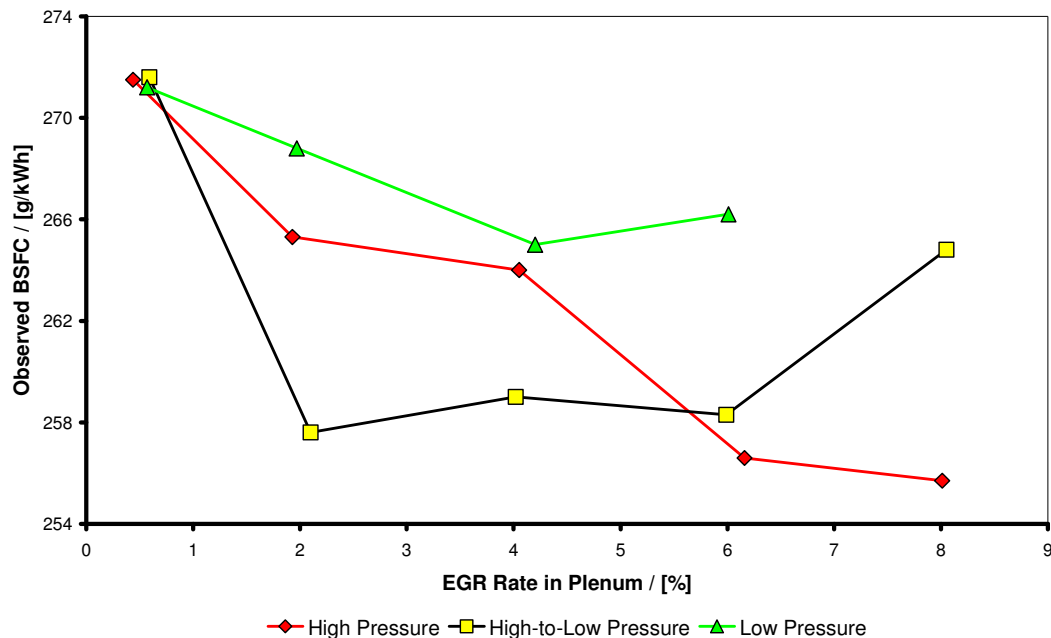


Fig. A5.5: Effect of EGR route on BSFC of Sabre engine at 5000 rpm, full load (reducing from ~18.0 to ~16.5 bar BMEP as EGR is added)

One of the primary reasons often reported for investigating cooled EGR is the possibility to operate a SI engine at $\lambda = 1$ at full load, with the attendant advantage of full after treatment of the exhaust gas stream with a three-way-catalyst. However, the TIT investigation showed that reduced enrichment operation without cooled EGR at the nominal maximum power condition in itself

causes a significant reduction in BMEP. This was because during normal Phase 1 operation the engine appeared to be operating with no specific requirement for component thermal protection fuelling. This is part of the reason for the reduction in BMEP at the 5000 rpm operating point since, due to the strategy of operating at LBT, fuel was removed as EGR was introduced and thus the air-fuel ratio increased towards $\lambda = 1$. One of the results apparent from Figures A5.2 and A5.5 is that, since the spark advance was set to KLSA, the introduction of cooled EGR effectively removed the efficacy of excess fuelling as a means of increasing power output. Furthermore, the rate at which fuel could be removed as EGR was introduced is not the same for all of the routes, as shown in Figure A5.6. The low-pressure route permits a reduced rate of AFR increase compared to the other two, with the high-to-low-pressure route slightly better than the high-pressure route. Both high- and high-to-low-pressure routes achieve $\lambda = 1$ at the comparatively low cooled EGR rate of 4%, although the low-pressure route almost achieves $\lambda = 1$ at the same EGR rate.

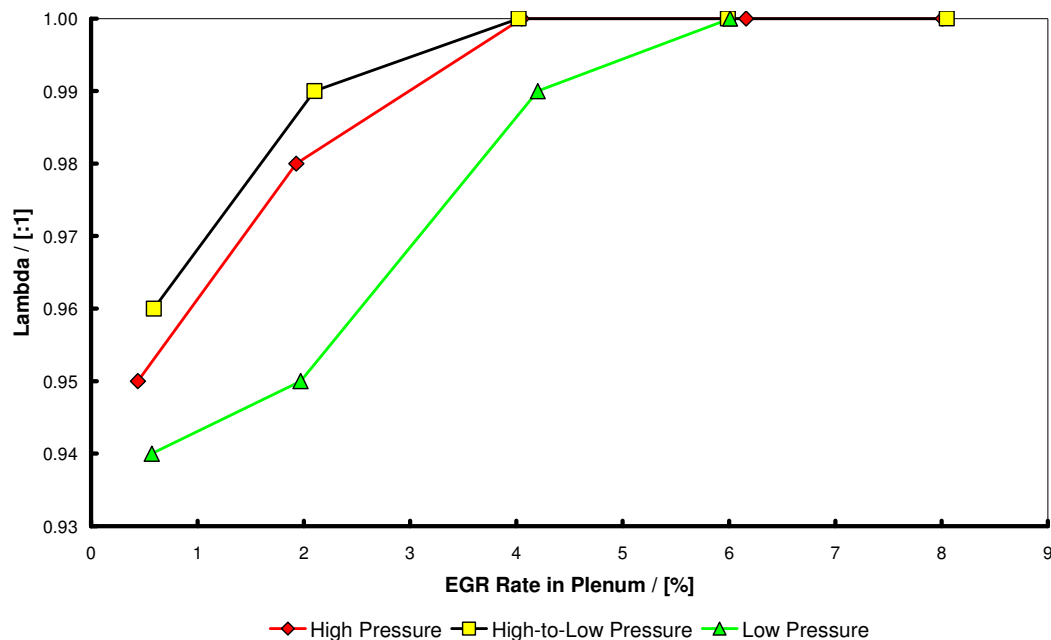


Fig. A5.6: Effect of EGR route on λ of Sabre engine at 5000 rpm, full load (reducing from ~18.0 to ~16.5 bar BMEP as EGR is added)

Another expected advantage of cooled EGR, and possibly the most important reason for considering it in the context of the removal of component thermal protection fuelling, is the potential reduction in turbine inlet temperature (TIT). The hope here is that the temperature reduction will be sufficiently great that diesel-level exhaust gas temperatures will be realized, and therefore low-temperature variable-geometry turbines (VGTs) can be adopted in a cost-effective manner in SI engines. While VGTs have been productionized for turbocharged SI engines (Kerkau *et al.*, 2006), the high exhaust temperature of the SI engine requires the application of more expensive metallurgy in the turbine (Gabriel *et al.*, 2007 and Sauerstein *et al.*, 2009). If exhaust temperatures below 900°C can be achieved, cheaper metallurgical solutions can be imagined, with benefits in piece price.

Figure A5.7 shows the effect of EGR route on TIT. The two routes which draw from before the turbine (i.e. the high- and high-to-low-pressure routes) both showed a clear response to increasing the EGR rate, with the high-pressure route being better at the higher rates achieved. However, at the point at which $\lambda = 1$ was achieved for both high and high-to-low-pressure routes (i.e. from Figure A5.6, 4% EGR flow) there was no significant difference between them in terms of TIT. The low-pressure route showed little response to EGR rate in terms of TIT. Since the key difference between the configurations tested was that, with the low-pressure route, no gas bypassed the turbine via the EGR cooler, it might be inferred from this that a significant proportion of the reduction in TIT observed for the other two configurations was due to a proportion of mass of gas bypassing the turbine via the EGR route as the EGR rate is increased, with the balance of the change coming from altered combustion due to the presence of the diluent in the charge. The subject of the effect on combustion will be returned to.

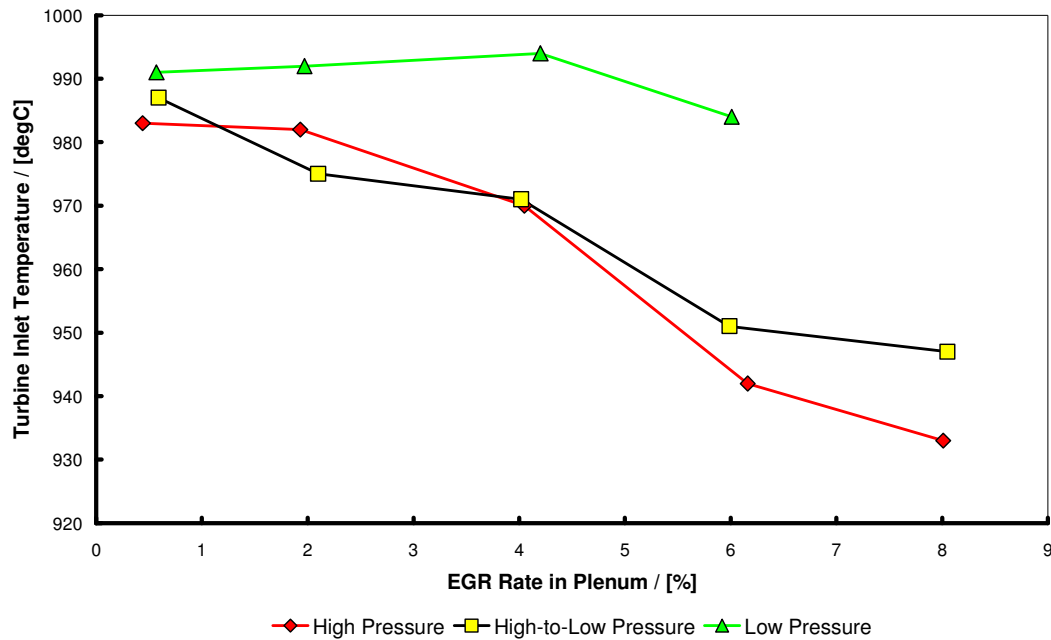


Fig. A5.7: Effect of EGR route on turbine inlet temperature of Sabre engine at 5000 rpm, full load (reducing from ~18.0 to ~16.5 bar BMEP as EGR is added)

None of the routes achieve a TIT of 900°C. Generally the high- and high-to-low-pressure routes perform best, realizing a TIT in the region of 930-940°C. For the high- and high-to-low-pressure cases, the data in Figure A5.7 suggests a rate of reduction in TIT of ~6°C per percent of cooled EGR introduced into the charge air. This result is entirely in line with the 6-7°C per percent EGR demonstrated by others using this approach (Cairns *et al.*, 2006 and Alger *et al.*, 2008).

An interesting effect on the charging system was that of the different EGR routes on the outlet temperature from the compressor. This is shown in Figure A5.8. For the constant-boost-pressure approach followed with the high-to-low- and low-pressure routes, i.e. those which feed the cooled EGR into the compressor entry, the outlet temperature from the compressor appeared to be constant or even slightly reduced with EGR rate. This is an effect of the diluent acting as a heat sink and is discussed later. For the high-pressure loop, however, and remembering from Figure A5.4 that the operating strategy was slightly different

with this configuration (insofar as the boost pressure was increased to try to maintain BMEP), the outlet temperature rose. This sort of response has been discussed in some researchers' work (for example, see Cairns *et al.*, 2006) when constant BMEP has been the desired operating condition, with the compressor having to supply the same mass air flow at concomitantly higher pressure ratios. With the large amounts of cooled EGR being employed by other researchers, this has led to the compressor outlet temperature exceeding 175°C under some conditions (Cairns *et al.*, 2006). The advantage in this engine of not having to employ significant levels of EGR in order to reduce component thermal protection fuelling serves to keep the compressor outlet temperature within safe limits for all operating conditions (i.e. less than 150°C).

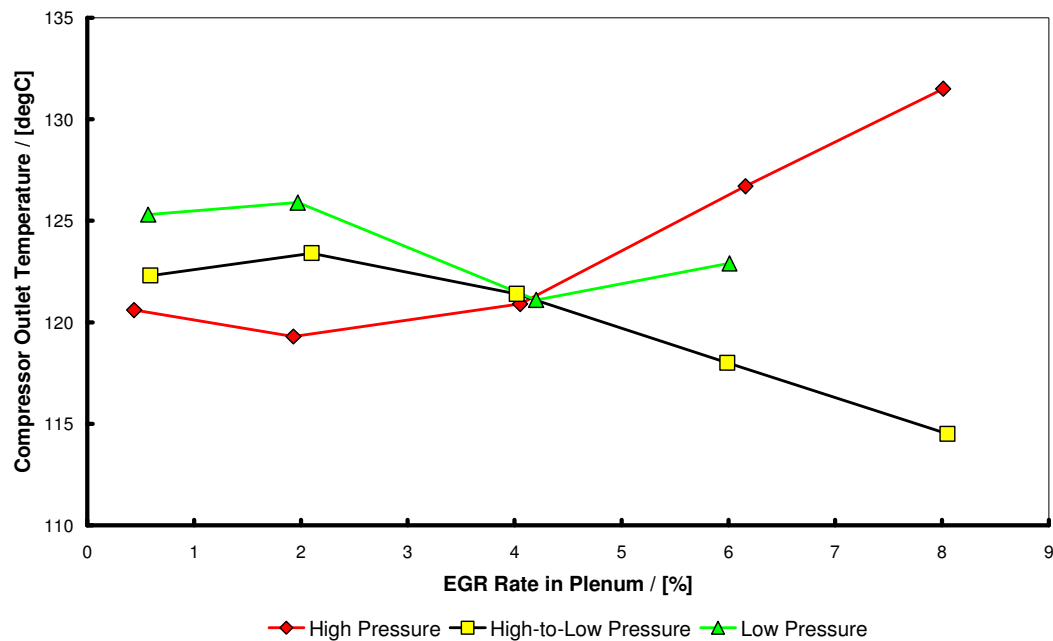


Fig. A5.8: Effect of EGR route on compressor outlet temperature of Sabre engine at 5000 rpm, full load (reducing from ~18.0 to ~16.5 bar BMEP as EGR is added)

It is interesting to note that in the work of Cairns *et al.* (2006), where a high-to-low-pressure cooled EGR loop was used, the general compressor outlet temperatures were slightly lower than those shown in Figure A5.8 at the 6-8%

EGR rate. Also, the compressor outlet temperature was reducing until the same level of EGR achieved here (see Appendix B of Cairns *et al.* (2006)). In general, the very high compressor outlet temperatures observed by those researchers were at the much higher EGR level of 16-20%, which the Sabre engine did not require (even though it could not flow this rate of EGR). In a manner similar to this investigation, Cairns *et al.* (2006) too were achieving $\lambda = 1$ operation at ~5% cooled EGR, although their tests were performed at 4000 rpm, an engine speed at which there is no requirement for cooled EGR in Sabre because $\lambda = 1$ operation is possible at this condition.

Because there is a higher ratio of triatomic to diatomic atoms in gasoline combustion products than in air, the EGR gas has a lower ratio of specific heats. This fact would to some extent explain the results of compressor outlet temperature in Figure A5.8. For the high-to-low- and low-pressure configurations, where EGR gas flows through the compressor, the increasing EGR proportion acts as a heat sink for the heat generated during compression. This is in a manner identical to that put forward for the reasoning behind its adoption in a combustion system, i.e. that the higher specific heat capacity of the diluent yields a lower temperature when compressed, either by the expanding flame front in a cylinder or during compression in a compressor. For the high-pressure loop configuration, the compressor only has air passing through it, and, in attempting to keep the BMEP constant, had to provide concomitantly greater boost pressure. Thus the outlet temperature from the compressor increases. In some respects, the pre-compressor introduction of cooled EGR produces similar effects to adding alcohol fuel to the charge air before the supercharger as reported in Chapter 5, which has also been reported for other supercharged engines utilizing pre-compressor injection of gasoline (for example, see Hooker *et al.* (1941) and Turner and Pearson (2001)).

As stated earlier, a general aim with the low-pressure route was to use the presence of the turbine before the exhaust gas take-off as a potential means of reducing gas temperature into the EGR cooler, to the benefit of reduced heat

exchanger capacity. This being the case, one would expect to see a lower EGR cooler outlet temperature for the low-pressure route than for either of the pre-turbine take-off configurations.

The results for EGR cooler outlet temperature are shown in Figure A5.9, and clearly show the reverse trend, i.e. the low-pressure route provided a higher EGR cooler outlet temperature at the higher EGR flow rates. This is surmised to be a function of the difference in EGR gas density within the cooler, itself a function of the pressure at the take-off point and the restriction in the system. The cooler itself was operated at the same volume flow of mains cooling water throughout the test work, and so any difference in the results is not believed to be due to a significant change in heat transfer capability on the liquid side of the heat exchanger.

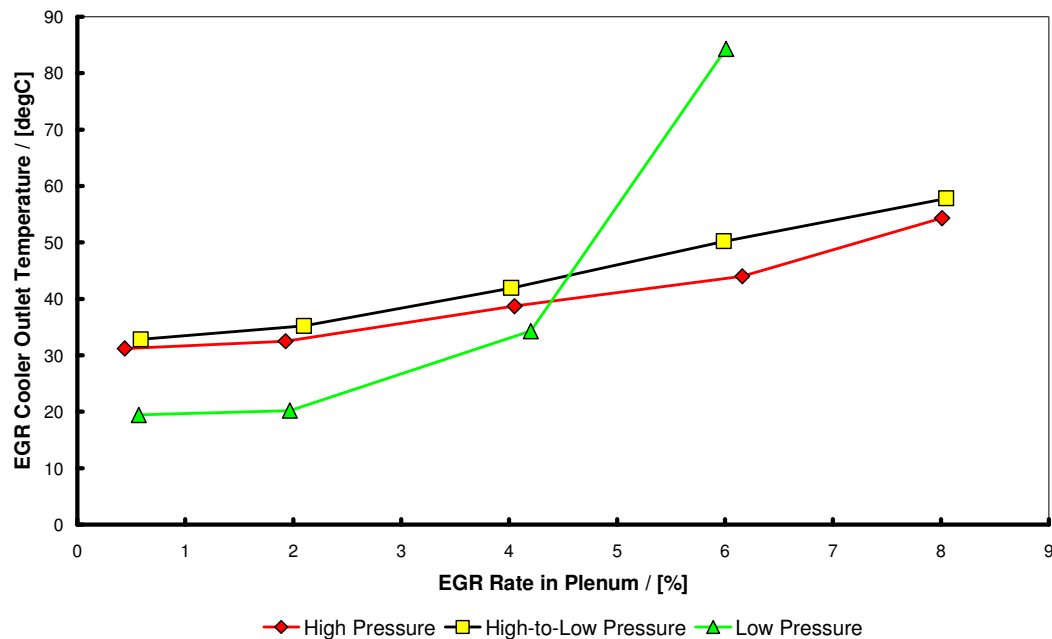


Fig. A5.9: Effect of EGR route on EGR cooler outlet temperature of Sabre engine at 5000 rpm, full load (reducing from ~18.0 to ~16.5 bar BMEP as EGR is added)

At low EGR gas flow rates, residence time in the cooler is high, and therefore the rate of heat exchange increases. The lower EGR cooler feed gas temperature for the low-pressure configuration would be compounded by this effect, and the outlet temperature would be lower. However, as the EGR flow rate increases the effect changes because mass flow rate increases and residence time reduces, so that the outlet gas temperature would increase. For the high- and high-to-low-pressure configurations there will be higher gas density in the cooler, which is presumed to promote greater rates of heat exchange.

The effects on the charging system can also be explained to a degree by the changes in turbine expansion ratio and exhaust back pressure (EBP) as the diluent was introduced. These changes are shown in Figures A5.10 and A5.11. In general, the expansion ratio of the turbine increased as the EGR rate in the plenum increased for all cases (see Figure A5.10). For the high- and high-to-low-pressure configurations, this reflected a requirement to extract more work from each unit of gas flowing through the turbine as a proportion of the mass flow was removed upstream of it (to flow around the EGR loop). The low-pressure configuration showed a smaller change in expansion ratio than the other two, in line with the smaller impact on the turbine resulting from the EGR gases being removed post-turbine. At the same time, the EBP is reduced quite markedly in the case of the high- and high-to-low-pressure routes due to the recycling of gas through the EGR loop. For the low-pressure route the EBP measurement point was before the gas take-off and so there is a reduced sensitivity shown. The combined effect of the changes in expansion ratio and EBP was relatively small and can be seen in Figure A5.12, where the turbine inlet pressure stays relatively uniform for all of the cases.

The effect of employing different EGR routes on the charging system of the Sabre engine was therefore not a severe one. However, it should be remembered that the engine did not require significant amounts of cooled EGR to realize very good fuel consumption, because it was believed to be operating at what is effectively a power-enriched condition at the start of the test. This in turn is believed to be due to its combination of synergistic technologies.

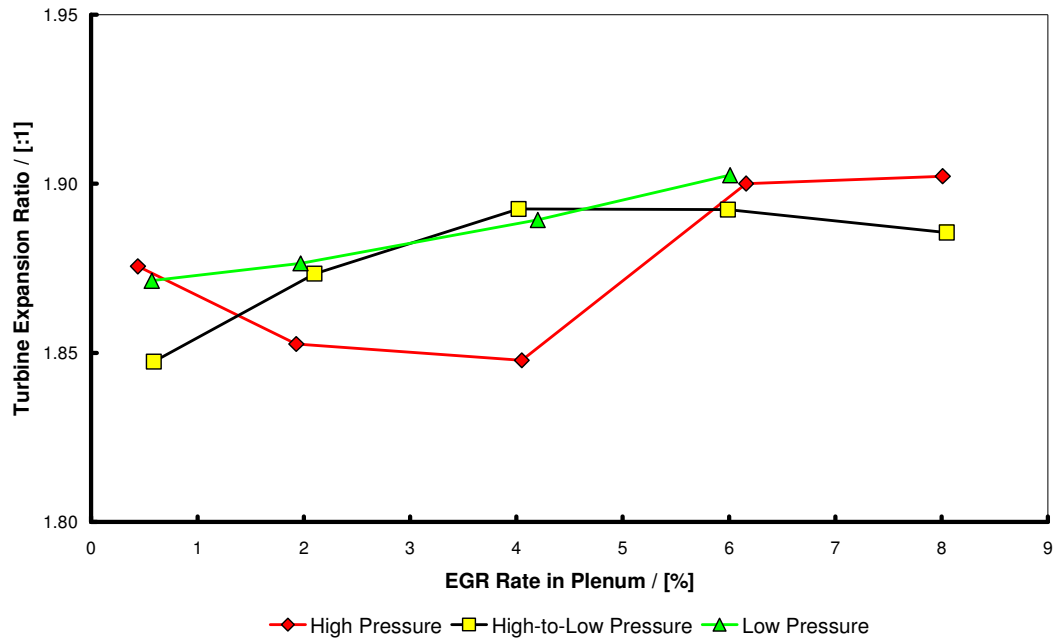


Fig. A5.10: Effect of EGR route on turbine expansion ratio of Sabre engine at 5000 rpm, full load (reducing from ~18.0 to ~16.5 bar BMEP as EGR is added)

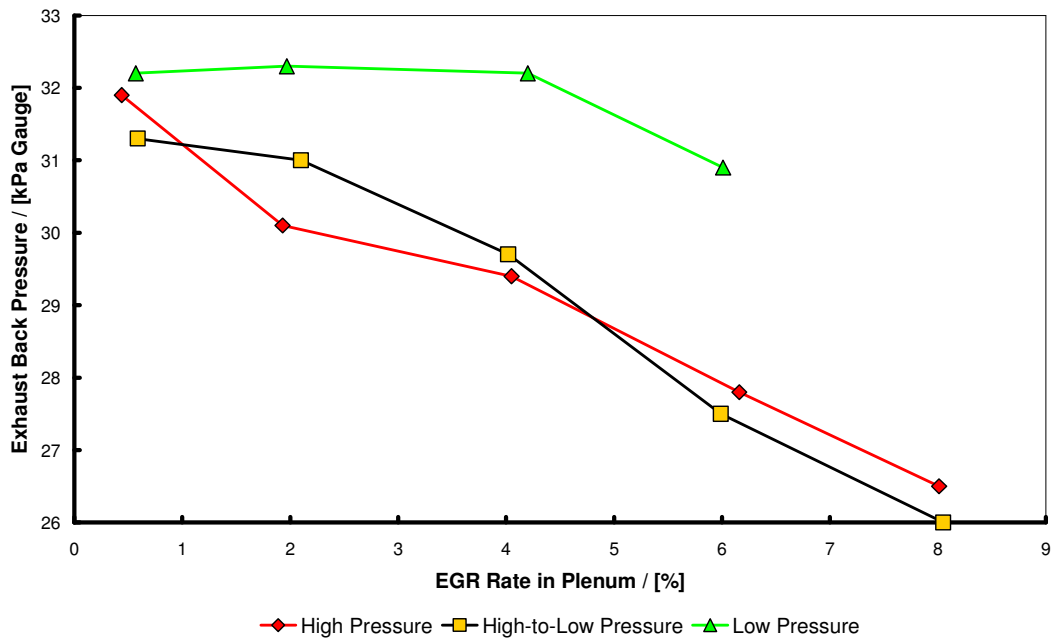


Fig. A5.11: Effect of EGR route on exhaust back pressure of Sabre engine at 5000 rpm, full load (reducing from ~18.0 to ~16.5 bar BMEP as EGR is added)

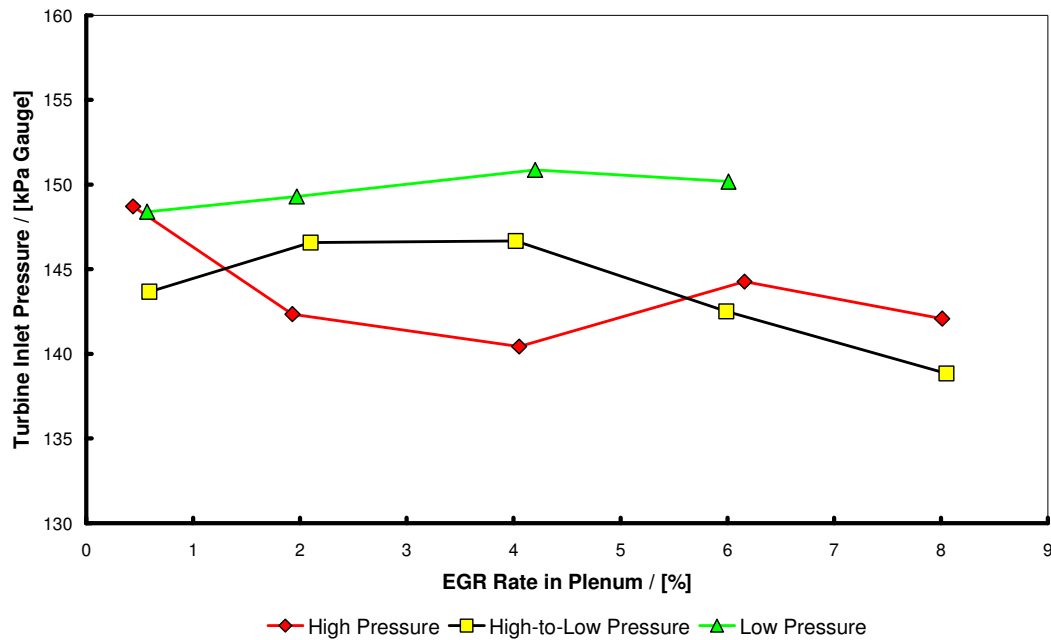


Fig. A5.12: Effect of EGR route on turbine inlet pressure of Sabre engine at 5000 rpm, full load (reducing from ~18.0 to ~16.5 bar BMEP as EGR is added)

A5.2 EFFECT OF EGR ROUTE ON COMBUSTION IN THE SABRE ENGINE

Figure A5.6 showed that it was possible to reach $\lambda = 1$ by introducing a relatively small amount of cooled EGR in the Sabre engine (~4% regardless of the route employed). However, for this specification of Sabre engine, operating as it was with a mismatched Phase 1 turbocharger, the effect on combustion stability as EGR was introduced was a severe one, as shown in Figure A5.13. As has already been remarked, combustion stability without EGR was already borderline-acceptable at just over 5% COV of IMEP. Figure A5.13 shows that increasing the rate of cooled EGR to 4% and simultaneously removing fuel enrichment rapidly degraded the COV of IMEP to ~9%. From the perceived flattening of the COV of IMEP for the two pre-turbine EGR take-off configurations after $\lambda = 1$ was achieved and while the proportion of cooled EGR was increased from 4 to 8%, this suggests that the bulk of the degradation in combustion

stability was due to the change in λ and not to the presence of increasing amounts of EGR.

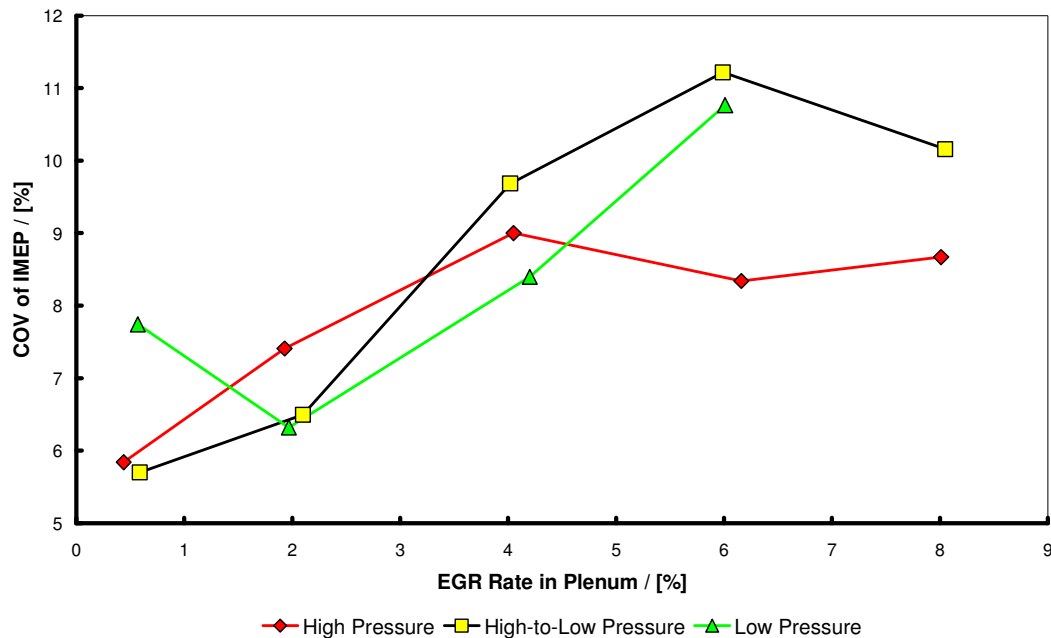


Fig. A5.13: Effect of EGR route on COV of IMEP of Sabre engine at 5000 rpm, full load (reducing from ~18.0 to ~16.5 bar BMEP as EGR is added)

The potentially complicating effect of the turbine inlet pressure on the mass of residuals trapped in the chamber is mitigated by the fact that this does not change rapidly as the proportion of cooled EGR is changed (see Figure A5.12). It has also been shown in Chapter 7 that, in general, due to the 3-cylinder configuration the average pressure in the exhaust port during overlap is lower than that in the inlet port (see Figure 7.9). From this, residual rate due to gas exchange is not believed to be a major contribution to combustion instability, and whatever is causing the combustion instability at high load in the Sabre engine is compounded when cooled EGR is introduced. This is presumed to be inadequate levels of charge motion at high load and was discussed in Chapter 8.

Regarding other combustion parameters, CA50 does not change greatly as the amount of EGR is introduced into the combustion system. This is shown in Figure A5.14, and is regardless of the cooled EGR route used. Figure A5.15 shows that KLSA does increase significantly as EGR is introduced, however: the general rate of increase is approaching 1° CA per 1% cooled EGR. At the same time, the combustion duration, represented by the 10-90% MFB interval, increases at a broadly monotonic rate with EGR, as shown in Figure A5.16. (Note that Figures A5.14 to A5.16 have all been plotted with the same number of crankshaft degrees on their abscissae to facilitate visual comparison of results.) These responses are well known in the literature and are in line with the discussion of cooled EGR results already made in Chapter 8.

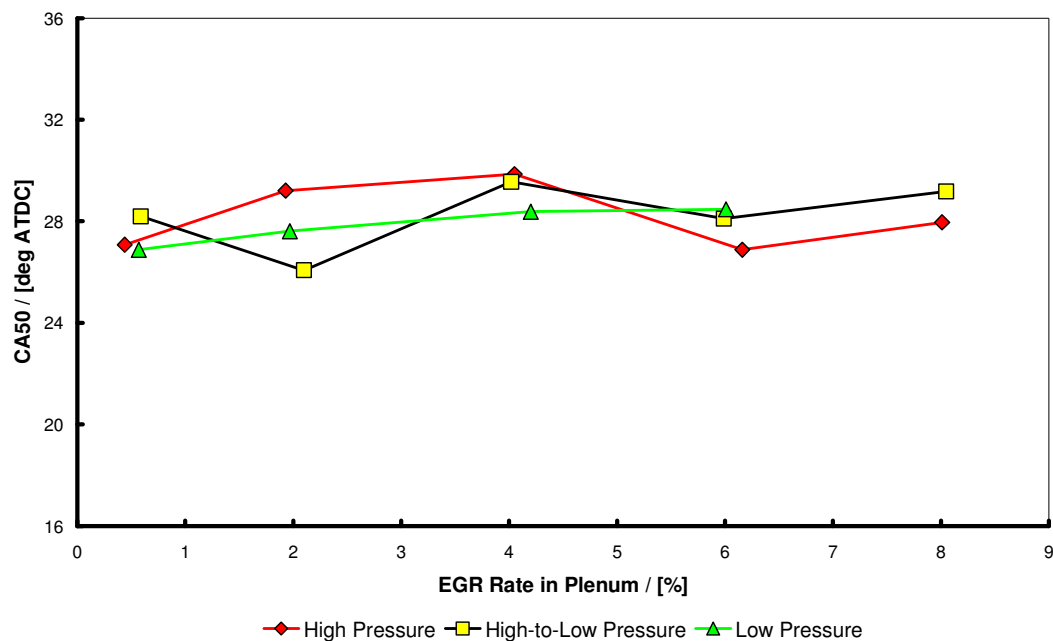


Fig. A5.14: Effect of EGR route on CA50 of Sabre engine at 5000 rpm, full load (reducing from ~18.0 to ~16.5 bar BMEP as EGR is added)

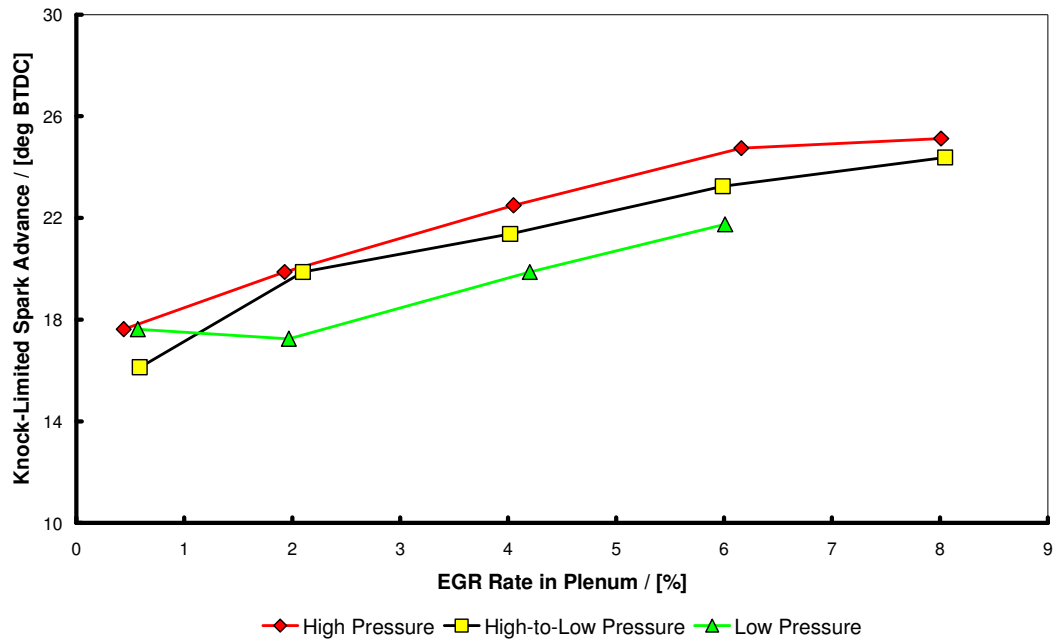


Fig. A5.15: Effect of EGR route on knock-limited spark advance for Sabre engine at 5000 rpm, full load (reducing from ~18.0 to ~16.5 bar BMEP as EGR is added)

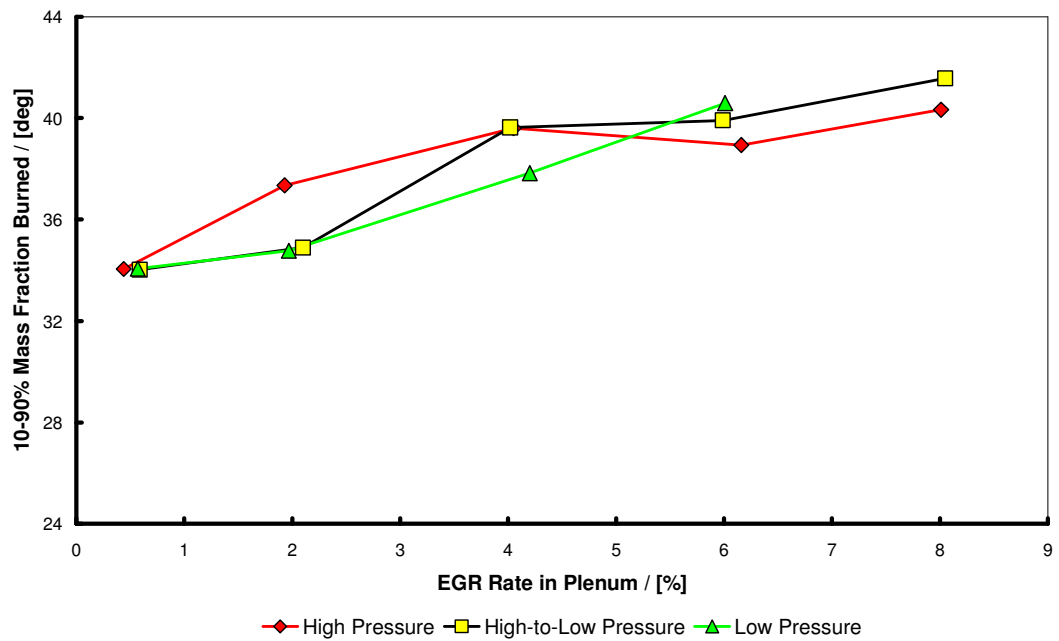


Fig. A5.16: Effect of EGR route on 10-90% MFB of Sabre engine at 5000 rpm, full load (reducing from ~18.0 to ~16.5 bar BMEP as EGR is added)

With the introduction of EGR into the charge air there is a reduction in oxygen proportional to the amount of EGR used. In the two approaches which kept plenum density constant, i.e. the high-to-low-pressure and low-pressure routes, one would expect a reduction in BMEP in line with the reduction in oxygen mass resulting from the introduction of EGR. This is generally shown to be the case in Figure A5.17. Despite the offset in the two lines, one can see that the BMEP is reducing broadly linearly with EGR introduction, although the reduction appears to be of the order of two percent reduction in BMEP for every one percent of EGR introduced.

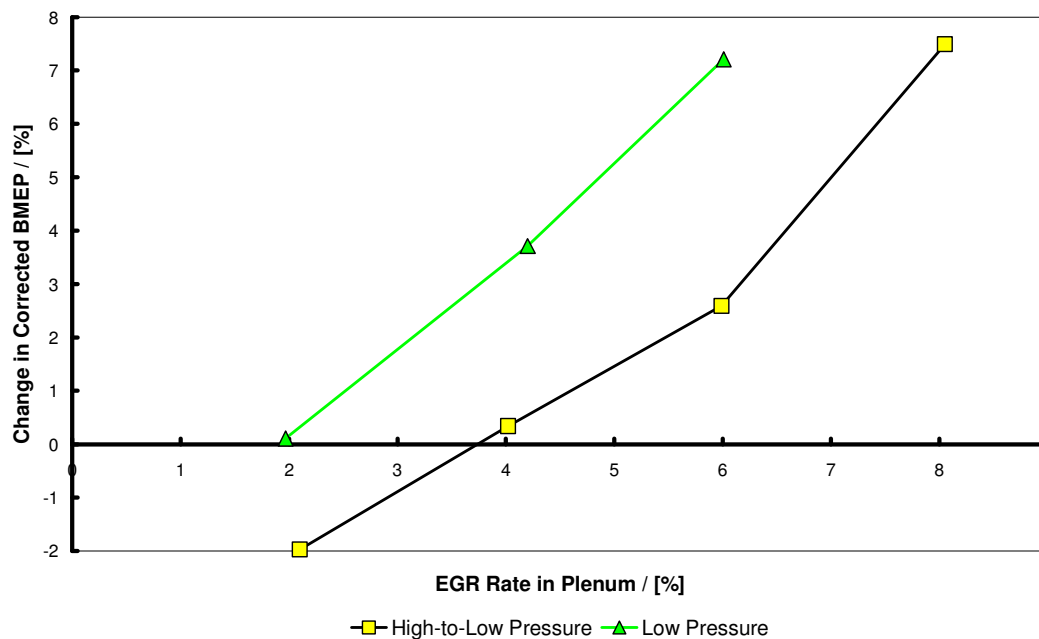


Fig. A5.17: Effect of EGR rate in plenum on change in corrected BMEP of Sabre engine at 5000 rpm, full load (reducing from ~18.0 to ~16.5 bar BMEP as EGR is added)

A5.3 SUMMARY AND CONCLUDING REMARKS

Overall, from the results presented here, the combustion system of the Sabre engine appears to respond less to the changes in cooled EGR route configuration than it does to the effect that these changes have on the charging system itself.

A factor to be borne in mind is that the Sabre engine, being a new design from the outset, represents a combination of features itself designed to ensure the best possible fuel consumption through a systems approach. The success of this approach has made it harder to realize, at this level of specific output, the same percentage improvement in fuel consumption as has been reported by other researchers starting from a less favourable position regarding engine configuration (Cairns *et al.*, 2006 and Alger *et al.*, 2008).

Therefore, from this investigation into the effects of different EGR routes on the full-load performance of the Sabre engine, the effect on the combustion system is believed ultimately to be dominated by the introduction of cooled EGR itself and to be largely independent of any interactions between the charging system and the configuration of the EGR route, which play a lesser role.

Appendix VI: Listing of Input Variables for Modelling of the Single-Cylinder Engine in Chapter 6

Figures A6.1 and A6.2 are a listing of the input variables for Lotus Engine Simulation used to generate the single-cylinder engine model discussed in Chapter 6 (Lotus Engineering Software, 2005). This model was used primarily to specify the exhaust system orifices used in order to mimic a turbocharger turbine and to put representative back pressure on the engine (Winterbone and Pearson, 1999). Inputting these variables to Lotus Engine Simulation will reproduce the basic engine model as used in this research and in the HOTFIRE research programme (Turner *et al.*, 2006a and Stansfield *et al.*, 2007).

Cylinder Geometric Data:

	Bore (mm)	Stroke (mm)	Rod Length (mm)	Pin Offset (mm)	Compression Ratio	Phase (ATDC)	Label
Cyl 1	88.0000	82.1000	142.00	0.80	10.00	0.00	Cylinder 1

Cylinder Transient Mass Data:

	Cyl Axis Angle (deg)	Piston Mass (kg)	Piston Pin Mass (kg)	Con-Rod Rot Mass (kg)	Con-Rod Recip Mass (kg)	Con-Rod Inertia (kg.m ²)
Cyl 1	0.00	0.00000	0.00000	0.00000	0.00000	0.00000

Intake Poppet Valve Data:

	Valve Open (deg)	Valve Close (deg)	Dwell at Max (deg)	Max Lift (mm)	MOP (deg)	Lift Option	Data Action	Opening Lash	Closing Lash	Label
Pval 1	27.00	55.00	0.00	9.350	105.00	User Lift	Fixed	0.20000	0.25000	240-9350

Exhaust Poppet Valve Data:

	Valve Open (deg)	Valve Close (deg)	Dwell at Max (deg)	Max Lift (mm)	MOP (deg)	Lift Option	Data Action	Opening Lash	Closing Lash	Label
Pval 2	53.00	25.00	0.00	9.350	-105.00	User Lift	Fixed	0.25000	0.25000	240-9350

Intake Port Data:

	No of Valves	Valve Throat Dia (mm)	Port Type	CF at 0.3 L/D	Label
Port 1	2	31.00	User Curve (common)	0.7175	#1 Inlet Port CF

Fig. A6.1: Input data listing for HOTFIRE single-cylinder engine model

Exhaust Port Data:

	No of Valves	Valve Throat Dia (mm)	Port Type	CF at 0.3 L/D	Label
Port 2	2	24.55	User Curve (common)	0.7364	#1 Exhaust Port CF

Intake Pipes (Ports) Data:

	Length (mm)	Diameter (mm)	No. of Meshes	Wall Thickness (mm)	Cooling Type	Wall Material	Wall Factor	Label
Pipe 1	0.000	49.000	8	1.63	Water Cooled	Aluminium	Friction Factor	#1 Inlet Port Pipe/Injector Housing
	14.440	48.570						
	28.880	48.130						
	43.320	47.680						
	57.770	47.220						
	72.200	46.750						
	86.640	46.270						
	101.800	45.790						
	109.000	45.440						
	130.000	45.440						

Exhaust Pipes (Ports) Data:

	Length (mm)	Diameter (mm)	No. of Meshes	Wall Thickness (mm)	Cooling Type	Wall Material	Wall Factor	Label
Pipe 5	0.000	42.660	6	1.63	Air Cooled	Steel	Surface Roughness (mm)	Trouser Piece
	11.220	42.660						
	26.000	42.660						
	33.670	42.400						
	44.890	41.670						
	56.110	40.680						
	67.330	39.480						
	78.550	38.230						
	89.780	37.100						
	96.000	40.000						
101.000	40.000							

Fig. A6.2: Input data listing for HOTFIRE single-cylinder engine model (concluded)

Appendix VII: Reproductions of Various Websites Given as References

In order to provide a historical record of information provided on various of the websites listed as references, several have been reproduced visually in this appendix. These are presented below, together with their reference as used in the text. However, some references, including the Kyoto Protocol (Website, 2006b), the California State Government's Assembly Bill 1493 (Website, 2002), Bentley Motors Limited's publication "Bentley and the future of biofuels" (Bentley Motors Limited, 2008) and the American Society of Mechanical Engineers's International Historic Mechanical Engineering Landmark publication on the Waukesha CFR Fuel Research Engine (Baxter and Yeo, unknown date), are believed to be obtainable for the foreseeable future, and so have not been reproduced here. Websites with data showing climate change have not been reproduced either since these are used merely to support the need to reduce greenhouse gas emissions from road vehicles.

Therefore, this appendix only reproduces web pages and documentation listed on websites where the data has been used to plot graphs in figures, or where the engineering concepts they describe are discussed and reviewed in the text.

A7.1 EC (2010)

Excerpt from page 3 of the reference showing historical data for the ACEA vehicle fleet, together with data for the manufacturers' associations for Japan (JAMA) and Korea (KAMA). The ACEA data was used to plot Figure 1.1.

Chart 1: Evolution of CO₂ emissions from new passenger cars by association (adjusted for changes in the test cycle procedure)

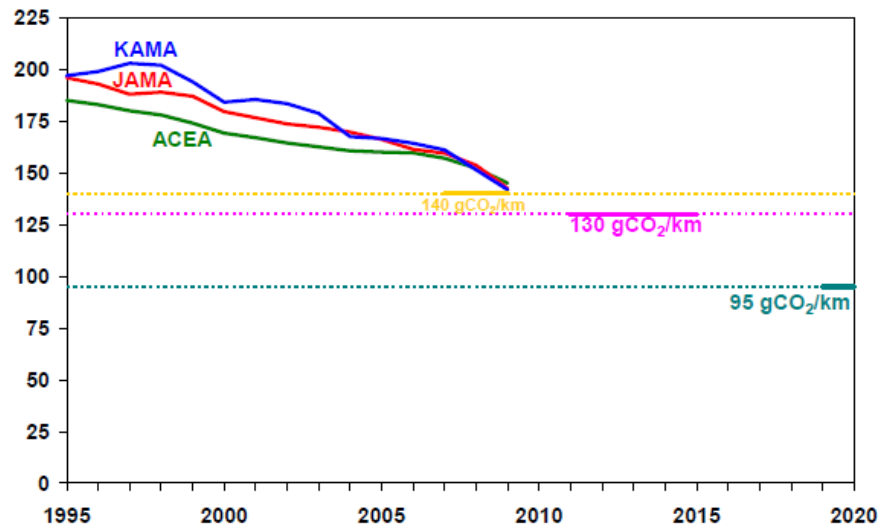


Table 1: Average CO₂ emissions from new passenger cars by association (adjusted for changes in the test cycle procedure)

gCO ₂ /km	2000	2001	2002	2003	2004	2005	2006	2007	2008	2009
ACEA	169.2	167.0	164.4	162.5	160.7	160.0	159.7	157.0	152.3	145.1
JAMA	179.6	176.6	173.7	172.0	169.7	166.2	161.4	159.5	153.7	142.6
KAMA	184.2	185.5	183.5	178.7	167.5	166.6	164.3	161.1	151.5	141.8

A7.2 SMMT (2011)

Excerpt from page 38 of the reference showing historical data for the UK vehicle fleet. This data was used to plot Figure 1.1.

Annex 1 - Historical CO₂ data

204. SMMT has published an annual CO₂ report since 2000 and has new car CO₂ data from 1997 onwards. This data is sourced from manufacturers own CO₂ figures (as supplied on the vehicle's first registration document) and checked with type approval data from the Vehicle Certification Agency (VCA) to ensure accuracy. Since 2003 the low volume of missing data was estimated by using other models in the range or using models of a similar segment/engine size and type. SMMT believes its database is the most accurate and reliable available and therefore provides the best source for analysing the UK's performance. The data is collated by SMMT's Motor Vehicles Registration Information Service (MVRIS). It links vehicles' CO₂ levels to the MVRIS new car registration database.

Table 17 - Average new car CO ₂ emissions in the UK (Source SMMT)			
Year	Average CO ₂ g/km	y/y % change	y/y % change on 1997
1997	189.8		
1998	188.4	-0.7%	-0.7%
1999	185.0	-1.8%	-2.5%
2000	181.0	-2.2%	-4.6%
2001	177.6	-1.9%	-6.4%
2002	174.2	-1.9%	-8.2%
2003	172.1	-1.2%	-9.3%
2004	171.4	-0.4%	-9.7%
2005	169.4	-1.2%	-10.7%
2006	167.2	-1.3%	-11.9%
2007	164.9	-1.4%	-13.1%
2008	158.0	-4.2%	-16.8%
2009	149.5	-5.4%	-21.2%
2010	144.2	-3.5%	-24.0%

A7.3 MCE-5 (2010)

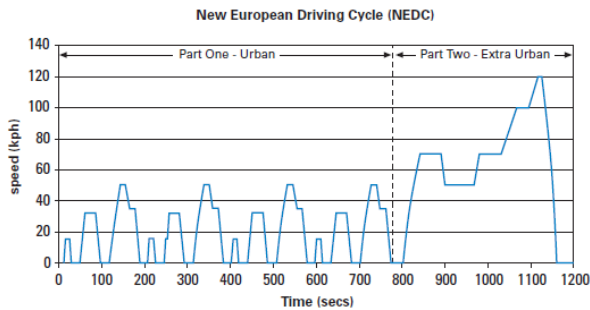
Excerpt from page 4 of the “Key results” brochure available on the MCE-5 website, reproduced solely for review purposes and to illustrate the approximately 30% reduction in fuel consumption generally seen when variable compression ratio mechanisms are applied to downsized 4-stroke spark-ignition engines.

MCE-5 VCRi: Pushing back the fuel consumption reduction limits

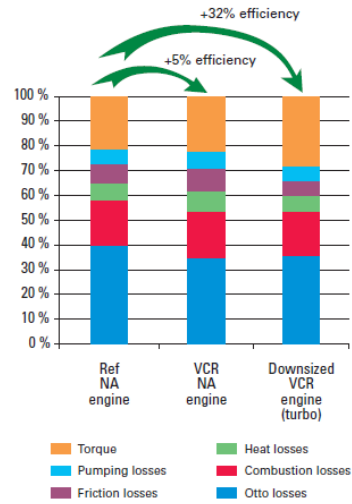
FUEL CONSUMPTION REDUCTION IN THE DRIVING CYCLE:

In the driving cycle (example: NEDC), MCE-5 VCRi reduces vehicle fuel consumption by combining the gains provided by downsizing-downspeeding with those provided by compression ratio optimization.

MCE-5 VCRi's limited friction losses also contribute to the results obtained. Note that the fuel consumption reduction is higher for powerful cars than for small ones.



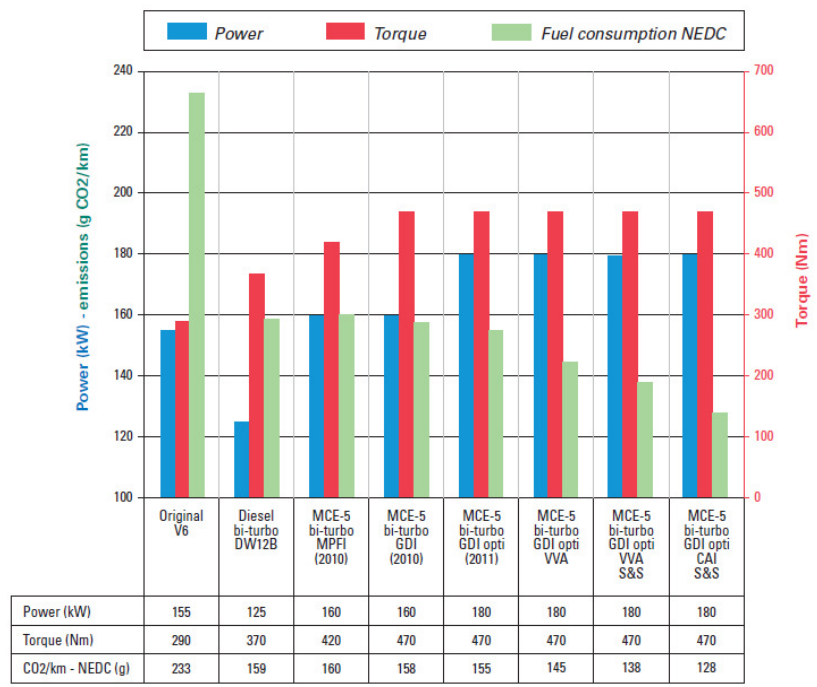
The forecasted fuel consumption reductions refer to the NEDC



VCR redefines the energy balance of engines

Excerpt from page 5 of the “Key results” brochure available on the MCE-5 website, reproduced solely for review purposes and to illustrate the approximately 30% reduction in fuel consumption generally seen when variable compression ratio mechanisms are applied to downsized 4-stroke spark-ignition engines.

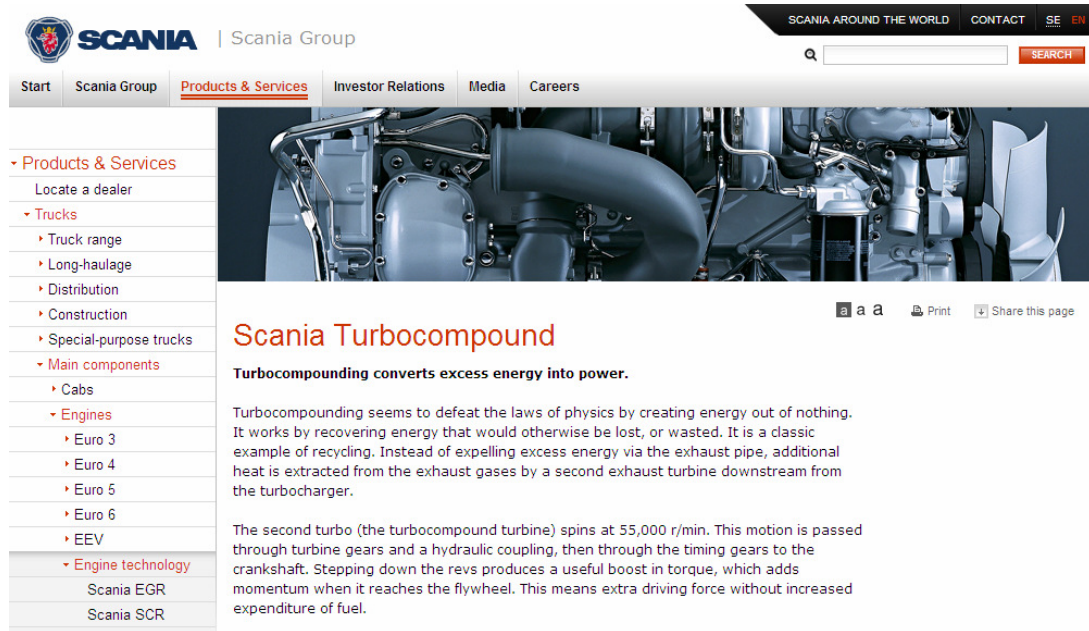
MCE-5 VCRi: Pushing back the fuel consumption reduction limits



On a Peugeot 407 type vehicle, the most basic MCE-5 VCRi MPFI reduces fuel consumption by 31%. The most sophisticated version of the MCE-5 VCRi planned for the near future could bring this reduction down to 45% while providing 16% more power and 62% more torque

A7.4 Website (2011a)

Scania Turbocompound web page.



SCANIA | Scania Group

SCANIA AROUND THE WORLD CONTACT SE EN

Start Scania Group **Products & Services** Investor Relations Media Careers

▾ Products & Services

- Locate a dealer
- ▾ Trucks
 - Truck range
 - Long-haulage
 - Distribution
 - Construction
 - Special-purpose trucks
- ▾ Main components
 - Cabs
- ▾ Engines
 - Euro 3
 - Euro 4
 - Euro 5
 - Euro 6
 - EEV
- ▾ Engine technology
 - Scania EGR
 - Scania SCR

Scania Turbocompound

Turbocompounding converts excess energy into power.

Turbocompounding seems to defeat the laws of physics by creating energy out of nothing. It works by recovering energy that would otherwise be lost, or wasted. It is a classic example of recycling. Instead of expelling excess energy via the exhaust pipe, additional heat is extracted from the exhaust gases by a second exhaust turbine downstream from the turbocharger.

The second turbo (the turbocompound turbine) spins at 55,000 r/min. This motion is passed through turbine gears and a hydraulic coupling, then through the timing gears to the crankshaft. Stepping down the revs produces a useful boost in torque, which adds momentum when it reaches the flywheel. This means extra driving force without increased expenditure of fuel.

A7.5 Website (2011b)

Page 1 of Digital Octane Panel document from DresserWaukesha (full document reproduced compliments of DresserWaukesha).

DRESSER Waukesha XCP™ Digital Octane Panel



Proven Fuel Rating Technology



Page 2 of Digital Octane Panel document from DresserWaukesha (full document reproduced compliments of DresserWaukesha).



The XCP™ Digital Octane Panel from Dresser Waukesha

Dresser Waukesha has taken the CFR® octane rating units– the Global Leader in Fuel Quality Testing – to a higher level of control and functionality with the new XCP™ Digital Octane Panel.

With advanced ease-of-use features including more automated functions and enhanced documentation, the Digital Octane Panel is now standard equipment on new production units, and may be retrofitted to most existing CFR units. The XCP platform is designed to accept future enhancements as they are made available!

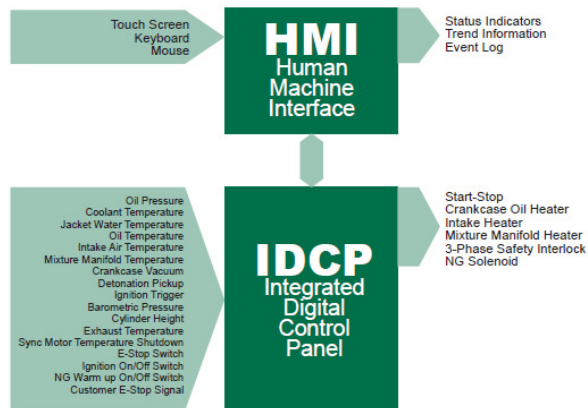
Designed with the operator in mind, the new Digital Octane Panel is user-friendly, intuitive and easily accommodates users with varying levels of operational expertise.

The XCP™ Digital Octane Panel Offers a Lot – And Delivers!

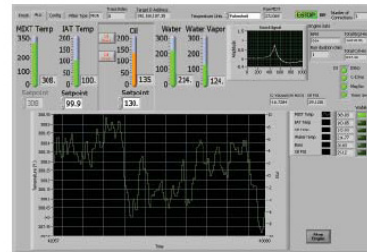
Ease of operation, increased functionality, and shortened training period are available through a completely re-designed operator panel with touch-screen functionality. More than 30 features are built in and more are coming. The easily configurable and adaptable XCP Digital Octane Panel has the technology built in to adapt to future enhancements/upgrades.

The Digital Octane Panel features a touch screen and keyboard interfaces for easier use.

System Diagram



Dresser Waukesha



Features

Easy-to-Use Panel Interface

The introduction of a touch screen user interface, standard keyboard and intuitive graphic panel translates to a shorter operator proficiency learning curve. Operators can become comfortable and more confident using a CFR with a Digital Octane Panel in days, not months.

The user-friendly touch panel is immediately recognized and accepted by today's computer-savvy work force. On-screen operation & maintenance and parts manuals, on-screen reports and internet capability are standard.

The new operation screens are clear and easy to use, reducing the opportunity for errors. Built-in prompts, automated calculations, and data logging allows operators to be quickly cross-trained for improved work flow.

Automated Data Recording

Better documentation – critical information for each rating is documented automatically using bold graphics and easy-to-read charts. Fuel rating files are now automatically generated based on fuel name and date and kept on easily accessible Microsoft® Excel® files.

More Consistent Results

Intuitive software and easy adjustments have been designed in to ensure the XCP will produce consistent reliable results from operator to operator.

Report Generation

As tests are completed, the XCP produces test results with all curves, calculations, tables, date stamps and engine records – a big time saver over manually recording results!

Increased Throughput

Lab supervisors may face the dilemma of a leaner work force and the need through the use of more cross trained operators to produce more octane tests per shift. Not only can more operators be trained on the easier to use XCP unit, there is no need to constantly monitor it when running a Falling Level procedure.

Reduced Maintenance

Incorporating the use of state-of-the-art technology improves durability and reduces maintenance. In addition, a built-in maintenance log records engine hours, cylinder hours and oil change intervals.

Safety

An emergency stop switch on the panel is an immediately recognizable part of its enhanced safety capabilities. The Digital Octane Panel meets all CE Mark requirements.

Retrofit Capability

The XCP platform is designed to accept future enhancements as they are made available!

The CFR octane rating units made since 1970 may be retrofitted with a Digital Octane Panel.

Planned Future Enhancements

- LIMS - Laboratory Information Management System
- MODBUS
- Enhanced Motor Protection
- Barometer
- Digital Octane Analyzer

Page 4 of Digital Octane Panel document from DresserWaukesha (full document reproduced compliments of DresserWaukesha).

Summary of Key Changes

Features	Legacy	New Digital Octane Panel	Benefits
Control System	Discrete Controls <ul style="list-style-type: none"> • 501C • Analog Meters • Knock Meter • Pressure Gauges • Mercury Thermometers • Hour Meters • Temperature Controller 	Fully Integrated Digital Controls <ul style="list-style-type: none"> • Digital Knock System • Digital Meters - On Screen • Actual Signals, Calculated Values, Trends • Transducers for Pressure • RTDs for Temperature • All Electronic • PID Closed Loop Controls 	<ul style="list-style-type: none"> • User Friendly • Easy to Read • Ease of Setup • Automatic Controls • More Information • More Robust • Automatic Data Log
Data Reports	<ul style="list-style-type: none"> • Manual Activity 	<ul style="list-style-type: none"> • Automatic Data Recording • Automatic Graphical Report Generation 	<ul style="list-style-type: none"> • Microsoft® Excel® • Preserved Data Integrity • Data Sharing • Archiving
Safeties	Discrete Controls <ul style="list-style-type: none"> • E-STOP (few installed) • Condenser Temperature Switchgag • Oil Pressure Switchgag • Magnetic Switch Contact • Motor Thermo Guard Switch • Mechanical Reset 	Fully Integrated Digital Controls <ul style="list-style-type: none"> • E-STOP Digital Input • Customer E-STOP Input (Remote) • Condenser Temperature RTD • Oil Pressure Transducer • Magnetic Switch Input • Motor Thermo Guard Input • On Screen Acknowledgement 	Ease of Setup <ul style="list-style-type: none"> • Automatic Event Log • Visual Status with Alarms • Integrated Shutdown System
Maintenance Log	<ul style="list-style-type: none"> • Manual Activity 	<ul style="list-style-type: none"> • Electronic Maintenance Log 	<ul style="list-style-type: none"> • Microsoft® Excel® • Easy Logging for Oil Changes, Carbon Blasting, Cylinder Installation, and Routine Maintenance • Electronic Operation, Maintenance, and Parts Manual (PDF)

Dresser, Inc.
Dresser Waukesha
 1101 West St. Paul Avenue
 Waukesha, WI 53188-4999
 T. 262 547 3311
 F. 262 549 2795

Bulletin 1262 10/09



www.dresser.com/waukesha

© 2009 Dresser, Inc. All rights reserved. Waukesha, CFR, and XCP are trademarks/registered trademarks of Dresser, Inc., Dresser Waukesha